Springer Theses
Recognizing Outstanding Ph.D. Research

Emilia Witkowska Nery

Analysis of Samples of Clinical and Alimentary Interest with Paper-based Devices

Springer

Springer Theses

Recognizing Outstanding Ph.D. Research

Aims and Scope

The series "Springer Theses" brings together a selection of the very best Ph.D. theses from around the world and across the physical sciences. Nominated and endorsed by two recognized specialists, each published volume has been selected for its scientific excellence and the high impact of its contents for the pertinent field of research. For greater accessibility to non-specialists, the published versions include an extended introduction, as well as a foreword by the student's supervisor explaining the special relevance of the work for the field. As a whole, the series will provide a valuable resource both for newcomers to the research fields described, and for other scientists seeking detailed background information on special questions. Finally, it provides an accredited documentation of the valuable contributions made by today's younger generation of scientists.

Theses are accepted into the series by invited nomination only and must fulfill all of the following criteria

- They must be written in good English.
- The topic should fall within the confines of Chemistry, Physics, Earth Sciences, Engineering and related interdisciplinary fields such as Materials, Nanoscience, Chemical Engineering, Complex Systems and Biophysics.
- The work reported in the thesis must represent a significant scientific advance.
- If the thesis includes previously published material, permission to reproduce this must be gained from the respective copyright holder.
- They must have been examined and passed during the 12 months prior to nomination.
- Each thesis should include a foreword by the supervisor outlining the significance of its content.
- The theses should have a clearly defined structure including an introduction accessible to scientists not expert in that particular field.

More information about this series at http://www.springer.com/series/8790

Emilia Witkowska Nery

Analysis of Samples of Clinical and Alimentary Interest with Paper-based Devices

Doctoral Thesis accepted by
the University of Campinas, Campinas, Brazil

Springer

Author
Dr. Emilia Witkowska Nery
Institute of Physical Chemistry
Polish Academy of Sciences
Warsaw
Poland

Supervisor
Prof. Lauro Tatsuo Kubota
Department of Analytical Chemistry,
Institute of Chemistry
University of Campinas
Campinas, SP
Brazil

ISSN 2190-5053 ISSN 2190-5061 (electronic)
Springer Theses
ISBN 978-3-319-28671-6 ISBN 978-3-319-28672-3 (eBook)
DOI 10.1007/978-3-319-28672-3

Library of Congress Control Number: 2016946307

Printed on acid-free paper

This Springer imprint is published by Springer Nature
The registered company is Springer International Publishing AG Switzerland

Supervisor's Foreword

When thinking about the development of analytical tools, especially those aiming at the concept of point-of-care, miniaturization has been an extensively exploited subject. In this context paper has been increasingly recognized as a powerful and interesting substrate for the development of analytical devices fulfilling the characteristics required in point-of-care testing. The paper-based analytical devices have been applied in many fields including clinical diagnosis, environmental monitoring, and food safety.

In the introduction of this thesis a short history of analytical devices constructed from paper is presented, summarizing the main advantages and disadvantages of the construction techniques, showing examples of methods of detection such as colorimetric, electrochemical, photoelectrochemical, chemiluminescence, and electrochemiluminescence. First chapter also includes comments about various types of paper presenting different thickness, porosity, etc., and therefore showing the applicability of paper in development of low-cost analytical devices. In the end, the future trends of production and application of these devices are discussed.

The main contributions provided by this thesis are as follows: the immobilization procedures of biological species on paper, the effect of the channel shape on the flow rate of the solution, preparation of electrodes on paper, and application of potentiometric sensors in electronic tongue systems. Aiming to render the paper channel bioactive, a variety of immobilization procedures were extensively investigated in order to identify methods, which enhance the activity and stability of analytical devices to greatest extent. As the analyte flows through the bioactive channel reacting during the percolation, the flow rate becomes a crucial parameter which can increase the efficiency of the reaction, thus impacting the sensitivity. With this in mind flow in several channel architectures was computer simulated and tested experimentally. Better sensitivity and resolution in case of the separation process during the percolation were the main goals of this part of work. As a consequence of these studies a proof of concept, paper-based device able to detect glucose and uric acid was developed. In this way, this part of the thesis provides guidelines for future research related to paper-based biosensors, identifying the best

methods of enzyme immobilization and channel construction needed to achieve optimum performance of such systems.

The preparation of paper-based electrodes applied as potentiometric sensors is another interesting contribution of this work. Thesis describes a detailed preparation procedure of a potentiometric sensor array, which is later used as an electronic tongue system. The characterization of the electrodes and their application in electronic tongue systems, which are able to classify precedence of mineral waters, as well as discriminate different wines and beers, are presented. Very few potentiometric, paper-based sensors were presented until today, therefore this work makes a valuable contribution to the field. This thesis also provides the first description of paper-based electrochemical electronic tongues, thus showing that it is possible to adapt complex multi-electrode systems to low-cost daily applications. It is important to stress that all these studies were carried out aiming to obtain devices fulfilling the requirements of the concept of point-of-care.

The results obtained during aforementioned studies have already inspired future projects related to application of organic solvents in paper-based analysis.

Campinas
December 2015

Prof. Lauro Tatsuo Kubota

Parts of this thesis have been published in the following:

Refereed Journal Articles

1. **E.W. Nery**, L.T. Kubota, *Integrated, paper-based potentiometric electronic tongue for the analysis of beer and wine*, Analytica Chimica Acta, 918, 60–68 (2016)

2. **E.W. Nery**, M. Santhiago, L.T. Kubota, *Flow in a paper-based bioactive channel—study on electrochemical detection of glucose and uric acid*, Electroanalysis, 28 (2016)

3. **E.W. Nery**, L.T. Kubota, *Evaluation of enzyme immobilization methods for paper-based devices—a glucose oxidase study*, J. Pharmaceut. Biomed., 117, 551–559 (2016)

4. **E. Witkowska Nery**, J.A. Guimaraes, L.T. Kubota, *Paper-based electronic tongue*, Electroanalysis, 27 (10), 2357–2362 (2015)

5. M. Santhiago, **E.W. Nery**, G.P. Santos, L.T. Kubota, *Microfluidic paper-based devices for bioanalytical applications,*Bioanalysis 6 (1), 89–106 (2014)

6. **E.W. Nery**, L.T. Kubota, *Sensing approaches on paper-based devices: a review*, Anal. Bioanal. Chem. 405, 24, 7573–7595 (2013)

Conference Submissions

1. **E.K. Witkowska Nery**, M. Santiago, L.T. Kubota, *Paper-based systems for the analysis of body fluid samples*, II School on Bioanalytical Chemistry, Maceió, Brazil, 2013

2. **E. Witkowska Nery**, J.A. Guimaraes, L.T. Kubota, *Flexible sensors for the analysis of foodstuffs*, 64th Annual Meeting of the International Society of Electrochemistry, Queretaro, Mexico, 2013

3. **E. Witkowska Nery**, L.T. Kubota, *Enzyme immobilization methods for enhanced stability of paper-based devices,* XVII EuroAnalysis 2013, Warszawa, Poland, 2013

4. **E.W. Nery**, M. Santhiago, L.T. Kubota, *The impact of different enzyme immobilization strategies on flow and reusability of paper-based microfluidic devices*, Gordon Research Conference, Physics & Chemistry of Microfluidics, Barga, Italy, 2013

5. M. Santhiago, **E.W. Nery**, L.T. Kubota, *Electrochemical detection in paper-based channels using microelectrodes*, Gordon Research Conference, Physics & Chemistry of Microfluidics, Barga, Italy, 2013

6. B.S. Miranda, C.C. Corrêa, **E.W. Nery**, F.C. Vasconcellos, L.T. Kubota, *Development and applications of point of care paper-based devices*, I School of Bioanalytical Chemistry, INCT Bioanálitica, Campinas, Brazil, 2012

7. **E. Witkowska Nery**, L.T. Kubota, *Development of paper based analytical device for detection of glucose*, International Workshop on Electrochemistry towards high performance systems: the use of nanomaterials, São Paulo, Brazil, 2011

Acknowledgements

Any work as extensive as a doctoral project cannot be completed without direct and indirect contributions. While mere words are inadequate to express all my gratitude they at least offer a chance to thank everyone who contributed to this achievement. I would like to give special thanks to the following people:

My supervisor Prof. Dr. Lauro Tatsuo Kubota for the opportunity to join LEEDS group, as well as for guidance and scientific freedom to develop this work.

CAPES and FAPESP foundations for the scholarships.

Employees of Institute of Chemistry at UNICAMP for their professionalism.

Colleagues from LEEDS Group for social and professional contributions.

Rúbia for invaluable help with paperwork and printing.

My mother and husband for taking care of the children at the time of writing.

Contents

Abbreviations

ANN	Artificial neural network
As	Anion-selective
BCG	Bromocresol green
BPB	Bromophenol blue
BPPA	Bis(1-butylpentyl)adipate)
BSA	Bovine serum albumin
ChOx	Cholesterol oxidase
CMC	Carboxymethyl cellulose
Cs	Cation-selective
DOS	Sebacic acid di(2-ethylhexyl) ester
EDC	1-Ethyl 3-(dimethylaminopropyl)carbodiimide
FAD	Flavin adenine dinucleotide
GOx	Glucose oxidase
HCA	Hierarchical cluster analysis
ISE	Ion-selective electrode
KNN	K-nearest neighbor
KTFPB	Potassium tetrakis[3,5-bis(trifluoromethyl)phenyl]borate
KTPClPB	Potassium tetrakis(4-chlorophenyl)borate
LbL	Layer-by-layer
LED	Light-emitting diode
LoD	Limit of detection
MES	4-morpholineethanesulfonic acid monohydrate
MLR	Multiple linear regression
NAD	Nicotinamide adenine dinucleotide
NHC	N-hydroxysuccinimide
o-NPOE	2-Nitrophenyl octyl ether
opad	Origami paper-based device
PARC	Pattern recognition and classification
PBS	Phosphate-buffered saline
PC	Principal component

PCA	Principal components analysis
PCR	Principal components regression
PDMS	Polidimetoxysilane
PEI	Polyethylenimine
PLS	Partial least squares
PVA	Polyvinyl alcohol
PVC	Polyvinyl chloride
SCE	Saturated calomel electrode
SIMCA	Soft independent modeling of class analogies
SMM	Separate solution method
TDMAC	Tridodecylmethylammonium chloride
TPPClMn	Chloride ionophore I
UOx	Uricase
μPAD	Paper-based microfluidic analytical devices

Introduction

Paper-based sensors have accompanied analytical chemistry for centuries in form of spot tests, litmus paper, and lateral flow assays based on nitrocellulose but just in the last few years this humble substrate has been rediscovered as a platform for integrated microfluidics. The ease of modification accomplished by common techniques such as painting, printing, and soaking, ability to form 3-D structures by simple folding and stacking, absorbency, high surface-to-volume ratio, biocompatibility, availability all over the world, and low cost are among others the reasons that made paper the first choice substrate for sensors.

Glucose is one of the most critical life compounds found in nature, and clinically it is used to evaluate diabetes. The World Health Organization estimates that 347 million people suffer from this disease worldwide. High levels of uric acid are related to conditions such as gout, Lesch–Nyan disease, obesity, diabetes, hypertension, and renal dysfunction. Cholesterol can aggravate medical conditions through its toxic derivatives or by depositing in arteries leading to plaque formation (atherosclerosis)

A few paper-based systems have already been proposed for quantification of those compounds, but **none of them have accomplished analysis of those three compounds in a single device**. Paper-based systems presented in the literature are based on the quantification of hydrogen peroxide, which is formed upon reaction of glucose, uric acid, and cholesterol with their oxidase enzymes. In all cases an auxiliary enzyme, namely peroxidase is used. The proposed system **will not employ peroxidase, reducing cost and complexity of the final device**.

In the majority of cases, devices described in the literature are not assessed in terms of storage stability. Paper-based devices are often designed for low-resource settings, where exposure to high temperatures during storage and transport is more than a threat; therefore stability of such sensors is of crucial importance. The choice of an adequate immobilization method could significantly prolong shelf-life of sensors based on enzymatic reactions. During this study a variety of immobilization methods based on different phenomena from simple absorption, through entrapment in gel, microencapsulation to covalent linkage, were compared in order to enhance storage stability of proposed sensors. In total 33 immobilization methods were

tested, and enzymatic activity was assessed for a period of 24 weeks considering two sets of samples, one stored in 4°C and other in ambient temperature. This study is intended **to identify methods of immobilization that could prolong storage stability of different types of sensors** (spot tests, lateral flow assays, sensors working in flow conditions).

Two detection **methods, electrochemical and colorimetric, were evaluated** as means of quantification of glucose, uric acid, and cholesterol on paper. In the case of colorimetric detection, different architectures were tested, including spot test, lateral flow assay, and tangential flow device. Various colorimetric agents were inspected in order to produce an **assay that would employ easily available and nontoxic compounds**. As cholesterol is not compatible with the first proposed method of fabrication (wax printing), a list of diverse fabrication methods was evaluated (cutting, impregnation with polymers). Chosen method should allow **retention of cholesterol samples in the proposed design** of the device, and permit sufficient resolution. Proposed device with electrochemical detection was designed to work in flow conditions, and several channel architectures were tested in order to **obtain optimum enzymatic reaction time and resolution of peaks**. Regardless the detection method developed systems should present **good repeatability in the range of concentrations encountered in blood and urine**.

Proposed system is not intended to compete with commercially available glucometers, which offer low detection limits and high accuracy. Instead, giving the high amount of medical disorders that alter the levels of glucose, uric acid, and cholesterol, the new paper-based system could serve in resource-limited settings as **a screening tool, indicating if the patient should seek medical help** or not.

Second part of this work was devoted to development of electronic tongue systems. Devices of this type are composed of several cross-sensitive sensors and can be trained to automatically discriminate samples from certain groups or perform multicomponent quantification. In this study potentiometric sensors were chosen, as this technique is simple, low cost, and does not require sophisticated equipment thus being consistent with the ideology of paper-based sensors. Development of an integrated system, with miniaturized reference electrode and using a minimum amount of sample was divided in three steps, each of them ending with a proof of concept application of proposed advances.

First, **individual, potentiometric, paper-based sensors** were developed. Different insulation, types of paper, and electrode materials were tested in order to obtain stable sensors able to perform measurements in liquid samples. Such developed working electrodes together with a miniaturized reference electrode of traditional architecture were applied to discriminate adulterations of forged mineral waters. Bottled water can be easily contaminated by intentional substitution with tap water or even neglectful packaging and storage. Proposed sensor matrix should be able to discriminate adulterated water samples.

In the next step an **integrated Ag/AgCl reference electrode** was introduced in the system. Based on the advances brought at this stage, material of working electrodes was changed from pencil graphite to silver to enhance sensitivity and general performance of the system. Integrated system composed of four working

electrodes and a paper-based reference was used to classify 34 different beers (12 types, 19 brands). This kind of system could potentially predict pH or alcohol content, classify unknown samples, or indicate presence of certain compounds, such as stabilizers, dyes, etc.

Last but not least, efforts were made **to minimize sample volume**. Amount of sample necessary for the analysis in the two previous examples was between 30 to 50 mL. Approaches intended to minimize sample volume included use of paper sample pads and measurement in flow conditions. Final device was applied to discriminate 11 wine types, as electronic tongue systems are often used for classification of alcohols, to detect falsification, classify samples by geographical origin, grape variety, or taste factors. Up to this date (08/2015) no potentiometric electronic tongue based on paper was proposed in the literature.

In summary, objectives of this work are:

- Platform for biomarker analysis
  - Reduction of cost and complexity by exclusion of peroxidase;
  - Employment of easily available and nontoxic compounds;
  - Analysis of cholesterol, glucose, and uric acid in a single device;
  - Evaluation and improvement of storage stability;
  - Comparison of electrochemical and colorimetric detection methods;
  - Satisfactory repeatability of measurements;
  - Working range of sensors in the range of concentrations encountered in blood and urine;
- Electronic tongue system
  - Development of an integrated system, with miniaturized reference electrode;
  - Electrode performance comparable with theoretical;
  - Usage of a minimum amount of sample;

Chapter 1
Paper as a Substrate for Sensors

Paper has been present in our culture for more than two thousand years, traditionally used to represent value, store information, for communication, sanitary use, packaging and many more. Recently, this material was rediscovered as a valuable substrate for electronic applications, sensors and microfluidic platforms.

1.1 Composition and Structure

The main constituent of paper is cellulose, the most abundant biopolymer in the world. Cellulose fibers present hierarchical structure. Thousands of β-glucose units form chains up to 5 μm long. Those partially crystallized chains form microfibrils held together by hydrogen bonds formed between hydroxyl groups. Microfibrils are later organized into fibrils which depending on the origin can be 2–5 mm long and 20–40 μm wide. In paper, the amorphous matter between cellulose fibrils is mainly composed of hemicellulose (heterogeneous, hydrophilic polysaccharide formed mainly by xylose, arabinose and mannose) and lignin (hydrophobic polymer composed of aromatic alcohols) [1, 2].

Paper properties, fiber length, lignin and hemicellulose content depend on the origin (plants, algae and bacteria) and pulping method. The main raw material is cellulose pulp obtained from plants, which can be prepared by chemical or mechanical treatment. In chemical pulping, fibers are separated after decomposition of lignin by means of high or low pH. This results in longer cellulose fibers and partial elimination of lignin. Paper prepared in this way is highly hygroscopic, and resistant as longer cellulose fibers provide strength. Mechanical pulp preparation, in which wood is simply ground results in shorter cellulose fibers leading to more opaque paper of reduced porosity. This kind of pulp also contains lignin and hemicellulose which can lead to paper aging (yellowing and brittleness), as well as pitch (resin and fatty acids) [1, 3]. Bacterial cellulose is less common, it is free from

E. Witkowska Nery, *Analysis of Samples of Clinical and Alimentary Interest with Paper-based Devices*, Springer Theses, DOI 10.1007/978-3-319-28672-3_1

lignin and hemicellulose, composed of nanofibrils of 3–8 nm, with high molecular weight, high crystallinity and mechanical strength [4].

Paper production is carried out by filtering of an aqueous solution of diluted pulp and additives. Mineral fillers such as calcium carbonate are used to increase brightness as well as reduce the surface roughness and cost of the final product. They can form up to 30 % of weight of paper and in the case of calcium carbonate can influence the paper-based analytical assay by forming carbonate buffer on a wetted surface [3, 5]. Chemical treatment such as acetylation, carboxymethylation and polymer additives such as starch, carboxymethyl cellulose, cellulose acetate, polyvinyl acetate are applied to increase mechanical strength of paper. Such polymers help also retain other additives incorporated into pulp. Other substances commonly added into the pulp include: adhesives, pH controllers, brighteners and dyes. Therefore chemical and physical properties can vary depending on the type of paper in question [1, 3].

Paper presents irregular mass distribution along the z direction (thickness). Sheets are usually denser in the center, becoming less compact near the surface. Swelling of paper is also directional, with up to 20 % increase in z axis when exposed to humidity and only up to 1 % increase in the longitudinal direction [1]. Often fibers present preferred orientation during the paper making process therefore fluid transport during an assay can be influenced by the way paper sheet was cut [3]. This type of structure often results in non-uniform wicking rates with differences observed within a single sheet of paper.

1.2 Advantages and Disadvantages of Paper as an Analytical Substrate

We observed an increasing interest in paper as a substrate for analytical platforms during the last decade. As it will be shown later, paper is not new to analytical chemistry, but it seems that just in the last few years was rediscovered as a substrate for sensors. Table 1.1 resumes some of its main properties that could lead to such increased interest.

However, this versatile substrate also presents some shortcomings. For example sheets (even from the same supplier) can vary in chemical composition. High absorbency not only results in easy modification but also in the difficulty of removing residues which are retained in the paper, even after washing. In some cases hydrophobization can serve as a solution. Droplets of reagents spread only slightly on hydrophobic paper, resulting in smaller, more densely packed detection regions, increasing the sensitivity of the assay and facilitating quantification, thus giving better results than from hydrophilic materials [6].

Phosphorescent impurities caused high background signals in some cases. Those problems could be diminished by means of irradiation with polychromatic UV light [6] or drying of the assay at 37 °C instead of room temperature [7]. Another issue is

Table 1.1 Properties of paper (adapted with modifications from [15])

	Property	Impact
Mechanical properties	Flexibility	Formation of complex 3D structures that will not tear when bent [14]
	High specific stiffness [13], lightness ($\sim$10 mg/cm^2) [16]	
	Thickness	Thickness of tens or hundreds of micrometers results in low (microliter) total volume required for the device preparation [17]
	Soft texture	Good contact with solid objects, collection of traces of analytes by swabbing [18]
Fibrous and porous structure	Absorbency	Defined total volume of the channels, dismisses the need of constant sample volume [19] and allow storage and delivery of an exact volume of reagents [12, 20], which relieves the final users from handling chemicals [21]; Allows enrichment of the sample via multiple addition/drying steps [22];
	Air permeability	Free diffusion of gas throughout the material [23] frees the system from air bubbles—one of the most common problems associated with microfluidic systems [24]; Increased collection and accumulation of gas results in rapid response of gas sensors [23]
	Network structure	Filtration of the sample e.g., contaminated with solids [19] Separation of analytes by means of chromatography [25]; Reduced fluid convection effects caused by random movement, vibration and heat result in increased accuracy of methods relying on time (chronoamperometry, chronopotentiometry) [26];
	High surface-to-volume ratio	Increased number of enzyme molecules or colorimetric probes that can be immobilized;
	Capillary action	Ability to wick fluids dispenses the use of pumps and permits fluid flow in all directions [8];
Natural origin	Compatible with biological samples [27]	Can increase thermal stability of immobilized molecules, including enzymes [28] and gold nanoparticles [29]; Easy to sterilize [30]; Chemically and biologically inert [31]; Presents chirality, which is advantageous in immobilization of antibodies and proteins [32];
	Disposability and biodegradability	Recyclable [33], rapidly degraded by microorganisms ($\sim$50 days) [34], and easily disposed of by incineration, thus eliminating the problem of contamination with biological material [35]

the uniformity of signal development. In some cases reporting molecules are carried out with liquid accumulating on the borders of the detection zone. In those cases several simple pretreatment techniques can be applied to at least partially immobilize or stabilize signal development, e.g. use of polymers such as poly(vinyl amine) [8], gelatin [9], poly(acrylic acid), and poly(ethylene glycol) [10].

As it was mentioned before dimensions of paper are greatly impacted by moisture, which can change lateral dimensions during printing deteriorating spatial resolution, lead to loss of electric contact of thin film electrodes, and reduce mechanical strength of the substrate [1, 11–14]. Combustion temperature of paper is around 200 °C, which makes it incompatible with some of the common microfabrication techniques.

Each material and fabrication technique has its advantages and disadvantages. Paper is abundant and easily available around the world, easy to store and transport. When compared with other microfluidic substrates paper (0.1 US$ cent/dm^2) is 200 times less expensive than polyethylene terephthalate (PET) and 1000 times less than glass [1, 36]. Development and market introduction of paper-based systems also requires a relatively small investment. As it will be shown in the next section a pair of scissors and a paper towel is all that is really needed to make a simple device of this material, which facilitates contributions of scientists around the world [35]. This kind of platform can spread widely not only among the scientific community but also could be easily applied in practical, real-life situations [35, 37], even in places without access to laboratory facilities e.g. developing world, military field or in case of an emergency [27, 29].

1.3 Methods of Fabrication

Most researchers working with paper emphasize the possibility of using low-cost techniques traditionally associated with paper industry, such as inkjet printing, screen printing, transfer printing etc. Printers can dispense various types of reagents like enzymes or colorimetric reagents enabling better defined detection areas or hydrophobic polymers to form walls. The choice of fabrication technique will depend mainly on the desired resolution, application and price. Diverse fabrication techniques of paper-based devices were already presented in the literature, with some of them resumed in Table 1.2. Regardless the method of fabrication barriers can be divided in the following types:

- hydrophobic wall created by modification of fibers with agents such as wax, photoresist, or alkyl ketene dimer;
- air–solid phase boundary as in cutting;
- physical barrier formed by blocking of the porous structure with a polymer such as polydimethylsiloxane, polystyrene, or polyurethane.

Table 1.2 Common fabrication techniques (adapted with permission from [15])

Technique		Resolution	Cost	High-throughput method	Advantages	Disadvantages
Cutting	Manual [49]	Very low	Very low	No	No contamination from chemicals; Fabrication of 3D structures from paper and tape; Applicable in resource-limited locations	Low-cost methods result in low resolution
	Computer-controlled cutting plotter [50, 51]	Low	Low	Yes		
	Laser cutter [12]	High	High	Yes		
	Mechanical drill [34]	Low	Moderate	Yes		
Printing	Wax printing [52, 53]	High	Low	Yes	Fast, automated method; Biodegradability of barriers; Only computer designed pattern needed;	Low popularity of wax printers
	Screen printing [54, 55]	Moderate	Very low	Yes	Deposition of thick layers is possible; No heat treatment	Patterned mesh is necessary, thus less applicable for prototyping
	Flexographic printing [56, 57]	High	Moderate	Yes	Low ink usage	Low ink viscosity; Limited compatibility of solvents
	Ink-jet printing [8, 58–63]	High	Low to moderate	Yes	Several print heads can be used at the same time; Only computer designed pattern needed; Applicable with modified office printers of extremely low cost and high availability;	Nozzle clogging; Temperature applied in thermal printers can affect ink properties; More sophisticated systems designed for microfabrication are costly;
	Laser printing [12]	High	Low	Yes	High availability; No additional treatment needed;	Only surface treatment;
	Transparency transfer printing [64]	Moderate	Low	Yes	Wax pattern printed on transparency can be transferred to any substrate, also of irregular shape	Manual positioning of transparency lowers resolution

(continued)

Table 1.2 (continued)

Technique	Resolution	Cost	High-throughput method	Advantages	Disadvantages
Drawing [40, 65, 66]	Very low	Very low	No	Extremely cheap and widely available; Resources as ballpoint pens filled with polymer and wax pencils can be used;	Very limited resolution
Dip-coating [54, 67]	Moderate	Very low	No	Inexpensive and widely available;	Metal or polymer template is needed—less applicable for prototyping
Plotting [68–70]	Low	Low	Yes	Less demanding viscosity ranges than in printing; Can be applied to any surface; Does not fold or bend sheets during the process;	Amount of liquid dispensed is difficult to control; Gradually replaced by printers; plotters are becoming hard to obtain
Photolithography [26, 71–73]	High	Moderate	Yes	Can be adapted to use low-cost facilities (hot plate, sunlight, and printer-produced mask)	Requires multistep process; Samples are prone to contamination with photoresist; Barriers are susceptible to damage when bent or folded;

Other functionalities, apart from hydrophobic contrast are often introduced into paper-based devices, including electrodes and circuitry drawn with a pencil [38, 39] or with conductive ink by means of a ballpoint pen [40]. Electrodes can be also painted [41], cut from carbon-nanotube-soaked paper [42] or printed through an adhesive tape stencil [43]. Other more sophisticated methods are also in use as for example thermal evaporation [44, 45], electron beam evaporation [46], sputtering [25, 47], laser annealing [17] and electroplating [48].

Several types of enclosures were also proposed ranging from simple wrapping in adhesive tape [14], lamination [74, 75], toner or polymer coatings [27, 54, 76] up to polymer and metal holders [53, 77, 78].

It was noted that paper has great potential as a substrate for integrated devices. Single sheet can incorporate pre-treatment steps like sample filtration, separation of analytes, and conduce simultaneously several independent measurements [19, 51]. With the development of electronic components on paper we can think of fully integrated devices with batteries providing power, digital sensors and displays presenting the results [1, 79].

1.4 History of Paper in Analytics

Until a few years back, paper-based sensing platforms usually provided only a "yes"/"no" information, and allowed to detect only one analyte per sample. Scientists differ about the starting date and the reasons that led to the increase in popularity of paper as a substrate for sensing platforms. Some attribute it to the developments in micro- and nanotechnologies that allow fabrication of new devices [46]. Others point out the growing trend to manufacture paper-based devices in an ever simpler manner (screen printing with a bar of wax [80], wax dipping [67], drawing with a wax pencil [65]). Those technologies, available for decades, have just now found application in sensor production. Most probably the necessity for simple, low cost, and disposable systems was the main reason why paper was rediscovered as a potential substrate not only for sensors but also for electronics.

First paper-based sensors appeared in the beginning of Current Era, evidence of those are given by Pliny the Elder in his Natural History [81]. This already almost 2000 years old work describes methods that could be considered a papyrus-based chromatography (estimation of quality of Tyrian purple) and a papyrus-based spot test for ferrous sulfate.

Next noteworthy example is the litmus paper, which could be considered a model to follow for all paper-based sensors. It is inexpensive, requires no signal amplification or additional equipment and almost no training, has a long shelf life and is extremely sensitive (sensitivity in picomolar range for paper indicating pH 11) [3]. Many attribute discovery of litmus paper to Gay-Lussac who described it in early 1800s [82].

In 1859 Hugo Schiff reported first paper-based test for uric acid that could be detected by precipitation with silver carbonate. This work demonstrated

possibilities (sensitivity) and expediency of spot-tests on filter paper [83]. In the late 19th century a number of researchers reported dry chemistry test papers and dipsticks. In 1883 G. Oliver described a method of detection of glucose and proteins in urine by means of a paper-based test stable in room temperature [84]. In 1906 Plesh presented a chromatography-based spot test for bilirubin from urine [85].

Another breakthrough dates back to 1937 when Yagoda reported the first test with walls defined by paraffin embossing [86]. This technique was later used in 1949 by Müller and Clegg to produce a device for chromatographic separation and reflectance-based detection of dyes and pigments [87].

The next major step was the Nobel Prize in Chemistry granted for partition chromatography to Archer Martin and Richard Synge in 1952 [88]. Initially this method was used for separation of organic substances such as amino acids, carbohydrates and lipids. Soon after paper chromatography was also adapted for inorganic ions, enabling separation of anions and cations [89]. Successful separation of amino acids and peptides by paper chromatography resulted in attempts to adapt this method to separation of proteins. The lack of positive outcomes led researchers to employ supporting electrolyte used in electrophoresis. Developed in the 50s of last century electrophoresis on paper proved useful in separation of proteins [90].

During the second half of the XX century several new types of tests have been proposed including the lateral flow assay, dot blot assay and many others. In 1956 A. Keston described the first colorimetric enzymatic glucose assay on filter paper based on reaction of o-toluidine with hydrogen peroxide. A year later, in 1957 J. Kohn used reported earlier urine glucose test strips for blood samples [84].

Many tests were also successfully commercialized during this time including Dextrostix by Ames company, for enzymatic detection of glucose (1964). In the 1970' the same company introduced the first commercial hand-held-battery-operated reflectance meter [84]. It was expensive, required a prescription, was rather large and heavy ($\sim$1 kg) but nevertheless proved to be a success and allowed to automatically assess the color change of enzyme-based glucose test strips [91, 92]. In 1988 Unipath brought to market the first immunoassay for human chorionic gonadotropin popularly known as the home pregnancy test [74].

In 1990 Allen et al. [93] reported equipment-free paper-based cholesterol detection system, in which concentration of cholesterol was proportional to the length of the strip on which color change was observed. Afterwards two important patents were deposited. In 1995 US Patent 5,409,664 describes similar assay for cholesterol but this time with walls made by printing of hydrophobic patterns or cutting [94]. In 2003 US Patent 6,573,108 reports the first tangential device currently described in literature as 3D μPAD (paper-based microfluidic analytical devices) or opad (origami paper-based device). Proposed system incorporated a filtration step for sample pretreatment, multiple channels and timers that would show when the assay is over. Walls could be made by screen printing, dipping in polymer with a template held against paper, or by a computer-controlled deposition system. Researchers proposed polymers such as heteropolysaccharides, acrylic

polymers and copolymers, and silanes [54]. This patent also contains reports detailing devices to detect glucose, nitrite and human chorionic gonadotropin.

The first years of the XXI century have thus far been marked by the rise of interest in paper as a substrate, first for electronics, and later for sensors. In 2008 first international conference on bioactive paper was held in Finland. Most recent articles cite the 2007 publication by Whitesides group [95] as the first modern analytical device on paper. In this article, the Harvard group presented a paper device with multiple channels capable of quantifying glucose and total protein concentration in samples of artificial urine. Regardless of who presented the possibility of manufacturing complex devices first, after the mentioned publication by Whitesides a huge growth of reports concerning paper-based devices was noted.

During the last two decades occurred a transition from simple devices to μPAD systems (paper-based microfluidic analytical devices) which can in many cases provide quantitative analysis, apply pretreatment, conduce multistep assays and work with several analytes at the same time. The formation of walls (hydrophobic, cut etc.) opened a new path for the devices on paper, since then they could contain multiple channels, containers, valves etc. Some of those novel functionalities will be covered in the following chapter.

1.5 Paper-Based Analytics During the Last Decade

As it was explained before paper-based analytics is not a new idea, but the explosive interest in paper as a substrate for sensor during the last decade led to implementation of many interesting features.

1.5.1 Enhanced Sensitivity and Signal Amplification

Enhanced sensitivity and accuracy was, for example achieved with the use of multiple indicators [96]. Each detection zone included several indicators that could be classified as: generating color on oxidation and losing color when oxidized. Nine detection zones were positioned around the sampling area, and the walls were made from photoresist. It was possible to quantify glucose (0.5–20 mmol/L), lactate (1–25 mmol/L), and uric acid (0.1–7 mmol/L) and the system presented accuracy above 90 % (single indicator system $\sim$ 70 %).

Other research groups described enhanced sensitivity achieved by means of small changes in architecture. Parolo et al. [97] reported a lateral flow assay in which the sample and conjugation pads were enlarged up to three times. The basics laws governing flow in paper network will be explained later in the text but in general it can be said that a narrowing of the channel accelerates the flow and a widening slows it down. By changing the size of the appropriate pad, authors could vary the time of interaction of the reagents. Best results were obtained with

maximum enlargement of both sample and conjugation pads, with eightfold improvement of limit of quantification. Another group investigated how narrowing of the detection pad (from 5 to 2 mm) impacts a lateral flow assay. Best results were obtained for 3 mm width and device was successfully implemented to analyze salivary cortisol [98]. Other strategy involved cutting filter paper into a star-like pattern [99]. Charged polyelectrolytes were used to create gradients on each branch. Even complex sample could be separated in the chemical gradient, and the analyte in question detected in a concentrated form on the tip. Rhodamine 6G was detected by Surface-enhanced Raman scattering in a complex mixture with attomolar limit of detection.

1.5.2 Three-Dimensional Architecture

3D systems are generally assembled by stacking and clamping of several paper layers, or interconnecting them with double-sided adhesive tape. Recently, third method was proposed in which layers are generated in a single sheet of paper.

First clamped device was described in the aforementioned 2003 patent [54]. In a so called origami paper-based device sheets are only clamped together and can be unfolded after reaction has taken place to allow easier quantification from whichever layer without the interference (i.e. color) from the adjacent layers. Similar technique was used later by Chen et al. [7] to assemble tests for glucose and uric acid. Single sheet patterned by means of photolithography was folded, forming a three-dimensional system, and clamped in an aluminum device holder. In another system Epicocconone dye was used as the fluorescent reagent to quantify bovine serum albumin in four simultaneous assays [73].

First system with layers interconnected with patterned double-sided adhesive tape was reported by Whitesides group in 2008. Layers of paper were patterned with photoresist and connected with each other by means of a double-sided adhesive tape. Report contained descriptions of a sample distribution system as well as glucose and protein assays [100].

Patterning complex channel architectures in a single sheet of paper was first presented by Schilling et al. [76]. In this case channel delimitated latterly with wax was enclosed between two layers of a laser printed toner. Device included channels for glucose and alkaline phosphatase assays and third for control. Apart from enabling fabrication of complex channel architectures enclosure (accomplished with toner, adhesive, lamination, or other coating) can protect the system from contamination, reagents from deactivation, and decrease the evaporation of fluid. The last feature is especially important when the fluid is supposed to wick for a considerable distance. Concept of fabrication of complex channels in a single sheet was recently expanded by several groups [101–103] and in all cases was based on printing properly aligned wax patterns on the top and bottom sides of the sheet. Vertical spreading of the wax pattern controls channel height while lateral spreading controls its width. Fully open, semi open and closed channels can be

fabricated in a single sheet. To obtain more complex structures device can be later enclosed between lamination sheets.

1.5.3 Timing and Valving

The wicking rate can be controlled not only by enclosing of the channel but also by controlling the humidity and temperature, viscosity of the fluid, as well as by modification of channel dimensions, and characteristics of the paper used. Control of the wicking rate is of great importance in assays where multiple steps are required, when reagents should interact for a defined period of time and to fabricate timers showing when quantification should take place.

Flow rate can be controlled by compression of a part of the channel. Pressure applied will reduce the pore size, increasing the resistance and hampering the flow [104]. Channels can be also crafted, for example with a plotter controlled knife to obtain patterns that can accelerate or delay the movement of a liquid. Cuts can be made without removing paper substrate from the channel, or cutting through but only by incising the surface. Flow is controlled by the number and orientation of the cuts (cuts perpendicular to flow cause delay, parallel accelerate). They can be made after the device is fabricated, and both enhancement and delay of flow can be accomplished on a single device. Colorimetric proof-of-concept assays for identification and quantification of metal ions were described employing this technique [105]. Precise time delays, that could vary between 1 min and 2 h were also obtained by deposition of paraffin wax inside the channels [106].

Fluid wicking through the modified area needed more time to pass through than it did through an unmodified channel. A proof-of-concept assay for glucose was described with a color dye appearing in an adjoining compartment (it could be also a luminescent or sound signal) informing the user when quantification should take place. Similar method was proposed by Yager group, in this case dissolvable sugar barriers were created allowing sequential delivery of the reagents. Different concentration of sucrose (10–70 % of saturation) applied for modification resulted in time delays spanning from minutes to almost an hour. Idea was successfully implemented to carry out a multi-step amplified immunoassay for a malaria diagnostic biomarker, PfHRP2 [107].

Sugars were also used to obtain dissolvable bridges that could be applied to automatically meter different volumes of fluid delivered from a common source. Sugar-based paste was placed in a mold and dried. Dried sugar element was used to interconnect two pads of nitrocellulose. After a certain volume of liquid passes through, the bridge dissolves, cutting-off the liquid flow. Range of volumes metered with this method spanned from 10 to 80 μL. Volume passed could be programmed with the width of the bridge and type of sugar used (trehalose or mannose) [108].

Valving was also obtained by means of modification with a surfactant. In this case fluidic valve was composed of two terminals, a cathode that would stop the fluid flow but was able to receive fluid coming from the opposite direction and an

anode through which fluid passed freely in both directions. A region of hydrophobic dots separates the anode and the cathode. From the side of the anode dots were modified with a surfactant, which would induce a change of the surface tension of the liquid approaching from the anode, allowing it to pass through the hydrophobic barrier of dots and to enter the cathode region. Once the diode was open, fluid could pass in both directions. Potential of the proposed system was exploited in an alkaline phosphatase assay, where fluid valve was used to deliver reagents at precise time intervals [109].

Another, this time magnetic valving method was presented by Li et al. [110]. In this case a magnetic valve could be automatically triggered (to close or open) by liquid flowing through a delay channel ending in a ionic resistor. Upon wetting of the ionic resistor (area with pre-deposited NaCl) resistance drop would lead to turning on of the electromagnet. System was fabricated by means of wax printing and laser cutting and incorporated a magnetized cantilever. It allowed to incubate and after specified amount of time transfer stored reagents to the reaction zone (normally-open valve), or control the volume of a solution delivered to the reagent zone (normally-closed valve). An alkaline phosphatase assay was described as a proof-of-concept application.

Alternative valving method is based on the fact that small gaps are formed between layers of a device fabricated from paper and double-sided adhesive tape. Those gaps can be filled with hydrophilic material to allow free flow, or pressure can be exerted on adjacent layers. “On” buttons formed by leaving gaps around a paper layer can be programmed by the user to generate a variety of flow patterns. The most important advantage of this approach is the programmability of a ready-made system as the choice of which channel will be used and which assay should be tested can be made after the device is finished [111].

1.5.4 Detection Methods

1.5.4.1 Optical Detection

Optical detection is the least expensive, simplest and universal [112]. A variety of detectors can be applied for optical sensing, including the most common devices such as scanners or cellphone digital cameras, more specialized such as spectrophotometers and fluorimeters to sophisticated equipment e.g. gel documentation systems.

An office scanner, provides high resolution and ensures focus of the digitalized image; furthermore, image intensity is not affected by the external lighting conditions. Scanners can be portable (e.g. pen scanners), they can be handled by unskilled personnel, and are widely used all over the world [19]. A digital camera can also be used as a detector and similarly as a scanner does not require any special skills. One shortcoming is that it cannot focus on objects that are too close (approximately 20 cm) [19, 113]. It is also possible to use cell phone cameras, and it is

worth remembering that around 67 % of the world's population owns a cell phone (data from 2011), with the largest growth of ownership in the developing world [114]. Results could be sent to a specialist or be analyzed by means of a user friendly software. If available cellphone hardware wouldn't be enough it is possible to construct cellphone-based readers that could direct light to exact position of the test [115] or provide pulses of energy required, for example, in electrochemiluminescence sensing [114]. Devices based for example on the Arduino platform can be developed and connected to a cell phone by means of a USB port or wireless.

Simple detectors can be fabricated with components readily available in any electronics supply catalog (light-emitting diodes, photodiodes, integrated chips, power sources, amplifiers and capacitors). Such systems were already described by several research groups and include photoelectric meters [116], portable color identifier systems [117] and transmittance colorimeters [72].

Not so common, but still useful options are spectrophotometers, fluorometers and photomultiplier tubes [114] that could be applied to optimize the fabrication process in the laboratory or in their portable versions used for on-site detection [113, 118]. Finally more sophisticated equipment can be used, such as microplate readers [27] and gel documentation systems [7], but they are rather expensive, not so popular, and therefore not fully compatible with simple paper-based sensors.

In the case of cameras and scanners, after digitalization, image can be analyzed with the use of a computer program such as Adobe Illustrator, Adobe Photoshop, GenePix, DigitalColor Meter, Corel PhotoPaint, ImageJ or other personalized software written in Python, MATLAB, etc. Images can be converted to color spaces: CMYK, RGB, grayscale, HSV, or CIE L*a*b* [27]. Depending on the color and hue of the image analyzed, the total value or just one channel of the color space can be used for quantification. Usually the quantitative response is given as the arithmetic mean of the pixel intensity within the detection zone after subtraction of the mean intensity for the control region.

As it was already mentioned, optical detection presents many assets nevertheless some variables must be taken into consideration, for example the fact that differences in illumination will cause variations in intensity and hue of a given color. This kind of problem can be solved by a white balance correction, subtraction of the background color, or comparison with a calibration curve of standards of known color and intensity [119, 120]. Comparison with standards can also be applied when different imaging devices are used e.g., when we want to compare results recorded by a camera, scanner, and a portable spectrometer. Nevertheless differences between the color of the wetted reaction zone and dry printed standard should be taken into account [120].

1.5.4.2 Equipment Free Optical Detection

Paper is usually associated with reading and writing, thus many efforts are directed to develop paper-based assays that would present they results in a similar straightforward fashion.

This idea was used in a blood typing device [61]. A hydrophilic pattern was delimitated with alkenylketene dimer by ink-jet printing. Letters "O" and a minus symbol were then painted with red ink. Hydrophilic regions formed letters "A", "B" and "X" as well as a vertical line (X being printed on top of previously painted O and the vertical line on top of the minus symbol together forming a plus sign). The letter A was modified with anti-A antibodies, the letter B with anti-B, and the letter X with both anti-A and anti-B antibodies. The vertical line was spotted with anti-D. Blood was introduced to each of the patterns and later washed out. For blood group A, agglutinated antibodies would color the A symbol and the X used to cross-out the-red printed O. The same would occur for blood group B, just that this time the letters B and X would become red. In the case of blood group O, no agglutination would take place, leaving the painted O pattern visible. For Rh-positive blood, agglutination would occur on the vertical line forming a plus; for Rh-negative blood, only the printed minus sign would be visible.

Another interesting qualitative approach was presented by Weaver et al. [121]. The "color barcode" consisted of 12 lanes, each of them conducing a different set of reactions, which were adapted from standard spot-test procedures. To perform the assay user rubs a portion of the pharmaceutical across the lanes, and dips the edge in water. Water carrying the pharmaceutical triggers reactions in each lane. Last lane serves as a timer, indicating when quantification should take place. After indicated time, user can compare the bar code with a library of attached standard, thus identifying active pharmaceutical ingredients (ampicillin, amoxicillin, rifampicin, isoniazid, ethambutol and pyrazinamide), substitutes (acetaminophen, chloroquine) as well as binders and fillers (chalk, talc and starch).

Quantitative optical detection is resumed in Fig. 1.1. Review article by Fu [122] excellently sums up recent advances in this field. Basically, the main approaches can be categorized into three groups: intensity, distance and time based. Intensity or hue-based readout systems (Fig. 1.1a) can include set of printed standards, that could be integrated on the devices [113] and would allow user to visually identify concentration of the sample. Intensity-based detection is probably the most common approach but can be affected by the user to user variability in the interpretation of intensity differences [72], lightning conditions, and devices of this type require at least minimum training.

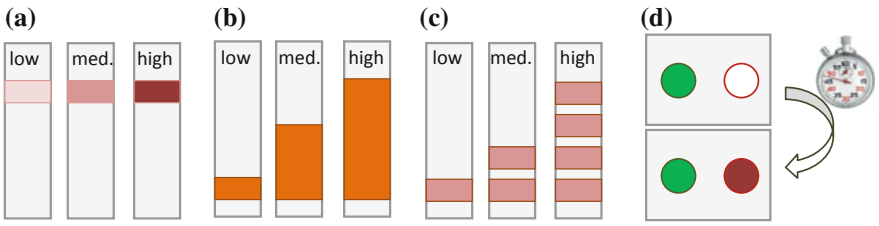

Fig. 1.1 Types of equipment-free quantification: **a** intensity-based, **b** distance-based, **c** ladder-bar, **d** time-based, adapted with changes from [122]

Distance-based quantification relies on spatial distribution of an indicator, which is deposited along the direction of the flow, in an expanded area. The length on which signal develops is proportional to measured quantity (i.e. concentration). There are two types of visualization, direct (Fig. 1.1b), where user matches the distance to a preprinted "concentration ruler" or a ladder-bar (Fig. 1.1c) where it is only necessary to count the number of areas on which signal developed. Tests of this type are less prone to user misinterpretation, and have potential for high quantitative resolution. Similar advantages can be cited for the time-based measurement. In this case user measures the time of the development of color in the two regions. In a device presented by Lewis et al. [123] the longer time needed for the second color reaction to take place indicated the higher concentration of heavy metal ions. Main disadvantage of this approach is the constant attention necessary to perform the test (up to 15 min).

Electrochemical Detection

The main advantage of electrochemical sensors in comparison with the optical detection is their insensitivity to interferents such as light and insoluble compounds [124]. Several groups observed that a paper matrix reduces the effect of convection of liquids caused by random motion, vibration, and heating by affixing a thin slab of liquid on the electrode surface [26, 114]. Furthermore an assay under stationary conditions can be easily transformed to a flow measurement. A pad of cellulose blotting paper can be connected to the outlet of the paper channel, allowing continuous wicking across the electrodes. This configuration facilitates plating of metals and cleaning of the electrodes and proved to be an excellent choice for measurements based on convection and hydrodynamic conditions.

Architecture of paper platforms allows electrolytes to be added from the back side of the electrodes in order to produce three-phase electrolyte/electrode/gas interfaces [125]. Large roughness and porosity results in an increased surface area of the deposited materials that can improve the sensor's response [126]. A rugged structure can also be a disadvantage when it comes to physical attachment of electrodes, which is sometimes hard to control [125]. In methods where the electrode is consumed on measurement, a modest amount of electrode material can result in a short lifetime of the device [43].

Apart from electrochemical workstations available in the laboratory, several simple detector systems have been proposed to permit field measurements. The first group includes homemade devices that can be fabricated from off-the-shelf components (amplifiers, voltage regulators, voltage inverters, batteries [127]). They are characterized by their simplicity and low cost, and could be adapted to work on batteries or to draw power from the network. They can be assembled at the place of need, which is important for applications in developing countries. One system of this type, namely CheapStat [128], an open source potentiostat can be assembled in the laboratory from separate components, build based on an assembled, programmed and tested CheapStat printed circuit board or bought ready-made from

IORodeo Inc. Similar Arduino-based systems could be constructed, at least partially taking advantage of the cell phone hardware.

Multimeters form the next class of low cost, potential electrochemical detectors. They are readily available and affordable (approximately $30) and could be useful for potentiometric measurements [129].

Commercial glucose meters are another group of detectors compatible with paper based platforms. The cost of the development of this technology has already been absorbed by the market; thus, we can take advantage of this sophisticated engineering for a reasonable price. They are designed to be operated by unskilled personnel and assays can be adapted to a variety of analytes and types of measurement, such as amperometry, chronoamperometry, anodic stripping voltammetry, and cyclic voltammetry [74, 124].

Integration is also an interesting approach, as paper-based electronics became an object of increased scientific attention few years before paper-based analytics. Paper-based transistors [130–134], batteries [135–137], diodes [4, 138, 139] and solar cells [36, 140, 141] are already available. Even logic circuits [142], RFID tags coupled to paper antennas [143], and digital displays, based on thermochromic [144–146], electrowetting [147], electrochromic [148] and electroluminescent [149] properties were already presented in the literature. Therefore it is possible to imagine fully integrated paper-based electrochemical systems, which is able to not only to conduce the assay, but also to detect the signal and to present it on a display. Unfortunately the cost of paper-based electronics is still too high in comparison with traditional methods. Therefore no fully integrated system made completely out of paper is yet available. Nevertheless some integrated platforms incorporating traditional electronic units were already presented. As an example we can cite an integrated platform for the fluorescent detection of β-D-galactosidase and albumin. Sensor and a galvanic cell battery are both made from paper. The fluidic battery serves as a power source for the UV LED used to illuminate the assay region. Sample is used both for the assay, and to re-dissolve electrolytes in the galvanic cells and thus initiate the half-reactions [150].

References

1. Tobjörk D, Österbacka R (2011) Paper electronics. Adv Mater 23:1935–1961. doi:10.1002/adma.201004692
2. Spence KL, Venditti R, Rojas OJ et al (2010) The effect of chemical composition on microfibrillar cellulose films from wood pulps: Water interactions and physical properties for packaging applications. Cellulose 17:835–848. doi:10.1007/s10570-010-9424-8
3. Pelton R (2009) Bioactive paper provides a low-cost platform for diagnostics. TrAC Trends Anal Chem 28:925–942. doi:10.1016/j.trac.2009.05.005
4. Legnani C, Vilani C, Calil VL et al (2008) Bacterial cellulose membrane as flexible substrate for organic light emitting devices. Thin Solid Films 517:1016–1020. doi:10.1016/j.tsf.2008.06.011

5. Lackinger E, Schmid L, Sartori J et al (2011) Novel paper sizing agents from renewables. Part 1: Preparation of a paper sizing agent derived from natural plant oils. Holzforschung 65:3–11. doi:10.1515/HF.2011.007
6. Ramasamy SM, Hurtubise RJ (1998) Oxygen sensor via the quenching of room-temperature phosphorescence of perdeuterated phenanthrene adsorbed on Whatman 1PS filter paper. Talanta 47:971–979
7. Chen X, Chen J, Wang F et al (2012) Determination of glucose and uric acid with bienzyme colorimetry on microfluidic paper-based analysis devices. Biosens Bioelectron 35:363–368. doi:10.1016/j.bios.2012.03.018
8. Hossain SMZ, Luckham RE, McFadden MJ, Brennan JD (2009) Reagentless bidirectional lateral flow bioactive paper sensors for detection of pesticides in beverage and food samples. Anal Chem 81:9055–9064. doi:10.1021/ac901714h
9. Cha R, Wang D, He Z, Ni Y (2012) Development of cellulose paper testing strips for quick measurement of glucose using chromogen agent. Carbohydr Polym 88:1414–1419. doi:10.1016/j.carbpol.2012.02.028
10. Mentele MM, Cunningham J, Koehler K et al (2012) Microfluidic paper-based analytical device for particulate metals. Anal Chem 84:4474–4480. doi:10.1021/ac300309c
11. Peng P, Summers L, Rodriguez A, Garnier G (2011) Colloids engineering and filtration to enhance the sensitivity of paper-based biosensors. Colloids Surf B Biointerfaces 88:271–278. doi:10.1016/j.colsurfb.2011.07.001
12. Bracher PJ, Gupta M, MacK ET, Whitesides GM (2009) Heterogeneous films of ionotropic hydrogels fabricated from delivery templates of patterned paper. ACS Appl Mater Interfaces 1:1807–1812. doi:10.1021/am900340m
13. Werner O, Quan C, Turner C et al (2010) Properties of superhydrophobic paper treated with rapid expansion of supercritical CO_2 containing a crystallizing wax. Cellulose 17:187–198. doi:10.1007/s10570-009-9374-1
14. Bracher PJ, Gupta M, Whitesides GM (2009) Shaped films of ionotropic hydrogels fabricated using templates of patterned paper. Adv Mater 21:445–450. doi:10.1002/adma.200801186
15. Nery EW, Kubota LT (2013) Sensing approaches on paper-based devices: a review. Anal Bioanal Chem 405:7573–7595
16. Jagadeesan KK, Kumar S, Sumana G (2012) Application of conducting paper for selective detection of troponin. Electrochem Commun 20:71–74. doi:10.1016/j.elecom.2012.03.041
17. Tseng S-C, Yu C-C, Wan D et al (2012) Eco-friendly plasmonic sensors: using the photothermal effect to prepare metal nanoparticle-containing test papers for highly sensitive colorimetric detection. Anal Chem 84:5140–5145. doi:10.1021/ac300397h
18. Ngo YH, Li D, Simon GP, Garnier G (2012) Gold nanoparticle-paper as a three-dimensional surface enhanced Raman scattering substrate. Langmuir 28:8782–8790. doi:10.1021/la3012734
19. Martinez AW, Phillips ST, Carrilho E et al (2008) Simple telemedicine for developing regions: camera phones and paper-based microfluidic devices for real-time, off-site diagnosis. Anal Chem 80:3699–3707. doi:10.1021/ac800112r
20. Fu E, Liang T, Spicar-Mihalic P et al (2012) Two-dimensional paper network format that enables simple multistep assays for use in low-resource settings in the context of malaria antigen detection. Anal Chem 84:4574–4579. doi:10.1021/ac300689s
21. Jarujamrus P, Tian J, Li X et al (2012) Mechanisms of red blood cells agglutination in antibody-treated paper. Analyst 137:2205–2210. doi:10.1039/c2an15798e
22. Gu Z, Zhao M, Sheng Y et al (2011) Detection of mercury ion by infrared fluorescent protein and its hydrogel-based paper assay. Anal Chem 83:2324–2329. doi:10.1021/ac103236g
23. Xu M, Bunes BR, Zang L (2011) Paper-based vapor detection of hydrogen peroxide: colorimetric sensing with tunable interface. Appl Mater Interfaces 3:642–647
24. Osborn JL, Lutz B, Fu E et al (2010) Microfluidics without pumps: reinventing the T-sensor and H-filter in paper networks. Lab Chip 10:2659–2665. doi:10.1039/c004821f

25. Yoshio L, Santhiago M, Gobbi AL et al (2012) Separation and electrochemical detection of paracetamol and 4-aminophenol in a paper-based microfluidic device. Anal Chim Acta 725:44–50. doi:10.1016/j.aca.2012.03.011
26. Nie Z, Nijhuis C, Gong J et al (2010) Electrochemical sensing in paper-based microfluidic devices. Lab Chip 10:477–83. doi:10.1039/b917150a
27. Coltro WKT, De Jesus DP, da Silva JAF et al (2010) Toner and paper-based fabrication techniques for microfluidic applications. Electrophoresis 31:2487–2498. doi:10.1002/elps.201000063
28. Zhang Y, Rochefort D (2011) Activity, conformation and thermal stability of laccase and glucose oxidase in poly(ethyleneimine) microcapsules for immobilization in paper. Process Biochem 46:993–1000. doi:10.1016/j.procbio.2011.01.006
29. Zhao W, Ali MM, Aguirre SD et al (2008) Paper-based bioassays using gold nanoparticle colorimetric probes. Anal Chem 80:8431–8437. doi:10.1002/cbic.200-800282.Analytical
30. Su S, Ali MM, Filipe CDM et al (2008) Microgel-based inks for paper-supported biosensing applications. Biomacromolecules 9:935–941. doi:10.1021/bm7013608
31. Kouisni L, Rochefort D (2008) Confocal microscopy study of polymer microcapsules for enzyme immobilisation in paper substrates. J Appl Polym Sci 111:1–10. doi:10.1002/app
32. Kim J, Wang N, Chen Y et al (2007) Electroactive-paper actuator made with cellulose/NaOH/urea and sodium alginate. Cellulose 14:217–223. doi:10.1007/s10570-007-9111-6
33. Noh H, Phillips ST (2010) Fluidic " Timers" for paper-based microfluidic devices materials supporting information. Anal Chem 82:8071–8078. doi:10.1021/ac1005537
34. Couderc S, Ducloux O, Kim BJ, Someya T (2009) A mechanical switch device made of a polyimide-coated microfibrillated cellulose sheet. J Micromech Microeng 19:055006. doi:10.1088/0960-1317/19/5/055006
35. Martinez AW (2011) Microfluidic paper-based analytical devices: from POCKET to paper-based ELISA. Bioanalysis 3:2589–2592. doi:10.4155/bio.11.258
36. Barr MC, Rowehl J a, Lunt RR et al (2011) Direct monolithic integration of organic photovoltaic circuits on unmodified paper. Adv Mater 23:3500–3505. doi:10.1002/adma.201101263
37. Zhao W, van der Berg A (2008) Lab on paper. Lab Chip 8:1988–1991. doi:10.1039/b814043j
38. Gimenez AJ, Yanez-Limon JM, Seminario JM (2011) ZnO-Paper Based Photoconductive UV Sensor. J Phys Chem C 282–287
39. ul Hasan K, Nur O, Willander M, Hasan K (2012) Screen printed ZnO ultraviolet photoconductive sensor on pencil drawn circuitry over paper. Appl Phys Lett 100:211104. doi:10.1063/1.4720179
40. Russo A, Ahn BY, Adams JJ et al (2011) Pen-on-Paper Flexible Electronics. Adv Mater 3426–3430. doi:10.1002/adma.201101328
41. Leung V, Shehata A-AM, Filipe CDM, Pelton R (2010) Streaming potential sensing in paper-based microfluidic channels. Colloids Surfaces A Physicochem Eng Asp 364:16–18. doi:10.1016/j.colsurfa.2010.04.008
42. Novell M, Parrilla M, Crespo G et al (2012) Paper-based ion-selective potentiometric sensors. Anal Chem 84:4695–4702. doi:10.1021/ac202979j
43. Yang Z, Suzuki H, Sasaki S, Karube I (1997) Design and validation of a low-cost paper-based oxygen electrode. Anal Lett 30:1797–1807. doi:10.1080/00032719708001698
44. Kim J, Lee H, Kim HS (2010) Beam vibration control using cellulose-based electro-active paper sensor. Int J Precis Eng Manuf 11:823–827. doi:10.1007/s12541-010-0099-8
45. Kim J, Yun S, Lee S-K (2007) Cellulose smart material: possibility and challenges. J Intell Mater Syst Struct 19:417–422. doi:10.1177/1045389X07083140
46. Tao H, Chieffo LR, Brenckle M et al (2011) Metamaterials on paper as a sensing platform. Adv Mater 23:3197–201. doi:10.1002/adma.201100163
47. Gullapalli H, Vemuru VSM, Kumar A et al (2010) Flexible piezoelectric ZnO-paper nanocomposite strain sensor. Small 6:1641–1646. doi:10.1002/smll.201000254

48. Cheng M-LL, Tsai B-CC, Yang J (2011) Silver nanoparticle-treated filter paper as a highly sensitive surface-enhanced Raman scattering (SERS) substrate for detection of tyrosine in aqueous solution. Anal Chim Acta 708:89–96. doi:10.1016/j.aca.2011.10.013
49. Wang W, Wu W-YY, Zhu J-JJ et al (2010) Tree-shaped paper strip for semiquantitative colorimetric detection of protein with self-calibration. J Chromatogr A 1217:3896–3899. doi:10.1016/j.chroma.2010.04.017
50. Yu J, Ge L, Huang J et al (2011) Microfluidic paper-based chemiluminescence biosensor for simultaneous determination of glucose and uric acid. Lab Chip 11:1286–1291. doi:10.1039/c0lc00524j
51. Yu J, Wang S, Ge L, Ge S (2011) A novel chemiluminescence paper microfluidic biosensor based on enzymatic reaction for uric acid determination. Biosens Bioelectron 26:3284–3289
52. Carrilho E, Martinez AW, Whitesides GM et al (2009) Understanding wax printing: a simple micropatterning process for paper-based microfluidics. Anal Chem 81:7091–7095. doi:10.1021/ac901071p
53. Ge L, Yan J, Song X et al (2012) Three-dimensional paper-based electrochemiluminescence immunodevice for multiplexed measurement of biomarkers and point-of-care testing. Biomaterials 33:1024–1031. doi:10.1016/j.biomaterials.2011.10.065
54. Hardman DJ, Slater JH, Reid AG et al (2003) Biochemical and immunochemical assay device. WO Pat WO/1998/032,018 17:1–17
55. Dungchai W, Chailapakul O, Henry CS (2011) A low-cost, simple, and rapid fabrication method for paper-based microfluidics using wax screen-printing. Analyst 136:77–82. doi:10.1039/c0an00406e
56. Määttänen A, Fors D, Wang S et al (2011) Paper-based planar reaction arrays for printed diagnostics. Sensors Actuators, B Chem 160:1404–1412. doi:10.1016/j.snb.2011.09.086
57. Olkkonen J, Lehtinen K, Erho T (2010) Flexographically printed fluidic structures in paper. Anal Chem 82:10246–10250. doi:10.1021/ac1027066
58. Abe K, Suzuki K, Citterio D (2008) Inkjet-printed microfluidic multianalyte chemical sensing paper. Anal Chem 80:6928–6934. doi:10.1021/ac800604v
59. Balu B, Berry AD, Hess DW, Breedveld V (2009) Patterning of superhydrophobic paper to control the mobility of micro-liter drops for two-dimensional lab-on-paper applications. Lab Chip 9:3066–3075. doi:10.1039/b909868b
60. Hossain SMZ, Brennan JD (2011) beta-Galactosidase-based colorimetric paper sensor for determination of heavy metals. Anal Chem 83:8772–8778. doi:10.1021/ac202290d
61. Li M, Tian J, Al-Tamimi M, Shen W (2012) Paper-based blood typing device that reports patient's blood type "in writing". Angew Chem Int Ed Engl 51:5497–5501. doi:10.1002/anie.201201822
62. Li X, Tian J, Garnier G, Shen W (2010) Fabrication of paper-based microfluidic sensors by printing. Colloids Surf B Biointerfaces 76:564–570. doi:10.1016/j.colsurfb.2009.12.023
63. Li X, Tian J, Shen W (2010) Progress in patterned paper sizing for fabrication of paper-based microfluidic sensors. Cellulose 17:649–659. doi:10.1007/s10570-010-9401-2
64. Lu Y, Lin B, Qin J (2011) Patterned Paper as a Low-Cost, Flexible Substrate for Rapid Prototyping of PDMS Microdevices via "Liquid Molding." Anal Chem 1830–1835. doi:10.1021/ac102577n
65. Liu H, Crooks RM (2012) A Paper-based electrochemical sensing platform with integral battery and electrochromic read-out. Anal Chem 84:1–3. doi:10.1021/ac203457h
66. Tai Y-L, Yang Z-G (2011) Fabrication of paper-based conductive patterns for flexible electronics by direct-writing. J Mater Chem 21:5938. doi:10.1039/c0jm03065a
67. Songjaroen T, Dungchai W, Chailapakul O et al (2012) Blood separation on microfluidic paper-based analytical devices. Lab Chip 12:3392–3398. doi:10.1039/c2lc21299d
68. Arena a., Donato N, Saitta G et al (2010) Flexible ethanol sensors on glossy paper substrates operating at room temperature. Sensors Actuators, B Chem 145:488–494. doi:10.1016/j.snb.2009.12.053

69. Bruzewicz D a, Reches M, Whitesides GM (2008) Low-cost printing of poly (dimethylsiloxane) barriers to define microchannels in paper. Anal Chem 80:1–9. doi:10.1021/ac702605a
70. Song Y, Lundeberg J, Brumer H (2012) Activated paper surfaces for the rapid hybridization of dna through capillary transport. Anal Chem 84:3311–3317
71. Apilux A, Dungchai W, Siangproh W et al (2010) Lab-on-paper with dual electrochemical/colorimetric detection for simultaneous determination of gold and iron. Anal Chem 82:1727–1732. doi:10.1021/ac9022555
72. Ellerbee AK, Phillips ST, Siegel AC et al (2009) Quantifying colorimetric assays in paper-based microfluidic devices by measuring the transmission of light through paper. Anal Chem 81:8447–8452. doi:10.1021/ac901307q
73. Liu H, Crooks RM (2011) Three-dimensional paper microfluidic devices assembled using the principles of origami. J Am Chem Soc 133:17564–17566. doi:10.1021/ja2071779
74. Liu H, Xiang Y, Lu Y, Crooks RM (2012) Aptamer-based origami paper analytical device for electrochemical detection of adenosine. Angew Chem Int Ed Engl 51:6925–6928. doi:10.1002/anie.201202929
75. Vella SJ, Beattie P, Cademartiri R et al (2012) Measuring markers of liver function using a micropatterned paper device designed for blood from a fingerstick. Anal Chem 84:2883–2891. doi:10.1021/ac203434x
76. Schilling KM, Lepore AL, Kurian J a, Martinez AW (2012) Fully enclosed microfluidic paper-based analytical devices. Anal Chem 84:1579–85. doi:10.1021/ac202837s
77. Lu J, Ge S, Ge L et al (2012) Electrochemical DNA sensor based on three-dimensional folding paper device for specific and sensitive point-of-care testing. Electrochim Acta 80:334–341. doi:10.1016/j.electacta.2012.07.024
78. Wang P, Ge L, Yan M et al (2012) Paper-based three-dimensional electrochemical immunodevice based on multi-walled carbon nanotubes functionalized paper for sensitive point-of-care testing. Biosens Bioelectron 32:238–243. doi:10.1016/j.bios.2011.12.021
79. Lee KB (2005) Urine-activated paper batteries for biosystems. J Micromech Microeng 15: S210–S214. doi:10.1088/0960-1317/15/9/S06
80. Apilux A, Siangproh W, Praphairaksit N, Chailapakul O (2012) Simple and rapid colorimetric detection of Hg(II) by a paper-based device using silver nanoplates. Talanta 97:388–394. doi:10.1016/j.talanta.2012.04.050
81. Elder P The (79AD) Natural History, 1601st edn.
82. Crosland M (1978) Gay-Lussac Scientist and Bourgeois. Cambridge University Press
83. Feigl F (1975) Development, present state and prospects of organic spot test analysis. In: Spot Test Org. Anal., 7th edn. Elsevier Scientific Publishing Company, p 1
84. Rocco RM (2006) Landmark papers in clinical chemistry, pp 323–324. In: Landmark Pap. Clin. Chem. Elsevier Science, p 522
85. Morgan ED, Wilson ID (2004) An early description of paper chromatography? Chromatographia 60:135–136. doi:10.1365/s10337-004-0316-7
86. Yagoda H (1937) Applications of confined spot tests in analytical chemistry. Ind Eng Chem Res 9:79–82. doi:10.1021/ac50106a012
87. Muller RH, Clegg DL (1949) Automatic paper chromatography. Anal Chem 21:1123–1125
88. Nobelprize.org The Nobel Prize in Chemistry 1952. In: Nobel Media AB 2014. http://www.nobelprize.org/nobel_prizes/chemistry/laureates/1952/. Accessed 29 May 2015
89. Stock R, Rice CBF (1974) Chromatographic methods, 3rd edn. Chapman and Hall and Science Paperbacks
90. Kunkel HG, Tiselius A, Andersen OS (1951) Electrophoresis of proteins on filter paper. J Gen Physiol 35:1–2
91. Newman JD, Turner APF (2005) Home blood glucose biosensors: a commercial perspective. Biosens Bioelectron 20:2435–2453. doi:10.1016/j.bios.2004.11.012
92. Oliver NS, Toumazou C, Cass a. EG, Johnston DG (2009) Glucose sensors: A review of current and emerging technology. Diabet Med 26:197–210. doi:10.1111/j.1464-5491.2008.02642.x

93. Allen MP, DeLizza A, Ramel U et al (1990) A noninstrumented quantitative test system and its application for determining cholesterol concentration in whole blood. Clin Chem 36:1591–1597
94. Allen MP (1995) Laminated assay device. 15:1–15
95. Martinez AW, Phillips ST, Butte MJ, Whitesides GM (2007) Patterned paper as a platform for inexpensive, low-volume, portable bioassays. Angew Chemie - Int Ed 46:1318–1320. doi:10.1002/anie.200603817
96. Dungchai W, Chailapakul O, Henry CS (2010) Use of multiple colorimetric indicators for paper-based microfluidic devices. Anal Chim Acta 674:227–233. doi:10.1016/j.aca.2010.06.019
97. Parolo C, Medina-Sánchez M, de la Escosura-Muñiz A, Merkoci A (2012) Simple paper architecture modifications lead to enhanced sensitivity in nanoparticle based lateral flow immunoassay. Lab Chip 386–390. doi:10.1039/c2lc41144j
98. Choi S, Lee J-H, Kwak BS et al (2015) Signal amplification in a microfluidic paper-based analytical device (μ-PAD) by confinement of the fluidic flow. BioChip J. doi:10.1007/s13206-015-9204-5
99. Abbas A, Brimer A, Slocik JM et al (2013) Multifunctional analytical platform on a paper strip: Separation, preconcentration, and subattomolar detection. Anal Chem 85:3977–3983. doi:10.1021/ac303567g
100. Martinez AW, Phillips ST, Whitesides GM (2008) Three-dimensional microfluidic devices fabricated in layered paper and tape. Proc Natl Acad Sci USA 105:19606–19611. doi:10.1073/pnas.0810903105
101. Jeong S-G, Lee S-H, Choi C-H et al (2015) Toward instrument-free digital measurements: a three-dimensional microfluidic device fabricated in a single sheet of paper by double-sided printing and lamination. Lab Chip 15:1188–1194. doi:10.1039/C4LC01382D
102. Renault C, Koehne J, Ricco AJ, Crooks RM (2014) Three-dimensional wax patterning of paper fluidic devices. Langmuir 30:7030–7036. doi:10.1021/la501212b
103. Li X, Liu X (2014) Fabrication of three-dimensional microfluidic channels in a single layer of cellulose paper. Microfluid Nanofluidics 1:1–9. doi:10.1007/s10404-014-1340-z
104. Shin JH, Park J, Kim SH, Park J-K (2014) Programmed sample delivery on a pressurized paper. Biomicrofluidics 8:054121. doi:10.1063/1.4899773
105. Giokas DL, Tsogas GZ, Vlessidis AG (2014) Programming fluid transport in paper-based micro fluidic devices using razor-crafted open channels
106. Noh H, Phillips ST (2010) Fluidic timers for time-dependent, point-of-care assays on paper. Anal Chem 82:8071–8078. doi:10.1021/ac1005537
107. Barry L, Tinny L, Elain F et al (2013) Dissolvable fluidic time delays for programming multi-step assays in instrument-free paper diagnostics. Lab Chip
108. Houghtaling J, Liang T, Thiessen G, Fu E (2013) Dissolvable bridges for manipulating fluid volumes in paper networks. Anal Chem 85:11201–11204. doi:10.1021/ac4022677
109. Chen H, Cogswell J, Anagnostopoulos C, Faghri M (2012) A fluidic diode, valves, and a sequential-loading circuit fabricated on layered paper. Lab Chip 12:2909–2913. doi:10.1039/c2lc20970e
110. Li X, Zwanenburg P, Liu X (2013) Magnetic timing valves for fluid control in paper-based microfluidics. Lab Chip 2609–2614. doi:10.1039/c3lc00006k
111. Martinez AW, Phillips ST, Nie Z et al (2010) Programmable diagnostic devices made from paper and tape. Lab Chip 10:2499–2504. doi:10.1039/c0lc00021c
112. Jokerst JC, Emory JM, Henry CS (2012) Advances in microfluidics for environmental analysis. Analyst 137:24. doi:10.1039/c1an15368d
113. Wang X, Chen H, Zhou T et al (2009) Optical colorimetric sensor strip for direct readout glucose measurement. Biosens Bioelectron 24:3702–3705. doi:10.1016/j.bios.2009.05.018
114. Delaney JL, Hogan CF, Tian J, Shen W (2011) Electrogenerated chemiluminescence detection in paper-based microfluidic sensors. Anal Chem 83:1300–1306. doi:10.1021/ac102392t

115. You DJ, Park TS, Yoon JY (2013) Cell-phone-based measurement of TSH using Mie scatter optimized lateral flow assays. Biosens Bioelectron 40:180–185. doi:10.1016/j.bios.2012.07.014
116. Maruo YY, Kunioka T, Akaoka K, Nakamura J (2009) Development and evaluation of ozone detection paper. Sensors Actuators B Chem 135:575–580. doi:10.1016/j.snb.2008.09.016
117. Li C, Vandenberg K, Prabhulkar S et al (2011) Paper based point-of-care testing disc for multiplex whole cell bacteria analysis. Biosens Bioelectron 26:4342–4348. doi:10.1016/j.bios.2011.04.035
118. Erçağ E, Uzer A, Eren S et al (2011) Rapid detection of nitroaromatic and nitramine explosives on chromatographic paper and their reflectometric sensing on PVC tablets. Talanta 85:2226–2232. doi:10.1016/j.talanta.2011.07.080
119. Hossain SMZ, Ozimok C, Sicard C et al (2012) Multiplexed paper test strip for quantitative bacterial detection. Anal Bioanal Chem 403:1567–1576. doi:10.1007/s00216-012-5975-x
120. Dungchai W, Chailapakul O, Henry CS (2009) Electrochemical detection for paper-based microfluidics. Anal Chem 81:5821–5826. doi:10.1021/ac9007573
121. Weaver A, Reiser H, Barstis T et al (2013) Paper analytical devices for fast field screening of beta lactam antibiotics and antituberculosis pharmaceuticals. Anal Chem 85:6453–6460. doi:10.1021/ac400989p
122. Fu E (2014) Equipment-free model of device development. Analyst 00:1–8. doi:10.1039/C4AN01003E
123. Lewis GG, Robbins JS, Phillips ST (2014) A prototype point-of-use assay for measuring heavy metal contamination in water using time as a quantitative readout. Chem Commun (Camb) 50:5352–5354. doi:10.1039/c3cc47698g
124. Nie Z, Deiss F, Liu X et al (2010) Integration of paper-based microfluidic devices with commercial electrochemical readers. Lab Chip 10:3163–3169. doi:10.1039/c0lc00237b
125. Hu C, Bai X, Wang Y et al (2012) Inkjet printing of nanoporous gold electrode arrays on cellulose membranes for high-sensitive paper-like electrochemical oxygen sensors using ionic liquid electrolytes. Anal Chem 84:3745–3750. doi:10.1021/ac3003243
126. Sarfraz J, Tobjörk D, Österbacka R et al (2012) Low-cost hydrogen sulfide gas sensor on paper substrates: fabrication and demonstration. IEEE Sens J 12:1973–1978
127. Lankelma J, Nie Z, Carrilho E, Whitesides GM (2012) Paper-based analytical device for electrochemical flow-injection analysis of glucose in urine. Anal Chem 84:4147–4152
128. Rowe A, Bonham AJ, White RJ et al (2011) Cheapstat: an open-source, "do-it-yourself" potentiostat for analytical and educational applications. PLoS One. doi:10.1371/journal.pone.0023783
129. Sevilla F, Alfonso RL, Andres RT (1993) The electrician's multimeter in the chemistry teaching laboratory: Part 2: Potentiometry and conductimetry. J Chem Educ 70:580. doi:10.1021/ed070p580
130. Zschieschang U, Yamamoto T, Takimiya K et al (2011) Organic electronics on banknotes. Adv Mater 23:654–658. doi:10.1002/adma.201003374
131. Jiang J, Sun J, Dou W et al (2011) In-plane-gate indium-tin-oxide thin-film transistors self-assembled on paper substrates. Appl Phys Lett 98:113507. doi:10.1063/1.3567946
132. Eder F, Klauk H, Halik M et al (2004) Organic electronics on paper. Appl Phys Lett 84:2673–2675. doi:10.1063/1.1690870
133. Kim Y, Moon D, Han J (2004) Organic TFT array on a paper substrate. IEEE Electron Device Lett 25:702–704
134. Lim W, Douglas E, Kim SH et al (2012) High mobility InGaZnO4 thin-film transistors on paper. Appl Phys Lett 94:4–7. doi:10.1063/1.3086394
135. Ferreira I, Brás B, Inácio J et al (2011) Solid-state paper batteries for controlling paper transistors. Electrochim Acta 56:1099–1105. doi:10.1016/j.electacta.2010.10.018
136. Lee KB (2006) Two-step activation of paper batteries for high power generation: design and fabrication of biofluid- and water-activated paper batteries. J Micromech Microeng 16:2312–2317. doi:10.1088/0960-1317/16/11/009

137. Hu L, Wu H, La Mantia F et al (2010) Thin, flexible secondary Li-ion paper batteries. ACS Nano 4:5843–5848. doi:10.1021/nn1018158
138. Yoon D-Y, Kim T-Y, Moon D-G (2010) Flexible top emission organic light-emitting devices using sputter-deposited Ni films on copy paper substrates. Curr Appl Phys 10:e135–e138. doi:10.1016/j.cap.2010.08.025
139. Lamprecht B, Thünauer R, Ostermann M et al (2005) Organic photodiodes on newspaper. Phys Status Solidi 202:R50–R52. doi:10.1002/pssa.200510010
140. Wang F, Chen Z, Xiao L et al (2010) Papery solar cells based on dielectric/metal hybrid transparent cathode. Sol Energy Mater Sol Cells 94:1270–1274. doi:10.1016/j.solmat.2010.03.023
141. Cha SI, Hwang KH, Seo SH, Lee DY (2011) TiO_2 Paper-Inserted sinter-free electrode for dye-sensitized solar cells. Nanosci Nanotechnol Lett 3:295–299. doi:10.1166/nnl.2011.1189
142. Ishida K, Masunaga N, Takahashi R et al (2011) User customizable logic paper (UCLP) with sea-of transmission-gates (SOTG) of 2-V organic CMOS and ink-jet printed interconnects. IEEE J Solid-State Circuits 46:285–292. doi:10.1109/JSSC.2010.2074330
143. Alimenti F, Virili M, Orecchini G et al (2011) A new contactless assembly method for paper substrate antennas and UHF RFID chips. IEEE Trans Microw Theory Tech 59:627–637
144. Siegel AC, Phillips ST, Wiley BJ, Whitesides GM (2009) Thin, lightweight, foldable thermochromic displays on paper. Lab Chip 9:2775–2781. doi:10.1039/b913540p
145. Yoon B, Ham D, Yarimaga O et al (2011) Inkjet printing of conjugated polymer precursors on paper substrates for colorimetric sensing and flexible electrothermochromic display. Adv Mater 23:5492–5497. doi:10.1002/adma.201103471
146. Hennerdal L, Berggren M (2011) Picture-to-picture switching in full-color thermochromic paper displays. Appl Phys Lett. doi:10.1063/1.3656972
147. Kim DY, Steckl AJ (2010) Electrowetting on paper for electronic paper display. Appl Mater Interfaces. doi:10.1021/am100757g
148. Andersson P, Forchheimer R, Tehrani P, Berggren M (2007) Printable all-organic electrochromic active-matrix displays. Adv Funct Mater 17:3074–3082. doi:10.1002/adfm.200601241
149. Kim J, Park SH, Jeong T et al (2010) Paper as a substrate for inorganic powder electroluminescence devices. IEEE Trans Electron Devices 57:1470–1474
150. Thom NK, Yeung K, Pillion MB, Phillips ST (2012) "Fluidic batteries" as low-cost sources of power in paper-based microfluidic devices. Lab Chip 12:1768. doi:10.1039/c2lc40126f

Chapter 2
Analysis of Glucose, Cholesterol and Uric Acid

2.1 Literature Review

2.1.1 Importance of Glucose, Cholesterol and Uric Acid

Glucose is one of the most critical for life compounds found in nature, acting as the primary fuel for glycolysis and being present in pathways of aerobic and anaerobic respiration [1]. Clinically it is used to evaluate diabetes, a metabolic disorder considered to be a major world health problem. In diabetes pancreas does not produce sufficient amounts of insulin, or the insulin produced is not used effectively. World Health Organization estimates that 347 million people worldwide have diabetes with more than 80 % of those living in low- and middle-income countries. It was also estimated that 1.5 million deaths were directly caused by diabetes in 2012, and that it will be the 7th leading cause of death in 2030. Diabetes increases the risk of heart disease and stroke, foot ulcers that together with infection can lead to limb amputation, retinopathy resulting in blindness and kidney failure [2]. Glucose in blood is normally in the range of 3.5–5.3 mmol/Land in urine 0.1–0.8 mmol/L [3].

Uric acid is the primary end product of purine metabolism, with daily production of about 350 mg and additional daily intake of around 300 mg. In most mammals uric acid reacts with uricase degrading to allantoin, which is then excreted from body with urine. A natural antioxidant, uric acid is responsible for up to 60 % of the free radical scavenging activity in human blood. High levels of uric acid are related with diseases such as gout, Lesch-Nyan disease, obesity, diabetes, hypertension, high cholesterol and renal dysfunction. Acute causes of abnormally high levels of uric acid include large alcohol intake, chemotherapy and diet rich in proteins. Prolonged high levels of this compound result in creation of monosodium urate crystals in tissues and areas around the joints. Patients suffer from recurrent flares of severe joint inflammation and are more prone to cardiovascular dysfunctions. Crystals can be naturally dissolved by lowering the serum uric acid level below

E. Witkowska Nery, *Analysis of Samples of Clinical and Alimentary Interest with Paper-based Devices*, Springer Theses, DOI 10.1007/978-3-319-28672-3_2

360 μmol/L [4]. Low concentration of uric acid was noted in cases of multiple sclerosis, Parkinson's disease and Alzheimer [5]. Uric acid in blood is normally in the range of 0.1–0.4 mmol/L and in urine 1.5–4.4 mmol/L [6].

Cholesterol is the most abundant of sterols, synthesized by animals. In vertebrates it is localized predominantly in liver. Cholesterol is almost absent in prokaryotes (e.g. bacteria) and rare in plants, where sterols with different side chains are dominant [7]. In human body, part of cholesterol is synthesized and rest comes from food of animal origin like meat, milk and eggs [8]. Cholesterol present in food can undergo autoxidation during processing and storage, forming metabolites of proved cytotoxicity, apoptotic and pro-inflammatory effects. Autoxidation is caused by contact with oxygen, exposure to sunlight, heating treatment and others. Those toxic derivatives of cholesterol can also be generated in human body through different oxidation mechanisms. Diseases that can be potentially initiated or aggravated include atherosclerosis, neurodegenerative processes and kidney failure [7]. Other diseases associated with abnormal levels of cholesterol include myocardial infarction, coronary heart disease, lipid disorders, liver failure and diabetes [9, 10].

Excess cholesterol present in blood can deposit in arteries and lead to plaque formation (atherosclerosis). A piece of thus formed plaque may break off, forming a blood clot, which in turn may block or decrease the blood flow in the heart, brain or other body part. In the case of severe blockage a heart attack or stroke can occur leading to surgery(bypass surgery, angioplasty, or stent placement), or even premature death [8].

Cholesterol travels through veins in particles called lipoproteins. The most common types are: very low density lipoproteins (VLDL), low-density lipoproteins (LDL), high density lipoproteins (HDL). Elevated levels of LDL cholesterol and reduced levels of HDL result in increased risk of developing blockages in the coronary arteries. Thus—taking men as an example—HDL less than 1.0 and LDL higher than 4.1 mmol/L are considered risk factors of cardiovascular disease (Table 2.1). The most recommended test to access serum cholesterol is the lipid panel or lipid profile in which the total, HDL, LDL cholesterol and fasting triglycerides levels are measured [8].

Table 2.1 Serum cholesterol levels, all data in mmol/L [8]

	Total cholesterol	LDL	Triglycerides		HDL
Normal	<5.2	<2.6	<1.7	Low	1.0 (men) 1.3 (women)
Borderline high	5.2–6.2	3.4–4.1	1.7–2.2	Medium	1.3–1.5
High	≥6.2	≥4.1	≥2.3	High	≥1.5

2.1.2 Methods of Quantification

2.1.2.1 Common Detection Methods

Glucose

Assessing glucose levels is among the most important analytical tasks, with glucose tests forming about 40 % of all blood tests in 2011 [11] and approximately 85 % of the world market of biosensors in 2005 [12].

Glucose is a reducing sugar, and early methods of its quantifications were based on its ability to reduce copper that could later form stable precipitates or colorimetric end-products (Benedict's solution, the Folin–Wu method). Unfortunately those methods could not differentiate glucose from other reducing sugars [1]. Nowadays synthetic boronic acids and glucose-binding proteins such as concanavalin A are used for sensitive and selective, non-enzymatic glucose sensing.

At present most methods utilize enzymes such as glucose oxidase or glucose dehydrogenase. Glucose dehydrogenase uses NAD^+ as a cofactor and produces NADH, is oxygen independent but the cofactors are relatively expensive and unstable [12]. Glucose oxidase (EC 1.1.3.4) is inexpensive and uses oxygen as a co-substrate (Eq. 2.1). Upon returning to its active state it transfers electrons to oxygen producing hydrogen peroxide that can be subsequently detected [12]. Operation range depends on the kind of microorganism from which the enzyme is extracted and most commonly falls between pH 4–7. Enzyme is highly specific to glucose but can be deactivated in solution containing Ag^+ ions, Hg^{2+}, Cu^{2+}. Glucose oxidase is the most common enzyme used in glucose biosensors, with all commercial optical sensors in 2011 relying on this enzyme [11].

$$\beta - D - glucose + H_2O + O_2 \overset{Glucose\ oxidase}{\rightarrow} D - glucono - 1,5 - lactone + H_2O_2 \tag{2.1}$$

$$D - glucono - 1,5 - lactone + H_2O \rightarrow gluconate + H^+ \tag{2.2}$$

In enzymatic optical glucose sensing we can distinguish measurement of the intrinsic UV fluorescence (Tryptophan in GOx and FAD coenzyme) which increases upon addition of glucose due to conformational change. Another group of methods is based on the consumption of oxygen usually utilizing luminescent complexes of ruthenium, platinum or palladium which are strongly quenched by oxygen. Glucose can be assessed also via measurement of changes in pH, with protons produced upon reaction of gluconolactone with water (Eq. 2.2), however the buffer capacity and the initial pH of the sample have to be taken into account. Another possibility is the quantification of hydrogen peroxide formed during the enzymatic reaction [11]. In this case commonly a second enzyme, namely peroxidase (e.g. from horseradish), is used to drive the oxidation of a chromophore. Commercial coupled systems include chromophores such as:

phenol/4-aminoantipyrine, amplex red (10-acetyl-3,7-dihydroxyphenoxazine) and o-dianisidine/sulfuric acid [1].

In the case of electrochemical enzymatic sensing both enzyme families, oxidases and dehydrogenases are widely used for electrooxidation of glucose. They present different redox potentials, cofactors and co-substrates, turnover rates and selectivity to glucose (oxidase is more selective and its cofactor is bound more strongly). Direct electron transfer between cofactor and enzyme is much too slow, and therefore mediators are used. Commercial electrochemical glucometers usually utilize mediators such as ferricyanide, ruthenium hexamine, Os complex, phenantroline or quinone. To prevent leaking of the electroactive components, redox hydrogels can be applied. The most used redox hydrogels directly catalyzing glucose electrooxidation are made from glucose oxidase enzyme and water-soluble polycationic polymers such as poly(4-vinylpyridine), poly(N-vinylimidazole) or poly(acrylamide)-copoly(N-vinylimidazole), with complexes of Os^{2+}/Os^{3+} [13].

Oxygen is being consumed upon the enzymatic reaction, thus it is possible to estimate the glucose concentration by the decrease of oxygen concentration. Oxygen can be monitored with a platinum or indium tin oxide (ITO) electrode [13].

Nevertheless most assays are based on amperometric monitoring of hydrogen peroxide, where peroxide is catalytically electrooxidized (commonly at about 0.6 V vs. SCE) or electroreduced (typically −0.1 V vs. SCE). Hydrogen peroxide can be also used to oxidize peroxidase which is later electroreduced directly or by means of a mediator. Electrooxidation catalysts include: platinum, palladium, nickel cyclam, ruthenium, ruthenium-platinum alloys, iridium dioxide, single-walled carbon nanotubes and polypyrrole functionalized multiwalled-carbon nanotubes. Most common electroreduction catalysts are: platinum, gold nanoparticles distributed in porous silicate; Cu^{2+}, Fe^{2+}; Zn^{2+} and Ce^{3+}-modified silicate xerogels [12, 13].

Other methods of glucose detection include separation by means of: high performance liquid chromatography, capillary zone electrophoresis or gas chromatography and posterior quantification by means of detectors such as: flame ionization, refractive index, nitrogen–phosphorus detector, pulsed amperometry, evaporative light scattering, UV, and fluorescence [1].

State of the art techniques tend to be non-invasive, directly measuring interstitial fluid, sweat or breath, or analyzing impedance of the skin and underlying tissue [12].

Uric Acid

Uric acid can be detected enzymatically, by means similar to mentioned before for glucose. During reaction with uricase (EC 1.7.3.3), uric acid is converted to 5-hydroxyisourate with formation of hydrogen peroxide. 5-hydroxyisourate is later converted to allantoin and carbon dioxide (Eq. 2.3). Hydrogen peroxide can be quantified colorimetrically or electrochemically, with or without the use of peroxidase.

$$uric\ acid + H_2O + O_2 \overset{Uricase}{\rightarrow} 5 - hydroxyisourate + H_2O_2 \rightarrow allantoin + CO_2 \tag{2.3}$$

Optimum pH depends on the microorganism from which the enzyme was extracted, but in general is in the range of 6.5–11. The enzyme has high specificity for uric acid but the reaction can be inhibited by uric acid analogues and compounds chelating copper [14].

Uric acid can be detected also without the use of uricase. In case of optical methods, most common approaches include direct spectrophotometric detection (maximum at 293 nm) [15] and reduction of phosphotungstic acid leading to formation of tungsten blue [16].

This compound can be also quantified electrochemically, but interferences from ascorbic acid, which presents similar oxidation potential at common electrodes (platinum, gold, carbon) have to be taken into account [17]. Other common interferents include dopamine, xanthine and hypoxanthine. Successful detection in the presence of those interferents was already described with gold electrodes modified with thiols, ground electrodes from glassy carbon and pyrolytic graphite [15], carbon paste electrodes electrochemically pretreated [18], with Nafion layer [19], with sodium do-decyl benzene sulfate [20], β-cyclodextrin [21] or cobalt Schiff base composite [22].

Another interesting approach is based on molecularly imprinted polymers. Lakshmi et al. [5] presented this kind of polymer prepared from melamine and chloranil, which after template removal was coated directly onto the surface of a hanging mercury drop electrode, via charge-transfer interactions. Later the same molecularly imprinted polymer was mixed with graphite into a sol-gel matrix, and the resultant composite used to modify the surface of a graphite electrode.

Similarly as with glucose, to avoid problems caused by interferents, uric acid can be at first separated by means of high performance liquid chromatography, gas chromatography or capillary zone electrophoresis and subsequently detected by one of the cited techniques.

Cholesterol

Chemical analysis of cholesterol was typically based on Liebermann-Burchard and Zak reactions. Upon reaction with various strong Bronsted and Lewis acids colored products are formed. Liebermann-Burchard reaction is carried out in acetic acid-sulfuric acid-acetic anhydride medium resulting in blue-green product. Zak reaction is performed in acetic acid-sulfuric acid medium with addition of Fe^{3+} ions, leading to red product. Both methods are unfortunately prone to interference from hemoglobin and bilirubin and use corrosive reagents [23].

Nowadays, serum cholesterol analysis is commonly accomplished using a three-enzyme assay. Since around 70 % of serum cholesterol is esterified, typically serum is first incubated with cholesterol esterase (EC 3.1.1.13) to release free

cholesterol (Eq. 2.4). Cholesterol is then enzymatically oxidized by means of cholesterol oxidase (EC 1.1.3.6) leading to formation of cholest-5-en-3-one and hydrogen peroxide (Eq. 2.5). In typical assay peroxidase enzyme is used to reduce hydrogen peroxide and subsequently oxidize an indicator molecule. Common indicators are 4-aminopyrine with phenol and 2,4,6-tribromo-3-hydroxybenzoic acid but other aforementioned methods of detection of hydrogen peroxide can also be applied [7, 10].

$$cholesterol\ ester + H_2O \overset{Cholesterol\ esterase}{\rightarrow} cholesterol + fatty\ acid \tag{2.4}$$

$$cholesterol + O_2 \overset{Cholesterol\ oxidase}{\rightarrow} cholest - 5 - en - 3 - one + H_2O_2 \tag{2.5}$$

Cholest-5-en-3-one can be also determined directly by spectrophotometric analysis at 240 nm [10].

2.1.2.2 Detection on Paper

Optical

An interesting system for the detection of glucose and uric acid is the above-mentioned platform by Dungchai et al. [6] which uses multiple indicators to achieve enhanced accuracy. With mixtures of 4-aminoantipyrine, 3,5-dichloro-2-hydroxybenzenesulfonic acid, o-dianisidinedihydrochloride, potassium iodide, acid black, and acid yellow it was possible to quantify glucose (0.5–20 mmol/L), lactate (1–25 mmol/L), and uric acid (0.1–7 mmol/L). Another worth mentioning system was constructed as a proof-of-concept device in a single sheet of paper [24]. 4-aminoantipyrine and 3,5-dichloro-2-hydroxy-benzenesulfonic acid were used as indicators. With the use of appropriate oxidase enzymes and horseradish peroxidase it was possible to quantify glucose (4–20 mmol/L), lactate (5–25 mmol/L), and uric acid (3–15 mmol/L) in artificial urine. Recently Fung et al. [25] described an equipment free, ladder-bar, glucose sensor. Three lines of goat anti-mouse IgG–horseradish peroxidase conjugate were deposited along a nitrocellulose strip. Sensing principle was based on different reaction times of successive lines due to the delay in the release of 3,3″,5,5′-tetramethylbenzidine from the reagent pad. Glucose concentration smaller than 5 μmol/L results in one line, 5–100 μmol/L in two lines and higher than 100 μmol/L in three lines.

Also equipment-free but this time distance-based measurement of cholesterol was proposed by Allen et al. [26] already a quarter-century ago. Proposed assay is based on cholesterol esterase, cholesterol oxidase and horseradish peroxidase and a reaction of hydrogen peroxide with dyes (3-methyl-2-benzothiazolinone hydrazine, N,N-dimethylaniline). Buffered solution of peroxidase is used as the wicking solution, which is transported by the wicking pad to sample region where a blood sample is spotted. Cholesterol from the sample reacts with cholesterol esterase and

oxidase from the subsequent pad, and later hydrogen peroxide formed upon this reaction passes to the measurement pad. The measurement pad is uniformly modified with aforementioned dyes. Length of the pad that changes color upon reaction is proportional to the cholesterol concentration in the sample. The same author deposited a patent [27] describing a laminated paper device for cholesterol detection based on similar sensing principle. Additionally authors indicated possible use of detergents such as polyoxyalkylenes, ethoxylatedalkylphenols, octylphenolethylene oxide condensates and polyoxyethylene lauryl ethers, or anionic detergents, such as bile acids. Other examples of uric acid, cholesterol and glucose sensors are resumed in Table 2.2.

Electrochemical

First multianalyte electrochemical system based on paper was presented by Dungchai et al. [3] in 2009. Hydrophilic channels were delimitated by means of photolithography and electrodes screen printed in the test zones. Three electrode system was used, including carbon with Prussian blue working and auxiliary electrodes and Ag/AgCl reference. Each of the three detection zones was modified with one of the following enzymes: glucose oxidase, lactate oxidase or uricase. Analytes in the control serum samples were detected by means of chronoamperometry, with the optimal detection potential for hydrogen peroxide (0 V). Device was capable of quantifying glucose (up to 100 mmol/L), lactate (up to 50 mmol/L), and uric acid (up to 35 mmol/L).

In 2010 Carvalhal et al. [38] described separation and quantification of ascorbic and uric acids. Gold electrodes were deposited on paper or polyester (two systems presented), and the linear range was between 0.05–0.2 mmol/L for uric acid and 0.05–0.4 mmol/L for ascorbic acid.

An interesting system for the detection of glucose was proposed by Liu and Crooks [39]. An integrated metal/air battery supplies power for the electrochemical sensor and electrochromic readout (visual quantification of Prussian blue spot). Prussian blue is reduced to its colorless counterpart prior to the assay. When a glucose sample in artificial urine is injected, urine activates the internal battery, which provides energy for the sensing assay. Paper forms two reservoirs one used by the sensor and other by the Al/air battery and is stacked between two ITO electrodes. Battery consists of an activated carbon cathode, paper reservoir forming a separator and metal foil anode.

Recently several systems applying graphene were also proposed including a wax printed platform comprising of a sample area and four channels leading to four test zones presented by Labroo et al. [40]. In each test zone two silver paste electrodes were interconnected with graphene-ink modified with appropriate enzyme. Device was used for multiplex detection of glucose, lactate, xanthine and cholesterol. Detailed assay procedures such as sample and stock solution preparation methods are not described, thus it is hard to analyze the system in detail. Another electrochemical detection system for cholesterol based on graphene was presented by

Table 2.2 Literature review on colorimetric detection of glucose, uric acid and cholesterol on paper

Analyte	Architecture	Indicator	Enzymes	Linear range	References
Glucose, uric acid	Spot-test	4-amino antipyrine + N-ethyl-N (3-sulfopropyl)-3-methyl-aniline sodium salt (for glucose) and +3,5-dichloro-2-hydroxy acid sodium (for uric acid)	Glucose oxidase, urate oxidase, horseradish peroxidase	0.3–1 mmol/L for both compounds	[28]
Uric acid	Lateral flow assay	3,5,3′,5′-tetramethyl benzidine and positively charged gold nanoparticles	Non mentioned, but detection is based on H_2O_2	0–0.7 mmol/L	[29]
Glucose, lactate, uric acid and cholesterol	Spot test	Graphene oxide@SiO_2@CeO_2 hybrid nanosheets having peroxidase activity and O-phenylenediamine, 2,2′-azinobis(3-ethylbenzothiozoline)-6-sulfonic acid, 3,3′,5,5′-tetramethylbenzidine	Respective oxidase enzymes	At least 0–30 mmol/L for all analytes	[30]
Glucose	Lateral flow assay with self-calibration	4-aminoantipyrine, 2,4,6-tribromo-3-hydroxy benzoic acid	Glucose oxidase, horseradish peroxidase	2.4–11.4 mmol/L	[31]
Glucose	3D wax patterned paper, double sided adhesive tape device with fluidic timer	Diethyl phenylenediamine and 1-chloro-4-naphthol	Glucose oxidase, horseradish peroxidase	0–5 mmol/L	[32]
Glucose, protein, alkaline phosphatase, alanine aminotransferase, and uric acid	Multiple lateral flow assay for demonstration of a new vapor-phase polymer deposition fabrication method	For glucose and uric acid:glucose test based on oxidation of potassium iodide, uric acid on commercially available kit	For glucose and uric acid: glucose oxidase, uricase and horseradish peroxidase	Glucose 0–2.8 mmol/L, uric acid 0–0.8 mmol/L	[33]

(continued)

Table 2.2 (continued)

Analyte	Architecture	Indicator	Enzymes	Linear range	References
Nitrite, albumin, glucose and uric acid	Multiple lateral flow assay for demonstration of a new paraffin stamping fabrication method	For glucose and uric acid:glucose test based on oxidation of potassium iodide and uric acid on the described earlier reagents used by Dungchai et al. [6]	For glucose and uric acid: glucose oxidase, uricase and horseradish peroxidase	Glucose 0–12 mmol/L and uric acid 0–5 mmol/L	[34]
Protein, cholesterol, glucose	Multiple wax printed lateral flow assay, qualitative	Glucose and cholesterol assays based on oxidation of potassium iodide	Glucose oxidase, cholesterol oxidase, horseradish peroxidase	Yes/no response for PBS buffer or 40 mmol/L cholesterol, and 5 mmol/L glucose	[35]
Glucose, nickel, glutathione	Lateral flow assay with barriers delimitated with wax, with distance-based, equipment-free detection	3,3′ diaminobenzidine in peroxidase substrate kit	Glucose oxidase, horseradish peroxidase	7–200 nmol/L	[36]
Glucose	Spot-test, reusable	Ceria nanoparticles	Glucose oxidase	0–100 mmol/L	[37]

Ruecha et al. [41]. System was based on three electrodes: an Ag/AgCl reference, carbon auxiliary electrode and graphene, polyvinylpyrrolidone and polyaniline modified carbon working electrode. After further modification of the working electrode with cholesterol oxidase it was possible to detect cholesterol by means of cyclic voltammetry in the range of 50 μmol/L–10 mmol/L.

Several worth mentioning systems coupled with readers were also described. For example use of a custom-made handheld electrochemical reader that enabled multiple simultaneous measurements [42]. Paper-based device comprises of eight modules, each of them includes a paper channel delimitated with wax and three screen printed carbon electrodes. Test zones were modified with one of the following enzymes: glucose oxidase, lactate oxidase or uricase and an electron-transfer mediator ($K_3[Fe(CN)_6]$). It was possible to quantify glucose (up to 20 mmol/L), lactate (up to 25 mmol/L), and uric acid (up to 10 mmol/L) by means of chronoamperometry. In another approach paper-based devices were adapted to work with commercially available glucometers [43]. Test strips were printed: with wax to obtain hydrophilic channel, with silver ink for wires and contact pads and with carbon ink to acquire four electrodes. Test were carried out for glucose (detection up to 2.8 mmol/L), cholesterol (0.5–5.2 mmol/L), lactate (1–11 mmol/L), and ethanol (up to 3 mmol/L).

Other systems include chemiluminescent detection of glucose and uric acid [44], and fluorescent detection of sodium, potassium, calcium, chloride, pH, glucose, bicarbonate, urea and creatinine using a smart phone-based fluorescence meter [45].

2.1.3 Quantification of Proteins

Enzyme immobilization studies, which will be described later in the text, indirectly led to investigation of protein quantification methods. As some enzyme immobilization methods include washing steps it was necessary to confirm the amount of enzyme present on paper. Without this information it would not be possible to compare the results between different immobilization methods tested. Proteins and the most abundant of them in human body albumin are also important clinical indicators.

2.1.3.1 Clinical Significance of Determination of Protein Levels

Measurement of total protein and albumin content in urine are one the most useful clinical markers for early stages of kidney disease (albumin > 30 mg/L). Increased levels of both total protein and albumin in urine are associated with increased risk of myocardial infarction, stroke, bladder cancer, diabetes, urinary tract infections [46, 47].

Tests for total urinary protein and albumin can be performed in three ways: a semi-quantitative estimation with a dipstick, determination of the protein to

creatinine ratio in a spot of urine and protein excretion using 24-h urine collection. Albumin is a single chain molecule and one of the most abundant proteins in urine, daily excretion is around 10 mg, comparing with daily protein excretion of around 100 mg. Concentration of albumin in urine is about 5000 times lower than in plasma [48].

Standard urine dipsticks (bis (3′,3″-diiodo-4′4″-dihydroxy-5′5″-dinitrophenyl)-3,4,5,6-tetrabromosulfonphthalein dye) usually quantify protein concentrations above 200–300 mg/L. Methods conventionally used in a laboratory to measure urinary albumin include nephelometry, immunoturbidimetry, enzyme-linked immunosorbent assays, radioimmunoassay and high-performance liquid chromatography [47, 48].

Serum total protein and albumin levels decrease in the case of depressed synthesis (end-stage liver disease, intestinal malabsorption syndromes, and protein-calorie malnutrition) or increased losses (nephrotic syndrome and severe burns). The only clinical cause of elevated serum albumin is acute dehydration [48].

Biuret reaction is the most widely applied method of measuring total serum protein. Serum proteins react with copper sulfate in sodium hydroxide forming violet complex. Albumin is usually measured by a dye-binding technique (e.g. bromocresol green, bromophenol blue, 2-(4′-hydroxyazobenzene) benzoic acid, tetrabromophenol blue), later globulin can be evaluated by subtraction of albumin content from the total amount of protein [47, 49]. Other popular tests include Bradford [50] and Lowry methods [51].

2.1.3.2 Detection of Proteins in Paper-Based Devices

Simple, qualitative spot tests for amino acids and proteins have been known for decades, as for example the Ninhydrin test. As already mentioned a range of dipsticks using dye binding techniques is commercially available. Literature review of recent paper-based protein detection platforms includes examples such as the use of tetrabromophenol blue. By means of this device with walls delimitated with photoresist, it was possible to quantify albumin in the range of 25 mg/L–5 g/L [52]. The same methodology but with bromophenol blue was applied in another device, this time cut manually. Tree shaped design included seven channels, which were used to performed simultaneous calibration during the assay. Device was tested in artificial urine and allowed to quantify albumin in the range of 0.08–5 mg/mL [53]. It is worth mentioning that both systems use citric buffer outside its working range (pH 1.8). A commercial assay kit for protein was used to prepare an origami paper-based device, with wax barriers. This platform allowed detection of albumin in human urine in the range 5–20 mg/mL and presented good correlation of the result with a commercial dipstick test [54]. Paper-based system was also constructed to perform electrophoresis, and was successfully applied to separate main proteins (IgG and albumin) in calf serum. Detection was based on direct

measurement of protein fluorescence [55]. Other recently presented systems are designed for IgG detection, and include: use of a chemiresistor [56] as well as potentiometric [57] and electrochemiluminescent [58] detection.

2.1.4 Enzyme Immobilization on Paper

Enzymes are biocatalysts performing and regulating processes in living matter. They are very effective, often display regio- and chemoselectivity, high activity and specificity and operate under mild conditions (physiological pH and temperature) [59].

Researchers often emphasize how properties of paper make it an ideal substrate for sensors for the developing world. It has to be remembered that those resource limited settings often lack proper refrigeration during storage and transport, can suffer from energy loss, lack of supplies etc. Even with so many reports describing new paper-based platforms being published, few of them explore their storage stability.

A large number of paper-based sensors is based, at least to some extent, on enzymatic reactions. Protein immobilization methods are known to increase shelf life of such sensors. In fact properly designed immobilization can be beneficial to almost all enzyme properties, such as activity, specificity, selectivity, reduction of inhibition and aforementioned stability. Stability is dictated by the nature and number of bonds between the enzyme and the support, degree of confinement, immobilization conditions and microenvironment created. Immobilized enzymes can gain new interesting properties, as higher volumetric activity or optimized performance under specific conditions (e.g. organic solvents, alkaline, acidic conditions, elevated temperatures). Other example is the possible reusability: enzyme can be recycled and used again reducing the overall cost. Enzyme attached to a support can form a selective sorbent for protein purification or can be used in systems for controlled release of drugs. On the other hand, poorly designed, immobilization can in some cases lead to decreased stability [60–62].

Immobilization methods can be classified as requiring support and support-free, or according to the nature of linkage, based on adsorption, covalent binding and cross-linking, entrapment and encapsulation.

When supports are necessary they should present high density of reactive groups and good compatibility with the surface of the enzyme. Popular supports include synthetic resins, biopolymers and inorganic polymers (silica, zeolites). Use of porous supports is an interesting approach, which permits good dispersion of enzyme molecules, and reduces possible interactions with the external environment, thus preventing aggregation, autolysis or proteolysis etc. Dry filter paper is able to absorb more than its weight when immersed in a solution. Non-volatile components will be retained in the paper structure after drying. Unmodified cellulose possesses a slightly anionic, hydrophilic surface, which can to some extent interact with tyrosine groups and offers few functional (carboxyl) groups. Fortunately paper usually

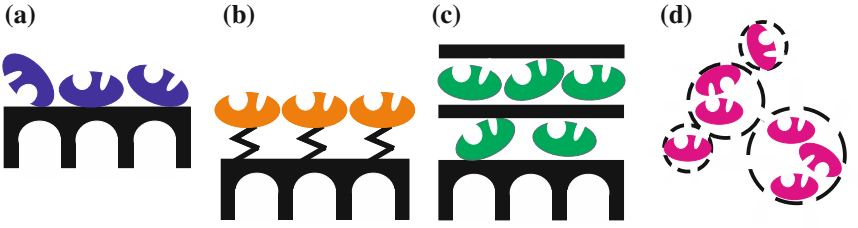

Fig. 2.1 Schematic representation of **a** adsorption, **b** covalent linkage, **c** entrapment, **d** encapsulation

incorporates also hemicellulose, lignin and other additives, therefore providing a wider range of possible reactive centers. Paper can be also chemically treated (i.e. oxidized) or coated with polymers in order to obtain functional groups of interest [60, 63].

Adsorption (Fig. 2.1a) is simple, inexpensive and does not modify the enzyme chemically. Interaction between the support and enzyme will depend on their character. Thereby hydrophobic supports will be more adequate for enzymes with lipophilic surface resulting in van der Waals interactions. Glycosylated enzymes and the ones with hydrophilic amino acid residues on the surface can interact via hydrogen bonds. Unfortunately this type of immobilization can result in subsequent leaching and the distribution of the enzyme in paper matrix is difficult to control. This method is also highly influenced by the reaction/deposition conditions, like pH that will impact the surface charge [61, 64].

Covalent binding (Fig. 2.1b) rigidifies structure of the enzyme. Usually short spacer arms are used between the enzyme and the support. Distorting agents such as heat, extreme pH or organic solvents will not be able to induce a conformational change of the enzyme that could lead to inactivation. As enzyme is tightly fixed problem with leaching is minimal. Covalent immobilization can also induce a favorable orientation of enzyme molecules. Nevertheless chemical modification can lead to denaturation during the immobilization process, and reaction residue can influence subsequent applications. If the enzyme is deactivated, the support, sometimes costly is also rendered useless. Bifunctional cross-linkers, such as glutaraldehyde can be used to produce carrier-free agglomerates of enzyme molecules or to bind enzymes to a support [60, 62, 65].

In the case of entrapment (Fig. 2.1c) enzymes are typically enclosed in a polymer matrix (organic polymer, sol-gel). This type of immobilization prevents direct contact with the environment, diminishing effects of gas bubbles, solvents and mechanical sheer, but can obstruct mass transfer. Sometimes additional covalent attachment is applied to prevent leakage. Layer-by-layer (LbL) assembly, can also be used. In this case support is consecutively exposed to polymer solutions of opposite charge. Adsorption of subsequent layers is achieved by electrostatic interactions and in some cases hydrogen bonds [63, 64].

Encapsulation (Fig. 2.1d) results in similar characteristics to entrapment. It is also possible to immobilize enzymes on colloidal particles that could be later used as a bioactive ink or added to the pulp during the papermaking process. In this case immobilization can be carried independently in an optimized environment [63].

Nowadays, genetically modified enzymes incorporating appropriate binding domains, which adhere spontaneously to cellulose and/or hemicellulose can be used for biochemical coupling with the support. In the case of paper many engineered enzymes with cellulose binding domains are already commercially available, but their price is usually higher [63].

This work will be focused on enzymes from oxidoreductase family, namely glucose oxidase, uricase and cholesterol oxidase. They are all multimeric, and were shown to dissociate under hydrostatic and osmotic pressure, increased temperature and extreme pH. However stabilization was accomplished by means of immobilization (entrapment, covalent linkage, adsorption) [66].

2.1.5 Flow in Paper Matrix

2.1.5.1 Fluid Mechanics in Micro and Nano-Scale

Microfluidic systems manipulate fluids in the amounts of 10^{-9}–10^{-18} L, inside channels with dimensions of few to hundreds of micrometres. In traditional fluid dynamics, the scale of flow greatly exceeds molecular levels, therefore flow is usually considered as continuous and molecular interactions can be neglected or represented just in physical constants such as viscosity. Scaling down of the fluid path leads to a transition regime between continuum and molecule dominated conditions. The basic hypothesis of continuum is no longer applicable. In a molecular size channel, molecules form discrete number of organized layers, resulting in apparent viscosity even 10^5 higher than macro scale values. Viscosity dominates over the forces of inertia resulting in fluid flow characteristic for low Reynolds numbers. Flow in microscale is laminar, thus fluids do not mix convectively. Surface forces like surface tension, van der Waals interaction etc. gain more significance. Heat transport has also a much greater impact and fluid can be driven not only by applied pressure difference but also with the use of electric fields, capillary force and gradients in interfacial tensions. Because of so many differences as compared with the macro scale, the design of a device equipped with channels of micrometer dimensions should be preceded by a thorough analysis of the behavior of the fluid in the system [67–70].

2.1.5.2 Flow in Paper Channel

Standard sheets used in paper-based sensing have thickness between 100–360 μm (Whatman n^{o} 1 Chromatography paper 180 μm, standard copy paper 80 g/m^2

106 μm, Whatman n° 3 Chromatography paper 360 μm). Therefore, microfluidics dictates the laws governing flow in paper networks. Paper is also porous, which means that liquid will be driven inside the matrix by capillary forces. In general, two kinds of flow can be distinguished, one being the wet-out process and the other the fully wetted flow.

In the first case, the fluid front is wicking along a dry, porous matrix, and the flow can be described by the Washburn equation [71]:

$$L^2 = \frac{\gamma D t}{4\mu} \tag{2.6}$$

where, L is the distance moved by the fluid front, D–the average pore diameter, t–time, γ–the effective surface tension and μ equals viscosity. According to the equation the fluid front velocity decreases with time. Movement of the liquid into the paper caused by surface tension is counteracted by the viscous resistance which grows with the increase of the fluid column.

The second kind of flow is the fully wetted case, usually only observed in the electrochemical flow-through sensors. In this type of devices samples travel along a wetted channel towards the wicking pad at the time when flow is already well established. Wicking of this nature can be described by the Darcy's law:

$$Q = -\frac{\kappa W H}{\mu} * \frac{\Delta P}{L} \tag{2.7}$$

where, Q–is the volumetric flow rate, κ–the fluid permeability of paper, WH–area of the channel perpendicular to flow and ΔP/L–the pressure difference along the channel. To analyze flux in a channel of varying width, device can be divided in segments. An analogy can be drawn to Ohm's law for computing current through a circuit of N resistors. ΔP will stand for voltage change, Q act as the fluidic counterpart of current, and $\frac{\mu L_i}{\kappa W_i H_i}$ as the resistance for each segment i. The same analogy can be used for fluidic elements in parallel, but in this case reciprocals of resistances add. Based on abovementioned equation, one can predict that all strips of constant width will have the same transport time if their length is equal. In contrast to the wetting process, velocity is constant in a constant-width fully wetted strip [72]. Even small changes in the architecture of the channel can significantly enhance performance of the sensors. Well planned device architecture can allow sequential delivery of reagents, achievement of desired reaction or incubation time and many others.

2.1.5.3 Computer Modeling

Numerical simulations of microfluidic devices could reduce the time from concept to prototype, helping to optimize the device. Task of architecture optimization is becoming increasing complex, and difficult to achieve experimentally especially

when counterintuitive effects have to be taken into account. Well-designed simulation could estimate performance of the system or help to explain and visualize experimental phenomena. Numerical techniques can be applied to study fundamental microfluidic problems as mixing, dispersion, controlled reagent delivery but also magnetic, magneto-rheological or acoustic phenomena. Transport of species including manipulation, sorting and storing, even chemical reactions and thermal analysis can all be simulated computationally.

Computer modeling is often based on discretization of differential equations, and can be classified by the method used for discretization as finite difference, finite element, finite volume, and boundary element methods. Some of the commercially available codes include Coventor, CFD ACE+, FLUENT and COMSOL Multiphysics. COMSOL provides a library of predefined models, including a Microelectromechanical Systems package, models for flow in porous media and many others. One model can incorporate different physical phenomena, for example fluid dynamics and mass transfer. Basically after problem formulation and choosing of the desired model, user has to define geometry, specify boundary conditions, apply material properties and select the desired mesh type. Incomplete mathematical description, too simplified model and numerical errors can lead to inaccurate results [73–77].

2.2 Materials and Methods

2.2.1 Reagents and Materials

Glucose Oxidase from *Aspergillusniger* 18.5 U/mg (Sigma Aldrich), Uricase 0880 4.6 U/mg (Sigma Aldrich), Cholesterol Oxidase from *Streptomyces sp.* 20 U/mg (Sigma Aldrich), soluble starch from companies Merck, Altair, Vetec, potassium iodide from Merck and Fisher, bovine serum albumin (Sigma Aldrich), Bradford reagent (Sigma Aldrich B6916-500ML), Folin-Ciocalteu (Sigma Aldrich F9252), Alginic acid Sodium salt from brown algae (Fluka 71238), Carboxymethyl cellulose 40 000, Whatman™ 3 Chr Paper, Whatman™ 1 Chr Paper, Whatman™ 20 Chr Paper, greaseproof Paper (Schoellershammer);

2.2.2 Equipment

CO_2 Laser cutter Gravograph LS 100, Ultraspec 2000 UV/VIS spectrophotometer, Pharmacia Biotech, Agilent Cary 500 spectrophotometer, MetrohmAutolab Potentiostat;

2.2.3 Substrate

As it was already mentioned different types of paper can substantially differ in chemical composition, structure etc. Therefore the following chapter will shortly describe the main types of substrate used in this work.

2.2.3.1 Types of Paper

Whatman™ Grade 1 Chr Cellulose Chromatography Paper-made from pure cellulose with no additives of any kind, 0.18 mm thick, with smooth finish. Linear flow rate for water equal 13 cm/30 min. High wet strength [78]. Relatively high absorbency 11 μL/cm^2 [79].

Whatman™ 3 Chr Chromatography Paper-made from pure cellulose with no additives of any kind, 0.36 mm thick, with smooth surface. Linear flow rate for water equal 13 cm/30 min. One of the most resistant chromatography papers, considering wet strength [78].

Standard copy paper-grammage of 80 g/m^2. Usually obtained after mechanical pulping. Made from bleached cellulose, with noticeable amount of alkyl ketene dimer (∼10 %) and fillers such as $CaCO_3$ (few%). Untreated paper is slightly hydrophobic with contact angle of 115^o [80, 81]. Thickness around 0.10 mm, with large fibers (diameter ∼ 20 μm) and low surface roughness (peak to valley ∼ 10 μm). Lacks microsized holes and presents sufficient wet strength to pass through a wet process [82].

Tracing paper-greaseproof Paper Schoellershammer–grammage of 90/95 g/m^2. Homogeneous surface with constant medium grammage, highly transparent, with long fibers and very low porosity. Chemically treated, usually by immersion in sulfuric acid which attacks the surface of fibers, forming an amyloid similar to starch. This amyloid fills areas between fibers resulting in enhanced impermeability to fats and water, higher tear strength and transparency [83, 84].

2.2.3.2 Analysis of Paper Surface

Paper surface was observed through an optical microscope (AmScope company) connected to a computer. Photographs of the surface at various magnifications (×4, ×10, ×40) were taken by means of AmScope software.

2.2.4 *Analysis of Glucose, Cholesterol and Uric Acid*

2.2.4.1 Optical Detection

Fabrication of Prototype Devices

Prototype devices were produced by wax printing described earlier by Carrilho et al. [85]. Basically, Whatman™ Grade 1 Chr was cut in A4 (210 mm × 297 mm) sheets and the desired pattern printed with a XEROX Phaser printer with a solid ink containing wax. Printed paper was later placed on a hot plate set at 110 °C for around 2 min. After cooling, and cutting out of the individual systems, devices were ready to use.

All devices prepared for preliminary tests were composed of a round sampling area with three channels leading to three detection zones situated around the sampling zone (Fig. 2.2). Size of each unit varied, sampling and detection zones: 4–6 mm, channels: 5–10 mm length, 3–4 mm width. Size of the base was equal 4 × 4 cm with 0.5 cm wings, which after bending act as supports. Real size of a finished internal wax pattern is slightly smaller due to lateral spreading of wax upon heating.

Choice of Colorimetric Method

Colorimetric assays proposed in this study are based on enzymatic reaction of an oxidase enzyme with its substrate (glucose, uric acid or cholesterol) to produce hydrogen peroxide. Hydrogen peroxide is later detected directly without the use of a peroxidase enzyme, in order to simplify the system and reduce the cost of the assay. Chosen method should provide rapid results, function in the pH range optimal for the enzyme, not inhibit the enzymatic reaction and allow storage for considerable amount of time.

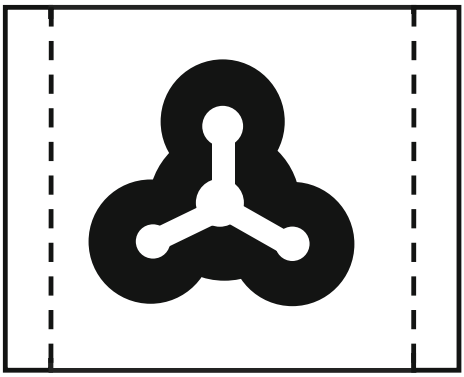

Fig. 2.2 Design of a sample device used during preliminary experiments

All subsequent tests were carried out first with hydrogen peroxide and later with glucose oxidase and glucose. Glucose oxidase is the least expensive, and least demanding in terms of pH, temperature and storage conditions of the three proposed enzymes.

Ferric Thiocyanate Assay-hydrogen peroxide generated upon enzymatic reaction reacts with Fe^{2+} to form Fe^{3+} ions. Ferric ion can be then monitored as a red thiocyanate complex (λ_{max} = 500 nm) [86]. Assay conditions: 5 mmol/L $FeSO_4$, 100 mmol/L KSCN in HEPES buffer (pH = 6.5);

Copper(II) ion and 2,9-dimethyl-1,10-phenanthroline method (DMP)-after reduction of Cu^{2+} by hydrogen peroxide, Cu^{+} forms a yellow colored complex (λ_{max} = 454 nm) with 2,9-dimethyl-1,10-phenanthroline. Method is not affected by reaction time and complex is stable under light. pH working range 5–9 [87]. Assay conditions: $CuSO_4 \cdot 5H_2O$ 10 mmol/L in 0.2 mmol/L PBS buffer, 2,9-dimethyl-1,10-phenanthroline 50 mmol/L in ethanol;

Iron(II) ion and 2,6-Bis(hydroxymethyl)-4-methylphenol method-hydrogen peroxide oxidizes Fe^{2+} to form Fe^{3+} ions. Ferric ion can be then monitored with 2,6-Bis(hydroxymethyl)-4-methylphenol. Assay conditions: 2,6-Bis(hydroxymethyl)-4-methylphenol 150 mmol/L in ethanol, $FeSO_4$ 10 mmol/L; pH working range of the assay is around 2, therefore it was not possible to detect hydrogen peroxide formed after enzymatic reaction of glucose. Paper-based devices in which enzymatic and colorimetric reactions are carried out in separate zones were prepared. Glucose first undergoes enzymatic reaction and later hydrogen peroxide is transported to a detection zone modified with the colorimetric reagent. Channel separating both areas was modified with small amounts of diluted acid (H_2SO_4 or H_3PO_4) to lower the pH to a range necessary for the colorimetric assay. In order to optimize the amount of acid, devices were impregnated with indicators that change color in the desired range (thymol blue: transition in pH 1.2–2.8, malachite green: transition in pH 0.2–1.8) or cut from pH indicator paper.

Starch-iodide method-hydrogen peroxide generated upon enzymatic reaction reacts with iodide ions to form iodine. In the next step iodine reacts reversibly with iodide ion yielding triiodide which can further react with iodine to form pentaiodide. Triiodide and pentaiodide are linear and can enter inside the amylose helix of starch. Charge transfer between starch and iodide, results in a change in coloration from colorless to blue-black (λ_{max} = 660 nm). Molybdenum ions were shown to enhance the reaction rate in the absence of peroxidase [88]. Assay conditions: KI 3 mmol/L, Na_2MoO_4 2.5 mmol/L, starch 10 mg/ml dissolved by gentle heating

Methylene blue-first methylene blue is reduced to colorless leucomethylene blue, for example by means of sodium thiosulfate. Later hydrogen peroxide can be used to oxidize it back to color methylene blue (λ_{max} = 660 nm). Different catalysts can be used, i.e. alumina supported metals [89, 90]. Different reaction conditions tested, varying concentrations of reagents, pH, with use of $KAl(SO_4)_2$ or in 1 mol/L NaOH/NaCl.

Differences in Hue and Repeatability of Digitalization

Preliminary tests were digitalized by means of a scanner and image analyzed in Corel Photo-paint ×5 using a histogram tool. Color was analyzed in RGB, CMYK and gray scale considering total signal for all the channels and each channel separately. In each case intensity of a blank area of the same size (number of pixels) and from the same device was subtracted from the mean intensity for the detection area. Maximum intensity was obtained for channels Magenta, Cyan and CMYK.

Differences in hue were observed during the preliminary experiments. It was also noted that the time during which scanner illuminates the samples is different for each digitalization.

To evaluate repeatability of quantification using a scanner, devices on which a glucose assay was carried out were scanned repeatedly 8 times and image analyzed in Corel Photo-paint ×5.

To address the hue issue different formulations of the starch-iodide reagent were prepared using combinations of potassium iodide (Merck, Fisher) and starch (Merck–two different batches, Altair, Vetec) from different brands. Those reagents were used to prepare spot-tests for preliminary assays with cholesterol and cholesterol oxidase. Two samples for each concentration (0–10 mmol/L) of cholesterol were prepared for each of the 8 formulations of reagents.

Solving the Autoxidation Problem

The starch-iodide method was chosen as the colorimetric assay, therefore attempts were made to solve the autoxidation problem. After around 30 min from spotting on paper, test zones changed color from colorless to brown (iodine ions). Subsequent approaches were tested:

- Optimization of pH
  Tests in PBS buffer of different pH (range 5–8, 3 replicates) were carried out, with 0.3 % hydrogen peroxide. Hydrogen peroxide was used as model analyte to avoid contributions related to different activity of glucose oxidase caused by pH change.
- Layer of liquid polymer (ethylene glycol, poly(vinyl alcohol)) on top of the detection zone modified with starch-iodide reagent;
- Protective cover cut from
  - adhesive tape (different brands and types used: Koretech, Adere–Tape Fix, Scotch);
  - transparent film with and without adhesive (Parafilm, food wrap, Tilibra book cover foil, Contact Vulcan adhesive foil);
  - lamination;

  protective layer covered both sides of paper leaving only sampling area bare.

New Fabrication Methods for Analysis of Cholesterol

Cholesterol is insoluble in water, thus stock solutions was prepared with the use of a surfactant, Triton X-100 [91]. Stock solutions with even minimal amounts of surfactant were not contained in paper channels delimitated with wax, and would spread freely in the paper matrix regardless the wax pattern. It was also not possible to observe a color change for the enzymatic spot tests which can indicate enzyme inactivation or most probably disturbed interaction between tri- and pentaiodide ions and starch. In subsequent tests ethanol was used to prepare stock solutions of cholesterol. Other methods used to dissolve cholesterol found in the literature include use of ether [92], hexane, chloroform [93], isopropanol [94] and liposomes [95].

Even without the use of a surfactant, cholesterol solution would pass through wax barriers, spreading evenly through paper, thus it became necessary to develop a new fabrication method, compatible with this kind of sample. New device could be cut from paper, or use a polymer that would physically shut paper pores.

In the case of polymers, solutions of different concentrations were prepared and used to draw simple structures on paper. Polymers tested include: polidimetoxysilane (PDMS), chitosan, polystyrene, polyvinyl chloride (PVC) and commercial waterproofing agents (NP Nanopool®, Germany and Waterproof spray by Sistem, Brazil). Details of polymer preparation are resumed in Table 2.3. Polymers were applied manually but in the future could be dispensed by an inkjet printer or used to fill simple gel or fountain pens. Test solutions included water, vegetable oil, as well as stock solutions of cholesterol in ethanol or Triton X-100.

Tests were performed also with paper without any delimitation, paper cut manually with scissors or paper punch, as well as a laser cutter. Depending on the type of paper and feature type (straight or curved lines) power of the laser cutter was adjusted to 5–12 % and velocity to 85–100 %. Pieces of paper could be suspended, or glued on top of a transparent film with adhesive.

Immobilization of the Colorimetric Reagent for Enhanced Uniformity of Color Development of Uric Acid Assay

Uric acid is poorly soluble in water, methods of dissolution found in the literature include use of buffers such as PBS [96], acetate, Tris-HCl [97], borate [98], additives of $LiCO_3$ or Na_2CO_3 [99], or dissolution in concentrated NaOH [100] with subsequent dilution with buffer. It was possible to prepare stock solution of desired concentration (10 mmol/L) only in NaOH or by addition of carbonates. During experiments uric acid was solubilized with addition of small amounts of K_2CO_3.

Using simple wax printed devices presented for glucose tests (Fig. 2.2) it was possible to distinguish only light coloration around the detection area, which could indicate that the starch-iodide reagent is being carried with the uric acid sample. After the experiment 3.0 % hydrogen peroxide was spotted on the detection zone

Table 2.3 Review of polymers applied to form barriers impermeable to cholesterol-methodology

Polymer	Preparation
Chitosan	Fibers: Chitosan fibers were pressed on top of paper channel delimitated with wax. Acetate buffer (pH- = 2.3) was passed through the channel for 15–20 min Powder: different quantities of chitosan powder were dissolved in acetate buffer. Several layers of polymer were deposited in case of more diluted solutions
PDMS	PDMS solution 5:1 (elastomer base: curing agent) was prepared and diluted with different solvents (toluene, isopropanol, hexane) to obtain a range of concentrations. After patterning with polymer, paper was dried in ambient temperature or in an oven set at 120 °C
PVC	PVC was dissolved in tetrahydrofuran obtaining a set of concentrations. Several layers of polymer were deposited in case of more diluted solutions.
Polystyrene	Polystyrene was dissolved in toluene and heated. Concentrated stock solution was dissolved to obtain set of concentrations
Commercial waterproofing agents	NP Nanopool®: Whatman n° 1 sheet was sent to NP Nanopool® (Germany) for modification. Channels were designed with nanostructured waterproofing product and sent back to Brazil. Unfortunately due to several issues with Brazilian post service sample was delivered completely soaked with rainwater. After drying channels were filled with the test solutions Waterproof spray by Sistem: First parts of a paper slip were covered with masking tape and sprayed with the waterproofing agent to create channels. Promising results led to fabrication of more advanced structures cut by means of laser cutter with supporting channels filled with the waterproofing spray

and strong black-blue coloration was only visible in the vicinity of the border. This effect was not seen during experiments with glucose and cholesterol. Usually mean intensity of pixels of a given area is used for quantification in a graphic program. If a great part of the detection area remains discolored it will influence the results, lowering sensitivity. Because of this reason different pretreatments were applied to immobilize the indicator in the detection zone. Some attempts to provide more uniform coloration were already described in the literature and include use of polyvinyl amine [101], gelatin [102], poly(acrylic acid) and polyethylene glycol [103].

During this work tests were carried out with gelatin, poly(acrylic) acid and poly [di(ethylene glycol)]. First paper strips were modified with one of the aforementioned reagents at different concentrations. After drying, the starch-iodide solution was deposited, and in sequence glucose oxidase (1 mg/mL) and glucose (10 mmol/L). More systematic tests were performed with gelatin.

Gelatin was dissolved by heating in PBS buffer pH = 6.5 to obtain a set of concentrations: 5, 10, 15, 20, 25 mg/mL. Two types of tests were performed a lateral flow assay and a spot test, both with gelatin deposited with one of the following manners:

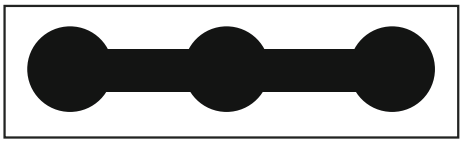

Fig. 2.3 Laser cut assay for layer-by-layer tests

a. starch-iodide reagent deposited and left to dry, subsequently modified with gelatin solution, test stored for 24 h in 4 °C;
b. starch-iodide reagent mixed with gelatin, test stored for 24 h in 4 °C
c. gelatin layer deposited and stored for 24 h in 4 °C, subsequently test area modified with starch-iodide reagent;

Test were stored for 24 h in 4 °C after deposition of gelatin to ensure uniform modification and drying of the polymer. Three samples of each test type were prepared (6 types) for all 5 concentrations, plus a test without gelatin. In the case of the lateral flow assay enzyme was deposited before the modified zone, and glucose sample was spotted in the beginning of the channel. After drying bottom of the paper slip was submersed in PBS buffer that would carry glucose to the enzymatic zone and later hydrogen peroxide to the detection area. In the spot test all the reagents were added on top of the starch-iodide modified area. To document the results photos were taken after 0, 2, 5, 10 and 20 min from starting of the test.

In the next step tests were carried out with uric acid and uricase. Tests included optimized assay with gelatin (10 mg/mL for lateral flow assay, gelatin on top of starch-iodide reagent) and a layer-by-layer approach. Test were performed in laser cut suspended devices shown in Fig. 2.3. Three types of assay were proposed, with zone A always serving as sampling area:

i. area B: LbL alginate/UOx-chitosan, 2 bilayers alginate 1 mg/mL, pH = 8.5, chitosan 0.5 mg/mL, pH = 7.5; area C:starch-iodide reagent under gelatin10 mg/mL;
ii. area B: LbL alginate-UOx, 2 bilayers alginate 1 mg/mL, UOx in borate buffer pH = 8.0; area C:starch-iodide reagent under gelatin10 mg/mL;
iii. area B: starch-iodide reagent under LbL alginate-UOx, 2 bilayers alginate 1 mg/mL, UOx in borate buffer pH = 8.0; area C: without modification;

4 tests of each type were prepared and 10 mmol/L uric acid was used in all cases.

Calibration Curves

Several attempts were made to perform lateral flow assays for uric acid and cholesterol. Some of the approaches are resumed in Fig. 2.4. Device visible in Fig. 2.4a was cut with laser leaving small uncut areas on the sides of channels (marked with arrows). Vicinity of the uncut area was modified with waterproofing

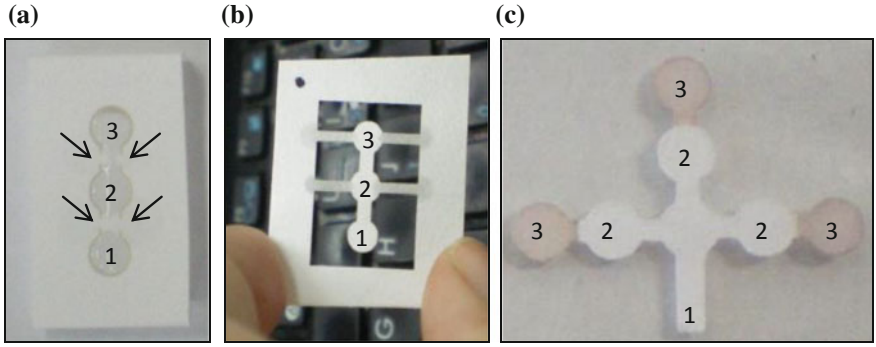

Fig. 2.4 Some devices used for uric acid and cholesterol assays. **a** Laser cut suspended. **b** Laser cut, suspended with long supporting channels. **c** Laser cut, on a layer of adhesive foil. *1*. sampling area, *2*. enzymatic area, *3*. detection area

agent. Due to small space dividing the assay area from the support, in some cases leaks would appear. Therefore another device was proposed (Fig. 2.4b) in which longer supporting channels filled with waterproofing agent would hold the device.

Third example shown on Fig. 2.4c is a laser cut assay, this time in physical contact with a support. Flux, observed in this case will be slightly different because of the interface formed between paper and an adhesive foil. Unfortunately it was not possible to obtain color change for lateral flow cholesterol assay. This compound could be only detected in spot tests. Probably cholesterol is too strongly retained in the paper matrix. All tests for uric acid resulted in uneven coloration around the detection zone. Because of this also uric acid was quantified in a spot test. In order to perform the tests, circles (diameter 5 mm) were cut by means of a laser cutter from Whatman n^{o} 1 chromatographic paper and glued on top of a transparent foil with an adhesive. For the lateral flow glucose assay device shown Fig. 2.4b was used, with 4 mm diameter sample, enzymatic and detection zones, and 2 mm × 2.2 mm channels.

Uric acid assay:

Spot test modified with 2 μL of starch-iodide reagent,
after drying, with 2 μL of 15 mg/mL gelatin solution,
after 24 h, with 2 μL uricase solution 18.4 U/mL,
all solutions prepared in 0.2 mmol/L PBS buffer pH = 8.0;
2 μL of sample solution was used to run the assay.

Cholesterol assay:

Spot test modified with 2 μL of starch-iodide reagent,
after drying, with 2 μL cholesterol oxidase solution 20 U/mL,
all solutions prepared in 0.2 mmol/L PBS buffer pH = 7.0;
2 μL of sample solution was used to run the assay.

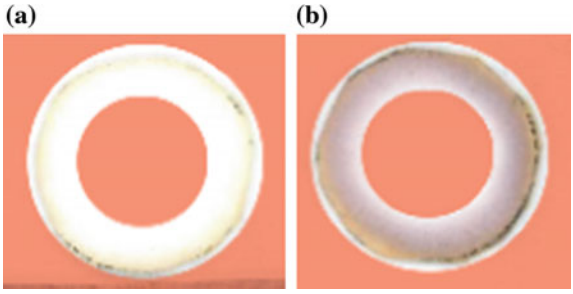

Fig. 2.5 Masking method used, for quantification of uric acid, **a** 0 mmol/L, **b** 5 mmol/L, masked area marked in *pink*

Glucose assay:

Enzymatic zone modified with 2 μL of glucose oxidase solution 18 U/mL,
Detection zone modified with 2 μL of starch-iodide reagent,
all solutions prepared in 0.2 mmol/L PBS buffer pH = 6.5.
8 μL of sample solution was used to run the assay.

Corel Photopaint ×5 was used for quantification. In the case of uric acid double mask was used (Fig. 2.5) to overcome the impact of discolored middle area.

Tangential Flow Devices

As an attempt to integrate all three assays in one device, a tangential flow system was proposed. Devices of this type, known also as 3D pads (three dimensional paper-based analytical devices), or opads (origami paper-based analytical devices) are usually assembled from several layers of paper. In this case to allow quantification of cholesterol, each paper layer was enclosed in a transparent adhesive foil. Layers were stacked together and clamped with a large paper clip. Both, paper and plastic foil were cut by means of a laser cutter. Each layer included a paper frame to stiffen the construction, and to obtain more constant thickness along the layer. Several variations of this device (Fig. 2.6) were proposed including:

a. 1st sampling layer (varying size and format),
   2nd four compartment enzymatic layer (with or without immobilization),
   3rd four compartment detection layer (with or without gelatin layer) (Fig. 2.6a);
b. as above but with an intermediate distributing layer between layers 1 and 2 (Fig. 2.6b);
c. as above but with an acrylate holder;

Device comprised of 4 detection zones, 1 for each analyte and 1 serving as a control. Sampling area could be in the future modified with agglutination antibodies, or cut from a plasma separation membrane (e.g. Vivid™ Plasma Separation Membrane, thickness 330 μm, material: asymmetric polysulfone). Layers are only stacked, thus it is possible to dismantle the device for quantification. Concentration of the reagents was equal as in the previous experiments destined to construct the

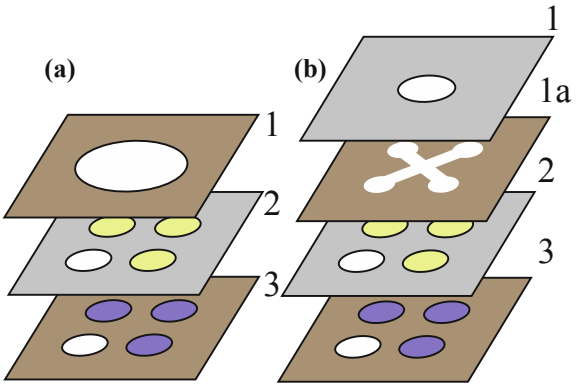

Fig. 2.6 Tangential flow device. **a** Without distribution layer, **b** with distribution layer. *1*. sampling area, *1a*. distribution layer, *2*. enzymatic zone, *3*. detection zone

calibration curves. To perform the test, 2–8 μL of the sample were spotted on the sampling area and subsequently 5–20 μL of water or buffer was added.

2.2.4.2 Methods of Enzyme Immobilization on Paper

Protein Quantification Methods

Next chapter will resume enzyme immobilization studies performed to prolong shelf life of proposed paper-based devices. In the case of some immobilization methods (encapsulation and methods that require washing steps) the final concentration of enzyme in the sample is not known. Therefore in order to compare activity of those samples it is necessary to quantify the amount of protein present. Several methods were tested, including the Bradford method [50], the Lowry method [51] with and without the use of surfactant, use of dyes such as bromocresol green [104] and bromophenol blue [47] as well as direct quantification (measurement of absorbance in the range of 200, 260–280 nm) [105].

Tests were performed:

a. in solution—to ensure correctness of execution;
b. on slips of unmodified paper—to guarantee that the lack of result is not caused by the absorption of reagents in the wax barrier;
c. on 1 × 1 cm devices with wax barriers—to guarantee that the lack of result is not caused by flow of reagents with subsequent additions. Two devices were used, one with a circular area of 3 mm and another in form of a square 1 × 1 cm (Fig. 2.7). Square device was used for the subsequent immobilization studies. Results obtained for those two tests did not present any significant differences, thus only protocols for the 1 × 1 device will be described in detail. To guarantee correctness of execution, samples of the enzyme immobilization study were encoded, and analyzed in random order. Serial number can be seen on the photograph presented in Fig. 2.7.

Fig. 2.7 Sample devices used for immobilization tests, to guarantee correctness of execution, all samples were encoded (*number* seen on the border)

Some of the methods of protein quantification are based on interaction with specific amino acids, thus they can be applicable only to certain proteins. For this reason BSA (bovine serum albumin) was used as a model protein, and GOx (glucose oxidase) as model enzyme, both in concentration between 10 and 40 mg/mL. Distilled water was used as control. In the case of spectrophotometric analysis Ultraspec 2000 UV/VIS spectrophotometer, Pharmacia Biotech, was used for all tests in solution (water or buffer solution used as blank) and Agilent Cary 500 spectrophotometer for tests on paper (Teflon used as blank).

Bromocresol green (BCG)

Based on the interaction between the indicator and proteins accompanied by a change in coloration to blue-green. In the case of this method several different protocols were found in the literature, thus preliminary tests were carried out using succinic acid buffer pH = 4.3, with or without the addition of sodium azide 4 mmol/L and with different dye concentrations (0.5–5.5 mmol/L). For the paper-based tests maximum concentration of the dye without the use of sodium azide was used.

Test in solution 100 μL succinic acid buffer pH 4.3 + 100 μL of BCG 5.5 mmol/L + 50 μL of sample or control;

Test on paper 10 μL succinic acid buffer pH 4.3 + 10 μL of BCG 5.5 mmol/L + 10 μL of sample or control;

Bromophenol blue (BPB)

Based on interaction between the indicator and proteins accompanied by a change in coloration to blue. Preliminary tests for the bromophenol blue method included samples of the dye dissolved only in ethanol, and ethanol with subsequent dilution 1:1 with buffer solutions (acetate buffer pH = 2.3; citrate buffer pH = 3.2;

succinic acid buffer pH = 4.3). Citrate buffer was chosen for the subsequent analysis.

Test in solution 100 μL citrate buffer pH 3.2 + 100 μL of BPB + 50 μL of sample or control;

Test on paper 10 μL citrate buffer pH 3.2 + 10 μL of BPB + 10 μL of sample or control;

Subsequently calibrations curves for tests in solution were constructed for both compounds (0.3–20 mg/mL), 3 replicates were prepared for each concentration. During tests on paper it was noted that the time between application of the indicator solution and the sample has a significant impact on the observed result. Also the order in which reagents were applied on paper had a major impact. In the case when the protein is spotted first (Fig. 2.8a) resulting coloration is uneven, with more intense color appearing in the place of spotting. When BPB was spotted first, color was even on the whole modified area (Fig. 2.8b). To obtain the same result with paper already containing protein, several deposition methods were tested with best results obtained with spraying (Fig. 2.8c).

Lowry method

Copper(II) forms a complex with peptide bonds under alkaline conditions, and in result is reduced to Copper(I). Monovalent copper in turn reacts with Folin-Ciocalteu reagent. Color changes from colorless (Lowry reagent) and yellow (Folin-Ciocalteu reagent) to blue (dark blue in the case of the modified assay).

Two versions of this assay were tested:

Lowry method

Reagent A 40 mg $CuSO_4$, 2 g K_2CO_3, 20 mg sodium potassium tartrate, 20 mL H_2O

Reagent B 80 mg NaOH, 2 mL H_2O

Lowry reagent 3 parts of A + 1 part of B

Test in solution 100 μL of sample or control + 100 μL of the Lowry reagent (10 min) + 25 μL of Folin-Ciocalteu reagent;

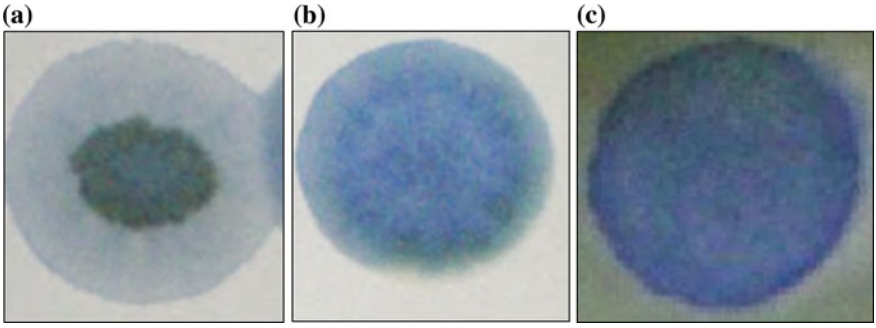

Fig. 2.8 BPB assays depending on the order of deposition **a** BSA + BPB, **b** BPB + BSA, **c** BSA + BPB Spray

Test on paper	10 μL of sample or control + 10 μL of the Lowry reagent (10 min) + 10 μL of Folin-Ciocalteu reagent;

Modified Lowry method (with surfactant)

Reagent A	40 mg $CuSO_4$, 2 g K_2CO_3, 20 mg sodium potassium tartrate, 20 mL H_2O
Reagent B	20 mg sodium dodecyl sulfate, 2 mL H_2O
Reagent C	80 mg NaOH, 2 mL H_2O
Lowry reagent	3 parts of A + 1 part of B + 1 part of C
Test in solution	100 μL of sample or control + 100 μL of the Lowry reagent (10 min.) + 25 μL of Folin-Ciocalteu reagent;
Test on paper	10 μL of sample or control + 10 μL of the Lowry reagent (10 min) + 10 μL of Folin-Ciocalteu reagent;

Bradford method

Method listed in Brazilian Pharmacopeia. It is based on the fact that proteins upon binding displace the absorption maximum of acidic solution of Coomassie Brilliant Blue G-250 from 465 to 595 nm (color change from brown to blue).

Test in solution: 100 μL of sample or control + 400 μL of Bradford reagent;

Test on paper: 10 μL of sample or control + 10 μL of Bradford reagent;

Paper pretreatment protocol: methanol 5 min, methanol/NH_4OH 5 mol/L(1:1) 10 min, methanol 2 min, methanol/CH_3COOH glacial (1:1) 10 min, rinsed several times in water;

Direct quantification

Aromatic rings of amino acids cause an absorbance peak at 280 nm and peptide bonds are responsible for peak around 200 nm. Secondary, tertiary and quaternary structure, and therefore factors such as pH, ionic strength affect absorbance. This method requires more sophisticated equipment than the colorimetric analysis (spectrophotometer instead of a scanner or camera) but it is nondestructive and does not require any additional reagents. First tests were carried out with a conventional spectrophotometer (Ultraspec 2000 UV/VIS, Pharmacia Biotech) by placing slips of modified paper directly on the optic path. Paper slips were immersed in water or oil. Arrangement of fibers in paper is not uniform throughout the paper therefore resulting repeatability of such tests was very low (light beam of small diameter). Next a spectrophotometer, with varian integrating sphere designed for solid samples was used (Agilent Cary 500) with Teflon serving as blank.

For tests in solution calibration curves (0.3–20 mg/mL) were prepared for both compounds, three replicates were made for each concentration.

For test on paper, 1 × 1 cm devices shown in Fig. 2.7 were modified with 10 μL of sample.

Enzymatic Activity, Optimization of Assay Conditions

Three methods have been proposed for the assessment of enzymatic activity. The most widely used in the literature is the measurement with an oxygen probe in

which the evaluation is based on oxygen consumption during the enzymatic reaction. Several cleaning and maintenance procedures have been conducted, but unfortunately the oxygen electrode found in the laboratory proved non-functioning. Other methods are based on indirect measurement and include reaction of hydrogen peroxide with luminol or potassium iodide. The number of variations of the luminol method in the literature is considerable, and the reaction conditions have to be optimized and adapted for use on paper. Since the first tests did not provide satisfactory results, the subsequent analysis was abandoned and starch-iodide method, already optimized for detection of hydrogen peroxide on paper was used.

First, pH was optimized for the glucose oxidize reaction with starch-iodide reagent. Tests were performed in solution, using Ultraspec 2000 UV/VIS spectrophotometer.

pH optimization assay: 0.8 mL of starch-iodide reagent of appropriate pH, 1.0 mL of PBS 0.2 buffer, 0.2 mL of 5 mmol/L glucose solution, quantification performed after 10 min from addition of the enzyme. Three samples were prepared for each pH tested.

Subsequently a calibration curve for enzymatic assay in solution was prepared (enzyme concentration 0.1–10 mg/mL) in pH 5.5.

Enzyme Immobilization Methods

Immobilization procedures are resumed in Table 2.4. Methods are divided in 5 groups: physical adsorption, entrapment in gel, layer-by-layer, covalent binding and encapsulation. Study includes using blockers (glycine, BSA), surface treatment (adsorption on a layer of polymer), use of protectants (mannitol, trehalose). Immobilization methods based on cellulose binding domains are not included, because they require use of modified enzymes that are more expensive and less available. Each sample was a square piece of Whatman n^{o} 1 paper with a 1 $\times$ 1 cm sample area defined with wax (XEROX Phaser printer). 10 μL of solution was needed to wet the paper completely, if not stated otherwise this volume was used for all modifications. All solutions, if not stated differently were prepared in PBS pH = 5.5. In the case of layer-by-layer methods paper was covered with 3 bilayers starting with anionic polymer. In the second and third bilayer cationic polymer was mixed with glucose oxidase to obtain final concentration of 2.5 mg/mL (92.5 U/mL) of enzyme. In the case of subsequent methods: EDC, EDC/NHS, entrapment in ammonium alginate and all encapsulation methods several batches with different concentration of reagents and reaction times were prepared. Table 2.4 lists only the optimized conditions of aforementioned methods. In the case of encapsulation methods, smaller capsules were dispersed on sample papers with a pipette, larger capsules were transported manually on paper and left to dry.

Table 2.4 Immobilization methods reviewed during this study, with their preparation procedure. Reprinted with permission from [129]

No.	Group	Method	Preparation procedure	References
1	Physical adsorption	Simple adsorption	10 μL of GOx 5 mg/mL (92.5 U/mL)	–
2		Bovine serum albumin (BSA) blocking	10 μL of GOx 5 mg/mL, after dry 10 μL of BSA 5 mg/mL	[106]
3		On a layer of collagen	10 μL of confectionary gelatin 10 mg/mL, after dry 10 μL of GOx 5 mg/mL	[102]
4		On a layer of stearic acid	10 μL of stearic acid 4.75 mg/mL, after dry 10 μL of GOx 5 mg/mL	[107]
5		On a layer of polyvinyl alcohol (PVA)	10 μL of PVA 11.5 mg/mL, after dry 10 μL de GOx 5 mg/mL	[65, 108, 109]
6		With mannitol	10 μL of GOx 5 mg/mL—mannitol 8 mg/mL	[6]
7		With trehalose	10 μL of GOx 5 mg/mL—trehalose 2.75 mg/mL	[110]
8	Entrapment in gel	In starch	10 μL of GOx 5 mg/mL—starch 10 mg/mL	[111]
9		In chitosan	10 μL of GOx 5 mg/mL—chitosan 1.5 mg/mL; Chitosan solution was first prepared in water with acetic acid and later diluted with PBS and Na_2HPO_4 to obtain the desired pH.	[65]
10		In polyvinyl alcohol (PVA)	10 μL of GOx 5 mg/mL—PVA 5 mg/mL	[65, 108, 109]
11		In dextran	10 μL of GOx 5 mg/mL—dextran 2 mg/mL	[64]
12		In ammonium alginate	10 μL of GOx 5 mg/mL – ammonium alginate 15 mg/mL	[112, 113]
13		In carboxymethyl cellulose (CMC)	10 μL of GOx 5 mg/mL—CMC 7 mg/mL	[64, 114]
14	Layer-by-layer	Sodium alginate-chitosan	Sodium alginate 4 mg/mL, chitosan 2 mg/mL	[115]
15		Sodium alginate-polylysine	Sodium alginate 4 mg/mL, polylysine 2 mg/mL	[115, 116]
16		Sodium alginate-polyethylenimine (PEI)	Sodium alginate 4 mg/mL, PEI 10 mg/mL	[117, 118]
17		Hyaluronic acid-chitosan	Hyaluronic acid 2 mg/mL, chitosan 2 mg/mL	[116, 119]
18		Hyaluronic acid-PEI	Hyaluronic acid 2 mg/mL, PEI 10 mg/mL	[116, 117]
19		Poly(vinyl sulfate)-chitosan	Poly(vinyl sulfate) 2 mg/mL, chitosan 2 mg/mL	[118, 120]
20		Poly(acrylic acid)-chitosan	Poly(acrylic acid) 5.6 mg/mL, chitosan 2 mg/mL	[118, 121]

(continued)

Table 2.4 (continued)

No.	Group	Method	Preparation procedure	References
21	Covalent linkage	Glutaraldehyde crosslinking	10 µL of GOx 5 mg/mL, when dry 10 µL of glutaraldehyde 2.5 %	[122]
22		Glutaraldehyde crosslinking with glycine blocking	10 µL of GOx 5 mg/mL, when dry 10 µL of glutaraldehyde 2.5 %, after 1:30 h, samples sprayed with 1 mol/L glycine	Modified method 21
23		Schiff base	Samples of paper were submerged in 100 g/L KIO_4 for 12 h, washed with water and dried with a paper towel. 10 µL GOx 10 mg/mL was spotted two times on each sample within an interval of 1 h. After 1 h 10 µL of 6 mg/mL of $NaBH_3CN$ was spotted on each device, which were, after 2 h washed several times with water	[123]
24		EDC[a] with glycine blocking	10 µL of EDC 20 mg/mL, GOx 10 mg/mL was spotted on each sample and left to react for 1 h in 4 °C. Subsequently more 10 µL EDC/GOx mixture was spotted and left for 2 h in 4 °C. After that time 10 µL of glycine was spotted on each sample	[124]
25		EDC[a]/NHS[b]	10 µL of 150 mg/mL EDC, 24 mg/mL NHS was spotted and left to react for 1 h in 4 °C. After that time more 10 µL was spotted and left to react for 3 h, also in 4 °C. Subsequently 10µL of GOx 10 mg/mL was spotted and after 2 h more 10 µL GOx	[125]
26		Potassium periodate, ethylenediamine, and glutaraldehyde activation	Paper substrate immersed in hot 0.1 M KIO_4 for 1:30 h. Washed with water to remove excess periodate and immersed in a solution of 12.5 mg/mL of ethylenediamnie for 2:30 h and in 2.5 % solution of glutaraldehyde for 1:30 h, washed 5 times with distilled water. 10 µL of GOx 10 mg/mL was deposited on each sample	[122]

(continued)

Table 2.4 (continued)

No.	Group	Method	Preparation procedure	References
27	Encapsulation	Sodium alginate	Solution of 30 mg/mL of sodium alginate and 20 mg/mL of GOx was added dropwise to 55 g/L of $CaCl_2$ under constant stirring	[126]
28		Sodium alginate—carboxymethyl cellulose (CMC)	Solution of 15 mg/mL of sodium alginate, 30 mg/mL of CMC and 20 mg/mL of GOx was added dropwise to 55 g/L of $CaCl_2$ under constant stirring	[126]
29		Sodium alginate—chitosan	Solution of 15 mg/mL of sodium alginate, 30 mg/mL of chitosan and 20 mg/mL of GOxwas added dropwise to 55 g/L of $CaCl_2$ under constant stirring	[112]
30		PEI	5 mL of a solution of 120 mg/mL PEI with 5 mg/mL GOx was added to 25 mL of cyclohexane with 0.1 % of Triton X 100 under constant stirring. 5 min after the emulsion was formed 1.2 mg of sebacoyl chloride in 1.2 mL of cyclohexane was added to the mixture. After 10 min of reaction, another 1.5 mL of sebacoyl chloride 1 mg/mL was added and left to react for 10 min. Reaction was stopped with 25 mL of cyclohexane and the capsules washed with water several times	[127]
31		Covalent attachment to PEI capsules	As the capsules from method 30 did not show any enzymatic activity they were used as a base to covalently attach GOx by means of glutaraldehyde crosslinking. For this purpose 10 mL of a suspension of PEI capsules from the previous study was mixed with 1 mL GOD 10 mg/mL and 4 mL of glutaraldehyde 2.5 % and left to react for 1 h under constant stirring. Capsules were washed with distilled water	Modified method 30
32		Covalent attachment to silica beads	1.5 g of chromatography silica beads was mixed with 5 mL of 10 mg/mL GOx and glutaraldehyde 2.5 % and left to react for 1 h. Afterwards washed with water	[109]

(continued)

Table 2.4 (continued)

No.	Group	Method	Preparation procedure	References
33		Chitosan	10 mL of 40 mg/mL chitosan, 20 mg/mL GOx mixture was added to 50 mL of cooking oil with 0.5 % of Tween surfactant and emulsified. After 5 min 0.8 mL of glutaraldehyde 25 % was added and left to react for 15 min 100 mL of distilled water was used to stop the reaction	[127]

[a]1-ethyl-3-(dimethylaminopropyl)carbodiimide
[b]N-hydroxysuccinimide

Impact of Enzyme Immobilization on Stability During Storage

In all cases 3 samples with enzyme and 1 control without glucose oxidase were prepared for storage in ambient temperature and the same set for storage in 4 °C for each day of measurement. Samples were measured after 1, 3 days and 1, 2, 3, 4, 5, 6, 7, 8, 10, 12, 14, 16, 20, 24 weeks of storage. In the case of complete loss of activity observed for a given method tests were terminated prematurely. Potassium iodide-starch method was used for the evaluation of enzymatic activity. Potassium iodide-starch reagent was prepared daily, as follows: 100 mg of starch was heated in 10 mL of PBS buffer (pH = 5.5; 0.1 mol/L) for several minutes, after cooling 50 mg of potassium iodide and 5 mg Na_2MoO_4 were added. Each time 1 mL of PBS buffer and 0.8 mL of potassium iodide-starch reagent were placed in the cuvette, after that the enzyme modified paper was submerged in a way as to not to obstruct the light path, and 0.2 mL of glucose solution 5 mmol/L was added. After 15 min the solution was mixed and the spectrum was taken.

Impact of Enzyme Immobilization on Flow in Paper Channel

Simple paper-based device was prepared with borders printed with wax (Fig. 2.9) comprising of buffer filled sponge providing the wicking solution, a 2.5 × 30 mm channel where the enzyme was immobilized and a wicking pad that guaranteed constant movement of the fluid.

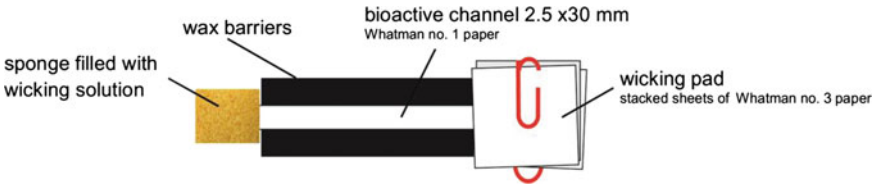

Fig. 2.9 Paper-based device for the analysis of flow in paper matrix. Reprinted with permission from [128]

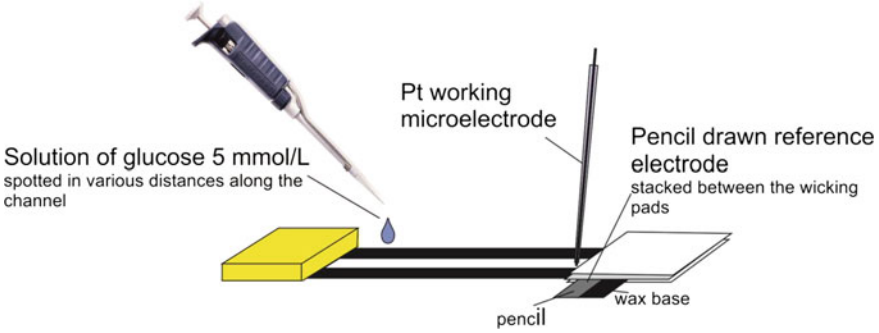

Fig. 2.10 Electrochemical analysis of flow in paper matrix. Reprinted with permission from [128]

Two distinct flow measurements were used to guarantee the correctness of the results. In the colorimetric attempt 1 μL of a blue food dye was spotted in the entrance and in the middle of the wetted channel. Objective of this study was to find out how immobilization influences already established flow in paper matrix. Movement of the colored solution was monitored with a series of photos made with a digital camera (Canon EOS 60D). Three devices for each immobilization method were prepared.

In the case of electrochemical measurement of flux, a pencil drawn reference electrode was placed between the device and wicking pads, a Pt working electrode was positioned in the end of the channel (Fig. 2.10). 1 μL of 5 mmol/L glucose in water was spotted in various distances along the channel and the time necessary to obtain the maximal response of the hydrogen peroxide on the electrode was measured. The applied voltage was equal 1 V. Three devices were prepared for each immobilization method.

Michaelis-Menten Kinetics

To analyze the metabolic activity of selected immobilization methods Lineweaver-Burk curve described by Michaelis-Menten kinetics was constructed. For this experiment only the most promising immobilization methods were selected. Therefore the tests were performed only with subsequent methods: in solution, adsorption, BSA blocking, entrapment in PVA, entrapment in starch, LbL sodium alginate-chitosan, LbL Hyaluronic acid—PEI, covalent linkage EDC/NHS. Enzymatic activity was evaluated accordingly to the previous tests (1 mL PBS; 0.8 mL of potassium iodide-starch; 0.2 mL glucose) for glucose concentrations equal 0, 0.5, 1, 5, 10, 50, 100, 200 mmol/L. Three samples were measured for each concentration. Measurements were conducted with the potassium iodide-starch reagent and different concentrations of hydrogen peroxide (0.025; 0.05; 0.1 mmol/L) to evaluate the extinction coefficient.

2.2.4.3 Electrochemical Detection

Optimization of Device's Architecture

Based on the literature data [72] and flow velocity obtained from previous experiments (Fig. 2.45) computation model of the paper network was constructed in COMSOL Mutliphysics v 4.3. "Darcy's Law" module was used to set the flux, and "Species transport in Porous Media" to describe the movement of the solution in the channel. The base fluid was water, which was later substituted with a fluid of concentration equal 1 mol/L. Permeability of paper $\kappa = 10^{-12}$ m^2, porosity 0.8, pressure in the entry of the channel equal 0 Pa and in the exit 130 Pa (adjusted according to experiments carried out in the bioactive channel), paper density equal 850 kg/m^3. Mesh type: "finer".

Several channel architectures were tested (Fig. 2.46), including:

- Straight channel—3 cm × 0.25 cm;
- Wide-narrow—2 cm × 0.4, 1 cm × 0.25 cm;
- Square—3 cm × 0.25 cm with a 0.5 cm^2 in the middle;
- Arrow—3 cm long, entrance 0.25, after 1.5 cm widening to 0.5, exit 0.25;
- Narrowing—3 cm long, entrance 0.4 cm, exit 0.2 cm;

After computer modeling all types of devices were fabricated and their analytical performance assessed by means of chronoamperometry. For those tests 1 μL of mixture of uric acid (1 mmol/L) and glucose (5 mmol/L) was spotted 5 mm from the entrance of the channel.

Analysis of Glucose and Uric Acid

Preliminary Tests

Previously described device, depicted in Fig. 2.10 was used for simultaneous detection of uric acid (direct) and glucose (indirect, after enzymatic reaction). For those tests enzyme was immobilized using Layer-by-layer method. It was possible to separate glucose and uric acid using PBS buffer pH = 5.5. After assembly, device was conditioned for 10 min counting from the complete wetting of the channel.

First tests were carried out with hydrogen peroxide, to verify if the separation is associated with modification by layer-by-layer, and enzyme present or with the cellulose matrix. It was possible to separate both compounds (hydrogen peroxide and uric acid), thus the separation ability was attributed to the cellulose matrix. It was also noted that the optimum pH for separation is 5.5.

Next, glucose solution (5 mmol/L) was passed through the bioactive channel and repeated cyclic voltammetry scans were registered. Signal started to deteriorate after 40 min. 0.7 V potential was chosen for future tests based on the CV curve format (not shown).

Table 2.5 Concentrations of glucose and uric acid in mixed samples

	I	II	III	IV	V	VI
Glucose (mmol/L)	10	7.5	5	4	3	2
Uric acid (mmol/L)	0.1	0.3	0.5	0.7	0.9	1.2

Preliminary Test Destined to Construct a Calibration Curve

Promising results led to preliminary experiments destined to construct a calibration curve. Mixed samples of glucose and uric acid were prepared with final concentrations of both compounds as stated in Table 2.5.

Three devices with narrowing channels were tested for each of the 6 samples. Experiments were carried out in random order, during two consecutive days.

Uniformity of Enzyme Immobilization

When a drop is placed on top of paper, each time it wicks slightly differently, depending on the arrangement of fibers. Because of this it was proposed that low repeatability of the results is related to the different time necessary for the solution to pass through the enzymatic zone. Center of the channel was cut and layer-by-layer immobilization was carried out by dipping. Problem arouse to connect back all parts of the channel. Several attempts were proposed, including:

- use of adhesive tape (Fig. 2.11a, e);
- paper clips (Fig. 2.11b);
- a device holder cut from a sponge, which provides support for while leaving the channel suspended (Fig. 2.11b–d);
- use of a plastic cover and pressure (Fig. 2.11c, d);
- interweaving of paper parts (Fig. 2.11e);

Electrode Positioning

Lack of repeatability could be also related to electrode positioning. As each device serves only for one measurement, electrode needs to be positioned anew each time. Therefore 10 mmol/L solution of uric acid was injected along the channel, later electrode was lifted, positioned again, and another three injections were made in the same way as before.

In the next step different manners of electrode positioning were tested, including:

- a sponge holder, with an electrode positioned on top—weight of the electrode provides always the same pressure over paper. Different sponge holders were prepared, providing or not providing support in the electrode area;
- a sponge holder, with an electrode positioned on the bottom (Fig. 2.12a)—weight of paper provides always the same pressure;

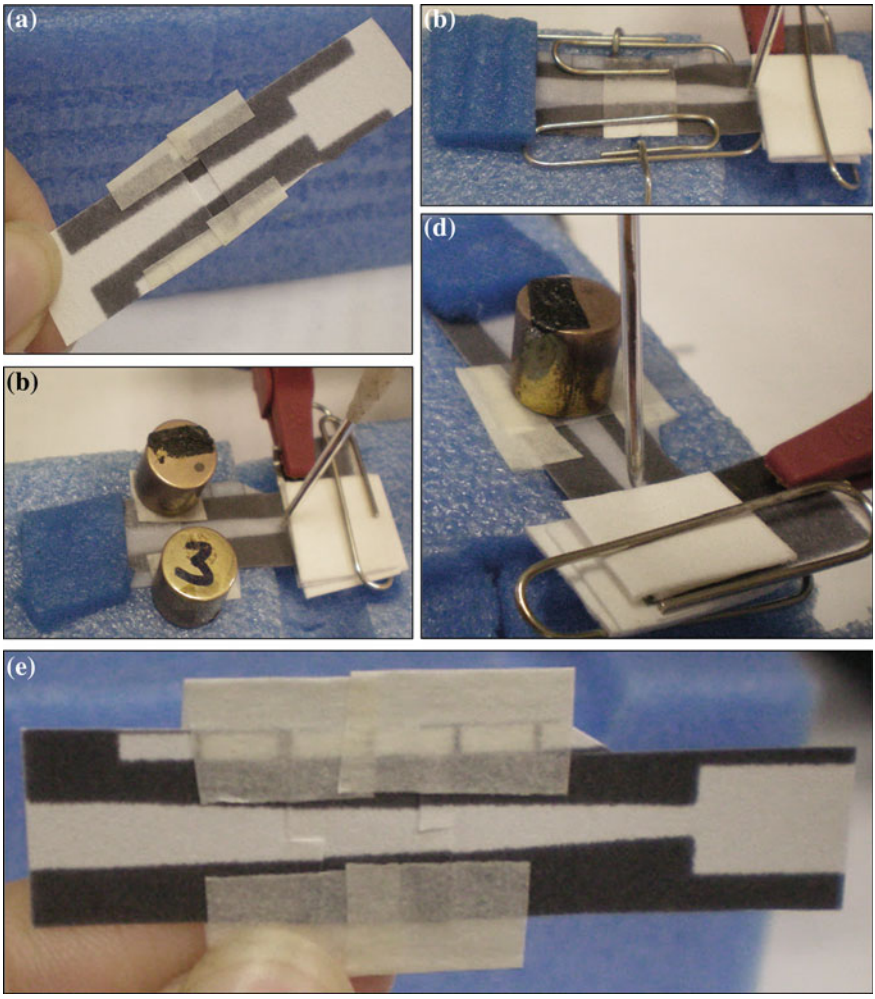

Fig. 2.11 Some of the approaches used to connect the enzymatic zone modified by dipping with the rest of the channel. **a** cut-out part secured with an adhesive tape, **b** placed on a sponge holder and hold with paper clips, **c** covered with plastic layer and pressed with weight on both sides of the channel, **d** covered with plastic layer and pressed with weight on *top* of the channel, **e** cut-out part interwoven and secured with an adhesive tape. Figure E reprinted with permission from [128]

- a Pt wire stacked across the width of the channel (Fig. 2.12b)—enclosed between layers of plastic, or bare;
- a Pt wire passing through paper in the middle of the channel (Fig. 2.12c);

In some of the tests a Pt wire was used instead of a microelectrode enclosed in a glass capillary.

Fig. 2.12 Some of the approaches used for electrode positioning. **a** with a sponge support, **b** with a Pt wire stacked across the width of the channel, **c** with a Pt wire passing through paper

Calibration Curve

After optimization calibration curves for both compounds were constructed. Mixed samples of glucose and uric acid were prepared with the final concentrations of both compounds as stated before in Table 2.5. 1 μL of the sample was spotted 5 mm from the entrance of the channel, where flow was already well established. Obtained signal consisted of two partially overlapping peaks. After computational resolution of peaks it was possible to construct calibration curves for both compounds based on the peak area (retention times and peak width would vary between the columns).

(Tutaj)Analysis of Glucose, Cholesterol and Uric Acid

Architecture

In the case of analysis of cholesterol, wax could not be applied for device's fabrication, thus subsequent systems were cut with a laser cutter. Two architectures were proposed, with one or two working electrodes. Two electrode system (Fig. 2.13a), takes advantage of the conservation of laminar flow in paper-based devices. Sample is spotted on a sample pad and travels through two channels of identical architecture, one channel is modified with glucose oxidase, other with cholesterol oxidase. Next, hydrogen peroxide formed upon enzymatic reaction flows together with rest of the sample (i.e. uric acid) to the detection zone. Due to conservation of laminar flow one electrode will detect hydrogen peroxide, which originated from cholesterol, and the other electrode from glucose. Uric acid will be detected on both electrodes.

In case of one electrode system (Fig. 2.13b), bioactive channels have different architecture. One of the channels is longer therefore longer time will be needed for part of the sample to pass. Again one channel is modified with glucose oxidase and the other with cholesterol oxidase, but this time reaction products and the remaining sample from the straight, shorter channel will arrive on the electrode first. Uric acid will be detected two times on the same electrode.

First devices for the two electrode measurements were cut from a single sheet of paper (Fig. 2.14). Longitudinal incision was made in the middle part of the channel which divided the channel into two enzymatic zones (glucose oxidase and cholesterol oxidase). Channel was too long and too thin to support its own weight when wetted and would bend down touching the surface beneath. In principle this

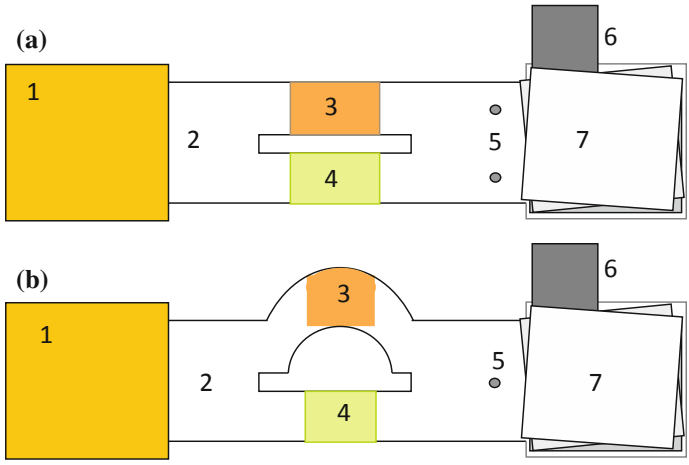

Fig. 2.13 Devices proposed for the analysis of glucose, uric acid and cholesterol. **a** two electrode system, **b** one electrode system. *1*. buffer filled sponge, *2*. sampling area, *3*. ChOx enzymatic zone, *4*. GOx enzymatic zone, *5*. working electrode(s), *6*. reference electrode, *7*. stack of wicking pads

Fig. 2.14 Prototype device for two electrode measurement

kind of device could be used after optimization, also as a one electrode system, if one of the channel parts would use some flow retardant. Based on the results of enzyme immobilization uniformity from other study (electrochemical system for glucose and uric acid) subsequent test used devices assembled from separate parts.

Different thicknesses of paper (Whatman n^{o} 1, 20, 3) were tested. Device was assembled by threading (Fig. 2.15a1, c) or interweaving of separate parts (Fig. 2.15a2, b). All types of devices (both type of linkage, different paper types) were after assembly tested with water samples to verify contact between separate parts.

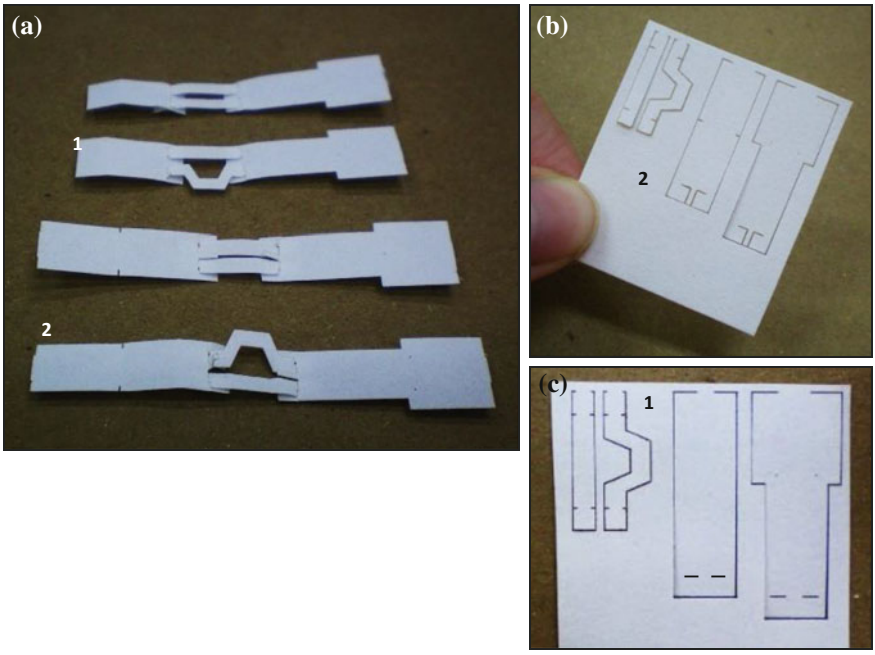

Fig. 2.15 Devices for the electrochemical analysis of glucose, cholesterol and uric acid *1*. bioactive channels passing through sample and detection pads. *2*. bioactive channels interwoven with sample and detection pads. **a** assembled systems. **b**, **c** laser cut systems prior to assembly

Dimensions:

- Sampling pad: 6 mm wide, composed of three areas
  - wicking area (to place a buffer filled sponge, or immerse in buffer solution) 1 cm long;
  - sampling area—1 cm long;
  - connection area—part of the channel with incisions or orifices 3 mm;
- Channels:
  - Straight—2.5 × 10 mm,
  - Curved—2.5 × 12 mm,
  - both with 3 mm connections on both sides;
- Detection pad:
  - connection area—part of the channel with incisions or orifices 3 × 6 mm;
  - detection area—13 × 6 mm with orifice(s) for electrode positioning;
  - wicking pad and reference electrode area—10 × 10;

Conservation of Laminar Flow

To guarantee the conservation of laminar flow necessary for functioning of the two electrode system one of the channels of the assembled device was placed in water and other in solution of a food dye (sponges filled with appropriate solutions placed on top of channels). Movement of solution was observed in all configurations of the device, with both types of linkage and with paper of different thicknesses.

Preliminary Tests and Optimization of the Architecture

Both two and one electrode systems were tested with mixtures of glucose, cholesterol and uric acid (10 mmol/L). Paper becomes more delicate upon wetting and would tear or deflect from the electrode in the two electrode system. In this case two platinum wires are exerting force upon small piece of paper (distance between electrodes 3 mm). One electrode system, did not provide repeatable results during the first tests. Therefore architecture was modified, including two constrictions of the channel, one in the sampling area (Fig. 2.16a), and another in the electrode area (Fig. 2.16b).

Sampling constriction facilitates deposition of the sample, and helps to guarantee equal distribution into both bioactive channels. Electrode constriction not only accelerates the flow, which should result in less broadened peaks, but also guides the streams originating from each channel to the electrode.

Fig. 2.16 Device with partially constricted channels. **a** sampling constriction, **b** electrode constriction

2.3 Results and Discussion

2.3.1 Substrate

As it can be seen on microscope pictures resumed in Fig. 2.17 all analyzed papers present homogenous structure. Both chromatography papers are to a large extent porous, with similar distribution, structure and size of fibers. Structure of copy and tracing papers is more compact, with no apparent microsized holes. In the case of copy paper fibers can be distinguished only at the highest magnification (×40) and their diameter is considerably smaller than in the case of chromatographic paper. Other, rounded structures of different light transmission properties can be also observed in the vicinity of the fibers, they can be associated with additives such as starch, $CaCO_3$ etc. Tracing paper forms a continuous structure with few, compact fibers of small diameter seen on the surface. This kind of structure could be expected after chemical treatment with sulfuric acid.

2.3.2 Optical Detection

2.3.2.1 Choice of Colorimetric Method

Ferric thiocyanate assay–highly reproducible assay in solution and on paper for hydrogen peroxide sample, depends on pH (<7). No change of coloration observed when glucose and glucose oxidase were used.

Copper(II) ion and 2,9-dimethyl-1,10-phenanthroline method (DMP)–method was successfully applied for tests in solution and on paper, for both hydrogen peroxide and glucose, with change of color from bright yellow to dark orange-yellow (Fig. 2.18a). Unfortunately after just 15 min the control zone of paper-based device also changed color. It was possible to quantify glucose on paper in the range 0.1–10 mmol/L. Promising method for paper-based detection of

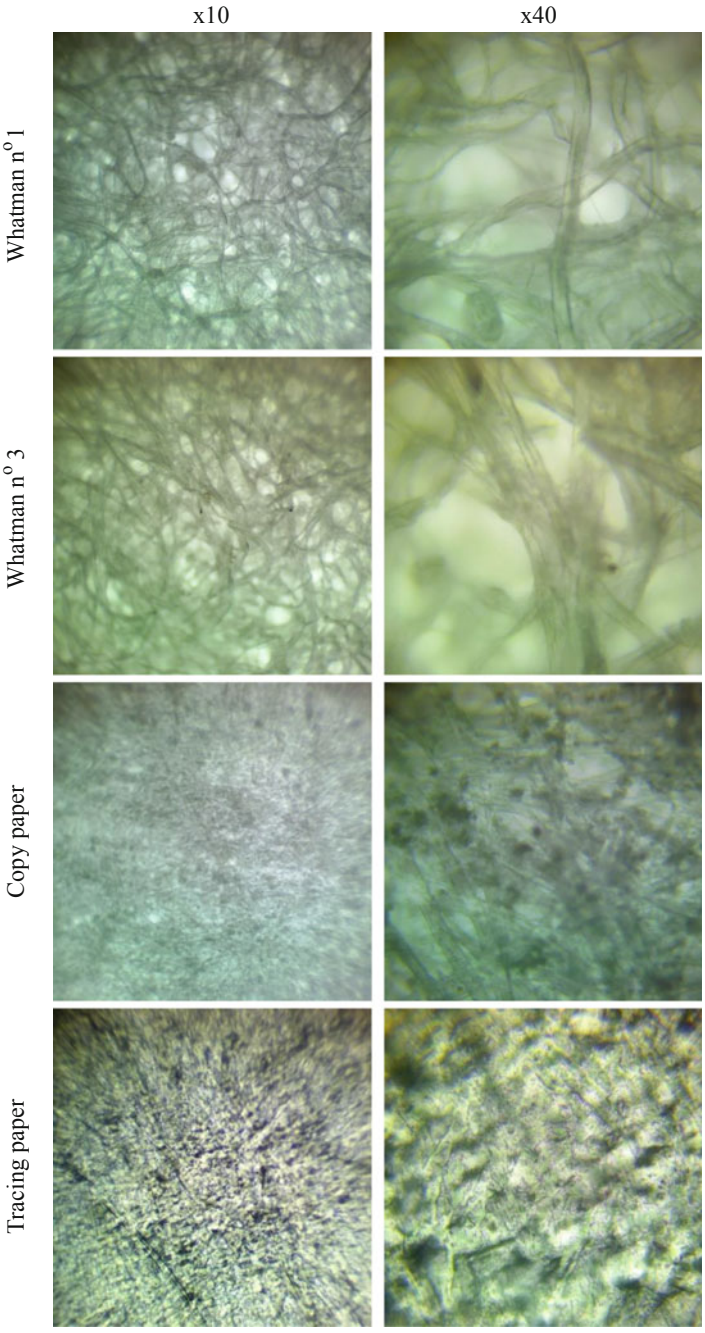

Fig. 2.17 Surface of different paper substrates seen through an optical microscope

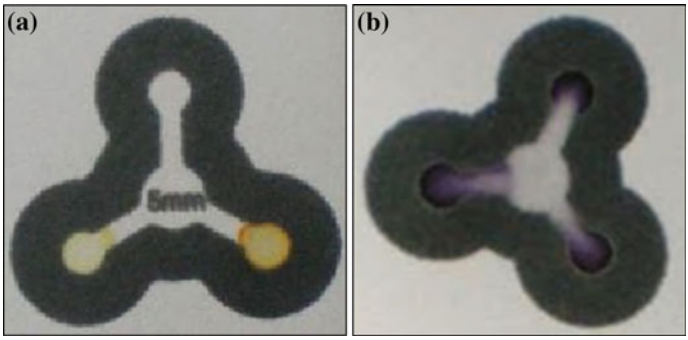

Fig. 2.18 Paper-based colorimetric reactions for the analysis of hydrogen peroxide. **a** Copper-DMP method (*left down* without GOx, *right down*–modified with enzyme), **b** Potassium iodide-starch method

glucose, nevertheless because of delicate changes in coloration, quantification should be made by means of a scanner or camera, and not by visual comparison with standards.

Iron(II) ion and 2,6-Bis(hydroxymethyl)-4-methylphenol method–reproducible results obtained in solution and on paper for hydrogen peroxide sample. pH working range $\sim$ 2, therefore was not possible to detect hydrogen peroxide formed after enzymatic reaction of glucose. Tests on paper where enzymatic and colorimetric reactions were carried out in separate zones were not reproducible.

Starch-iodide method–drastic change in coloration from colorless to black blue (Fig. 2.18b), for reaction in solution and on paper, for both hydrogen peroxide and glucose. Method uses easily accessible, non-toxic reagents and has a wide pH working range. After around 30 min due to autoxidation of iodide-starch reagent control zone changes coloration to some extent. It was possible to quantify glucose on paper in the range 0.1–10 mmol/L. Based on described results starch-iodide method was chosen for subsequent tests.

Methylene blue–assay carried out successfully only for hydrogen peroxide and only in solution. Leucomethylene blue solution is unstable and oxidizes spontaneously.

2.3.2.2 Differences in Hue and Repeatability of Digitalization

Repeatability of digitalization: The standard deviation of intensity of a given area for 8 subsequent scans was equal 3.9 units (total value for CMYK), which contributes to $\sim$1.5 % of maximum signal (histogram range: 0–255). Repeatability is associated not only with digitalization but also manual positioning of the masking tool in the computer program.

Differences in hue: Least reproducible and least intensive results were obtained when corn starch from Altair company was used to prepare the starch-iodide

reagent. Potassium iodide from Fisher resulted in weaker signal than Merck, both reagents were still before their expiration date. Observed differences were associated with inappropriate storage (i.e. humidity). The lowest standard deviation between two assays and highest linearity of the calibration curve for cholesterol were obtained for combination of potassium iodide from Merck and starch from Vetec. Different concentrations of amylose, amylopectin and proteins in starches of different suppliers can cause variations in hue and intensity.

2.3.2.3 Solving the Autoxidation Problem

Single Factor Anova was performed to test if pH has any impact on color intensity (pH range 5–8, 3 replicates). When intensity was expressed in CMYK, data divided into two groups, with no difference between results ($F < F_{crit}$) for pH 5, 5.5, 7 and 6, 8. Higher intensities were observed for the first group. In the case of Cyan channel no significant difference was observed between results for all pH values. Therefore single channel should be used for subsequent data analysis.

After dissolving starch-iodide reagent in 0.1 mmol/L PBS buffer (pH = 6.5 used) autoxidation would not occur for 1–2 weeks depending on storage conditions. This time could be prolonged further with use of covers. Use of liquid polymers was discarded due to inhibition of colorimetric reaction and hydrophobization of the modified region. All adhesive tapes used during study contained glucose present in glue. Sugars are often used in glue formulations as a non-toxic and inexpensive modulator of viscosity. Covers without adhesive only stacked against paper by means of paper clips did not exert any effect on shelf life. Lamination had positive effects on storage stability but heat applied during the process led to deactivation of enzymes and adhesive also contained glucose. Finally transparent, adhesive book cover foil from Con-tact Vulcan was used to fabricate the cover as it was the only material tested which did not cause false positive reaction with glucose oxidase. Device was tested during a period of 4 weeks in ambient conditions and brown colorations from iodine ions did not appear.

2.3.2.4 New Fabrication Methods for Analysis of Cholesterol

Table 2.6 resumes results of tests carried out with different polymers. PDMS, polystyrene and commercial waterproofing spray by Sistem were able to retain all test solutions.

In the case of paper slips without any boundary the size of the detection area depends on the precision of deposition, temperature and homogeneity of paper. The greatest problem in this case is the delimitation of the area in the graphic program. Manual cutting or use of paper punch results in low resolution and reproducibility.

In the case of manual application of polymers resolution and reproducibility are also very low, thus a device presented in Fig. 2.19e was proposed. In this case parts of the device which are important to the assay, as the reaction or the detection zone

Table 2.6 Review of polymers applied to form barriers impermeable to cholesterol

Polymer	Preparation	Example
Wax	Test solutions spread freely through wax barriers (Fig. 2.19a)	Fig. 2.19a
Chitosan	Fiber: chitosan fiber partially dissolved clogging paper pores (Fig. 2.19b). Unfortunately using fiber is not practical and does not allow good resolution Powder: it was not possible to replicate results obtained with chitosan fiber using powder, independently of the concentration	Fig. 2.19b
PDMS	Polymer spread over the paper independently of the drying method and concentration used. All devices regardless the solvent used were able to retain water, vegetable oil and both cholesterol stock solutions (with Triton X-100 and ethanol). Simple devices were drawn on top of a laser printed design (Fig. 2.19c)	Fig. 2.19c
PVC	Independently of the concentration simple devices were not able to retain any of the test solutions	
Polystyrene	Simple devices prepared with diluted polystyrene solution were able to retain all test solutions (Fig. 2.19d)	Fig. 2.19d
Commercial waterproofing agents	NP Nanopool®: Some parts of the channel designed along the whole paper sheet did not retain the test solutions, except water which was retained perfectly each time. Results were inconsistent probably due to prolonged contact with water during shipment Waterproof spray by Sistem: Prepared devices were able to retain all test solutions. Figure 2.19e shows a device cut with laser cutter with 4 supporting channels (uncut parts of the structure, market with arrows) filled with waterproofing spray	Fig. 2.19e

are precisely cut by means of a laser cutter. Device is suspended on paper structure by means of channels filled with a waterproofing polymer.

2.3.2.5 Immobilization of the Colorimetric Reagent for Enhanced Uniformity of Color Development of Uric Acid Assay

Paper modified with poly[di(ethylene glycol)] appeared oily, and black-blue coloration was only visible in the area unmodified with the polymer. Poly(acrylic acid) also resulted in oily appearance of the paper, and paper strips modified with higher concentrations became twisted upon drying. Color resulting from the enzymatic and colorimetric reactions was clearly visible but reproducibility of the assay was very low. Uniformity of color development was highly dependent on the method used for polymer application.

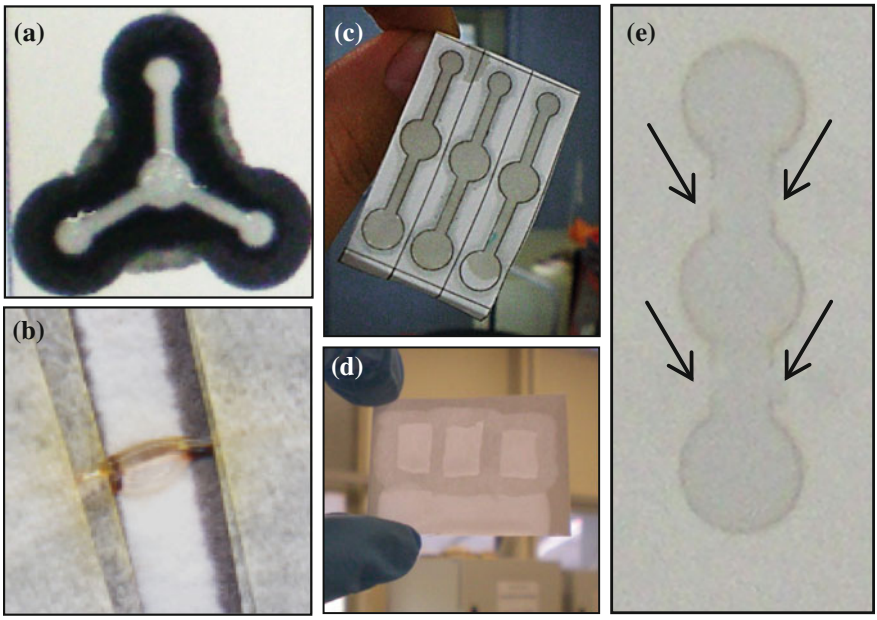

Fig. 2.19 **a** Device with wax barriers filled with Triton X-100, **b** Partially dissolved chitosan fiber. **c** Simple device with borders delimitated with PDMS retaining solution of Triton X-100, **d** Simple polystyrene device retaining solution of Triton X-100 (*center*) and vegetable oil (lower external part of paper), **e** laser cut device with supporting channels marked with *arrows*

Gelatin proved to be more promising, thus more detailed study was performed. In cases where gelatin was on top or mixed with the starch-iodide reagent it should additionally protect it from oxidation, not only enhancing the buniformity of color development but also the shelf life of the final device. Results are resumed in Fig. 2.20.

All the tests with gelatin resulted in more uniform color development than tests without the polymer. In case of lateral flow assay without gelatin, indicator is carried with the flux resulting in uneven coloration spread on larger area. All spot tests showed some level of uniformity in color development, with lighter middle area where solutions were added and darker edges. In both lateral flow assay and spot test best result was obtained with gelatin deposited on top of the starch-iodide reagent. Optimum concentrations were 10 mg/mL for lateral flow assay and 15 mg/mL for the spot test.

Lateral flow assays for uric acid prepared with LbL technique were designed to separate enzymatic and colorimetric reactions. Glucose assay did not present problems with uneven coloration. Thus if only hydrogen peroxide would pass to the detection zone in the uric acid assay color should develop evenly. Unfortunately in all cases color developed forming a ring around the detection zone (Fig. 2.21). Most reproducible results were obtained for the first assay (LbL alginate/UOx-chitosan in

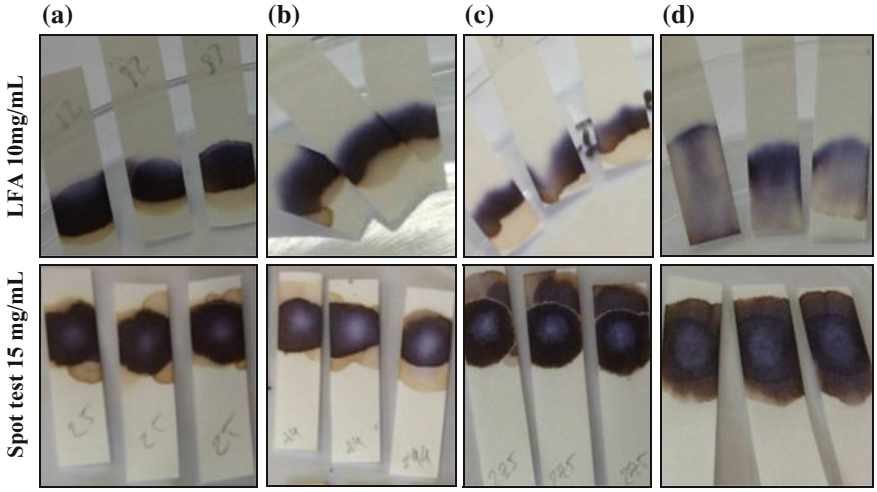

Fig. 2.20 Photographs of lateral flow assays and spot tests taken after 20 min. Only the concentrations of gelatin which gave the best results are shown. **a** Starch-iodide under gelatin layer. **b** Starch-iodide mixed with gelatin. **c** Starch-iodide on top of gelatin layer. **d** Starch-iodide without gelatin

Fig. 2.21 Uric acid test

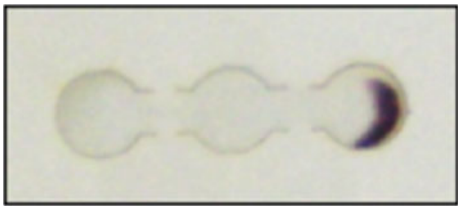

the middle zone, starch-iodide reagent under gelatin in detection zone). Similar results were obtained for the third type of assay (starch-iodide under LbL in the middle zone) but interestingly color did not appear in the middle zone were the starch-iodide reagent was deposited, but in the third area, in the same ring format as in the previous assay. Starch-iodide was therefore carried with the fluid. Second assay, without chitosan in LbL formulation was the least reproducible.

2.3.2.6 Calibration Curves

Uric acid: With the results obtained by means of a spot test it was possible to construct a calibration curve presenting good linearity $R^2 = 0.993$ in the range of interest 0.1–2.5 mmol/L. Calibration curve (Fig. 2.22) is described by equation $y = 12.7 \pm 0.44x + 4.4 \pm 0.30$, $N = 3$. Limit of detection, estimated according to IUPAC Gold Book as the concentration of the analyte giving a signal equal to the blank plus 3× the standard deviation of the blank is equal 0.10 mmol/L.

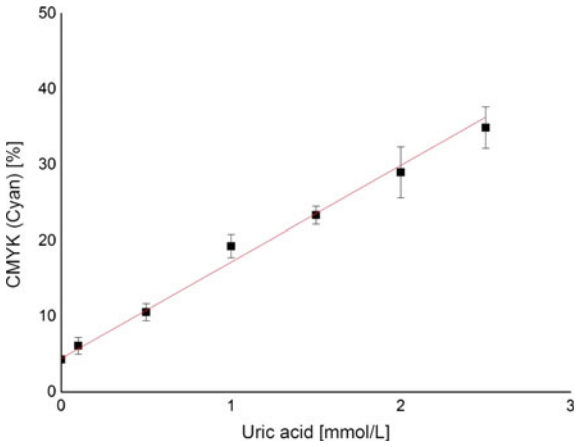

Fig. 2.22 Calibration curve for uric acid–colorimetric method, spot test with starch-iodide indicator immobilized in gelatin

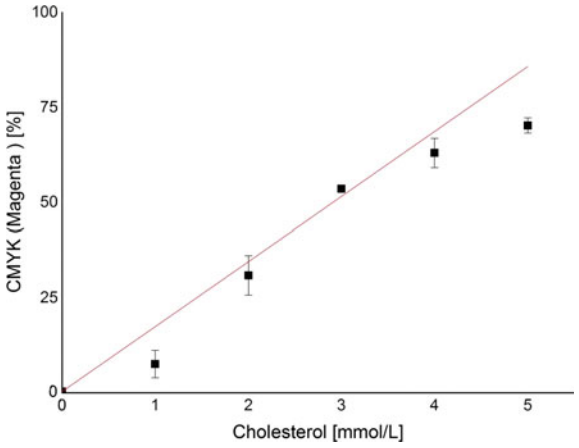

Fig. 2.23 Calibration curve for cholesterol–colorimetric method, spot test

Cholesterol: With the results obtained by means of a spot test it was possible to construct a calibration curve presenting good linearity $R^2 = 0.991$ in the range of interest 1.0–5.0 mmol/L. Calibration curve (Fig. 2.23) is described by equation $y = 17.08 \pm 0.74x + 0.33 \pm 0.49$, $N = 3$, with limit of detection equal 0.02 mmol/L.

Glucose: With the results obtained by means of a lateral flow assay it was possible to construct a calibration curve presenting good linearity $R^2 = 0.938$ in the range of interest 0.2–5 mmol/L. Calibration curve (Fig. 2.24) is described by equation $y = 11.97 \pm 1.25x + 3.7 \pm 2.6$, $N = 3$. Limit of detection, is equal 0.2 mmol/L.

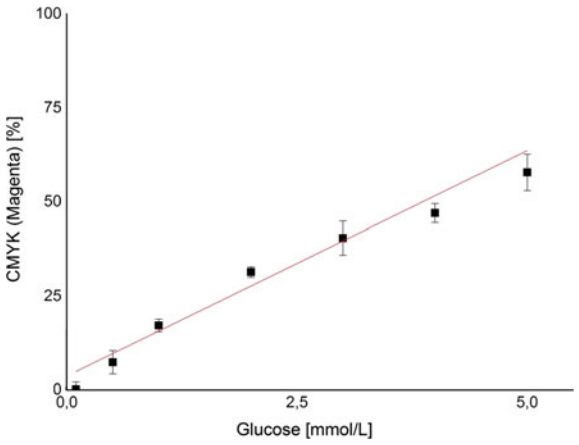

Fig. 2.24 Calibration curve for glucose–colorimetric method, lateral flow assay

2.3.2.7 Tangential Flow Devices

Devices without the intermediate distribution layer, resulted in an uneven coloration (Fig. 2.25c). Inclusion of a distribution layer allowed to obtain uniform coloration for the glucose assay, and similar ring type result as observed in the spot test for uric acid.

Figure 2.25b shows two type of acrylate covers with different sizes of the sampling orifice. Without the acrylate holder it was difficult to reproducibly clamp

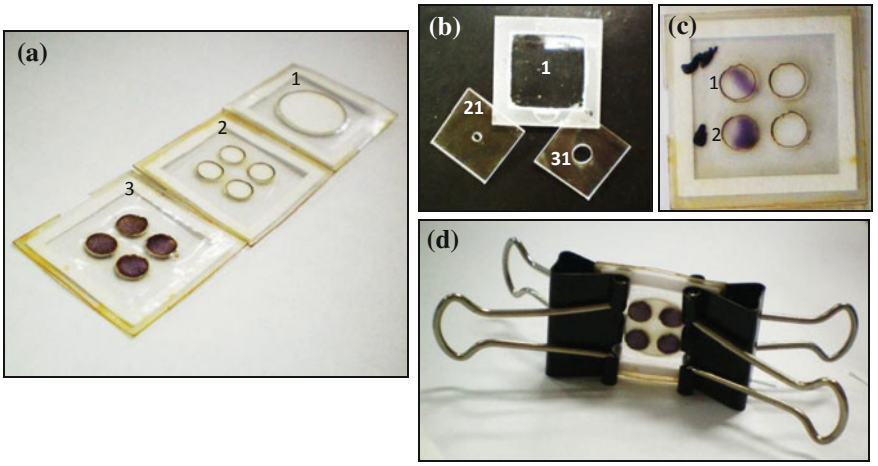

Fig. 2.25 Photographs of a sample tangential flow device. **a** individual layers: *1*. sampling layer, *2*. enzymatic layer, *3*. detection layer (test with H_2O_2); **b** acrylate holder: *1*. base, *2*. cover with a small sampling orifice, *3*. cover with a large sampling orifice; **c** Results obtained for a device without distribution area *1*. uric acid, *2*. glucose; **d** assembled device, clamped between two paper clips

the device. Paper clips exerted more pressure in certain points of the assay, and their positioning had great influence on uniformity of color development. When device was enclosed in a holder with a cover tightly fitting the bottom piece, color development seemed slower and did not reach the same intensity as with open device. It was proposed that lack of readily available oxygen can be the cause of such results, therefore a slightly smaller cover with a larger sampling orifice was proposed (Fig. 2.25b3).

It was not possible to detect cholesterol in any of the devices. To overcome this problem, in order to move cholesterol from the sampling layer, an organic solvent should be used or surfactant added to the running buffer. Cholesterol oxidase modified paper could be also in direct contact with the sampling pad, in this way enzyme could react with cholesterol in the sampling area and later only hydrogen peroxide would flow to the detection zone. It was possible to quantify glucose and uric acid with results similar to obtained in previous tests (the same linear working range but lower repeatability).

2.3.3 Methods of Enzyme Immobilization on Paper

2.3.3.1 Protein Quantification Methods

All tested methods were successfully applied for measurements in solution.

Bromocresol green-in the case of bromocresol green method positive results of the preliminary tests on paper (Fig. 2.32) for BSA samples, and weak results for GOx led to formation of calibration curves (tests in solution) in the range of 0.3–20 mg/mL for both compounds. Linear dependence was observed for BSA samples (Fig. 2.26) and no trend for the GOx (Fig. 2.27), therefore method was discarded from subsequent tests on paper. Differences observed for those two compounds can be related to smaller number of amino acid residues participating in reaction in the case of GOx.

Bromophenol blue-after promising results of the preliminary bromophenol blue tests (Fig. 2.32) for both BSA and GOx, calibration curves were constructed for both compounds (tests in solution). Higher sensitivity was observed for BSA (Fig. 2.28) as compared with GOx (Fig. 2.29). Curve for GOx was described by equation $y = 0.42x + 1.96$, $SD = 0.04$ for $N = 3$. It was noted that the order of deposition of reagents is crucial for the reproducibility of the results (tests on paper). If the protein was deposited first (which would be the case of the immobilization studies) the dye would spread only on a small area forming regions of uneven coloration. To overcome this problem dye could be deposited first or sprayed (Fig. 2.30) on top of the protein instead of spotted (Fig. 2.31). Even with those two modifications it was not possible to obtain sufficient reproducibility to construct a calibration curve for GOx for tests on paper and only for BSA.

Lowry method–for both variations of the Lowry method no changes in coloration was observed for any of the paper samples (Fig. 2.32). Both variations of the test

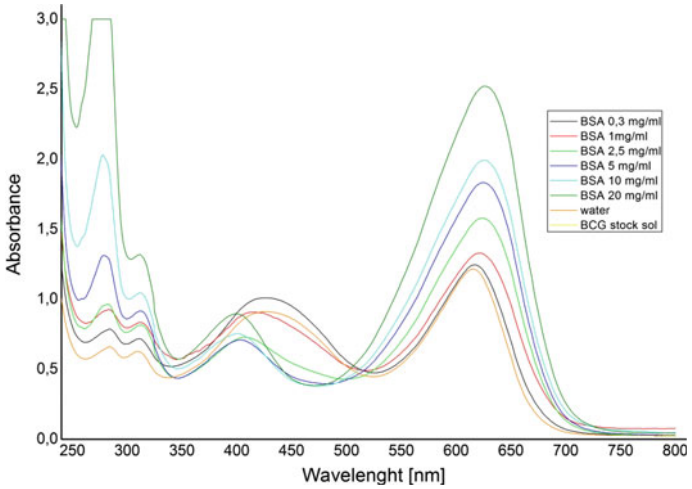

Fig. 2.26 Absorption spectrum for different concentrations of BSA, bromocresol green method, tests in solution

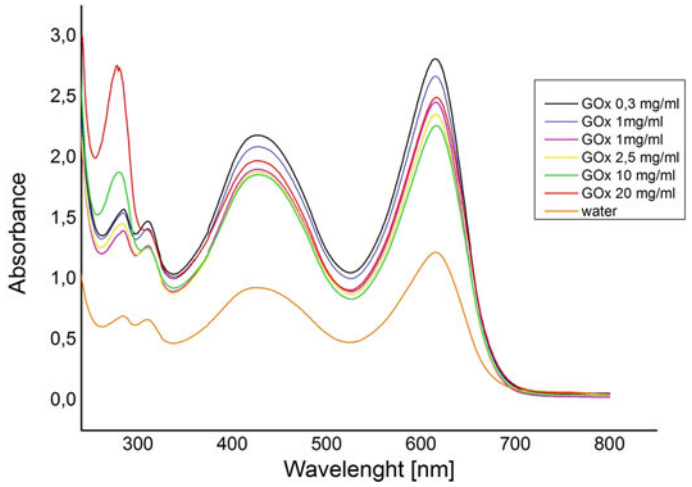

Fig. 2.27 Absorption spectrum for different concentrations of GOx, bromocresol green method, tests in solution

(with or without the surfactant) were correctly executed, as was confirmed in the experiments carried out in solution.

Bradford method–in the case of Bradford method all samples (water, BSA and GOx) resulted in change of coloration of the modified paper (Fig. 2.32). It was presumed that false positive result obtained for the water sample can be caused by

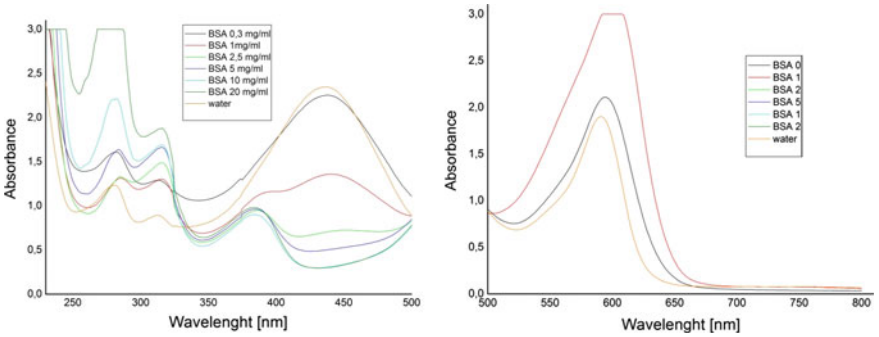

Fig. 2.28 Absorption spectrum for different concentrations of BSA, bromophenol blue method, tests in solution. Due to high intensity observed for concentrations above 1 mg/mL of BSA spectrum was divided in two ranges with higher concentrations masked for wavelengths above 500 nm

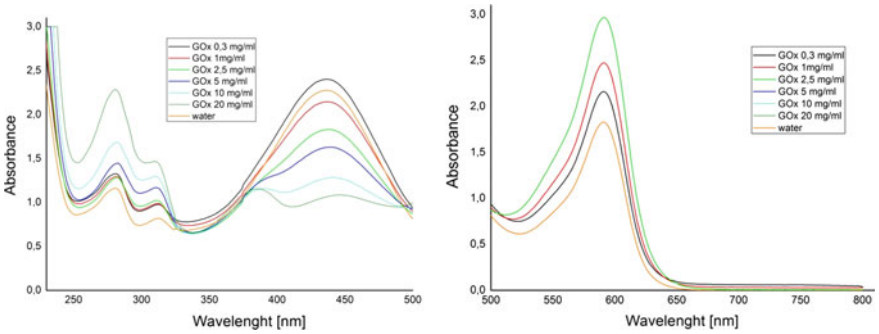

Fig. 2.29 Absorption spectrum for different concentrations of GOx, bromophenol blue method, tests in solution. Due to high intensity observed for concentrations above 2.5 mg/mL of GOx spectrum was divided in two ranges with higher concentrations masked for wavelengths above 500 nm

contamination of paper. Therefore a cleaning procedure was applied, including washing in methanol, methanol with ammonium hydroxide, methanol with acetic acid and distilled water, but even with such prepared paper the results remained unchanged. Tests in solution confirmed correct execution of the test.

Direct quantification-absorption spectra for BSA and GOx are shown in Figs. 2.33 and 2.34. Sensitivity is lower for GOx but clear dependence of absorbance at 280 nm with concentration can be seen for both compounds.

For tests on paper intensity around 280 nm is too low, but proteins can be quantified by the absorption peak at 200 nm (Figs. 2.35 and 2.36).

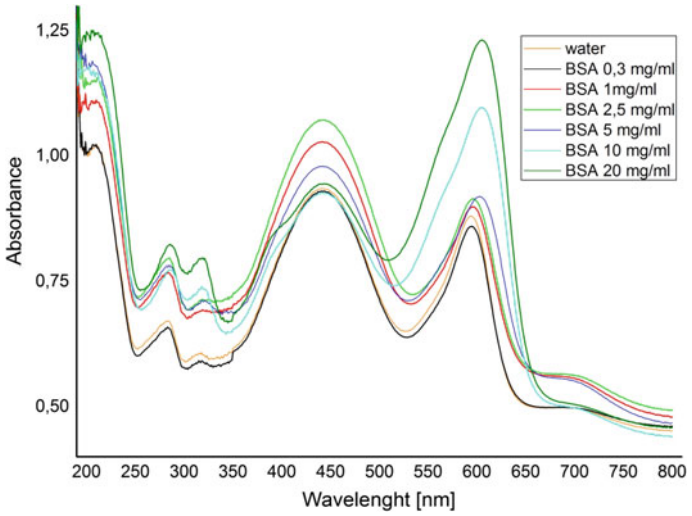

Fig. 2.30 Absorption spectrum for different concentrations of BSA, bromophenol blue method, tests on paper, BPB deposited with spray

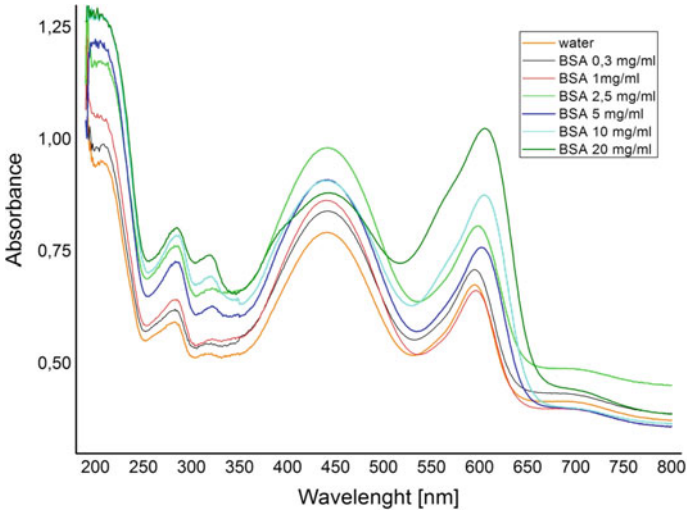

Fig. 2.31 Absorption spectrum for different concentrations of BSA, bromophenol blue method, tests on paper, BPB deposited with a pipette

Calibration curves were constructed for both BSA and GOx on paper using inclination of the spectrum in the region of 204–220 nm (N = 3). Data show linear dependence for concentrations between 0.3 and 5 mg/mL for BSA $y = -0.0031x + 0.0008$, $R^2 = 0.9961$, and for 1–20 mg/mL GOx $y = -0.0021x + 0.0004$, $R^2 = 0.9999$.

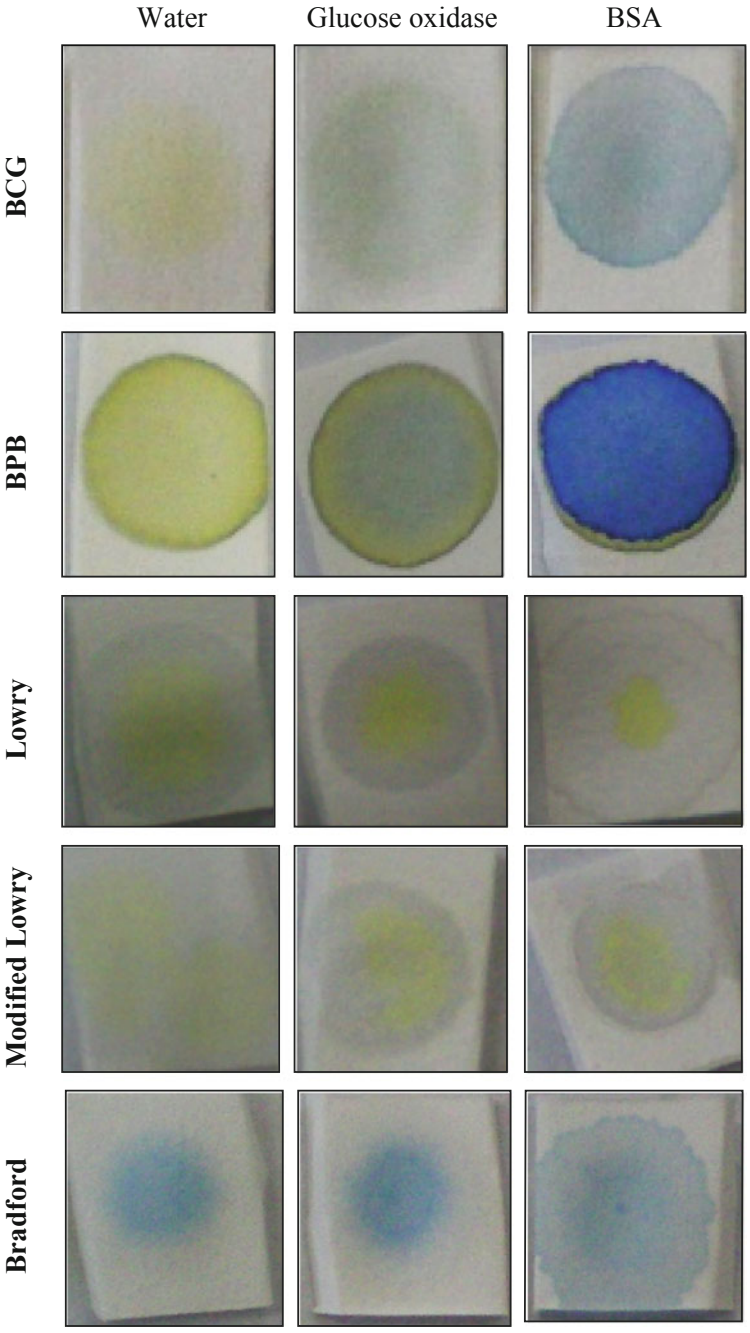

Fig. 2.32 Comparison of all methods for quantification of proteins, tests on paper

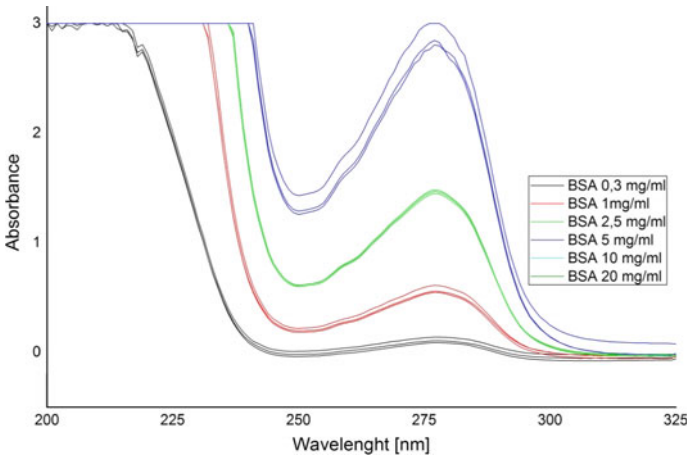

Fig. 2.33 Absorption spectrum for different concentrations of BSA, direct quantification, tests in solution

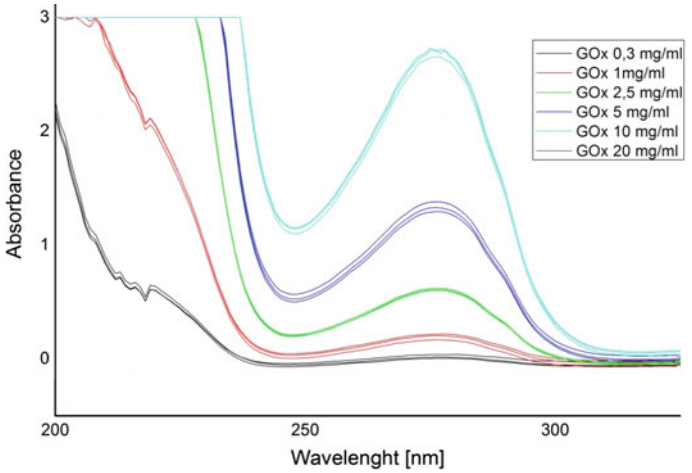

Fig. 2.34 Absorption spectrum for different concentrations of GOx, direct quantification, tests in solution

2.3.3.2 Enzymatic Activity, Optimization of Assay Conditions

Based on data presented in Fig. 2.37 subsequent tests were performed in pH 5.5. Highest activity and low standard deviation was observed for assay performed in this condition. Calibration curve for the amount of enzyme used for reaction, showed linearity in the region between 0.5 and 5 mg/mL, $y = 0.5x - 0.4$, $R^2 = 0.982$, $N = 3$. For immobilization studies 5 mg/mL enzyme concentration was chosen.

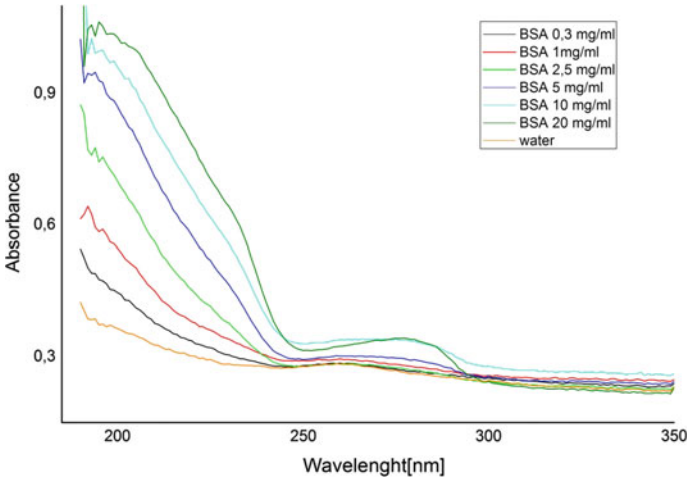

Fig. 2.35 Absorption spectrum for different concentrations of BSA, direct quantification, tests on paper

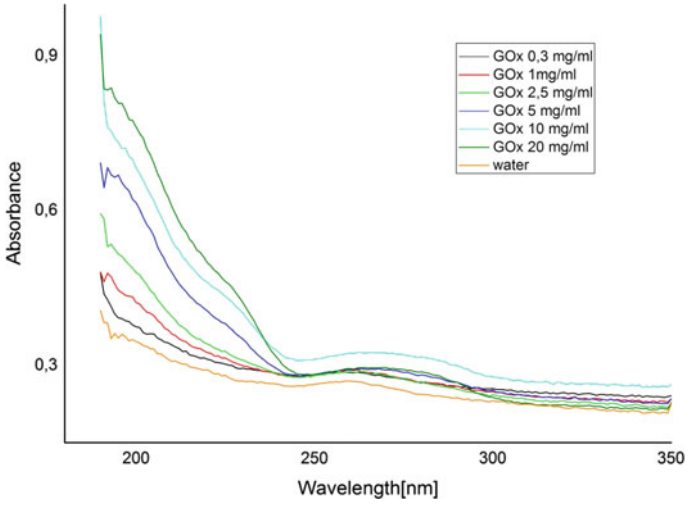

Fig. 2.36 Absorption spectrum for different concentrations of GOx, direct quantification, tests on paper

2.3.3.3 Enzyme Immobilization on Paper-Quantification of Proteins

Direct quantification was applied to confirm amount of protein present after immobilization. Each time before assessment of enzymatic activity paper devices were analyzed for the amount of protein present. Table 2.7 summarizes the results of quantification of protein for all the immobilization methods tested. After

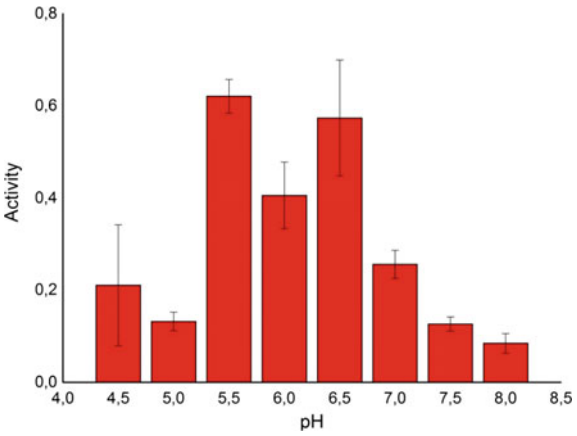

Fig. 2.37 Activity of enzymatic reaction depending on pH. Activity expressed as absorbance maximum in the range 570–580 nm. Standard deviation for N = 3

analyzing the standard deviation and comparing measured and theoretical protein content it can be clearly seen this method is only capable to quantify protein in case of: simple adsorption, adsorption on stearic acid, on PVA, with mannitol, entrapment in starch, chitosan, PVA, dextran, alginate, CMC and LbL sodium alginate-PEI technique (Table 2.7 blue marked methods). In case of encapsulation methods, and covalent linkage with washing steps higher standard deviation between the samples would be acceptable, but analysis of spectra (not shown) confirms that this method is not applicable. In the case of glutaraldehyde linkage it was noted that after just 3 days for samples stored in room temperature and 1 week for storage in 4 °C a new band appeared around 240 nm, which was accompanied by complete loss of activity. It clearly shows that the crosslinking reaction continues slowly deactivating the enzyme. High background signal was noted for: BSA blocking, adsorption on collagen, LbL alginate-chitosan, LbL alginate-polylysine, LbL Hyaluronic acid–chitosan, LbL hyaluronic acid–PEI, LbL poly(vinyl sulfate)–chitosan, LbL poly(acrylic acid)-chitosan, glutaraldehyde crosslinking with glycine blocking, EDC and EDC/NHS (Table 2.7 brown marked methods). Activation with potassium periodate, ethylenediamine and glutaraldehyde colored the paper and it was not possible to obtain spectra in the region of interest.

2.3.3.4 Impact of Enzyme Immobilization on Stability During Storage

Results of enzymatic activity will be analyzed using the theoretical quantity of protein used for preparation of samples. This fact should not have any impact on most of methods, apart from encapsulation, activation with potassium periodate, ethylenediamine and glutaraldehyde, as well as Schiff base method.

Figures 2.38, 2.39, 2.40, 2.41 and 2.42 resume the initial (24 h) activity of immobilization samples (N = 3) with normalized absorbance. Range of the results for the initial enzymatic activity was very large, two methods (LbL alginate-chitosan

Table 2.7 Theoretical and experimental protein content in samples prepared with different immobilization methods

				Theoretical protein concentration (mg protein/cm^2)	Average protein concentration measured (mg protein/cm^2)	St. dev. (N = 18)
Physicaladsorption		1	Simple adsorption	0.05	0.05	0.002
		2	BSA blocking	0.05	0.03	0.009
		3	On collagen	0.05	0.02	0.002
		4	On stearicacid	0.05	0.05	0.002
		5	On PVA	0.05	0.05	0.004
		6	With mannitol	0.05	0.06	0.002
		7	With trehalose	0.05	0.06	0.008
Entrapment in gel	Simple	8	In starch	0.05	0.05	0.002
		9	In chitosan	0.05	0.05	0.003
		10	In PVA	0.05	0.05	0.003
		11	In dextran	0.05	0.06	0.002
		12	In ammoniumalginate	0.05	0.05	0.002
		13	In CMC	0.05	0.05	0.003
	Layer-by-layer	14	Sodiumalginate—chitosan	0.05	0.04	0.019
		15	Sodiumalginate—polylysine	0.05	0.02	0.007
		16	Sodiumalginate—PEI	0.05	0.05	0.006
		17	Hyaluronicacid—chitosan	0.05	0.01	0.030
		18	Hyaluronicacid—PEI	0.05	0.04	0.003
		19	Poly(vinylsulfate)—chitosan	0.05	0.00	0.025
		20	Poly(acrylicacid)—chitosan	0.05	0.02	0.033
Covalentlinkage		21	Glutaraldehydecrosslinking	0.05	0.02	0.025
		22	Glutaraldehyde crosslinking with glycine blocking	0.05	0.02	0.005
		23	Schiffbase I	0.20	0.04	0.006
		24	EDC with glycine blocking	0.20	-0.02	0.029
		25	EDC/NHS II	0.20	0.01	0.020
		26	KIO_4, ethylenediamine, and glutaraldehyde activation	0.10	–	–
Encapsulation		27	Sodiumalginate II	unknown	0.04	0.007
		28	Sodiumalginate—CMC	unknown	0.02	0.025
		29	Sodiumalginate—chitosan	unknown	0.05	0.012
		30	PEI	unknown	–	–
		31	Covalent attachment to PEI capsules	unknown	–	–
		32	Covalent attachment to silica beads	unknown	0.05	0.007
		33	Chitosan	unknown	0.03	0.022

Possible protein quantification

High background signal prevents reliable quantification

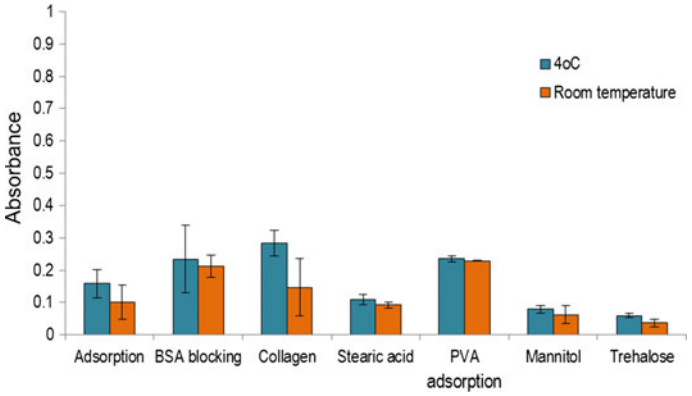

Fig. 2.38 Initial enzymatic activity of adsorption methods. Reprinted with permission from [129]

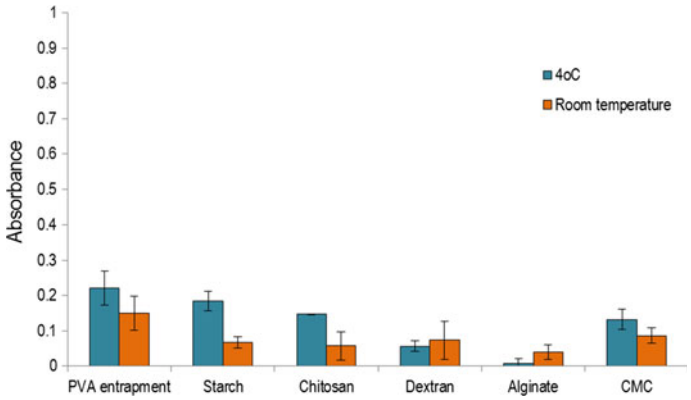

Fig. 2.39 Initial enzymatic activity of simple entrapment methods. Reprinted with permission from [129]

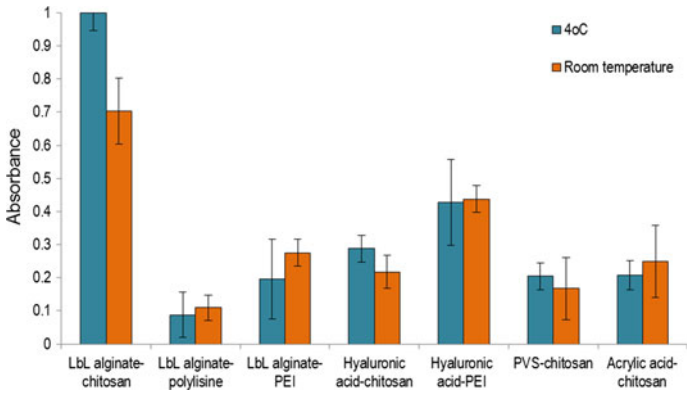

Fig. 2.40 Initial enzymatic activity of LbL entrapment methods. Reprinted with permission from [129]

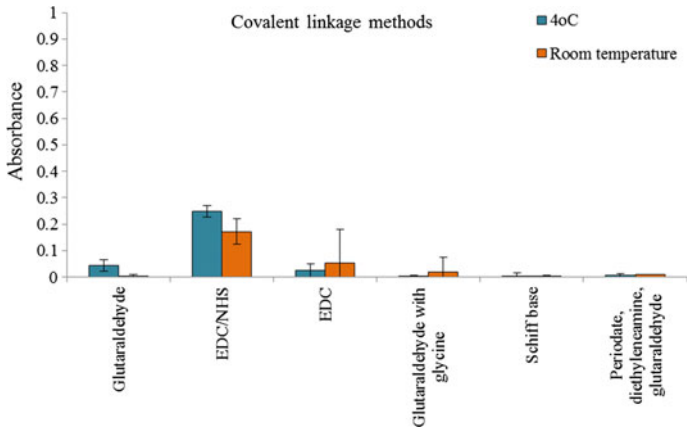

Fig. 2.41 Initial enzymatic activity of covalent linkage methods. Reprinted with permission from [129]

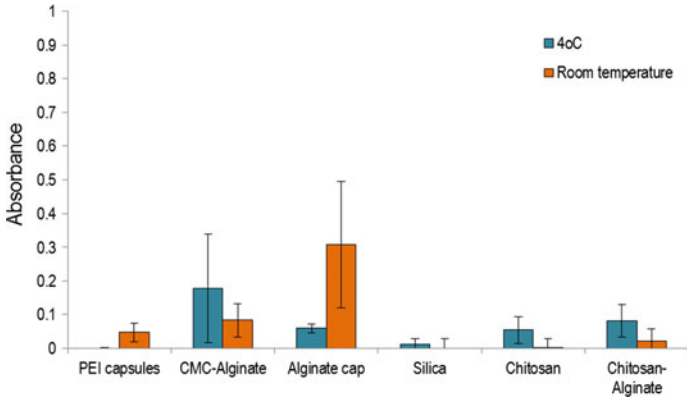

Fig. 2.42 Initial enzymatic activity of encapsulation methods. Reprinted with permission from [129]

and EDC/NHS) presented absorbance higher than the working range of the spectrophotometer (>3) in those two cases presented results are after 48 h.

Table 2.8 resumes the impact of storage temperature and time on enzymatic activity; results are shown as percentage of the initial activity observed for each method after 24 h. Methods in which activity dropped to 0 % after just 1 day of storage were not included in the summary.

Choice of enzyme immobilization method will depend mostly on the application, and the characteristic in question: long term stability, stability in room temperature, work in flow conditions, ease of preparation etc. Selected method should meet both catalytic (selectivity, stability, productivity) and non-catalytic (ease of separation, minimum leakage etc.) requirements. There is no general universally applicable

Table 2.8 Impact of time and temperature of storage on enzymatic activity. Reprinted with permission from [129]

				Day 1	Day 3	Week 1	Week 2	Week 3	Week 4	Week 5	Week 6	Week 7	Week 8	W 10	W 12	W14	W16	W 20	W 24
Physicaladsorption	1	Simple adsorption	4°C	>75 %			>50 %							>25 %			>10 %		<10 %
			RT	>75 %		>50 %	>25 %									>10 %		<10 %	
	2	BSA blocking	4°C	>75 %											>50 %			>25 %	>10 %
			RT	>75 %						>50 %					>25 %			<10 %	
	3	On collagen	4°C	>75 %			>50 %									>25 %			>10 %
			RT	>75 %				>50 %			>25 %							<10 %	
	4	On stearicacid	4°C	>75 %		>50 %					>25 %								<10 %
			RT	>75 %			>25 %				<10 %								
	5	On PVA	4°C	>75 %			>50 %								>25 %				<10 %
			RT	>75 %	>50 %		>25 %									>10 %		<10 %	
	6	With mannitol	4°C	>75 %				>50 %				>25 %						>10 %	<10 %
			RT	>75 %	>50 %				>25 %					<10 %					
	7	With trehalose	4°C	>75 %				>50 %				>25 %					>10 %		
			RT	>75 %					>50 %		>25 %			17 %		>10 %			
Entrapment in gel	8	In starch	4°C	>75 %					>50 %						>25 %				>10 %
			RT	>75 %							>50 %						>25 %		<10 %
	9	In chitosan	4°C	>75 %			>50 %					>25 %							<10 %
			RT	>75 %							>50 %					>10 %		<10 %	
	10	In PVA	4°C	>75 %	>50 %				>25 %									>10 %	<10 %
			RT	>75 %		>50 %										>10 %		<10 %	
	11	In dextran	4°C	>75 %													>50 %	>25 %	>10 %
			RT	>75 %		>50 %					>25 %					>10 %		<10 %	
	12	Ammonium alginate	4°C	>75 %	>25 %	<10 %													
			RT	>75 %		<10 %													
	13	In CMC	4°C	>75 %					>50 %	>25 %			>10 %					<10 %	
			RT	>75 %			>50 %							>25 %	>10 %			<10 %	

Table 2.8 (continued)

Layer-by-layer	14	Alginate—chitosan	4°C	>75 %		>50 %	>25 %			>10 %
			RT	>75 %	>50 %	>25 %			>10 %	<10 %
	15	Alginate—polylysine	4°C	>75 %		>50 %			>10 %	<10 %
			RT	>75 %		>50 %	>25 %	>10 %		<10 %
	16	Alginate—PEI	4°C	>75 %		>50 %				>10 %
			RT	>75 %	>50 %	>25 %	>10 %			<10 %
	17	HA-chitosan	4°C	>75 %	>50 %		>25 %		>10 %	<10 %
			RT	>75 %		>50 %	>25 %	>10 %	<10 %	
	18	Hyaluronica cid-PEI	4°C	>75 %		>50 %	>25 %		>10 %	<10 %
			RT	>75 %	>50 %	>25 %		>10 %		<10 %
	19	PVS-chitosan	4°C	>75 %	>50 %		>25 %		>10 %	<10 %
			RT	>75 %	>25 %			>10 %	<10 %	
	20	PAA-chitosan	4°C	>75 %		>50 %	>25 %		>10 %	<10 %
			RT	>75 %	>25 %		>10 %		<10 %	
Covalentlinlage	21	Glutaraldehyde	4°C	>75 %	<10 %					
			RT	>75 %	>50 %	<10 %				
	22	Schiffbase	4°C	>75 %		>50 %		>25 %	<10 %	
		II						%		
			RT	>75 %	<10 %					
	23	EDC I	4°C	>75 %		>50 %	>25 %		<10 %	
			RT	>75 %	>50 %	>10 %		<10 %		
	24	EDC with glycine	4°C	>75 %		>50 %		>25 %	>10 %	
			RT	>75 %	>25 %			>10 %	<10 %	
	25	EDC/NHS II	4°C	>75 %	>50 %		>25 %		>10 %	<10 %
			RT	>75 %	>50 %			>25 %	>10 %	<10 %
Encapsulation	26	Sodiumalginate II	4°C	>75 %	>50 %			<10 %		
			RT	>75 %	>25 %	<10 %				
	27	Alginate—CMC	4°C	>75 %		>50 %		>25 %	<10 %	
			RT	>75 %	>50 %			>10 %	<10 %	

method for enzyme immobilization, and also in this study it is difficult to cite one outstanding result.

For storage in 4 °C for periods up to 8 weeks simple adsorption in paper would probably be the choice. It shows rather low initial activity (~17 %) as compared with LbL sodium alginate-chitosan (highest initial activity of all the methods), but is extremely easy to prepare and does not require any other chemicals except the enzyme. All adsorption methods showed rather low initial activity (from 7 to 30 % as compared with LbL sodium alginate-chitosan method). BSA blocking method stands out, as it showed the longest storage stability regardless the temperature, it's easy to prepare and in resource limited settings powdered milk could be used instead of purified albumin.

In the case of entrapment methods very distinct results were observed for simple methods where enzyme was mixed with the polymer and LbL. For storage in lower temperatures entrapment in dextran would be the recommended method, it is simple, inexpensive and showed activity above 75 % of the initial value after 14 weeks (4 °C)—best results from all the methods tested.

Storage stability in room temperature was highest for entrapment in starch and chitosan (simple entrapment). Initial activity was even lower for the simple entrapment methods than for adsorption, probably because of the lesser accessibility of the enzyme when enclosed in polymer. Simple entrapment methods are extremely easy to prepare, on the contrary to LbL which require multiple addition steps and drying. Layer-by-layer methods, showed high initial activity, unfortunately deactivation progressed very fast. Highest initial activity from all the methods tested was observed for LbL sodium alginate-chitosan. This method retained more than 50 % of initial stability after 10 weeks for storage in 4 °C but only for 3 weeks when stored in room temperature. Longest stability was observed for LbL sodium alginate-PEI 60 % after 20 weeks (4 °C).

Covalent linkage on paper is extremely inconvenient, requires multistep preparation and it is almost impossible to wash out the chemicals after reaction. Chemical residues can cause interference in posterior applications or slowly deactivate the enzyme as it was seen in case of glutaraldehyde crosslinking. Some treatments (oxidation with periodate, prolonged submersion etc.) affect the physical properties of paper, making it easier to tear, or compromising its flexibility. If despite this covalent linkage would be the method of choice EDC/NHS presented best results in this group. It retained 50 % of activity after 8 weeks of storage at room temperature.

Capsules produced in our laboratory by the syringe method were rather big: sodium alginate ~ 1.5 mm; sodium alginate-CMC ~ 2–2.5 mm; sodium alginate-chitosan ~ 4 mm (Fig. 2.43). Size of those capsules could be diminished by using other encapsulation methods like spray drying, but specialized equipment would be necessary. Chitosan capsules produced by interphase polymerization were smaller 0.5–1 mm. Small capsules and silica beads did not hold to paper, and could be used to produce bioactive paper when mixed in pulp. After complete drying, capsules changed their form becoming flat and completely covered the surface of paper. Inconsistent results were found for encapsulation in alginate with much

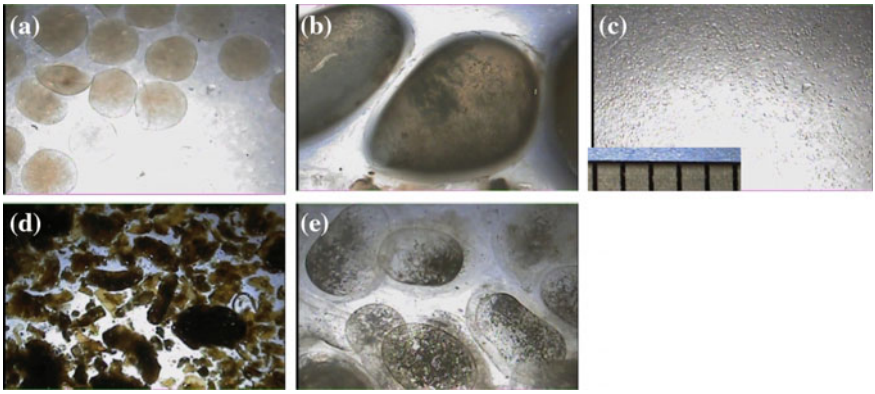

Fig. 2.43 Microscopic images of capsules produced during this study. **a** Sodium alginate. **b** Sodium alginate-chitosan, **c** Covalent linkage to silica capsules, **d** Chitosan, **e** Sodium alginate-CMC; scale in mm for all images marked on **c**

higher initial activity for storage in room temperature, this can be explained by the incapability to relate the activity with quantity of enzyme present in each sample, high standard deviation was also observed in this case. Method of choice would be encapsulation in sodium alginate-CMC as it retained more than 50 % of activity after 8 weeks of storage in room temperature.

No methods showed satisfactory results after 24 weeks of storage. This study showed that protective agents such as sugars, that are widely used to prolong shelf life of enzymes stored in solution have no positive impact on storage stability of glucose oxidase on paper, blocking agents such as glycine or BSA should be used instead (Table 2.8).

2.3.3.5 Impact of Enzyme Immobilization on Flow in Paper Channel

In the colorimetric method the measurement error grows with time of the experiment, as the borders of the dye spot travelling through paper channel become more and more diffused (Fig. 2.44). Distance/time plot (not shown) demonstrates that the

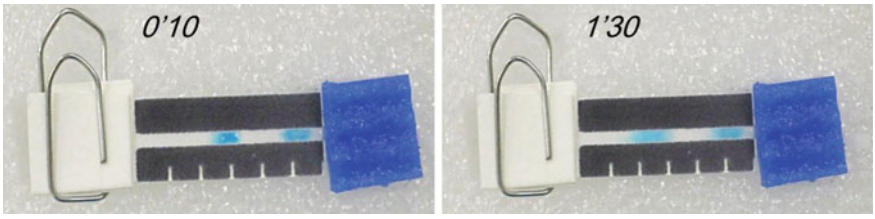

Fig. 2.44 Photograph of the device after 10 and 90 s from application of the dye

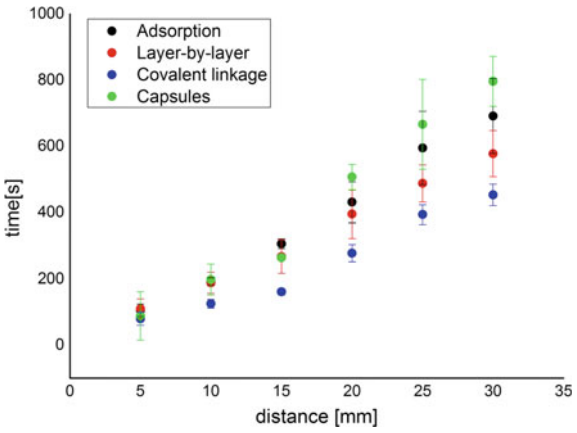

Fig. 2.45 Flow velocity in a bioactive paper-channel. Reprinted with permission from [128]

flow is most slowed down in case of covalent linkage. Other methods of immobilization result in similar velocity but adsorption showed the lowest reproducibility.

In the case of electrochemical method, on the contrary to the colorimetric attempt the fastest flow was observed for the covalent linkage. Unfortunately, the chemical residue present after immobilization resulted in much higher background signal (baseline ~ 25 nA) in comparison with other immobilization methods (~0.5–2.5 nA). This chemical residue could be the cause of slowness observed in the colorimetric attempt. The second fastest was Layer-by-layer method, which also presented the highest linearity. Flow velocity in a channel with adsorbed enzyme and microcapsules was similar (Single Factor Anova $F < F_{crit}$). In some cases capsules upon drying partially clogged the channel. Adsorption was the least reproducible method in both measurements. Results of the electrochemical measurement are presented in Fig. 2.45.

2.3.3.6 Michaelis-Menten Kinetics

Table 2.9 summarizes the calculated values of V_{max} and Km for free and immobilized GOx. Only methods considered most promising were tested in this study. All immobilization methods showed increase in the Km value as compared with the free enzyme. It can be related to the lower accessibility of the active sites of immobilized GOx.

Lesser Km value indicates higher affinity of enzyme and substrate, which results in faster response. The lowest increase was noted for EDC/NHS method (2.8 times higher) which could be explained by the fact that covalent linkage methods tend to specific orientation of the enzyme. Entrapment in starch and BSA blocking showed the highest increase of Km (6.6 and 5.4 times respectively). Optimization of the

Table 2.9 Kinetic parameters for free and immobilized GOx

	Km (mmol/L)	V_{max} ((μmol/L)/min)
In solution	2.9	8.7
Adsorption	11.1	4.8
BSA blocking	15.8	3.8
Entrapment in PVA	10.6	4.9
Entrapment in starch	19.0	5.4
LbL sodium alginate-chitosan	12.6	4.5
Lbl hyaluronic acid–PEI	9.0	5.1
Covalent linkage EDC/NHS	8.1	5.2

amount of BSA and the concentration of starch should be considered in those cases, as to retain their impact on stability but reduce the accessibility effects.

V_{max} describes the velocity with which the substrate occupies all active sites of all the enzyme molecules. Decrease of V_{max} in all cases shows that no simple inhibition is taking place (competitive inhibition $-V_{max}$ remains constant, uncompetitive inhibition $-V_{max}$ decreases but Km remains constant, competitive inhibition–both Km and V_{max} decrease), nevertheless mixed inhibition effects can still be present.

2.3.4 Electrochemical Detection

2.3.4.1 Analysis of Glucose and Uric Acid

Optimization of Device's Architecture

In order to maximize the electrochemical response, several channel architectures were analyzed. Architectures were chosen in a way as to change the time of reaction of the analyte with enzyme deposited always in the middle of the channel, and the velocity with which hydrogen peroxide reaches the electrode. Results of computer modeling and chronoamperometric measurements are resumed in Fig. 2.46. Results of computer modeling demonstrate how water (blue) is substituted by another liquid of concentration 1 mol/L (red). Purpose of the visualization was to show the flow front (rounded or perpendicular), diffusion zone etc. and not velocity which was one of the input data (pressure difference).

In a straight channel (Fig. 2.46) straight flow front is observed, with constant velocity throughout the channel. Chronoamperometric analysis shows good separation of both compounds, with two broadened peaks and analysis time of 30 min. In architecture "Wide-narrow", flow has a constant velocity till the enzymatic reaction zone, after which channel narrows therefore higher speed is obtained when reaching the electrode. Peaks are still broadened, but the time of analysis is slightly

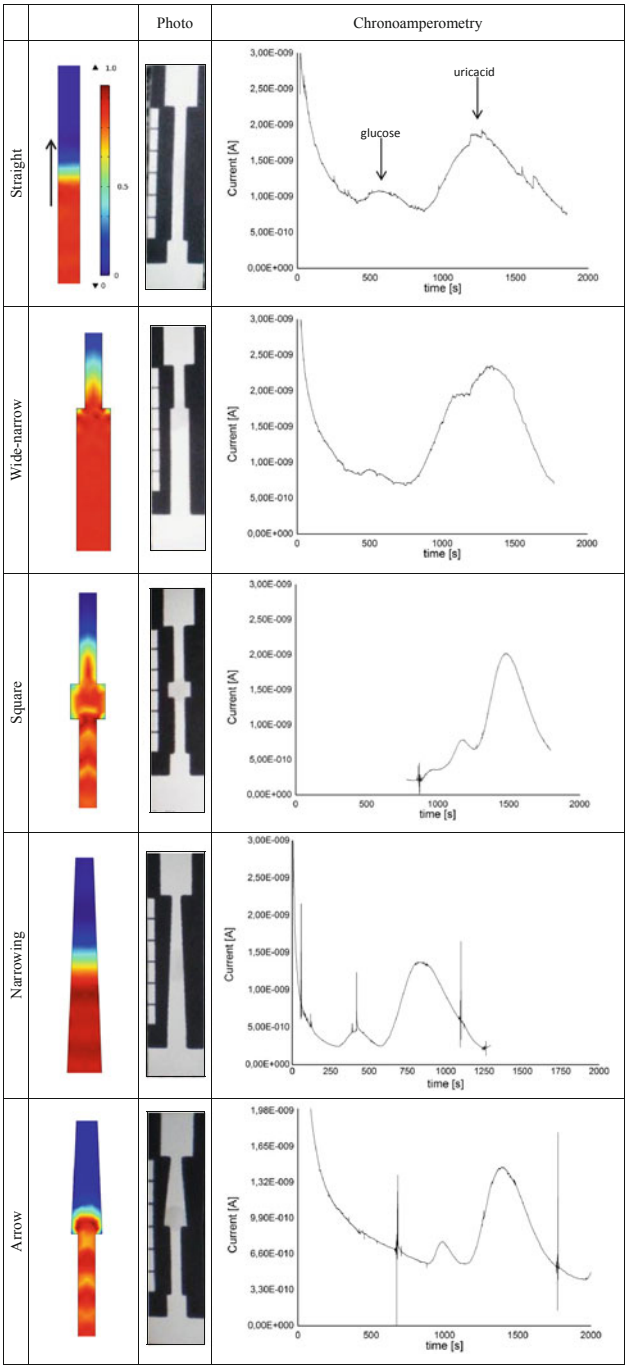

Fig. 2.46 Results of computer modeling and chronoamperometric measurements for different channel architectures. Reprinted with permission from [128]

shorter. Interesting is also the wider diffusion zone observed in architecture "Wide-narrow" as compared with other types of channels. In architecture "Square", flow is being slowed down inside a wider, square enzymatic reaction zone, and accelerates again after leaving it. Peaks are partially superimposed but the time of analysis drops to around 16 min. In architecture "Narrowing" flow gets gradually faster along the channel. Chronoamperometric measurements showed the shortest time necessary for both peaks to appear ($\sim$15 min). It is worth noting that architecture "Narrowing" conserves the straight, perpendicular flow front of a straight channel weather other architectures do not. In architecture "Arrow" flow slows down entering the enzymatic reaction zone and later gradually accelerates. Peaks are well separated with around 18 min time of analysis.

Architectures "Narrowing" and "Arrow" were subjected to more detailed tests and due to greater reproducibility "Narrowing" channel was used in subsequent experiments.

The intensity of the signal was not commented because, as it will be seen later, on this stage it mainly depends on positioning on the electrode.

Preliminary Test Destined to Construct a Calibration Curve

Repeatability of the obtained signal was too low to construct a calibration curve. Not only the intensity of peaks differed but also the relative position and time needed for analysis. It was noted that flow on each device is slightly different, especially during wetting of the enzymatic zone. During spotting, solution wicks differently each time depending on the arrangement of fibers. This characteristic is especially visible when numerous layers are being deposited.

Uniformity of Enzyme Immobilization

When paper is dipped, fibers are covered uniformly with the solution. Thus this method was used to deposit enzyme on paper. Unfortunately in this case part of the channel has to be cut-out to perform the immobilization. When pieces simply overlap and are hold by means of an adhesive tape (Fig. 2.11a) they tend to deflect upon wetting. In this way contact is not uniform over the entire width of the channel. Exerting more pressure by means of paper clips and a device holder (Fig. 2.11b), does not solve the problem if the channel remains loose. Flow is greatly enhanced in channels covered with a small piece of plastic, or stacked between two plastic slips, due to capillarity between paper and the cover and not only through the paper fibers. In this way time of reaction is too short to obtain satisfactory signal for glucose. Flow was even faster when pressure was exerted on top of the channel (Fig. 2.11d) as compared with pressure on the sides (Fig. 2.11c). Best results were obtained for the device in which small incisions were made in the middle of the channel and pieces were interwoven (Fig. 2.11e). In this case pressure

was exerted not only on the sides (adhesive tape) but also in the middle of the channel, allowing reproducible wetting.

Nevertheless, even after solving the problem of flow through the bioactive area, device continued to present large discrepancies between individual systems.

Electrode Positioning

As it can be seen of Fig. 2.47 it is necessary to develop a more elaborate positioning method, to ensure repeatability of the results. Peaks obtained after repositioning of the electrode are 2–3 times lower than the ones registered before. Differences exist also between peaks obtained with the same position of the electrode, for example the first three peaks differ in height, peak width at ½ height and therefore area. But those differences could be diminished by more accurate spotting of the sample.

In the next step various manners of repeatable electrode positioning were proposed. In the case of sponge holders tested during the experiments it was not possible to obtain repeatable results, as paper was deflecting when becoming wet. When electrode was positioned on top, paper would deflect from the electrode resulting in lack of electrical contact, and too high pressure resulted in tears. Results were not repeatable even when the electrode area of the channel was supported on a slip of plastic placed in the sponge holder. This fact can be attributed to fibrous structure of paper, which results in electrode tip positioning on top or between the fibers. Similar problems (deflection, tears) were observed when the electrode was placed under the paper device (Fig. 2.12a).

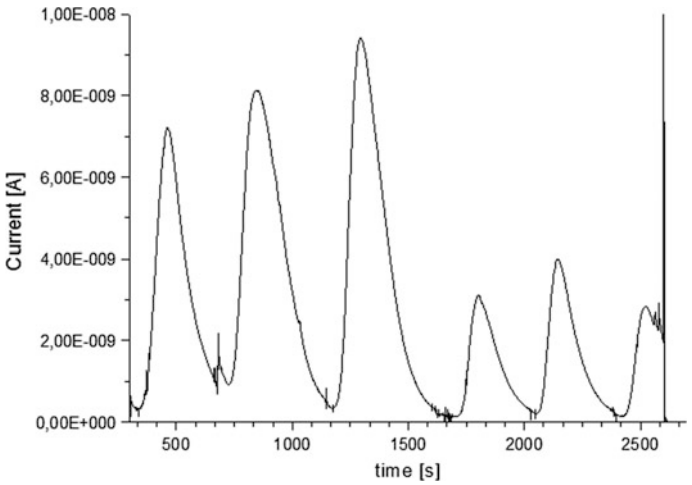

Fig. 2.47 Signal repeatability for consecutive injections of 10 mmol/L uric acid solution. After three injections electrode was lifted and repositioned

A Pt wire was used instead of a capillary enclosed microelectrode, allowing new configurations. First the wire was stacked across the width of the channel (Fig. 2.12b), but again wet paper would twist and deflect from the electrode, resulting in lack of electrical contact, regardless if the wire was positioned on top or bottom side of the channel. When electrode was enclosed between two layers of plastic measurements became repeatable. Unfortunately, obtained signal was characterized by high background and noise. Next, a small orifice was made 3 mm from the end of the channel, and Pt wire was gently forced through (Fig. 2.12c). In this way paper surrounds the circumference of the electrode, resulting in repeatable contact. After promising results calibration curve was constructed.

Calibration Curve

Glucose: After optimization of the device (Fig. 2.48) it was possible to construct a calibration curve, presenting good linearity ($R^2 = 0.980$) in all examined range (2.0–10.0 mmol/L). Calibration curve (Fig. 2.49) is described by equation $y = 2.22 (\pm 0.14) \cdot 10^{-6}x - 2.01(\pm 0.83) \cdot 10^{-6}$, N = 3. Limit of detection, estimated as the concentration of the analyte giving a signal equal 3 × the standard deviation of the blank is equal 1.4 mmol/L.

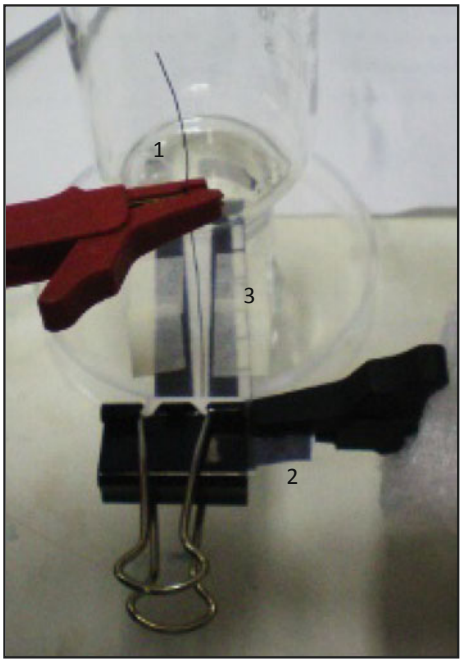

Fig. 2.48 Final device for the detection of glucose and uric acid. *1*. Pt wire working electrode, *2*. reference electrode drawn with a pencil, *3*. bioactive channel

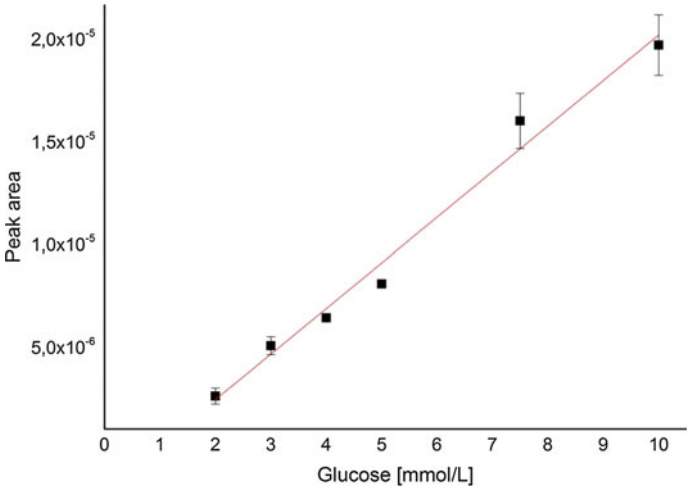

Fig. 2.49 Calibration curve for glucose–electrochemical method, lateral flow assay, with bioactive channel, immobilization by means of layer-by-layer (potential 0.7 V, 1 μL of sample). Reprinted with permission from [128]

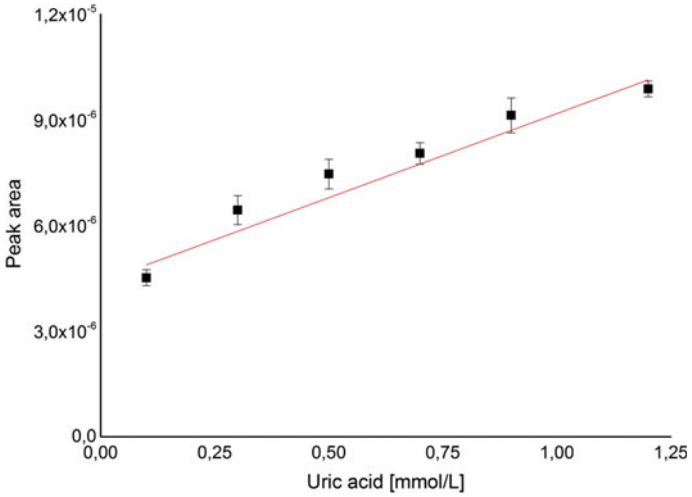

Fig. 2.50 Calibration curve for uric acid–electrochemical method, lateral flow assay, with bioactive channel, immobilization by means of layer-by-layer (potential 0.7 V, 1 μL of sample). Reprinted with permission from [128]

Uric acid: It was possible to construct a calibration curve, presenting good linearity ($R^2 = 0.958$) in all examined range (0.1–1.2 mmol/L). Calibration curve (Fig. 2.50) is described by equation $y = 4.78(\pm 0.44) \cdot 10^{-6}x + 4.40(\pm 0.34) \cdot 10^{-6}$, N = 3.

2.3.4.2 Analysis of Glucose, Cholesterol and Uric Acid

Architecture

Assembly of the devices shown in Fig. 2.13 proved difficult as the parts were small and delicate. Papers of different thickness were tested. Thickness of sample and detection pads did not impact the assembly but the bioactive channels were easier to set up when made from thicker paper (Whatman n°3).

Two assembly methods were proposed. In the case of threading incisions were made on both sides of the bioactive channels and each channel was forced through a small orifice in the sample and conjugation pads. This type of assembly proved to be more secure and would not dismantle upon usage. In the other device proposed, incisions were made only on one side of the channels, and sample and conjugation pads had fitting angular incisions. Device prepared in this way was easier to assembly, and channels would not tear or crumple so often but it was prone to dismantle upon usage. No inconsistencies were noted between devices of the same type upon wetting of the channels. More secure contact between pieces of paper of the threaded device allowed for faster wetting of consecutive parts. Threaded device was chosen for subsequent tests.

Conservation of Laminar Flow

As it can be seen on Fig. 2.51 regardless the architecture of the channel laminar flow is maintained after the junction. Diffusion is present on the boundary between two flowing solutions but apart from that flow is undisturbed till the end of the channel, which confirms the possibility of application of two electrode system.

Preliminary Tests and Optimization of the Architecture

After modification of the one electrode system and inclusion of two constrictions it was possible to obtain signal as seen in Fig. 2.52. Three maximums are visible in

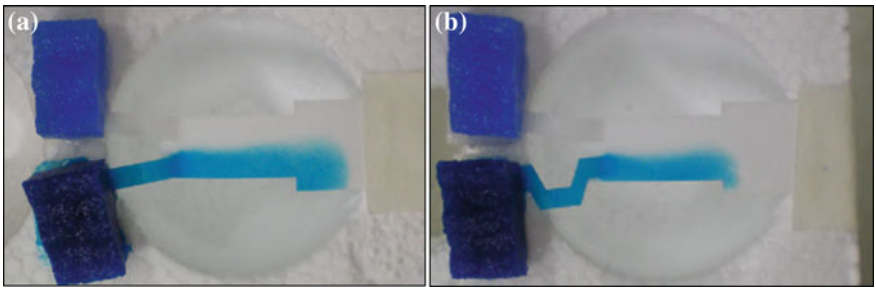

Fig. 2.51 Visualization of laminar flow upon leaving of the channel

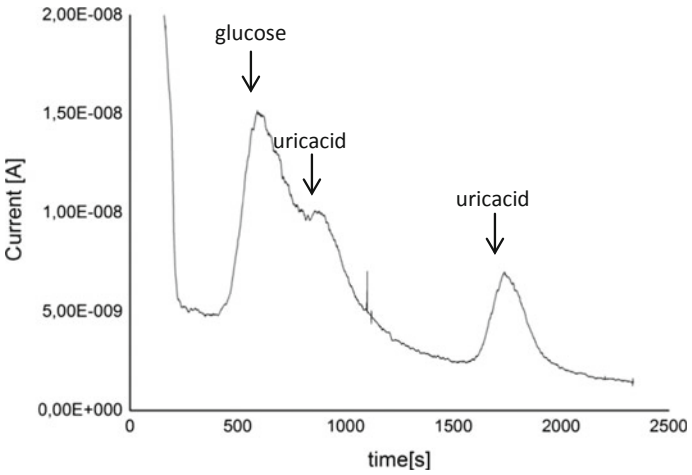

Fig. 2.52 Response of one electrode system, mixed sample glucose and uric acid

the graph, associated with uric acid (two maximums) and glucose (one) which proves that use of a one electrode system with channels of different length would be a promising solution to detect all three compounds.

It was not possible to detect cholesterol in any of the experiments. Probably another carrier solution should be used to move cholesterol molecules across paper matrix (addition of surfactant, organic solvent etc.). Additional tests confirmed activity of cholesterol oxidase used in this study.

2.4 Partial Conclusions

Table 2.10 resumes parameters of calibration curves obtained for devices with both types of detection. Only as a reminder, normal levels of compounds of interests are: glucose 3.5–5.3 mmol/L (blood), 0.1–0.8 mmol/L (urine), cholesterol 5.2 mmol/L (blood), uric acid 0.1–0.4 mmol/L (blood), 1.5–4.4 mmol/L (urine). Therefore proposed devices with colorimetric detection at current stage of development could be applied for the quantification of all compounds in blood, but in the case of borderline high levels of cholesterol and glucose only providing qualitative response. Regardless this shortcoming this kind of sensor still can be applied as an initial point of care screening device quantifying normal levels of compounds of interest or indicating the need of more specialized assistance in case of higher concentrations. In order to increase the working range of this sensor other geometry, with greater surface area of the detection zone could be applied. Inversely to the test with blood in the case of urine, device would be able to quantify glucose in all range, even for higher than normal levels, but the working range for high concentrations of uric acid would have to be increased.

Table 2.10 Analytical parameters of developed systems with colorimetric and electrochemical detection. Presented range in mmol/L

	Colorimetric detection			Electrochemical detection		
	Equation	R^2	Range	Equation	R^2	Range
Glucose	$y = 11.97 \pm 1.25x + 3.7 \pm 2.6$	0.938	0.2–5.0	$y = 2.22(\pm 0.14) \cdot 10^{-6}x - 2.01(\pm 0.83) \cdot 10^{-6}$	0.980	2.0–10.0
Cholesterol	$y = 17.08 \pm 0.74x + 0.33 \pm 0.49$	0.991	1.0–5.0	–	–	–
Uric acid	$y = 12.7 \pm 0.44x + 4.4 \pm 0.30$	0.993	0.1–2.5	$y = 4.78(\pm 0.44) \cdot 10^{-6}x + 4.40(\pm 0.34) \cdot 10^{-6}$	0.958	0.1–1.2

System with electrochemical detection could quantify both uric acid and glucose in blood but for test with urine would have to be optimized for lower concentrations of glucose (i.e. longer enzymatic reaction time) and higher concentrations of uric acid (i.e. other electrode material).

Sensitivity is not the only consideration when choosing the best detection method. Preliminary tests were performed with real samples (results not shown) in order to indicate future steps of development. Electrochemical detection can be affected by fouling of proteins on the electrode surface, resulting in higher background current and lower detection signal. It is also prone to interference related to detection of other electroactive compounds present in the sample. Furthermore other species present in the sample could react with hydrogen peroxide formed upon enzymatic reaction before it can be detected on the electrode. In the case of colorimetric detection the biggest concern is the color of the sample. Probably delicate coloration due to urine samples would not affect results obtained with proposed starch-iodide method, but intense color associated with red blood cells would surely have a negative impact on sensitivity. To overcome this obstacle sampling zone could be modified with agglutination antibodies, or fabricated from a plasma separation membrane.

One issue arises from the developments described above—device would have to work in flow conditions, therefore the problem of cholesterol retention on paper would have to be solved. In order to move cholesterol from the sampling layer, an organic solvent could be used or surfactant added to the running buffer. Cholesterol oxidase modified paper could be also in direct contact with the sampling pad, in this way enzyme could react with cholesterol in the sampling area and later only hydrogen peroxide would flow to the detection zone. This type of construction could result in interference observed in uric acid and glucose assays due to hydrogen peroxide originating from the cholesterol reaction, therefore another architecture would have to be proposed. Layers of the device could function as flaps, and in this way alternately be moved to contact specified areas of the device.

Apart from the device also the detection system should be considered. For resource limited setting one-component systems are preferred. With two components, namely a disposable test and a reader, it is highly possible that the system will not function due to lack of supplies (disposable tests) or malfunction of the equipment and absence of technical support. In the case of electrochemical systems efforts are being made to develop ever more affordable but not less reliable readers but still with this kind of detection some kind of specialized equipment will always be necessary. Detection system could be disposable together with the test but this kind of one-component integration of electrochemical devices is not always possible for a reasonable price. When thinking of colorimetric system, equipment free quantitative detection can be accomplished by appropriate design of the device (distance or time-based detection). Cell phone cameras and downloadable software could also be used for intensity-based quantification. In this way detector of this two-component system could be easily replaced by another telephone, by simply installing appropriate software.

Summarizing, for extremely low cost applications, in order to reach wider public and be applicable in real-life situations system should be self-contained and one component, use unprocessed sample, not require any specialized training and be easy to interpret. Based on the results obtained during this work, in the nearest future abovementioned requisites would be met easier with colorimetric systems.

References

1. Galant a. L, Kaufman RC, Wilson JD (2015) Glucose: detection and analysis. Food Chem 188:149–160. doi:10.1016/j.foodchem.2015.04.071
2. WHO Diabetes WHO Fact sheet. http://www.who.int/mediacentre/factsheets/fs312/en/. Accessed 1 June 2015
3. Dungchai W, Chailapakul O, Henry CS (2009) Electrochemical detection for paper-based microfluidics. Anal Chem 81:5821–5826. doi:10.1021/ac9007573
4. Perez-Ruiz F, Dalbeth N, Bardin T (2014) A review of uric acid, crystal deposition disease, and gout. Adv Ther 32:31–41. doi:10.1007/s12325-014-0175-z
5. Lakshmi D, Whitcombe MJ, Davis F et al (2011) Electrochemical detection of uric acid in mixed and clinical samples: a review. Electroanalysis 23:305–320. doi:10.1002/elan.201000525
6. Dungchai W, Chailapakul O, Henry CS (2010) Use of multiple colorimetric indicators for paper-based microfluidic devices. Anal Chim Acta 674:227–233. doi:10.1016/j.aca.2010.06.019
7. Morzycki JW (2014) Recent advances in cholesterol chemistry. Steroids 83:62–79. doi:10.1016/j.steroids.2014.02.001
8. Birtcher KK, Ballantyne CM (2004) Cardiology patient page. Measurement of cholesterol: a patient perspective. Circulation 110:e296–e297. doi:10.1161/01.CIR.0000141564.89465.4E
9. Ding S-N, Shan D, Zhang T, Dou Y-Z (2011) Performance-enhanced cholesterol biosensor based on biocomposite system: Layered double hydroxides-chitosan. J Electroanal Chem 659:1–5. doi:10.1016/j.jelechem.2011.04.003
10. MacLachlan J, Wotherspoon a. TL, Ansell RO, Brooks CJW (2000) Cholesterol oxidase: sources, physical properties and analytical applications. J Steroid Biochem Mol Biol 72:169–195. doi:10.1016/S0960-0760(00)00044-3
11. Steiner M-S, Duerkop A, Wolfbeis OS (2011) Optical methods for sensing glucose. Chem Soc Rev 40:4805–4839. doi:10.1039/c1cs15063d
12. Newman JD, Turner APF (2005) Home blood glucose biosensors: a commercial perspective. Biosens Bioelectron 20:2435–2453. doi:10.1016/j.bios.2004.11.012
13. Heller A, Feldman B (2008) Electrochemical glucose sensors and their applications in diabetes management. Chem Rev 108:2482–2505
14. Information on EC 1.7.3.3—factor-independent urate hydroxylase. http://www.brenda-enzymes.org/enzyme.php?ecno=1.7.3.3. Accessed 3 June 2015
15. Kanďár R, Drábková P, Hampl R (2011) The determination of ascorbic acid and uric acid in human seminal plasma using an HPLC with UV detection. J Chromatogr B: Anal Technol Biomed Life Sci 879:2834–2839. doi:10.1016/j.jchromb.2011.08.007
16. Steel E (1958) The determination of uric acid in biological materials. Biochem J 68:306–309
17. Piermarini S, Migliorelli D, Volpe G et al (2013) Uricase biosensor based on a screen-printed electrode modified with Prussian blue for detection of uric acid in human blood serum. Sensors Actuators, B Chem 179:170–174. doi:10.1016/j.snb.2012.10.090
18. Ca X, Kalcbeb K, Neuhold C, Owrevc B (1994) An improved voltammetric method for the determination of trace amounts of uric acid with electrochemically pretreated carbon paste electrodes. Talanta 3:407–413

19. Zen J-M, Hsu C-T (1998) A selective voltammetric method for uric acid detection at Nafion®-coated carbon paste electrodes. Talanta 46:1363–1369
20. Shankar SS, Swamy BEK, Chandrashekar BN, Gururaj KJ (2013) Sodium do-decyl benzene sulfate modified carbon paste electrode as an electrochemical sensor for the simultaneous analysis of dopamine, ascorbic acid and uric acid: a voltammetric study. J Mol Liq 177:32–39
21. Ramirez-Berriozabal M, Galicia L, Gutierrez-Granados S et al (2008) Selective electrochemical determination of uric acid in the presence of ascorbic acid using a carbon paste electrode modified with b-cyclodextrin. Electroanalysis 20:1678–1683
22. Amiri M, Bezaatpour A, Pakdel Z, Nekoueian K (2012) Simultaneous voltammetric determination of uric acid and ascorbic acid using carbon paste/cobalt Schiff base composite electrode. J Solid State Electrochem 16:2187–2195
23. Burke RW, Diamondstone BI, Velapoldi R a, Menis O (1974) Mechanisms of the Liebermann Burchard and Zak color reactions for cholesterol. Clin Chem 20:794–801
24. Li X, Liu X (2014) Fabrication of three-dimensional microfluidic channels in a single layer of cellulose paper. Microfluid Nanofluidics 1:1–9. doi:10.1007/s10404-014-1340-z
25. Fung KK, Chan CPY, Renneberg R (2009) Development of enzyme-based bar code-style lateral-flow assay for hydrogen peroxide determination. Anal Chim Acta 634:89–95. doi:10.1016/j.aca.2008.11.064
26. Allen MP, DeLizza A, Ramel U et al (1990) A noninstrumented quantitative test system and its application for determining cholesterol concentration in whole blood. Clin Chem 36:1591–1597
27. Allen MP (1995) Laminated assay device. United States Patent 5409664, 15:1–15
28. Chen X, Chen J, Wang F et al (2012) Determination of glucose and uric acid with bienzyme colorimetry on microfluidic paper-based analysis devices. Biosens Bioelectron 35:363–368. doi:10.1016/j.bios.2012.03.018
29. Kumar A, Hens A, Arun RK et al (2015) A paper based microfluidic device for easy detection of uric acid using positively charged gold nanoparticles. Analyst 140:1817–1821. doi:10.1039/C4AN02333A
30. Deng L, Chen C, Zhu C et al (2014) Multiplexed bioactive paper based on GO@SiO2@CeO2 nanosheets for a low-cost diagnostics platform. Biosens Bioelectron 52:324–329. doi:10.1016/j.bios.2013.09.005
31. Zhu WJ, Feng DQ, Chen M et al (2014) Bienzyme colorimetric detection of glucose with self-calibration based on tree-shaped paper strip. Sensors Actuators, B Chem 190:414–418. doi:10.1016/j.snb.2013.09.007
32. Noh H, Phillips ST (2010) Fluidic timers for time-dependent, point-of-care assays on paper. Anal Chem 82:8071–8078. doi:10.1021/ac1005537
33. Demirel G, Babur E (2014) Vapor-phase deposition of polymers as a simple and versatile technique to generate paper-based microfluidic platforms for bioassay applications. Analyst 139:2326–2331. doi:10.1039/c4an00022f
34. Garcia PDT, Cardoso TMG, Garcia CD et al (2014) A handheld stamping process to fabricate microfluidic paper-based analytical devices with chemically modified surface for clinical assays. RSC Adv 4:37637–37644. doi:10.1039/C4RA07112C
35. Carrilho E, Martinez AW, Whitesides GM (2009) Understanding wax printing a simple micropatterning process for paper based Microfluidics.pdf. 81:7091–7095
36. Cate DM, Dungchai W, Cunningham JC et al (2013) Simple, distance-based measurement for paper analytical devices. Lab Chip 13:2397–2404. doi:10.1039/c3lc50072a
37. Ornatska M, Sharpe E, Andreescu D, Andreescu S (2011) Paper bioassay based on ceria nanoparticles as colorimetric probes. Anal Chem 83:4273–4280. doi:10.1021/ac200697y
38. Carvalhal RF, Kfouri MS, Piazetta MHDO et al (2010) Electrochemical detection in a paper-based separation device. Anal Chem 82:1162–1165. doi:10.1021/ac902647r
39. Liu H, Crooks RM (2012) A paper-based electrochemical sensing platform with integral battery and electrochromic read-out. Anal Chem 84:1–3. doi:10.1021/ac203457h

40. Labroo P, Cui Y (2014) Graphene nano-ink biosensor arrays on a microfluidic paper for multiplexed detection of metabolites. Anal Chim Acta 813:90–96. doi:10.1016/j.aca.2014.01.024
41. Ruecha N, Rangkupan R, Rodthongkum N, Chailapakul O (2014) Novel paper-based cholesterol biosensor using graphene/polyvinylpyrrolidone/polyaniline nanocomposite. Biosens Bioelectron 52:13–19. doi:10.1016/j.bios.2013.08.018
42. Zhao C, Thuo MM, Liu X (2013) A microfluidic paper-based electrochemical biosensor array for multiplexed detection of metabolic biomarkers. Sci Technol Adv Mater 14:054402. doi:10.1088/1468-6996/14/5/054402
43. Nie Z, Deiss F, Liu X et al (2010) Integration of paper-based microfluidic devices with commercial electrochemical readers. Lab Chip 10:3163–3169. doi:10.1039/c0lc00237b
44. Yu J, Ge L, Huang J et al (2011) Microfluidic paper-based chemiluminescence biosensor for simultaneous determination of glucose and uric acid. Lab Chip 11:1286–1291. doi:10.1039/c0lc00524j
45. Awqatty B, Samaddar S, Cash KJ et al (2014) Fluorescent sensors for the basic metabolic panel enable measurement with a smart phone device over the physiological range. Analyst 139:5230–5238. doi:10.1039/C4AN00999A
46. Hortin GL, Sviridov D (2008) Analysis of molecular forms of albumin in urine. Proteomics - Clin Appl 2:950–955. doi:10.1002/prca.200780145
47. Pugia MJ, Lott J, Profitt J, Cast TK (1999) High-sensitivity dye binding assay for albumin in urine. J Clin Lab Anal 13:180–7
48. Polkinghorne KR (2006) Detection and measurement of urinary protein. Curr Opin Nephrol Hypertens 15:625–630. doi:10.1097/01.mnh.0000247502.49044.10
49. Busher JT (1990) Serum albumin and globulin. In: Walker H, Hall W, Hurst J (eds) Clinical methods: the history, physical, and laboratory examinations, 3rd edn. Butterworth Publishers, pp 497–499
50. Bradford MM (1976) A rapid and sensitive method for the quantitation of microgram quantities of protein utilizing the principle of protein-dye binding. Anal Biochem 72:248–254
51. Lowry OH, Rosebrough NJ, Farr L et al (1951) Protein measurement with the Folin phenol reagent. J Biol Chem 193:265–275. doi:10.1007/s10982-008-9035-9
52. Martinez AW, Phillips ST, Butte MJ, Whitesides GM (2007) Patterned paper as a platform for inexpensive, low-volume, portable bioassays. Angew Chemie - Int Ed 46:1318–1320. doi:10.1002/anie.200603817
53. Wang W, Wu W-YY, Zhu J-JJ et al (2010) Tree-shaped paper strip for semiquantitative colorimetric detection of protein with self-calibration. J Chromatogr A 1217:3896–3899. doi:10.1016/j.chroma.2010.04.017
54. Sechi D, Greer BP, Johnson J, Hashemi N (2013) Three-dimensional paper-based microfluidic device for assays of protein and glucose in urine. Anal Chem 85:10733–10737
55. Luo L, Li X, Crooks RM (2014) Low-voltage origami-paper-based electrophoretic device for rapid protein separation. Anal Chem 86:12390–12397
56. Pozuelo M, Blondeau P, Novell M et al (2013) Paper-based chemiresistor for detection of ultralow concentrations of protein. Biosens Bioelectron 49:462–465. doi:10.1016/j.bios.2013.06.007
57. Szucs J, Gyurcsányi RE, Gyurcsµnyi E et al (2012) Towards protein assays on paper platforms with potentiometric detection. Electroanalysis 24:146–152. doi:10.1002/elan.201100522
58. Wu L, Ma C, Zheng X et al (2015) Paper-based electrochemiluminescence origami device for protein detection using assembled cascade DNA–carbon dots nanotags based on rolling circle amplification. Biosens Bioelectron 68:413–420. doi:10.1016/j.bios.2015.01.034
59. Sheldon RA. (2007) Enzyme immobilization: the quest for optimum performance. Adv Synth Catal 349:1289–1307. doi:10.1002/adsc.200700082

60. Mateo C, Palomo JM, Fernandez-Lorente G et al (2007) Improvement of enzyme activity, stability and selectivity via immobilization techniques. Enzyme Microb Technol 40:1451–1463. doi:10.1016/j.enzmictec.2007.01.018
61. Hanefeld U, Gardossi L, Magner E (2009) Understanding enzyme immobilisation. Chem Soc Rev 38:453–468. doi:10.1039/b711564b
62. Cao L (2005) Immobilised enzymes: Science or art? Curr Opin Chem Biol 9:217–226. doi:10.1016/j.cbpa.2005.02.014
63. Pelton R (2009) Bioactive paper provides a low-cost platform for diagnostics. TrAC Trends Anal Chem 28:925–942. doi:10.1016/j.trac.2009.05.005
64. Brady D, Jordaan J (2009) Advances in enzyme immobilisation. Biotechnol Lett 31:1639–1650. doi:10.1007/s10529-009-0076-4
65. Sheldon RA (2007) Enzyme immobilization: the quest for optimum performance. Adv Synth Catal 349:1289–1307. doi:10.1002/adsc.200700082
66. Guzik U, Hupert-Kocurek K, Wojcieszyńska D (2014) Immobilization as a strategy for improving enzyme properties-application to oxidoreductases. Molecules 19:8995–9018. doi:10.3390/molecules19078995
67. Ho C-M (2001) Fluidics- the link between micro and nano sciences and technologies. IEEE MEMS 2001:375–384
68. Whitesides GM (2006) The origins and the future of microfluidics. Nature 442:368–373. doi:10.1038/nature05058
69. Stone H, Kim S (2001) Microfluidics: basic issues, applications, and challenges. AIChE J 47:1250–1254
70. Kleinstreuer C (2013) Theory. In: John Wiley & Sons I (ed) Microfluid. Nanofluidics Theory Sel. Appl. pp 1–8
71. Washburn EW (1921) The dynamics of capillary flow. Phys Rev 17:273–283. doi:10.1103/PhysRev.17.273
72. Fu E, Ramsey SA, Kauffman P et al (2011) Transport in two-dimensional paper networks. Microfluid Nanofluidics 10:29–35. doi:10.1016/j.biotechadv.2011.08.021.Secreted
73. Dickinson EJF, Ekstrom H, Fontes E (2014) COMSOL multiphysics: finite element software for electrochemical analysis. A mini-review. Electroch 40:71–74
74. Segal IA (2015) Finite element methods for the incompressible Navier-Stokes equations. Delft Institute of Applied Mathematics
75. Schilling E, Yager P (2009) Microfluidic tutorial-a highly biased primer. http://faculty.washington.edu/yagerp/microfluidicstutorial/tutorialhome.htm. Accessed 10 June 2015
76. Erickson D (2005) Towards numerical prototyping of labs-on-chip: modeling for integrated microfluidic devices. Microfluid Nanofluidics 1:301–318. doi:10.1007/s10404-005-0041-z
77. Kleinstreuer C (2013) Modeling and simulation aspects. In: Microfluid. Nanofluidics Theory Sel. Appl., 1st edn. Wiley, pp 363–373
78. Whatman™ Cellulose chromatography paper. https://www.fishersci.com. Accessed 16 June 2015
79. Bracher PJ, Gupta M, Whitesides GM (2010) Patterned paper as a template for the delivery of reactants in the fabrication of planar materials. Soft Matter 6:4303–4309. doi:10.1039/c0sm00031k
80. Sayyah SM, El-salam HMA, Khaliel AB, Mohamed EH (2011) Graft polymerization of acrylonitrile onto paper and characterization of the grafted product. J Appl Polym Sci 120:1411–1419. doi:10.1002/app
81. Vesel A, Mozetic M, Hladnik A et al (2007) Modification of ink-jet paper by oxygen-plasma treatment. J Phys D Appl Phys 40:3689–3696. doi:10.1088/0022-3727/40/12/022
82. Hu L, Wu H, La Mantia F et al (2010) Thin, flexible secondary Li-ion paper batteries. ACS Nano 4:5843–5848. doi:10.1021/nn1018158
83. Papel Vegetal Schoellershammer. http://www.microservice.com.br/. Accessed 16 June 2015
84. Hanlon JF, Kelsey RJ, Forcinio H (1998) Paper and paperboard. In: Handbook of package engineering, 3rd edn. CRC Press, pp 44–49

85. Carrilho E, Martinez AW, Whitesides GM et al (2009) Understanding wax printing: a simple micropatterning process for paper-based microfluidics. Anal Chem 81:7091–7095. doi:10.1021/ac901071p
86. Tian K, Dasgupta PK (1999) Automated measurement of lipid hydroperoxides in oil and fat samples by flow injection photometry. Anal Chem 71:2053–2058. doi:10.1021/ac9813181
87. Matsui S, Echigo S, Shishida K (1998) Comparison among the methods for hydrogen peroxide measurements to evaluate advanced oxidation processes: application of a spectrophotometric method using copper (II) ion and 2,9-Dimethyl-1,10-phenanthroline. Environ Sci Technol 32:3821–3824
88. Repka V (1999) Improved histochemical test for in situ detection of hydrogen peroxide in cells undergoing oxidative burst or lignification. Biol Plant 42:599–607. doi:10.1023/A:1002687603731
89. Dhaouadi A, Monser L, Sadok S, Adhoum N (2006) Flow-injection methylene blue-based spectrophotometric method for the determination of peroxide values in edible oils. Anal Chim Acta 576:270–274. doi:10.1016/j.aca.2006.06.026
90. Salem I, El-Maazawi MS (2000) Kinetics and mechanism of color removal of methylene blue with hydrogen peroxide catalyzed by some supported alumina surfaces. Chemosphere 41:1173–1180. doi:10.1016/S0045-6535(00)00009-6
91. Wisitsoraat A, Karuwan C, Wong-ek K et al (2009) High sensitivity electrochemical cholesterol sensor utilizing a vertically aligned carbon nanotube electrode with electropolymerized enzyme immobilization. Sensors 9:8658–8668. doi:10.3390/s91108658
92. Galanos DS, Vazis G MA, Kapoulas VM (1964) Serum glycerides, free cholesterol, and cholesterol. J Lipid Res 5:242–244
93. Sackett GE (1925) Modification of Bloor's Method for the determination of cholesterol in whole blood or blood serum. J Biol Chem 64:203–205
94. Martin SP, Lamb DJ, Lynch JM, Reddy SM (2003) Enzyme-based determination of cholesterol using the quartz crystal acoustic wave sensor. Anal Chim Acta 487:91–100. doi:10.1016/S0003-2670(03)00504-X
95. Moraes ML, de Souza NC, Hayasaka CO et al (2009) Immobilization of cholesterol oxidase in LbL films and detection of cholesterol using AC measurements. Mater Sci Eng, C 29:442–447. doi:10.1016/j.msec.2008.08.040
96. Babaei A, Zendehdel M, Khalilzadeh B, Taheri A (2008) Simultaneous determination of tryptophan, uric acid and ascorbic acid at iron(III) doped zeolite modified carbon paste electrode. Colloids Surfaces B Biointerfaces 66:226–232. doi:10.1016/j.colsurfb.2008.06.017
97. Hasebe Y, Nawa K, Ujita S, Uchiyama S (1998) Highly sensitive flow detection of uric acid based on an intermediate regeneration of uricase. Analyst 123:1775–1780. doi:10.1039/a802214c
98. Chen Y, Meng Y, Tang J et al (2010) Extraction of uricase from Candida utilis by applying polyethylene glycol (PEG)/ NH 4) 2 SO 4 aqueous two-phase system. 9:4788–4795
99. Tiffany TO, Jansen JM, Burtis C et al (1972) Enzymatic kinetic rate and end-point analyses of substrate, by use of a GeMSAEC fast analyzer. Clin Chem 18:829–840
100. Chandra U (2011) Determination of dopamine in presence of uric acid at poly (Eriochrome Black t) film modified graphite pencil electrode. Am J Anal Chem 02:262–269. doi:10.4236/ajac.2011.22032
101. Hossain SMZ, Luckham RE, McFadden MJ, Brennan JD (2009) Reagentless bidirectional lateral flow bioactive paper sensors for detection of pesticides in beverage and food samples. Anal Chem 81:9055–9064. doi:10.1021/ac901714h
102. Cha R, Wang D, He Z, Ni Y (2012) Development of cellulose paper testing strips for quick measurement of glucose using chromogen agent. Carbohydr Polym 88:1414–1419. doi:10.1016/j.carbpol.2012.02.028
103. Mentele MM, Cunningham J, Koehler K et al (2012) Microfluidic paper-based analytical device for particulate metals. Anal Chem 84:4474–4480. doi:10.1021/ac300309c

104. Duly EB, Grimason S, Grimason P et al (2003) Measurement of serum albumin by capillary zone. J Clin Pathol 56:780–782
105. Grimsley GR, Pace CN, Pace NC (2003) Spectrophotometric determination of protein concentration. In: Current protocols in protein science. Wiley, p Supplement 33
106. Rendl M, Bönisch A, Mader A et al (2011) Simple one-step process for immobilization of biomolecules on polymer substrates based on surface-attached polymer networks. Langmuir 27:6116–6123. doi:10.1021/la1050833
107. Zanon NCM, Oliveira ON, Caseli L (2011) Immobilization of uricase in Langmuir and Langmuir-Blodgett films of fatty acids and a possible uric acid colorimetric sensor. J Colloid Interface Sci 373:69–74. doi:10.1016/j.jcis.2011.07.095
108. Olkkonen J, Lehtinen K, Erho T (2010) Flexographically printed fluidic structures in paper. Anal Chem 82:10246–10250. doi:10.1021/ac1027066
109. Pierre C (2004) The sol-gel encapsulation of enzymes. Biocatal Biotransformation 22:145–170. doi:10.1080/10242420412331283314
110. Schilling KM, Lepore AL, Kurian J a, Martinez AW (2012) Fully enclosed microfluidic paper-based analytical devices. Anal Chem 84:1579–85. doi:10.1021/ac202837s
111. Mulhbacher J, McGeeney K, Ispas-Szabo P et al (2002) Modified high amylose starch for immobilization of uricase for therapeutic application. Biotechnol Appl Biochem 36:163–170. doi:10.2147/IJN.S33835
112. Liu Q, Michael A, Yu X (2007) Immobilization and bioactivity of glucose oxidase in hydrogel microspheres formulated by an emulsification—internal gelation—adsorption—polyelectrolyte coating method. Int J Pharm 339:148–156. doi:10.1016/j.ijpharm.2007.02.027
113. Zhang Y, Zhi T, Zhang L et al (2009) Immobilization of carbonic anhydrase by embedding and covalent coupling into nanocomposite hydrogel containing hydrotalcite. Polymer (Guildf) 50:5693–5700. doi:10.1016/j.polymer.2009.09.067
114. Wu XJ, Choi MMF (2004) Spongiform immobilization architecture of inotropy polymer hydrogel coentrapping alcohol oxidase and horseradish peroxidase with octadecylsilica for optical biosensing alcohol in organic solvent. Anal Chem 76:4279–4285. doi:10.1021/ac049799d
115. Alkasir RSJ, Ornatska M, Andreescu S (2012) Colorimetric paper bioassay for the detection of phenolic compounds. Anal Chem 84:9729–9737. doi:10.1021/ac301110d
116. Mertz D, Vogt C, Hemmerlé J et al (2011) Tailored design of mechanically sensitive biocatalytic assemblies based on polyelectrolyte multilayers. J Mater Chem 21:8324. doi:10.1039/c0jm03496g
117. Deng C, Chen J, Nie Z, Si S (2010) A sensitive and stable biosensor based on the direct electrochemistry of glucose oxidase assembled layer-by-layer at the multiwall carbon nanotube-modified electrode. Biosens Bioelectron 26:213–219. doi:10.1016/j.bios.2010.06.013
118. Lvov YM, Grozdits G, Us C (2010) Layer-by-layer nanocoating for paper fabrication. US Pat 1–10
119. Lu H, Rusling JF, Hu N (2007) Protecting peroxidase activity of multilayer enzyme-polyion films using outer catalase layers. J Phys Chem B 111:14378–14386. doi:10.1021/jp076036w
120. Hoshi T, Saiki H, Anzai J-I (2003) Amperometric uric acid sensors based on polyelectrolyte multilayer films. Talanta 61:363–368. doi:10.1016/S0039-9140(03)00303-5
121. Ma J, Cai P, Qi W et al (2013) The layer-by-layer assembly of polyelectrolyte functionalized graphene sheets: a potential tool for biosensing. Colloids Surfaces A Physicochem Eng Asp 426:6–11. doi:10.1016/j.colsurfa.2013.02.039
122. Wang S, Li S, Yu Y (2004) Immobilization of cholesterol oxidase on cellulose acetate membrane for free cholesterol biosensor development. Artif Cells Blood Substit Immobil Biotechnol 32:413–425. doi:10.1081/LABB-200027479
123. Albayrak N, Yang S (2002) Immobilization of Aspergillus oryzae beta-galactosidase on tosylated cotton cloth. Enzyme Microb Technol 31:371–383

124. Isobe N, Lee D-S, Kwon Y-J et al (2011) Immobilization of protein on cellulose hydrogel. Cellulose 18:1251–1256. doi:10.1007/s10570-011-9561-8
125. Saxena U, Goswami P (2010) Silk mat as bio-matrix for the immobilization of cholesterol oxidase. Appl Biochem Biotechnol 162:1122–1131. doi:10.1007/s12010-010-8923-2
126. Blandino A, Macías M, Cantero D (2003) Calcium alginate gel as encapsulation matrix for coimmobilized enzyme systems. Appl Biochem Biotechnol 110:53–60
127. Alexakis T (1992) Microencapsulation of DNA within cross-linked chitosan membranes
128. Witkowska Nery E, Santhiago M, Kubota LT (2016) Flow in a paper-based bioactive channel—study on electrochemical detection of glucose and uric acid. Electroanalysis 28
129. Witkowska Nery E, Kubota LT (2015) Evaluation of enzyme immobilization methods for paper-based devices—a glucose oxidase study. J Pharm Biomed Anal 117:551–559

Chapter 3
Electronic Tongue Systems for the Analysis of Beverages

3.1 Literature Review

3.1.1 Sensor Arrays

The easiest way to classify sensor arrays is by dividing them into ones composed from sensors selective to one analyte and with sensors sensitive to different constituents of the sample (Fig. 3.1). Arrays composed of repeated sensors of one type can provide enhanced reliability, which is especially important when working with miniaturized sensors. Matrix of this type will also allow to measure spatial distribution of a given compound for example by growing a cell culture on top of the array. Arrays composed of sensors sensitive to different constituents of the sample can be used to measure concentration of various species at the same time or generally characterize the sample like in the case of electronic nose and tongue systems.

In one of IUPAC technical reports electronic tongues are described as follows: "The electronic tongue is an analytical instrument comprising an array of non-specific, low-selective, chemical sensors with high stability and cross-sensitivity to different species in solution, and an appropriate method of PARC and/or multivariate calibration for data processing [1]".

The first reference concerning mimicking olfactory organ appeared in 1982 [2]. A sensor array was applied to simulate receptors situated in the nose and pattern recognition used to identify different stimulation patterns. Just 3 years later, in 1985, the first system for liquid analysis, an electronic tongue was proposed by Otto and Thomas [3]. From that time desire to model, replace and improve human olfactory and taste systems drove scientists to develop new sensor arrays for gaseous and liquid samples. Design of those devices resembles biological recognition systems (Fig. 3.2) in which arrays of non-specific sensors present in the tongue or nose are used to gather information. This complex data is later processed and analyzed in the brain which provides decision about the sample (recognition,

E. Witkowska Nery, *Analysis of Samples of Clinical and Alimentary Interest with Paper-based Devices*, Springer Theses, DOI 10.1007/978-3-319-28672-3_3

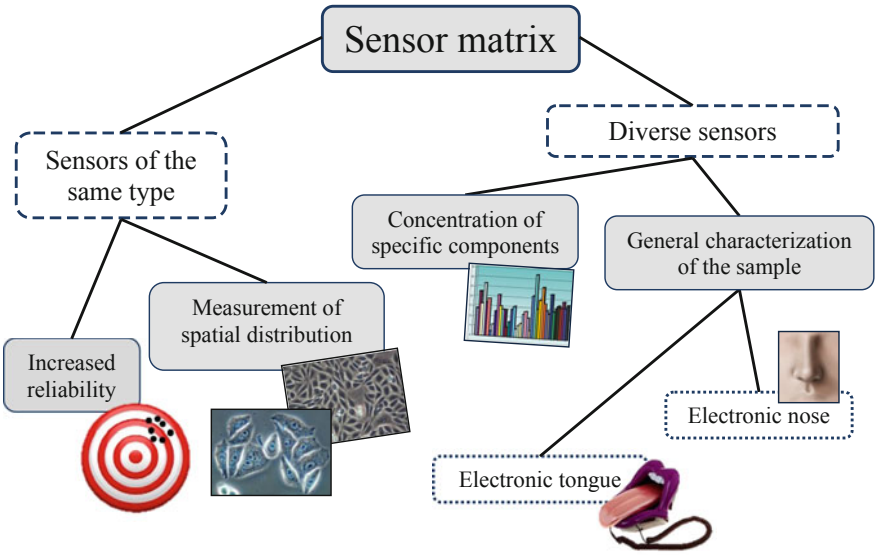

Fig. 3.1 Classification of sensor arrays

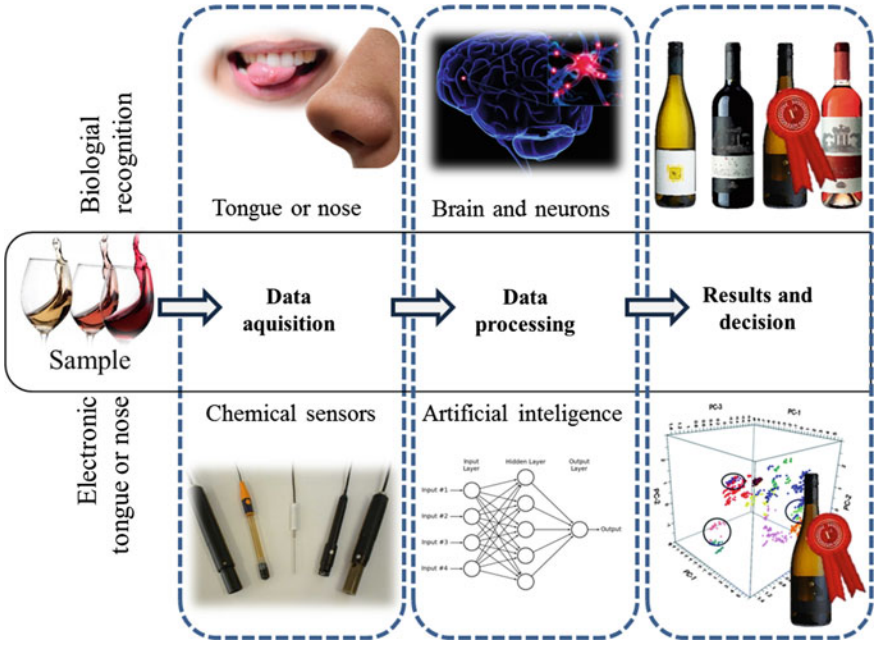

Fig. 3.2 Comparison of biological recognition with electronic nose and tongue systems

identification or quantification). Instead of brain, arrays of chemical sensors use methods of artificial intelligence and chemometry [4, 5].

Artificial and natural systems have a common working principle, but differ in design. Natural receptors are not selective, appear in great excess (10^8), use biochemical processing and produce periodical peaks of signal. In comparison artificial sensors are selective or partially selective, present low redundancy (~ 10), use chemical processing and produce steady-state response dictated by the continuous sample delivery. In natural systems due to great number of sensors data has to be synthesized. In electronic tongues and noses one sensor results in one signal. Biological data analysis relies on a huge database, integration of data from other senses and compensation of drift. Computer-based data analysis similarly to natural systems can integrate information from other instruments but disposes of a limited database and drift compensation is rather weak [5].

3.1.2 Analytical Techniques

Electronic noses usually comprise of sensors utilizing metal-oxide semiconductor materials, conducting polymers or metaloporphyrin films. Electronic tongue systems described till today are based on different sensing principles, with most common being potentiometry and amperometry, very few systems employ biosensors, optical sensors and piezoelectric mass sensors.

Traditional voltammetric systems employ three electrodes: reference, auxiliary and working electrode. Measurements are performed in a non-equilibrium state and signal is a current-potential relationship. Voltammetric sensors applied to electronic tongue systems usually present a favorable signal to noise ratio when compared with potentiometry, thus being better suited to lower concentration applications. Muitidimensionality is also higher including number of electroactive components present, number of working electrodes, scanning range etc. Many modes of measurement are possible: square wave, cyclic voltammetry, pulse voltammetry. In the case of pulse voltammetry information is extracted mainly from the exponential decay after each pulse. Electrodes can be made from different metals (copper, nickel, palladium, silver, tin, titanium, zirconium, gold, platinum, rhodium etc.), carbon (paste, glassy carbon, graphite etc.) and numerous other materials, not to mention the number of possible modifications including enzymatic. The principle of operation limits their application to redox-active substances [1, 5, 6].

Impedimetric sensors can also be applied to electronic tongue measurements, with a full scan of different AC frequencies or just a selected number of discrete values. First electronic tongue of this type comprised of electrodes modified with Langmuir-Blodgett films made from composite and nanostructured conducing polymers (polyaniline, polypyrrole, perylene derivatives, sulfonated polystyrene) [7].

In the case of piezoelectric mass sensors additional voltage can be detected when the piezoelectric material excited at a specific frequency is exposed to mechanical

stress (adsorption of an analyte). Sensors are usually fabricated from quartz crystals and can incorporate different chemosensitive layers. Surface Acoustic Wave sensors were already used to access mechanical and electrical properties such as viscosity, permittivity, conductivity but as the working principle is based on adsorption response is highly correlated, thus lowering the information gain [5].

Optical methods can be applied to detect species difficult to analyze electrochemically (e.g. not charged, not electroactive). Wide range of indicators includes chemically responsive dyes, enzymes, antibodies. Different modes of operation are also possible, such as signal lifetime or intensity accomplished by detection of absorbance, luminescence, reflectance etc. [5].

Hybrid systems comprising of sensors of different modalities are also possible, including a so called electronic panel: an array of gas, electrochemical liquid sensors and optical system of LEDs [8].

Potentiometry that will be one of the subjects of the forthcoming work will be revised in more detail later in the text.

3.1.3 Signal Processing

3.1.3.1 Signal Types

Signal can be acquired from steady state conditions, or utilize dynamic measurement for example when electronic tongues are operated with automated flow systems. Dynamic components of the signal include e.g. transient response corresponding to the introduction of a sample. In this case new dimension of data is added, namely kinetic resolution, improving modeling ability and diminishing the impact of interferents. Sensors response speed versus primary and secondary species can vary, thus providing additional information allowing better differentiation of samples [5, 6].

3.1.3.2 Data Preprocessing and Processing

Data preprocessing is crucial for successful analysis removing redundant information, enhancing signal-to-noise ratio etc. Simplest techniques include centering, based on subtraction of some matrix M from the original data matrix, and scaling, where data is multiplied by matrix W on the left. Autoscaling is a combination of centering and scaling by columns. Those simple treatments are often used to equalize contribution of different variables or to process different blocks of data. Non-linear transformations and other simple treatments such as extraction of the root or logarithm can also significantly improve subsequent analysis and modeling.

Data smoothing methods such as moving the average or Savitzky–Golay method can be applied to remove random noise. More complex treatments include multiplicative scattering correction, orthogonal signal correction and variable selection.

To improve data quality and allow analysis of large datasets, processing methods such as Fourier deconvolution and transformation or wavelet analysis can be used. Traditionally the Kalman Filter was used for signal smoothing and resolution of overlapping peaks, but it lost importance after introduction of computers [5, 9, 10].

3.1.3.3 Chemometry

Numerous chemometric methods were already applied to extract information from electronic tongue systems. They can be used for qualitative and quantitative analysis.

Qualitative approach can be used for data exploration to isolate useful information (detect outliers, indicate patterns or trends), or for discrimination and classification (attribute samples to a particular class). Qualitative methods can be divided into two groups: supervised and unsupervised. If it is possible it is recommended to use supervised methods based on two sets of data. In this approach first a classification model is constructed based on a library of known samples, later a separate library of responses is used to test the model. Performance of the model is given as the proportion of correctly classified samples.

The other group is the prediction methods, which are used for multivariate calibration, i.e.to determine the concentration of analytes from multiple measurements (e.g. voltammetric data, multiple electrodes). Multivariate calibration can be achieved by deconvolution of data to obtain contributions of individual analytes and later use simple calibration methods (peak area etc.) or by treating the data as whole and applying multivariate regression [6, 9–11].

Some of the most popular chemometric techniques will be presented in more detail:

Principal components analysis (PCA)—unsupervised method, reduces the number of variables of a large multivariate data matrix, without the loss of important information. Data is projected onto new coordinates, with new axes known as principal components (PC). First PC incorporates the largest amount of common variance. The next is orthogonal to the first. In the case of linear data the majority of variance can be usually described with just 2 or 3 PCs (correlation and redundancy in the original data). This method uses linear projection, therefore random noise (not fitting the model) is stored in latter PCs. Data matrix X is reduced into two smaller matrices, scores (T), and loadings (P). Samples are plotted on a scores plot and their relative position indicates relative similarity between the samples. Similar samples appear at similar positions [10]. Loadings matrix summarizes the properties of each variable, being the correlation between the original variables and the components. Equally to scores, variables located closely in the loadings plot give similar information. The higher (absolute) the loadings value the more important is the variable.

Hierarchical cluster analysis (HCA)—unsupervised method, commonly used to produce dendrograms, diagrams showing relationships between individual samples

within the dataset. Samples are paired as branches of the dendrogram, by calculating the distance (e.g. Euclidean) between each sample [10].

K-nearest neighbor (KNN)—supervised method, assigns similar patterns to one class depending on distance between points in the pattern space. Type of distance (e.g. Euclidean) and K value are the only changeable parameters. K describes the number of neighbors which indicate the class [12].

Soft independent modelling of class analogies (SIMCA)—supervised method, mathematically defines clusters observed in PCA, creating individual PC models for each cluster [10].

Multiple linear regression (MLR)—suitable for systems in which the response is a linear sum of individual responses for each analyte. MLR relates data (X) to a vector of corresponding values (y) by a regression vector (b), noise and nonlinearities are stored in a separate residual matrix (E) [10].

Principal components regression (PCR)—performs regression based on the scores and loadings plot generated by PCA. User chooses how many PCs should be used for the regression, inclusion of all PCs will result in MLR. Use of fewer PCs usually increases accuracy, removing unnecessary information [10].

Partial Least Squares (PLS)—used when the number of independent variables significantly exceeds the number of data points. Set of latent variables (analogues to PCs in PCA) is created based on both data matrix (X) and the target vector (y)(and not just X like in PCR) maximizing the covariance between them.

Non-Linear PLS—inner relationship between the experimental loading and scores to results is based on a non-linear polynomial function. Useful in cases when electrode is close to saturation, or interferences between analytes occur [10].

Artificial neural network (ANN)—is a machine learning tool, composed of units called neurons, arranged in layers. Each neuron of a given layer receives the same input information (x). The sum of each input is multiplied by weight (w) and added a bias (b) and just then subjected to a transfer function (f( )) of chosen kind (linear, sigmoid, tan sigmoid etc.). Error is minimized by altering weights between neurons. Depending on network parameters and initial weights, neural networks are capable of producing an infinite number of different models, thus requiring a more experienced user [10].

3.1.4 Potentiometric Sensors for Electronic Tongue Systems

3.1.4.1 Working Principle

Potentiometric methods are based on measuring the electromotive force (SEM) of the cell consisting of a working electrode and a reference electrode immersed in the sample solution in zero-current conditions. Usually a Ag/AgCl reference electrode is used. Basic equation describing the functioning of potentiometric sensors is the Nerst equation:

$$E = E^0 + \frac{RT}{nF} \ln Q \tag{3.1}$$

where, E is the electrode potential in V, E^0 is the standard electrode potential, R is the universal gas constant; T—absolute temperature; F—Faraday constant, n—number of electron transferred, Q is the reaction quotient.

Ion-selective electrodes form the largest group among potentiometric sensors. In this case, potential is a function of the activity of ionic species in the sample. A charge separation occurs due to selective partitioning of ionic species between the ion-selective membrane and the solution. The main disadvantages of this technique are temperature-dependence, detection limited to charged species, sensitivity to electrical noise, need of conditioning and possible interference from adsorbed species that can affect the charge transfer. Nevertheless, ion-selective electrodes are low cost, easy to fabricate, small and portable, consume little energy, have a well-known principle of operation, and present the highest similarity to natural molecular recognition [5, 13–15].

3.1.4.2 Cross-sensitivity

Cross-sensitivity is the ability of a particular sensor to respond reproducibly to a number of different species in solution. It was proved in the paper by Ciosek et al. that including cross-sensitive sensors into the array of ion-selective electrodes allows better discrimination of beverages (milk, fruit juice, tonic) with very high degree of accuracy (90–100 %) [16]. This kind of array better mimics biological systems, which are composed of partially or non-selective sensors of little variety (about 100 different types of olfactory receptors and several dozens identified in the taste buds of mammals) [1]. The smell or taste sense supply a complex data pattern, comprising of multiple, individual, cross-sensitive responses [6]. Notwithstanding, they are able to recognize thousands of compounds, some of them with very low detection limits and very similar in structure, e.g. stereoisomers.

In the case of potentiometric sensors selectivity coefficients are generally used to describe sensors cross-sensitivity. This coefficients describe what is the change in potential for an electrode in presence of an interfering ion, when compared with the primary ion. In the case of liquid membrane electrodes, its value depends on the properties of ionophore and other membrane components and ion mobility in the membrane. They are expressed according to the Nicolsky–Eisenman equation:

$$E = E_0 + RT/(z_A F) \ln \left[a_A + \sum_B K_{A,B}^{pot} (a_B)^{\frac{z_A}{z_B}} \right] \tag{3.2}$$

where E is the measured potential; E_0 is a constant including the standard potential of the electrode, the reference electrode potential, and the junction potential; z_A and z_B are the charge numbers of the primary ion (A), and interfering ion (B),

respectively; a_A and a_B are the activities of the primary and interfering ion; $K_{A,B}^{pot}$ is the potentiometric selectivity coefficient for the primary ion A against the interfering ion, B; R is the universal gas constant; T—absolute temperature; F—Faraday constant;

If $K_{A,B}^{pot} > 1$ the ion-selective electrode responds to the interfering ion more selectively.

Selectivity coefficient can be determined in several ways:

A. Mixed solution methods

   a. Fixed interference method-most commonly used mixed solution method. Based on measuring electromotive force (emf) of a solution with constant activity of an interfering ion a_B and varying activity of the primary ion a_A. The emf values obtained are plotted versus the logarithm of the activity of the primary ion. The intersection of the extrapolated linear ranges of this plot indicates the value of a_A that is used for calculations:

$$K_{(A,B)}^{pot} = a_A/(a_B)^{(z_A/z_B)} \tag{3.3}$$

   b. Fixed primary ion method
   c. Two solution method
   d. Matched potential method

B. Separate solution method (SSM)

This method is based on consecutive measurements of solutions containing only the main ion (Eq. 3.4) and only the interfering ion (Eq. 3.5)

$$E_A = E_0 + \frac{RT}{z_A F} ln a_A \tag{3.4}$$

$$E_B = E_0 + \frac{RT}{z_A F} \ln\left(K_{A,B}^{pot} a_B^{z_A/z_B}\right) \tag{3.5}$$

Next, based on the above mentioned equations selectivity coefficient is defined [17]:

$$K_{A,B}^{pot} = a_A^{(1-z_A/z_B)} e^{(E_B - E_A) z_A F/(RT)} \tag{3.6}$$

3.1.4.3 Types of Ion Selective Electrodes

Ion selective electrodes can be classified by the type of material used for membrane formation into: solid membranes (glass, crystalline), liquid membranes (polymer)

and sensitized (enzymatic). In this work liquid membrane ISE will be used, and thus this group will be described in more detail.

Liquid Membrane Electrodes

The principal component of a ion selective electrode is the electroactive membrane, which covers the solid contact or separates two electrolytes. Membrane allows selective extraction of ions from the solution, generating potential dependent on the concentration of the extracted ion. The basic components of the membrane are: ionophore, ionic additives and the polymer matrix.

Ionophore is a lipophilic, macrocyclic, molecule–sized compound, charged or neutral, which defines membranes selectivity. Neutral ionophores include valinomycin selectively binding potassium ions, and hexyl trifluoroacetyl benzoate selective to carbonate. Metal porphyrins used for determination of nitrate and bis-[4-(1,1,3,3-tetramethylbutyl)phenyl] phosphate selective to calcium ions are examples of charged ionophores. Ionophores exist in nature, where they are responsible for transport of species through cell membranes. In the case of ISEs they are used to reversibly complexate ions and transport them into the membrane, reducing the total free energy needed for the transfer. Structure of the ionophore, its cavities or semi-cavities allow for selective interactions. Therefore selectivity derives from the difference in binding strength between the given ionophore and different ions. In the case of strongly hydrophilic ions, free ionophore is transported to the liquid phase, forms a complex with the ion and is transported back to the membrane. Lipophilic ions cross the phase independently and are complexated in the membrane. In membranes without ionophore or with ionophores without any chemical recognition abilities transport of ions from the liquid depends only on lipophility of the compound. Selectivity of this type of membranes is with accordance with the Hofmeister series:

for cations: $Cs^+ > Ag^+ > K^+ > NH_4^+ > Na^+ > Li^+ > Ca^{2+} > Pb^{2+} > Cu^{2+}$

for anions: $ClO_4^- > SCN^- > I^- > NO_3^- > Br^- > NO_2^- > Cl^- > HSO_3^- > SO_4^{2-} > HPO_4^{2-}$ [15, 18].

Ionic additives ensure constant ratio of free and complexated ionophore and permselectivity i.e. no significant amount of the counter ions penetrates the membrane. They are formed by a hydrophilic ion that can freely penetrate to the liquid phase of the sample and a lipophilic counterion that remains in the membrane. Charge of the transported ion depends on the selectivity of the membrane (cation, anion) and the working principle of the ionophore. Similarly to liquid chromatography hydrophilic ion is exchanged for a cation or an anion. Thanks to lipophilic salts the net charge of the membrane remains constant. Other advantages include enhanced permeability and decrease in anionic interference. Electrical resistance of the membrane also reduces. Ratio of the ionic additive and ionophore should be strictly defined because it can act as a ion exchanger, inducing a selective response to lipophilic ions in case of insufficient amount of ionophore [15, 18].

Polymer matrix stands for around 99 % of membranes weight, it provides mechanical stability and elasticity. Polymers used in membranes should present glass transition temperature below the room temperature in order to be fluid enough to allow diffusion of the membrane components. In the case of polymers with higher glass transition temperature plasticizer must be added. When polymers such as silicone rubber, poly (vinylidene chloride) and soft polyurethane are used plasticizer can be added to modify the ion selectivity. If present, plasticizers are usually used in ratio 2:1. They lower the glass transition temperature, enhance plasticity, elasticity and malleability of the membrane. Plasticizer has to be chosen with care as it has to dissolve all the membrane components. As its polarity can influence the selectivity of the membrane, they can also result in problems with leaking. Membrane should allow free diffusion, present ionic conductivity and adequate mechanical properties. It should be also lipophilic, to better retain the ionophore and the lipophilic salt. The most frequently ISEs are based on polyvinyl chloride (PVC) with addition of esters of organic salts and ethers serving as plasticizers [15, 18, 19].

Construction of Ion Selective Electrodes

Ion selective electrodes can be divided by construction as electrodes of classical architecture and solid-contact electrodes. Electrodes of classical architecture present symmetrical arrangement, membrane separates the test solution and the inner solution (constant concentration of ionic species). They require periodical exchange of the internal solution and are difficult to miniaturize. Solid-contact electrodes are asymmetrical, without internal solution. Membrane is in direct contact with metal (coated wire electrodes). They generally show poor stability and rely on blocked charge transfer across the interface between purely ionic conductor (membrane) and purely electronic conductor. Interface becomes a condenser and parasitic capacitance will affect the signal stability even when minimal electrical current passes. Short time measurements (dozens of minutes) are possible due to potential stabilization based on side reactions with species penetrating the polymer. Oxygen is an especially good depolarizer in this case, but other redox species also present this effect. Their advantages are the possibility of miniaturization and low fabrication cost [13, 18].

Selectrodes (rods of porous graphite impregnated with liquid membrane without polymer) and coated wire electrodes (polymer membrane deposited on noble metals (Pt, Au or Ag) respond similarly to classical ISEs of corresponding composition but present chaotic, rapid potential changes (up to 10 mV/h) [18]. Stabilization of solid-contact membrane ISE potential was already attempted in several ways:

- Electrode of I kind (metal in a solution of its salt)—not appropriate for ionophore-based membranes, permeable to water which forms thin film on metal surface. Because of the small volume, concentration of metal salt changes drastically with dissolution and depends on the external conditions.

- Electrode of II kind–successfully applied for ISE selective to Cl^-, Br^-, and SCN^- and other anions forming poorly soluble precipitates with silver. Membranes are deposited on the corresponding electrode of II kind: Ag/AgX.
- Membrane doping with an appropriate redox system, which components are concentrated near the electronically conducting substrate. Redox components soluble in the membrane material result in appearance of sensitivity to the redox potential of the medium. Therefore an intermediate transduction layer was proposed. This fast and thermodynamically reversible ion to electron transduction system can be formed by electron—ion exchanging resins or *p*-type conducting polymers. Single piece sensors, in which conducting polymer is incorporated in the membrane are also possible.
- Quasi-classical ISEs with a hydrogel layer between the contact and membrane–present low stability due to drastic diffusion driven composition changes of the water layer.
- Replacement of PVC by other polymers, that absorb much smaller amounts of water. Polymers include methacrylic—acrylic copolymers (higher resistance than PVC) and silicone rubbers (e.g. RTV 3140 Dow Corning).
- Increase in the electrical capacity of the transducer layer. It can be accomplished by doping of the transduction layer with carbon materials such as carbon nanotubes and porous graphite. Resultant capacity is of a double layer nature rather than redox [14, 18].

3.1.4.4 Paper-Based Potentiometric Sensors

Few systems were proposed until today employing paper in potentiometric analysis. In the first approach paper was used to maintain continuous liquid stream during the flow-injection measurements. Electrodes of classical architecture were placed against a slip of paper that would carry the liquid. First attempts of this type appeared in mid-1980' e.g. system for the analysis of chloride in tap water and sewage [20] and traces of fluoride [21]. Similar systems were proposed throughout the years, with the most modern described by Szucs et al. in 2011. Two coated wire electrodes modified with membranes selective to Ag^+ and Ca^{2+}(pseudo-reference) were used to indirectly quantify IgE. Assay was based on dissolution and later quantification of silver deposited after standard dot-blot assay. Electrodes were stacked against a nitrocellulose membrane slipon both sides of the silver blot and sealed with two silicone rubber sheets [22].

First fully paper-based potentiometric sensor was described by Novell et al. Filter paper was impregnated with carbon nanotube ink (carbon nanotubes in a water–surfactant mixture). This conductive paper was later enclosed between two layers of plastic mask leaving a small orifice in the end filled with a ion-selective membrane. Electrodes sensitive to K^+, NH_4^+, and pH were constructed and thoroughly characterized, presenting sensitivity of 56–58 mV/dec [23]. The same type of sensor was used to construct a paper cell, in which one ISE and a reference

electrode were sandwiched together leaving a 50 µl cavity. Lithium selective electrode (sensitivity of 56 mV/dec) was used to analyze Li levels in blood. Recovery from blood and serum samples compared with atomic emission spectroscopy was between 87 and 115 % [24]. Whitesides group proposed a paper-based sensor with borders printed with wax, and screen-printed Ag/AgCl electrodes [25]. Slip of paper with one of the Ag/AgCl electrodes was stacked against a ion-selective membrane and an end of paper-based channel formed on a second slip of paper. On the other side of the channel another Ag/AgCl electrode working as a reference was printed. Electrodes selective to K^+, Na^+ and Ca^{2+} were equipped with ion-selective membrane, whereas Cl^- ions were measured directly by stacking two pieces of paper without the membrane. Electrodes presented good selectivity 22.9 mV/dec for a divalent calcium ions, $\sim$54 mV/dec for K^+, Na^+ and 61 mV/dec for Cl^- but in a lower concentration range than devices presented by Novel et al.

3.1.4.5 Detectors

First analogue detectors had a resolution of only 1–2 mV. When they were substituted by digital meters the resolution of 0.1 or even 0.01 mV was achieved, and the stability and reproducibility of the electrode became limiting to the system. Currently potentiometric detectors span from self-calibrating devices able to compensate the influence from temperature, portable, handheld meters to multichannel systems capable of recording several signals at the same time. They are based on two designs, and can be classified as potentiometers and direct reading instruments. Potentiometers use compensation method, where emf of an unknown cell is compared directly to a known standard cell. They are more appropriate for cells with low internal resistance ($\leq 10^5$ Ω), for high resistance electrodes like the glass electrode high impedance voltmeters are used. In direct reading instruments electrode is connected to a high-resistance field effect transistor or a voltage follower. Potential measured in a solution of interest is compared to the one obtained in a standard solution [26].

Potentiometric detectors are low cost and their simple design allows to assemble them from readily available electronic components. Nevertheless even simpler device could be applied, such as a meter bridge or a multimeter. Digital multimeters have a high input impedance, thus will not withdraw current from the cell during measurement. It is enough to set the multimeter in the voltmeter mode and connect two electrodes [27]. It was proposed recently to connect multimeter to a capacitor to enhance sensitivity. In this case capacitor is charged for a designated time and later its discharge is measured through the multimeter [28, 29].

3.1.5 Application of Sensor Arrays

As already mentioned sensor arrays have several types of application, one of them being the artificial taste concept. In this case, the goal is to mimic human taste assessment in situations when human expert panel is not applicable because of process conditions (automatic process control especially on industrial scale), sample type (poisonous/extreme condition samples) or because of economic reasons (time-consuming and expensive sensory panels). Measurement can be qualitative, identifying particular constituent of the sample, classifying samples or recognizing adulteration. Quantitative approaches are based on simultaneous determination of multiple species for example for process control, or to reduce the impact of interferents [6].

Applications include food industry, where electronic tongue systems can be used for quality control, optimization of bioreactors, control of ageing and aforementioned automated control of taste. In case of chemical industry sensor arrays can be used to detect functional groups or attest products purity. Clinical in vivo monitoring, non-invasive diagnostics, or assessment of tastes of pharmaceuticals are only some of possible medical uses. Electronic tongues can be also applied to environmental monitoring to monitor pollution or detect leaks of toxic substances [5].

3.1.5.1 Discrimination of Forged Mineral Water Samples

Mineral waters currently dominate the soft drink market worldwide [30]. Unfortunately bottled water can be easily contaminated by intentional substitution with tap water or even neglectful packaging and storage. Issues concerning bottled water that does not meet generally accepted standards were already reported in Asia: Bangladesh [31], India, China [32]; Middle East: Iran [33]; Africa: Nigeria [34], Tanzania [35], Ghana [36] and South America: Brazil [37].

Samples are abundant and low cost and problem impacts mainly individual households and tourists thus sensing system that has the best chance of implementation should be inexpensive, widely applicable and the assay easy to perform. Composition of mineral waters coming from different sources can vary considerably (Table 3.1). Additionally, the type of contamination is usually hard to predict and can include inorganic and organic species as well as bacteria. With so many possible contaminants it is difficult to name one sensor that could identify that adulteration has taken place. As was already mentioned electronic tongues comprising of several cross-sensitive sensors can be trained to automatically discriminate samples from certain groups, and could serve as a platform indicating adulteration of bottled water.

Some of the electronic tongues proposed for the analysis of water until today are resumed in Table 3.2. Potentiometry is the main technique, but voltammetric and mixed arrays are also present. All studies are designed for qualitative analysis of the samples.

Table 3.1 Chemical composition of some Brazilian, bottled commercial mineral waters, values in mg/L as stated on the label

Brand	Spring	HCO_3^-	Ca^{2+}	Cl^-	F^-	Mg^{2+}	NO_3^-	K^+	Na^+	SO_4^{2-}
Acquissima	Santa Inês	94.98	16.49	0.59	0.04	2.75	0.16	3.211	13.3	6.54
Lindoya	São Luis	257.28	46.21	1.51	0.2	16.03	1.3	3.418	14.95	3.83
Lindoya	N. Sra. Das Brota III (P1)	40.86	6.103	2.08	0.03	1.969	8.52	2.555	7.73	0.19
Crystal	Yguaba	91.63	3.858	1.06	0.93	0.735	0.01	1.632	30.46	1.36
Frescca	São Francisco	73.17	12.55	1.41	0.12	2.45	0.5	2.74	8.22	0.1
Bonafont	Painera	7.53	1.402	0.58	0.05	0.586	4.53	1.669	1.212	0.06
Bonafont	Painera I	17.38	2.572	3.33	0.02	1.594	3.01	1.731	4.142	2.73
Pureza Vital	Sta Catarina	90.67	19.98	0.18	0.04	0.132	0.16	2.849	9.541	0.1
Pureza Vital	Primavera	137.14	24.2	9.84	0.09	14.22	2.44	3.084	3.086	1.14
Pureza Vital	St Antônio	7.57	1.561	1.82	0.01	0.437	1.2	0.737	1.755	0.7
Pureza Vital	Levíssima	4.85	0.622	1.57	0.01	0.309	0.33	0.636	1.481	0.39
S. Lourenço	Oriente	258.88	26.49	1.38	0.11	11.21	0.91	30.52	30.17	2.42
	St.dev.	89.2	13.9	2.6	0.3	5.9	2.5	8.2	10.3	2.0

Table 3.2 Literature review of electronic tongue systems proposed for the analysis of water

Technique	No. of sens.	Type of sensors	Samples	Data analysis	References
Large-amplitude pulse voltammetry	2	Au and Re wires	Discrimination of bottled mineral water from KCl solution and tap water, as well as natural water samples from different locations (tap water, lake etc.)	Discrete cosine transform	[38]
Potentiometry	16 of 8 types +1	Liquid membrane ion-selective electrodes and a standard pH electrode	Discrimination of eight brands of mineral water, tap and Oligocene water and ten brands of apple juices	ANN	[39]
Potentiometry	12	Thic film RuO_2, C, Ag, Ni, Cu, Au, Pt and Al and rod electrodes from Sn, Pb and graphite	Discrimination of six mineral waters, two tap waters and an osmotized sample	PCA, ANN	[40]
Potentiometry	18 of 6 types	Thick-paste electrodes Cu, RuO_2 of 10 Ω/sq, RuO_2 of 1 MΩ/sq, Ag, Pt, AgCl	Discrimination of five brands of natural mineral water, one sparkling and one tap water	ANN, Linear Discriminant Analysis	[41]
Hybrid	8	Six ion selective field effect transistors, an interdigitated platinum electrode and a silicon diode used as a temperature sensor	Discrimination of thirteen brands of mineral water	HCA, PCA, SIMCA	[42]
Pulse voltammetry	1	Ag wire	Discrimination of six brands of mineral water	PCA, Sammon's nonlinear mapping	[43]
Potentiometry	7	Commercial α-Astree II E-tongue (Alpha MOS company, Toulouse, France), ion selective field effect transistor	Discrimination of three brands of mineral water	PCA, HCA, SIMCA, Discriminant factorial analysis	[44]

(continued)

Table 3.2 (continued)

Technique	No. of sens.	Type of sensors	Samples	Data analysis	References
Potentiometry	7	Commercial α-Astree II E-tongue (Alpha MOS company, Toulouse, France), ion selective field effect transistor	Discrimination of six brands of bottled mineral waters, one spring water (non-carbonated, still), and tap water	PCA, HCA, Linear discriminant analysis	[45]
Potentiometry	5	Commercial ion selective electrodes	Discrimination of five brands of mineral water	Independent component analysis, linear discriminant analysis, Learning vector quantization	[46]

3.1.5.2 Classification of Beverages

Analysis of beverages is gaining popularity because of several factors, like interest in determination of geographical origin, evaluation of gustatory properties and optimization of process control. Increased concern of consumers, economic factors and indirectly authenticity assessment are the main reasons to determine the geographical origin of food products. The European Union established food quality schemes based on region, as a result products of certain geographical origin became more costly. Some products like ham, cheese, wine are often associated with a specific geographical areas, thus making them susceptible to fraud. Authenticity assessment links not only with origin but also as in the case of wines with aging time and method (oak barrel etc.). Increase in quality of agricultural production generated the need of more optimized process control necessary to maintain high safety standards, uniformity within a brand, quality and commercial viability of the end product [8, 47, 48].

Beer

The Beer: Global Industry Guide (May 2015) by Research and Markets shows that beer manufacturing industry demonstrated considerable growth over the past 5 years, and it is expected that it will continue to grow for another five. Annual revenue reached 494.4 billion $ in 2014 with market consumption of 176.4 billion l. Beer is currently the third most consumed beverage in the world (1st water, 2nd tea), and the first considering alcoholic beverages [49, 50].

Beers are usually categorized by factors such as color, flavor, alcohol content, production method, fermentation method, type and origin.

Traditionally beer was produced by the brewing and fermentation of malted barley and hops, and according to the purity law only those two ingredients together with water could be used. Nowadays because of economic reasons barley is often partially substituted with corn, rice or sugars. Additives also include chemical stabilizers and antioxidants. There is a growing resentment of consumers related to such practices, often poorly described on the label. The investigation of basic beer attributes is also important for the manufacturer, in order to obtain products with accordance to consumer preferences. Recently low-alcohol beers are increasing their share in the beer market, it is therefore important to evaluate components determining flavor of regular beers to obtain a similar product but with reduced alcohol content [49–52].

It was already proven that drinking beer in small amounts has the same beneficial effects as wine drinking, but this fact did not gain public recognition. Many new studies seek to convince public opinion by analysis of compounds beneficial for health in beer samples. Beer is rich in vitamins, especially of the B group (i.e. folic acid) and numerous micro-elements, like silicon, magnesium and potassium. Beer has also an antioxidant activity due to polyphenolic compounds [49–52].

Beer composition and physico-chemical parameters depend on:

- water
  - Sodium contributes to beer body and character;
  - Chloride highlights malt sweetness;
  - Sulfate enhances bitterness;
  - Calcium contributes to the pH;
  - Magnesium is an important nutrient for the yeast;
- additives
  - substitution of barley (source of sugar), for economic reasons or to obtain special beer types (wheat, corn, rice, fruits, sugar);
  - flavorings such as fruit and herbs;
  - preservatives;
- hops and malt
  - content of alpha and iso-acids, which influence flavor (bitterness), foam stability and have bacteriostatic effects;
  - preparation of malt (without pretreatment, caramelized, roasted);
  - content of polyphenolic compounds-responsible for color intensity, antioxidant activity, flavor (bitterness, astringency and harshness) and stability;
  - moment of addition of hops (during or after brewing, before or after filtration of the wort);
- brewing
  - time and temperature;
  - presence and type of filtration;
- fermentation
  - time and temperature;
  - open or closed fermenters;
  - type of yeast used (low or high fermentation);
- aging
  - ageing promotes esterification of alcohols and acids, decomposition of polyphenols;

Major components are water, ethanol, carbohydrates, subsequently proteins, organic acids, amino acids, higher alcohols, esters, ketones (including diacetyl) and salts. Polyphenolic compounds include phenolic acids (ferulic, cinnamic, chlorogenic, vanillic, gallic, caffeic, and p-coumaric, syringic), derivatives of flavan-3-ol (catechin, epicatechin, procyanidin, prodelphinidin) and flavone glycosides [52–56].

Some of the electronic tongue systems proposed for the analysis of beer and wine are resumed later in the text in Table 3.5.

Wine

Report of the International Organization of Vine and Wine for the 2014 shows that the global consumption of wine is steadily increasing, the amount consumed outside Europe is also growing and reached 39 % (America 23 %, Asia 10 %). Total revenue for 2013 achieved 25.7 billion €(increase as compared with previous years), with an increase in value of all 10 top exporters (France, Italy, Spain etc.).

The most important chemical classification in the case of wine is based on geographical origin, grape variety, subsequently taste factors (e.g. astringency), relative age and wine style (red, white, rose). Elemental composition and main chemical properties are resumed in Tables 3.3 and 3.4.

Several studies cite Sr, Mn, Mg, Li, Co, Rb, B, Cs, Zn, Al, Ba, Si, Pb, and Ca as the most discriminating elements. Study of 65 wine types showed that impact of the winery and vineyard can be correlated with elements such as: Be, Na, P, Ti, Zn, As, Rb, Cd, Sb, Cs, La, Pr, Dy, Er, Tm, Yb, Tl [47, 57].

Wine composition depends on [47, 48, 58–61]:

- location of the vineyard
  - proximity to ocean > sodium, to roads and industry > cadmium and led;
- soil composition, use of fertilizers, pesticides, herbicides etc. irrigation

Table 3.3 Elemental wine composition [47]

Major elements	10–1000 mg/L	Ca, K, Na, Mg,
Minor elements	0.1–10 mg/L	Al, Fe, Cu, Mn, Rb, Sr, Zn
Trace elements	0.1–1000 µg/L	Ba, Cd, Co, Cr, Li, Ni, Pb, V

Table 3.4 Main chemical parameters of wine [48, 57]

Wine	White	Red
Total acidity (g/L)	5.1–9	5.6–8.7
Alcohol (vol.%)	9.1–13.3	9.9–12.7
Reducing sugars (g/L)	0.7–16.5	1.0–13.1
SO_2 total (mg/L)	23–203	10–110
pH	2.9–3.58	3.21–3.91
Total phenolics (mg/L)	144–503	893–3262
Tartaric acid (g/L)	–	1.26–5.74
Malic acid (g/L)	–	1.28–4.44
Lactic acid (g/L)	–	1.24–3.54
Glycerol (g/L)	–	6.69–10.52

  - soil rich in B, Cr, Mn, Mo, W, and Zn > sugar, polyphenol and amino acids;
- winemaking process
  - crushed grapes > Cu and Zn, grapes separated from rachises > Al, Cu, Fe, Zn, Mn and Sr;
  - clarification with bentonites > Al, Cd, Hf, rare earth elements, Pb, U, and Zr, filtration > Co, Cr, Fe, and Ni and rare earth elements;
  - type of wine (red, white, rose)–concentrations of isoamylic alcohol, higher major alcohols, ethyl hexanoate, acetates, ethyl octanoate, 4-vinyl-guaiacol and decanoic acid;
- ageing and storage
  - oak barrels > Al, Fe and V
  - ageing promotes esterification of alcohols and acids, decomposition of polyphenols;
  - oxidative ageing more vigorous at the beginning, and tends to slow down as the wine matures;
  - screw-capped bottles > Sn
  - glass bottles > rare earth elements, colored glass > Cr
- intentional adulteration
  - ethanol–to modify alcohol content
  - tartaric acid–to modify total acidity
  - tannic acid–to modify astringency
  - SO_2–to modify sulfur content
  - acetic acid–to modify volatile acidity
  - sucrose–to modify content of reducing sugars
  - acetaldehyde–to obtain fruity flavor

Some of the electronic tongue systems proposed for the analysis of wine are resumed in Table 2.7 in Chap. 2 (Table 3.5).

3.1.6 Paper-Based Electronic Tongues

Until the time of writing no electrochemical, paper-based electronic tongue was described in the literature. Optical systems include two approaches. First system proposed by Pumtang et al. in 2011 uses a matrix of UV cured polydiacetylenes (two monomers in ratios 0:100, 50:50, 20:80, 10:90, 5:95 and 100:0) to colorimetrically identify organic solvents. Fourteen common organic solvents and a deionized water sample were tested and 9 of the solvents formed separate clusters in PCA plot [70]. A year after the same group described another matrix [71], this type made from eight different diacetylene monomers polymerized by UV radiation. After reducing the number of different monomers and PCA analysis it was possible

Table 3.5 Literature review of electronic tongue systems proposed for the analysis of wine and beer

Technique	No of sens.	Type of sensors	Samples	Data analysis	References
Analysis of wine					
Hybrid	14 + (5 + 3) + 11	14 metal–oxide–semiconductor gas sensors, 5 conducting polymer and 3 rare-earth bisphthalocyanines electrochemical sensors, 11 LEDs	Discrimination of six Spanish red wines (two regions, one grape type, 3 aging periods)	PCA, polar plots of the percentage variation	[8]
ICP-MS	–	63 monitored elements	Discrimination of 65 red wines (five different vineyards, five different wineries)	Canonical variate analysis	[47]
Potentiometry	22	Membrane and chalcogenide glass sensors	Evaluation of astringency of 32 white and green (type of Portuguese white wine) wines, 8 rose and 15 red wines	Common component and specific weight analysis–for comparison of electronic tongue and FTIR data, PLS and Variable Importance in Prediction statistics	[48]
Potentiometry	7	Commercial α-Astree II E-tongue (Alpha MOS company, Toulouse, France), ion selective field effect transistor	Prediction models with sensory evaluation or LC–MS/MS. Korean rice wines brewed from nine cultivars (amino acid and fatty acid content). Good correlation with fatty acids, amino acids, ribose, lactate, succinate, and tryptophan content and taste.	PLSR, PCA	[62]
Cyclic voltammetry	3	Glassy carbon, gold and platinum	Discrimination of four types of rice wines of different aging periods (3, 5, 8 and 10 years), 30 bottles of each type	SIMCA, PLSDA, KNN, ANN, support vector machine	[58]

(continued)

Table 3.5 (continued)

Technique	No of sens.	Type of sensors	Samples	Data analysis	References
Potentiometry	6	Chalcogenide glass and membrane ion selective field effect transistor	Discrimination of 6 commercial from 9 homemade wines according to the grape variety and quantitative prediction of volumetric alcoholic degree and pH	PCA, SIMCA, PLS	[59]
Potentiometry	23	14 sensors with chalcogenide glass and crystalline membranes, 2 metallic (Pt and Sb), 6 with plasticised polymer membranes and pH glass electrode	Discrimination of 20 samples of Barbera d'Asti and 36 samples of Gutturnio wine by vintage and denomination. Prediction of total and volatile acidity, pH, ethanol content, tartaric acid, sulphur dioxide, total polyphenols, glycerol and response of human sensory panel	PCA, PLS, ANN, SIMCA	[57]
Potentiometry	12	Metallo-porphyrins doped PVC membranes	Discrimination of Verdicchio D. O.C wine from 9 different cantinas and produced in different years. Prediction of SO_2, L-malic acid, and total phenols content	PCA, PLS	[63]
Beer analysis					
Voltammetry	4	Commercial screen-printed electrodes (carbon, gold, carbon/Co-Phtahlocyanine and platinum)	Discrimination of 25 types of beers (alcohol free, pilsner, doppel bock, strong lager). Prediction of the European Brewery Convention color index and the alcoholic strength	PCA, PLS, linear discriminant analysis	[51]

(continued)

Table 3.5 (continued)

Technique	No of sens.	Type of sensors	Samples	Data analysis	References
Potentiometry	21	PVC membrane ISE	Discrimination of 51 samples of 10 types of beer in different bottle sizes. Prediction of alcohol content.	PCA, linear discriminant analysis, ANN	[52]
Hybrid	6 + 5	6 modified graphite-epoxy voltammetric +15 potentiometric	Discrimination of 25 beer brands, with clusters related to different beer types	PCA, linear discriminant analysis	[54]
Potentiometry	10	5 types of PVC membrane ISE	Discrimination of 5 beer brands	PLS, ANN	[64]
Potentiometry	12	Polymer membrane deposited on screen-printed carbon paste/Prussian Blue electrodes	Discrimination of 5 beer brands, 3 "tastes"	PLS, PCR	[65]
Potentiometry	6	PVC membrane ISE	Discrimination of 5 beer brands	PCA, ANN	[55]
Voltammetry	4	Biosensors	Determination of ferulic, gallic and sinapic acids in 15 spiked samples (one beer type)	ANN	[66]
Voltammetry	3	Carbon paste/phthalocyanine biosensors	Discrimination of 4 beer packaging and type (alcoholic, non-alcoholic, bottle, can) inside one brand, before and after aging procedure	PCA, linear discriminant Analysis, ANN	[56]
Voltammetry	6	Conducting polymers	Discrimination of 21 lager beers (dark, pale; with alcohol and alcohol free). Prediction of isohumulone and ethyl alcohol.	PCA, PLS	[67]

(continued)

Table 3.5 (continued)

Technique	No of sens.	Type of sensors	Samples	Data analysis	References
Potentiometry	29	PVC membrane ISE	Discrimination of 50 beers of different types (lager beers, ales, wheat beers, etc.). Comparison with sensory panel. Prediction of 20 attributes out of 42	PCA, PLS, canonical Correlation analysis	[68]
Potentiometry	18	PVC and chalcogenide glass membranes and a pH glass electrode	Discrimination of 50 beers of different types (lager beers, ales, etc.). Prediction of real extract, alcohol and polyphenol content and bitterness	PLS, canonical Correlation analysis	[69]

to discern clusters of 18 organic solvents and 5 types of gasoline (separate experiments).

In 2013 a fluorimetric electronic tongue was proposed for the identification of 7 heavy metal ions (Hg^{2+}, Cd^{2+}, Co^{2+}, Cu^{2+}, Ni^{2+}, Zn^{2+}, and Ag^{+}). Nine detection zones delimitated with wax were modified with different derivatives of a boron-based fluorescent dye. All heavy-metal ions appeared in separate clusters in a HCA dendrogram. It was possible to distinguish all heavy-metal ions at mmol/L concentrations [72]. The same group recently published work concerning similar colorimetric device using nine commercially available heterocyclic azo indicators. 2 ml of sample was continuously drawn through the device to concentrate the species of interest. It was possible to identify Hg^{2+}, Cu^{2+} and Zn^{2+} in samples of sea and tap water (HCA analysis) and all heavy metal ions formed separate clusters in HCA and PCA plots [73].

3.2 Materials and Methods

3.2.1 Reagents and Materials

Polyvinyl chloride(Sigma Aldrich 81392), 2-Nitrophenyl octyl ether(Sigma Aldrich 73732),sebacic acid di(2-ethylhexyl) ester(Sigma Aldrich 84818), potassium tetrakis(4-chlorophenyl)borate(Sigma Aldrich 60591), KTFPB(potassium tetrakis [3,5-bis(trifluoromethyl)phenyl]borate), tridodecylmethylammonium chloride (Sigma Aldrich 91661), sodium ionophore X(Sigma Aldrich 71747), valinomycin (Sigma Aldrich 60403), BBPA (bis(1-butylpentyl)adipate)), ETH 129 Calcium ionophore II (Sigma Aldrich 21189), TPPClMn (chloride ionophore I, meso-tetraphenylporphiryn manganese(III)-chloride complex), TDMAC (tridodecylmethylammonium chloride), 4-morpholineethanesulfonic acid monohydrate (Sigma Aldrich), Whatman™ 3 Chr Paper, Whatman™ 1 Chr Paper, Whatman™ 20 Chr Paper;

3.2.2 Equipment

CO_2 Laser cutter Gravograph LS 100, Metrohm Autolab Potentiostat, pH meter (Corning model 350)

3.2.3 Development of Potentiometric Sensors

3.2.3.1 Choice of Electrode Material

Conductive paths were painted with silver paste along 10 × 2 cm strips of paper and subsequently sintered at 100 °C for 30 min. Paths were also drawn with a pencil. Pencils of different grading differ in the amount of clay as compared to graphite. Therefore pencils ranging from hard (H), medium (HB) to soft (2B and 6B) were used to draw the paths on paper. In another attempt graphite powder (1–2 μm) was mixed with mineral oil–Nujol (2:1 wt%) and deposited on top of pencil drawn conductive path. A cellulose acetate based graphite paste was also prepared with 50/50(v/v) mixture of acetone and cyclohexanone, 7.5 % (wt%) of cellulose acetate and 30 % (wt%) of graphite powder. Resistivity of the path was measured with a standard multimeter.

3.2.3.2 Choice of Insulation

Paths drawn with a pencil and painted with silver ink were covered with different types of insulators, leaving only the endings of the paths bare to allow measurement. Insulators used included: melted candle wax, adhesive tape and lamination sheet as well as different types of glue (cyanoacrylate "Super bondex", two component epoxy glue "Araldite", one component synthetic resin glue "Prego liquido") and a liquid insulator "Fita isolante líquida" from Quimatic. First resistivity of the path was measured to evaluate impact of insulation. Later water was spotted on top of insulated fragment, or the middlepart of the "electrode" submerged in solution in search of potential defects in insulation. In the last step potassium selective PVC membrane was deposited on one of the ends.

3.2.3.3 Type of Paper

Impact of paper type was evaluated, by drawing electrodes on standard copy paper, Whatman™ Grade 1 and 3 papers and tracing paper. Electrodes were subsequently laminated leaving a small orifice where a potassium sensitive membrane was deposited. After conditioning overnight, experiments were carried out leading to a construction of a calibration curve for potassium. 4 sensors of each type were tested.

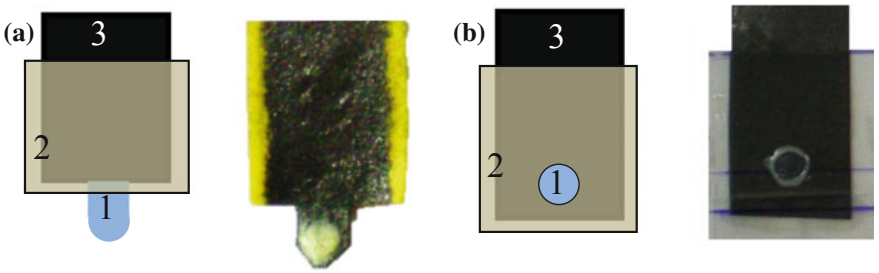

Fig. 3.3 Two principal architectures of potentiometric sensors used in this work. **a** Tip electrode, **b** orifice electrode. *1*. membrane, *2*. insulation, *3*. pencil drawn paper. Adapted with permission from [77]

3.2.3.4 Electrode Architecture

Two electrode architectures were proposed, tip and orifice electrodes. In the first type (Fig. 3.3a) the tip of the paper slip was not insulated and dipped in membrane solution, therefore membrane enclosed paper from all sides. In the second approach membrane was spotted in an ø 5 mm orifice in the insulation (Fig. 3.3b). In each case paper was first impregnated with wax to prevent absorption of water passing through the membrane.

3.2.3.5 Optimized Fabrication Procedure

For the discrimination of forged water samples electrodes were prepared as follows:

- wax was printed on both sides of Whatman™ Grade 1 paper;
- sheet was heated to evenly spread the wax throughout the whole paper structure;
- 25 × 10 mm slips were cut;
- electrical connection was drawn on top with a 6B pencil for several minutes to obtain steady resistance;
- lamination sheet was cut into 25 mm wide slips;
- Ø 5 mm punch was used to cut holes in one side of the lamination, 8 mm from the bottom;
- electrodes were inserted in the lamination sheet and subjected to lamination;
- individual electrodes were cut;
- two layers of membrane mixture 5 μL each, were deposited in the orifice;
- electrodes were conditioned in their respective conditioning solutions (Table 3.6) for at least 12 h before measurement;
- electrical connection was made by means of standard mini alligator clip;

3.2.4 Discrimination of Forged Water Samples

3.2.4.1 Electrode Matrix for the Discrimination of Forged Water Samples

Ion-selective electrodes were chosen based on chemical composition of bottled mineral waters presented in Table 3.1. Ions that presented the highest standard deviation between different brands were (in descending order): Ca^{2+}, Na^{+}, K^{+}, Mg^{2+}, NO_3^{-}. The highest standard deviation was observed for carbonate ion but as it is related with type of water (sparkling or still) and could be influenced by the time between opening of the bottle and measurement, carbonate-sensitive electrode was not included in the matrix. To obtain better discrimination capability two ion-selective (Cl^{-}, NO_3^{-}) and two cross-sensitive sensors (Na^{+}/K^{+}, Ca^{2+}/Mg^{2+}) were used. Final matrix was therefore composed of four sensors, which composition is resumed in Table 3.6.

Composition of the Ca^{2+}/Mg^{2+} selective electrode was elaborated and optimized based on cited references for Ca^{2+} and Mg^{2+} membranes. Other electrodes were prepared without changes. In each case membrane components as described in Table 3.6 were thoroughly mixed in 0.5 mL of tetrahydrofuran until homogenous (30 min to 2 h).

3.2.4.2 Reference Electrode

During study with forged water samples a home-made Ag/AgCl reference electrode was used for all measurements. A Pt wire was inserted in the tip of a 3.5 cm glass capillary during its sealing, electrode was filled with a saturated KCl solution. An Ag wire with electrochemically deposited layer of AgCl (5 mA, 2 h, HCl 1 mol/L,

Table 3.6 Composition of ion-selective membranes used for discrimination of forged mineral water samples. Adapted with permission from [77]

Electrode type	Plasticizer (mg)	Lipophilic salt (mg)	Polymer (mg)	Ionophore (mg)	Conditioning solution (mmol/L)	References
Cl^{-}	o-NPOE 66.0	TDMAC 0.08	PVC 33.0	TPPClMn 1.0	0.01 NaCl	[16]
Na^{+}/K^{+}	o-NPOE 62.0	KTFPB 2.05	PVC 30.7	Valinomycin 0.2; ionophore X 5.15	0.01 NaCl, 0.01 KCl	[16]
Ca^{2+}/Mg^{2+}	o-NPOE 63.8	KTFPB 0.6	PVC 30.4	ETH 129 1.3; ETH 1117 1.0	0.01$CaCl_2$, 0.01 $MgCl_2$	[39, 74]
NO_3^{-}	DOS 59.6	TDMAN 0.4	PVC 33.3	ETH 500 6.67	0.01 $NaNO_3$, 0.01 NaCl	[75]
K^{+}	o-NPOE 65.0	KTFPB 0.4	PVC 32.6	Valinomycin 2.0	0.01 KCl	[39]

Table 3.7 Composition of solutions used to construct calibration curves. Adapted with permission from [77]

Electrode type	Base electrolyte (mmol/L)	Additions (mmol/L)
Cl^-	0.01 $NaNO_3$	0.1 NaCl
Na^+/K^+	K^+: 0.01 $NaNO_3$ Na^+: 0.01 KNO_3	K^+: 0.1 KNO_3 Na^+: 0.1 $NaNO_3$
Ca^{2+}/Mg^{2+}	0.01 NaCl	0.1 $CaCl_2$
NO_3^-	0.01 NaCl	0.1 $NaNO_3$
K^+	0.01 $NaNO_3$	0.1 KNO_3

Pt reference electrode) was immersed in the KCl solution and affixed in the capillary with a rubber stopper.

3.2.4.3 Electrode Characterization

Calibration curve and sensitivity—four sensors of each type were prepared and a calibration curves separate for each type of electrode, were constructed. Table 3.7 resumes composition of solution used to construct calibration curves. Appropriate amounts of additions of solution containing ion in question were injected to 100 mL of base electrolyte.

Volume of consecutive additions was calculated to change the logarithm of activity according to Table 3.8.

Selectivity—selectivity coefficients were determined by the (SSM) separate solution method using 0.1 mmol/L solutions of inorganic salts: nitrates of appropriate cations and sodium salts in the case of anions. All solutions were buffered using 0.005 mol/L MES (4-morpholine ethane sulfonic acid monohydrate) with final pH adjusted with solutions of 0.1 mmol/L NaOH or 0.1 mmol/L H_2SO_4. The activities of ions in aqueous solutions were calculated according to the DebyeHueckel approximation.

Signal repeatability—two solutions of distinct activity (log a −3.25 and −2.25) of ion in question were prepared for each electrode type. Solutions were measured alternately 3 times each.

3.2.4.4 Electronic Tongue

Electronic tongue was composed of four working electrodes (Cl^-, NO_3^-, Na^+/K^+, Ca^{2+}/Mg^{2+}) and a miniaturized Ag/AgCl reference electrode of traditional

Table 3.8 Volume and value of log a for consecutive additions

Volume (mL)	0.002	0.002	0.008	0.028	0.088	0.280	0.892	2.900	10.500	15.300
log a	−5.75	−5.45	−4.97	−4.45	−3.94	−3.44	−2.94	−2.45	−1.96	−1.72

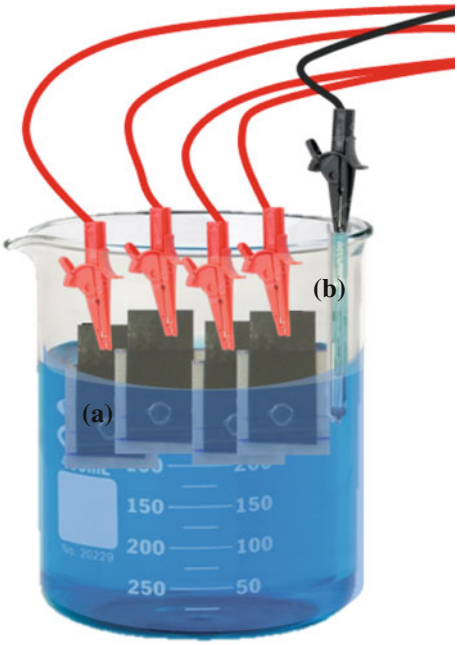

Fig. 3.4 Electronic tongue for the analysis of water samples. **a** Working electrodes, **b** reference electrode

architecture. During measurement all 4 sensors (multiplexed) and reference electrode were placed in the sample, under stirring, signal was measured for 5 min to guarantee its stabilization. Schematic representation of the measurement system is presented in Fig. 3.4.

To acquire signal from all electrodes at the same time a home-made system consisting of a multiplexer fabricated in our laboratory connected to a standard pH meter (Corning model 350) was used. Together with a PC this system allows electrode multiplexing, control over agitation velocity and data acquisition. The multiplexer is based on an acquisition card (model ACL-8111 ADLink Technology) and an analogic switch (ADG201) with software written in VISUAL BASIC 4.0. Detailed architecture, schematics, and logical structure can be found in [76].

3.2.4.5 Water Samples

9 different mineral waters from natural springs in Caxambu, Minas Gerais, Brazil and 2 commercial bottled mineral waters were obtained. Detailed composition as stated on the label or information chart provided by spa gardens "Parque das Águas" is presented in Table 3.9.

Samples present great range of concentrations of individual ions, with differences above 100 mg/L for Ca^{2+}, CO_3^{2-}, Na^+ and K^+. Apart from abovementioned three representative forged water samples were obtained. One coming from a lake

Table 3.9 Composition of mineral water samples in mg/L, as stated on the label or in the information chart provided by spa gardens "Parque das Águas", Caxambu-MG, Brazil (adapted with permission from [77])

	Crystal Yguaba[a]	Bio Pure Pietra[a]	Dom Pedro	Viotti	Beleza	Mayrink 1	Mayrink 3	Duque de Saxe	Princ. Isabel	Leopoldina	Venancio	Max–Min
Ca^{2+}	4.22	6.596	42.89	21.8	114.63	13.63	15.63	117.43	129.46	–	121.84	125.24
Mg^{2+}	0.999	3.915	–	4.13	69.5	2.92	2.43	64.64	33.78	10.94	74.82	73.821
CO_3^{2-}	108.32	51.51	241.89	119.67	1237.07	82.75	84.55	1041.37	865.89	458.31	1161.04	1185.56
Na^+	38.299	3.6	18.9	12	136	7	6	82	71	39	102	132.4
Cl^-	2.38	0.1	1	8	1.5	<0.25	<0.25	0.5	1	<0.25	1.5	7.9
K^+	2.262	1.846	19.6	11	116	6.37	7.5	86	74	36	84	114.154
SO_4^{2-}	7.32	0.06	4.96	3	9	1	2	7	6	–	8.5	8.94
F^-	0.26	0.05	0.92	0.31	2.6	0.13	0.17	1.5	1.7	0.52	2	2.55
PO_4^{3-}	0.51	0.11	<0.03	0.03	<0.03	<0.03	<0.03	<0.03	<0.03	0.03	0.03	0.48
Sr^{2+}	0.046	0.033	1.67	0.918	9.73	0.529	0.572	6.29	5.37	2.99	7.06	9.697

[a]Commercial bottled mineral waters

in the city of Caxambu and two samples of tap water from distinct places in Campinas, Sao Paulo, Brazil. Each of the 14 samples was divided in three parts and each part was measured separately in random order.

3.2.4.6 Chemometric Analysis

All chemometric analysis was performed in Pirouette 3.11(Infometrix). Principal Components Analysis was conducted with the mean result obtained for each sample. Initial potential data was mean-centered to equalize the relevance of each factor.

To guarantee the correct classification of adulterated and not adulterated samples, KNN analysis was performed. Data was divided in two parts, first KNN analysis was performed with 2/3 of the total data (28 samples, 3 variables, data mean-centered). In the next step this model was used to classify the remaining 14 samples.

3.2.5 Integration of Reference Electrode

3.2.5.1 Preparation of Silver Electrodes

Silver nanoparticles–prepared according to [78], as follows:

- 1.7 g polyvinylpyrrolidone dissolved in 35 mL of ethylene glycol and heated under stirring to obtain clear light yellow coloration;
- 25 mg KBr, 50 mg NaCl and 700 mg $AgNO_3$ dissolved in 7 mL of ethylene glycol and added dropwise to PVP solution;
- heated for 4 h 170 °C;

Two portions of above mixture were prepared, to one 200 mg $FeCl_3$ inn 5 mL H_2O was added in order to obtain Ag/AgCl nanoparticles [79]. Products were washed with water and centrifuged at 15,000 rmp, two times. Supernatant was discarded, and sediment dried and stored in dark at 4 °C.

Tollens reaction–several variations of electroless plating of silver by Tollens reaction were found in the literature [80, 81]. In this work reaction was performed with and without $SnCl_2$.

Reagent A: 250 mg $SnCl_2$ dissolved in 25 mL of water with 1 mL of 35 % HCl.
Reagent B: 3.5 g $AgNO_3$ dissolved in 60 mL of H_2O
0.35 g NaOH dissolved in 14 mL of H_2O
Both solutions mixed NH_3OH added till solution clarifies
Reagent C: 7 g of glucose, 0.57 g of tartaric acid dissolved in 140 mL of H_2O

Electrode patterns as shown in Fig. 3.5 were laser cut from Whatman™ Grade 1 paper. Dimensions: 1 × 1 cm^2 pad for electrical connection, 2 × 0.3 cm long conductive path and 0.5 cm round electrode area, with 0.4 orifice cut in the lamination sheet. For all methods of silver deposition two sets of four paper electrodes

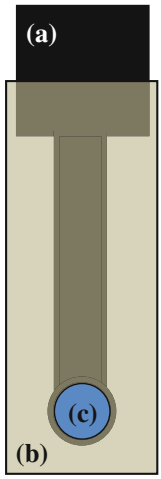

Fig. 3.5 Architecture of the electrode used for optimization of silver deposition. **a** Paper electrode, **b** lamination sheet, **c** ion-selective membrane

as shown on Fig. 3.5 were prepared. One set was covered with wax before silver deposition and the other left bare.

Types of deposition tested:

- Electrolube Conductive paint (silver content 45 %),1 layer 120 °C for 2 h;
- SPI Conductive Silver Paint, 2 layers, 120 °C for 2 h;
- Tollens with $SnCl_2$–Reagent A 10 min, Reagent B + C 70 °C for 2 h;
- Tollens–Reagent B + C 70 °C for 2 h;
- Tollens on Electrolube–1 layer of Electrolube Conductive paint left to dry, Reagent B + C 70 °C for 2 h;
- Nanoparticles–two component epoxy resin "Araldite" mixed with silver nanoparticles (1:2 wt%);
- Nanoparticles with graphite–two component epoxy resin "Araldite" mixed with graphite and silver nanoparticles (1:1:2 wt%);
- Nanoparticles with graphite–mineral oil (Nujol) mixed with graphite and silver nanoparticles (1:1:2 wt%);
- Nanoparticles with graphite–mineral oil (Nujol) mixed with silver nanoparticles (1:2 wt%), deposited on a layer of Electrolube silver paint;

Electrodes which presented sufficiently low resistivity were covered with Na^+ selective membrane and a calibration curve for sodium was constructed.

3.2.5.2 Fabrication of Ag/AgCl Reference Electrode

First Ag/AgCl nanoparticles were mixed with two component epoxy resin "Araldite" or Nujol (2:1 wt%) and deposited on an electrode painted with Electrolube silver paint. In the second approach electrodes were painted with SPI Conductive Silver Paint or with Electrolube silver paint later subjected to Tollens

reaction. Thus produced electrodes were treated with sodium hypochlorite (2 depositions of 10 μL of commercial bleach, each time left to react for 15 min) [82]. To test performance of thus prepared electrodes, their signal was measured (potentiometry, zero current) in 0.01 mol/L KCl versus a commercial Ag/AgCl reference electrode from Methrom.

3.2.5.3 Optimized Fabrication Procedure

Based on experiments concerning fabrication of Ag and Ag/AgCl electrodes in subsequent tests electrodes were prepared as follows:

1. Electrode pattern was laser cut from Whatman™ Grade 1 paper (Fig. 3.6a);
2. Two layers of SPI Conductive Silver Paint were painted;
3. Electrode pattern was sintered for 2 h at 120 °C;
4. Melted wax was deposited on the back side of the electrode, and the excess removed (Fig. 3.6b);
5. Individual electrodes were freed from the handling sheet;
6. Pattern was cut by hand from the lamination sheet (Fig. 3.6c);

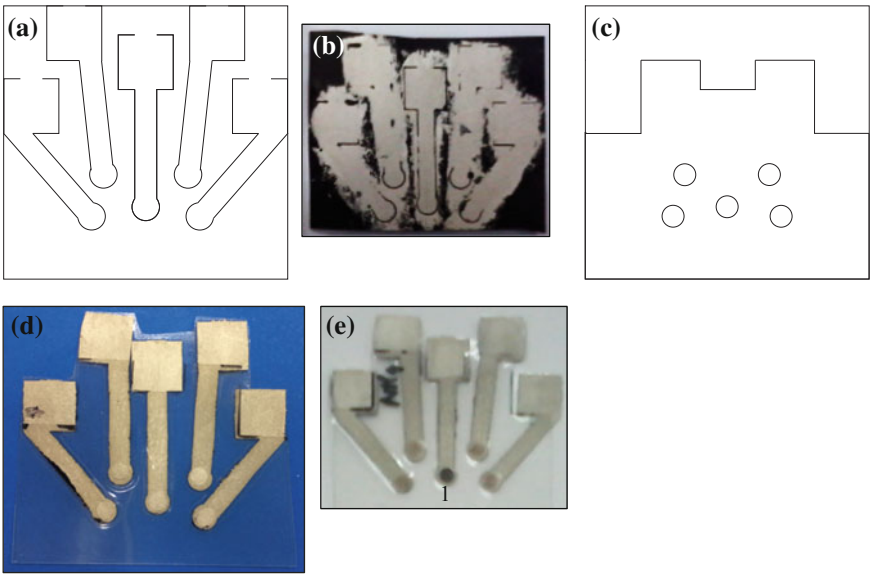

Fig. 3.6 Electronic tongue system for the analysis of beer samples. **a** Electrode pattern. **b** Electrodes painted with conductive paint and impregnated with wax. **c** Lamination pattern. **d** Assembled device. **e** Device ready for measurement–with ion selective membranes and Ag/AgCl reference electrode (1). Figures (a) and (c) adapted with permission from [84]

7. Device underwent lamination (Fig. 3.6d);
8. Two layers of appropriate membrane solution were spotted on working electrodes;
9. Bleach was spotted on top of reference electrode, excess removed after reaction and the electrode washed with distilled water;
10. Device was conditioned in appropriate mixed conditioning solution (Fig. 3.6e);

Device presented in Fig. 3.6 is designed in a way that working electrodes are positioned on a circle around the reference electrode, therefore all electrodes are in equal distance to the reference (Fig. 3.6e1). Lamination sheet is left uncut in the back side of the contact pads to stiffen the construction.

3.2.6 Discrimination of Beers

3.2.6.1 Electrode Matrix for the Discrimination of Beer Samples

Ion-selective electrodes were chosen based on chemical composition of beers and on response of sensing matrixes described in the literature (Table 3.5). To obtain better discrimination capability three ion-selective (Na^+, Ca^{2+}, NH_4^+) and one cross-sensitive sensor (anion-selective (AS)) were used. Final matrix was therefore composed of four sensors, which composition is resumed in Table 3.10.

Mixed conditioning solution used for electronic tongue conditioning: NH_4Cl 0.01 mmol/L, $CaCl_2$ 0.01 mmol/L, KH_2PO_4 0.05 mmol/L, KCl 0.02 mmol/L.

Table 3.10 Composition of ion-selective membranes used for discrimination of beer samples adapted with permission from [84]

Electrode type	Plasticizer (mg)	Lipophilic salt (mg)	Polymer (mg)	Ionophore (mg)	Conditioning solution (mmol/L)	References
Na^+	o-NPOE 66.0	KTPClPB 0.15	PVC 32.85	ionophore X 1.0	0.01 NaCl	[39]
Ca^{2+}	DOS 64.8	KTPClPB 0.85	PVC 33.0	ETH 129 2.15;	0.01 $CaCl_2$	[39]
NH_4^+	BPPA 64.7	KTPClPB 1.0	PVC 32.3	Nonactin 2.0	0.01 NH_4Cl	[39]
AS	o-NPOE 64.3	TDMAC3.5	PVC 322	–	0.01 NaCl or 0.05KH_2PO_4, 0.25 Na_2HPO_4	[12]

Table 3.11 Composition of solutions used to construct calibration curves

Electrode type	Base electrolyte (mmol/L)	Additions (mmol/L)
Na^+	0.01 KNO_3	0.1 $NaNO_3$
Ca^{2+}	0.01 NaCl	0.1 $CaCl_2$
NH_4^+	0.01 $CaCl_2$	0.1 NH_4Cl
AS	0.01 $Ca(NO_3)_2$	0.1 NaCl

3.2.6.2 Electrode Characterization

Calibration curve and sensitivity—four sensors of each type (integrated in one device) were prepared and a calibration curves separate for each electrode type (Table 3.11), were constructed.

Selectivity–was measured as described before, during studies four sensors of each type integrated in one device were used.

Signal repeatability–solution used in repeatability study consisted of NH_4NO_3, $NaNO_3$, $CaCl_2$ and NaCl in concentrations equal 0.005 mmol/L or 0.01 mmol/L. Three electronic tongues were used for this study each consisting of one electrode of each type.

3.2.6.3 Electronic Tongue

Electronic tongue was composed of four working electrodes (AS, NH_4^+, Na^+, Ca^{2+}) and an integrated Ag/AgCl reference electrode (Fig. 3.6). During measurement all 4 sensors (multiplexed) and reference electrode were placed in the sample (Fig. 3.7), under stirring, signal was measured for at least 5 min to guarantee its stabilization.

3.2.6.4 Beer Samples

Thirty four different beers (12 types, 19 brands) were tested during this study (Table 3.12).

3.2.6.5 Chemometric Analysis

Analysis of All Beer Samples (34 Samples)

PCR–discrimination of different beer types–for this study non-beer samples were deleted from the dataset (Radler and distilled lemon alcoholic drink), as they were classified as outliers. Data was range scaled before analysis. Samples were grouped into types such as: Pilsner (including Pilsner 0 %), Lager, Stout, Weiss, Malzbier, Munich, Ale, Schwarzbier, Dark.

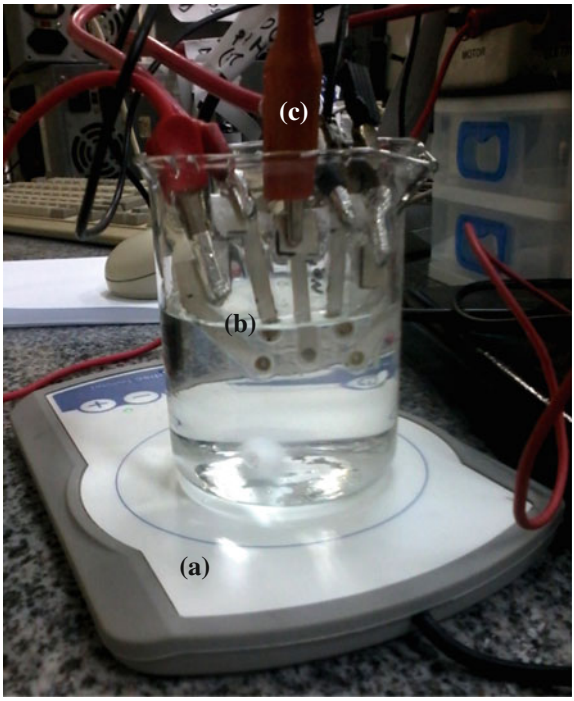

Fig. 3.7 Electronic tongue system for the analysis of beer samples. **a** Magnetic stirrer, **b** electronic tongue with integrated reference, **c** alligator clip connectors

KNN–presence of antioxidants and stabilizers–all 34 samples, two replicates were analyzed using the KNN algorithm (2 neighbors). Data was range scaled before analysis. Classification was based on the presence of antioxidants and stabilizers, as stated in Table 3.12.

PLS–prediction of pH–before measurement with electronic tongue, pH of samples was measured with standard pH meter. Data was mean-centered before analysis.

PLS–alcohol content–electronic tongue response was correlated with alcohol content as stated on the label (Table 3.12). Data was mean-centered before analysis.

Analysis of Pilsner Beers (13 Samples)

PCA–discrimination of Pilsner beers—the 34 sample data set tested during this study included 13 Pilsner beers, because of large volume of data this group was analyzed separately. Different pretreatment techniques were tested to enhance separation of brands, including: mean-centering, auto-scaling, range scaling, variance scaling and no pretreatment.

Table 3.12 List of beer samples. Adapted with permission from [84]

	Brand	Type	Name	Fermentation	Alc. vol. %	Origin	Brewery	Unmalted cereals	Carbohyd.	Dye	Other addtives	Antioxidant	Stabilizer	pH	Serial number
1	Ashby	Weiss	Weiss	High	6.7	Amparo SP	Cervejaria Ashby Ltda	No	Yes	No	Wheat	INS 316	INS 405	4,529	L214001110315
2	Ashby	Pilsen	Pilsen	Low	4.8	Amparo SP	Cervejaria Ashby Ltda	Yes	Yes	No	No	INS 316	INS 405	4,419	L210001100215
3	Zehn bier	Weiss	Weiss	High	5.5	São Luiz Brusque SC	Hezbier Cervejaria Ltda	No	No	No	Wheat	No	No	4,211	2360
4	Zehn bier	Galer	Pilsen extra	Low	5.6	São Luiz Brusque SC	Hezbier Cervejaria Ltda	No	No	No	No	No	No	4,58	2367
5	Brahma	Malzbier	Malzbier	Low	4	Jacarei SP	Ambev SA	Yes	Yes	Yes	No	INS 316, INS 221	INS 405	3,96	jc23:132
6	Bavaria	Pilsen	Bavaria Pilsen	Low	4.6	Ponta grossa PR	Heineken Brasil	Yes	Yes	No	No	INS 316, INS 224	INS 405	3,851	l505507600713
7	Kaiser	Radler	Kaiser Radler	Low	2	Ponta grossa PR	Heineken Brasil	No	Yes	No	Lemon juice	No	No	2,997	l434907602322
8	Bavaria	Pilsen	Premium Puro malte	Low	4.8	Jacarei SP	Heineken Brasil	No	No	No	No	INS 316, INS 224	INS 405	4,106	l5069076f0048
9	Devassa	Pilsen	one #vemprapelada	Low	4.7	Itu SP	Brasil Kirin SA	Yes	No	No	No	INS 316	INS 405	4,191	l8502744
10	Skol	Pilsen	Pilsen	Low	4.7	Sete Lagoas MG	Ambev SA	Yes	Yes	No	No	INS 316, INS 221	INS 405	3,836	nm13:22 1
11	Skol	Distilled	Beats Senses	Not app.	7.9	Jacarei SP	Ambev SA	No	Yes	INS 150 C	Lemon juice, Acidulants INS 330 INS 334, Acidity regulators INS 331 III INS 296	Other	Other	2,642	jc09:34 3
12	Itaipava	Malzbier	Cerveja Malzbier	Low	4.2	Teresopolis RJ	Cervejaria Petropolis	Yes	Yes	INS 150 C	No	INS 316, INS 223	INS 405	4,005	3222213

(continued)

Table 3.12 (continued)

	Brand	Type	Name	Fermentation	Alc. vol. %	Origin	Brewery	Unmalted cereals	Carbohyd.	Dye	Other addtives	Antioxidant	Stabilizer	pH	Serial number
13	Schin	Munich	Cerveja Escura tipo Munich	Low	4.,5	Itu SP	Brasil Kirin SA	Yes	Yes	INS 150 C	No	INS 136	INS 405	4,025	l8499234
14	Caracu	Stout	Cerveja escra forte	High	5.4	Jacarei SP	Ambev SA	Yes	Yes	INS 150 C	Roasted malt	No	No	4,101	jc02142
15	Kaiser	Lager	Receita lager tradicional	Low	4.5	Jacarei SP	Heineken Brasil	Yes	Yes	No	No	INS 316, INS 224	INS 405	3,996	l5036076g0437
16	Budweiser	Lager	Limited edition UFC	Low	5	Jacarei SP	Ambev SA	Yes	No	No	No	No	No	4,164	201214jc
17	Bohemia	Pilsen	Pilsen	Low	5	Jaguariuna SP	Ambev SA	Yes	Yes	No	No	INS 316, INS 221	INS 405	4,031	ja0922
18	Itaipava	Pilsen	Pilsen	Low	4.5	Boituva SP	Cervejaria Petropolis	Yes	Yes	No	No	INS 316, INS 223	INS 405	4,094	56192711
19	Stella Artois	Lager	Lager	Low	5	Jacarei SP	Ambev SA	Yes	No	No	No	No	No	4,07	jc13303
20	Brahma	Pilsen	Chopp	Low	4.8	Uberlandia MG	Ambev SA	Yes	Yes	No	No	INS 316, INS 221	INS 405	3,87	tm1559
21	Crystal	Pilsen 0 %	Crystal 0 %	Low	0	Boituva SP	Cervejaria Petropolis	Yes	Yes	No	No	INS 316, INS 223	INS 405	4,032	520081
22	Antarctica	Pilsen	Antarctica Subzero	Low	4.6	Jacarei SP	Ambev SA	Yes	Yes	No	No	INS 316, INS 221	INS 405	4,049	jc17312
23	Schin	Pilsen 0 %	Schin Zero Alcool 0	Low	0	Itu SP	Brasil Kirin SA	Yes	Yes	No	Malt extract	INS 316	INS 405	3,975	l850654
24	Crystal	Pilsen	Pilsen	Low	4.5	Boituva SP	Cervejaria Petropolis	Yes	Yes	No	No	INS 316, INS 223	INS 405	4,162	2811201
25	DaDoBier	Pilsen	DaDoBier Lager	Low	5	Santa Maria RS	Santamate IND Ltda	No	Yes	No	No	INS 316	INS 405	4,243	le051im
26	Bohemia	Schwarzbier	Bohemia Escura	Low	5	Jacarei SP	Ambev SA	Yes	Yes	INS 150 C	No	INS 316, INS 221	INS 405	3,852	jc22414
27	Schin	Pilsen	Cerveja Pilsen	Low	4.7	Itu SP	Brasil Kirin SA	Yes	No	No	No	INS 316	INS 405	4,207	l8512550

(continued)

Table 3.12 (continued)

	Brand	Type	Name	Fermentation	Alc. vol. %	Origin	Brewery	Unmalted cereals	Carbohyd.	Dye	Other addtives	Antioxidant	Stabilizer	pH	Serial number
28	Heineken	Lager	Heineken Lager	Low	5	Jacarei SP	CKBR SA	No	No	No	No	No	No	4,256	l5044076g1659
29	Xingu	Pilsen	Extra pilsen premium gold	Low	5.4	Jacarei SP	CKBR SA	Yes	No	No	No	INS 316, INS 224	INS 405	3,991	l4288076b1454
30	Eisenbahn	Weiss	Weizenbier	High	4.8	Blumenao S.C.	Cervejaria Sudbrack Ltda	No	No	No	Wheat	No	No	4,25	60
31	Bohemia	Dark	Escura, cerveja extra escura	Low	5	Petropolis RJ	Ambev SA	Yes	Yes	INS 150 C	Acidulant INS 270	INS 316	INS 405	3,971	pr1315
32	Devassa	Tropical Ale	Devassa Ruiva	High	4.8	Itu SP	Brasil Kirin SA	No	No	No	Unspecified Malts	INS 316	INS 405	4,205	L8502404
33	Xingu	Ale	Unique red	High	4.6	Jacarei SP	CKBR SA	Yes	Yes	INS 150 C	No	INS 316, INS 224	INS 405	3,937	l5019076b0535
34	Xingu	Stout	Original Black	High	4.6	Jacarei SP	CKBR SA	Yes	Yes	INS 150 C	No	INS 316, INS 224	INS 405	3,989	L4291076b0137

Analysis of Other (Non-Pilsner) Beer Types

KNN–type of fermentation, presence of unmalted cereals, carbohydrates and caramel dye-data was range scaled in the case of all KNN analyses. With lowest number of misclassifications for 1 and 2 neighbors.

3.2.7 Minimization of Sample Volume

In the first attempt flow-through devices with electrodes integrated in the channel were tested. Architecture was based on the device constructed for simultaneous detection of glucose and uric acid. Several devices, resumed in Fig. 3.8 were proposed (wicking pads, reference electrodes not market on the drawings). Different channel architectures were tested in order to:

- maximize the contact of the sample with the membrane;
- reduce spaces prone to retention of the liquid.

Device was wax printed and in the first tests electrodes were drawn with pencil graphite (Fig. 3.8a2). Sodium selective membrane was spotted from the front and back to fully cover the electrical contact (Fig. 3.8a1). Two tests were carried out: an electrochemical measurement and a visualization of flow with a colored solution (food dye) passing through the channel.

In another attempt electrodes was prepared as before (4.2.5.3 Optimized fabrication procedure), with two modifications. First, all electrodes were aligned as shown in Fig. 3.9. In this the case distance between working electrodes and Ag/AgCl reference is not constant, nevertheless this architecture was chosen for studies on minimization of sample volume. Two architectures were tested, similarly to studies on discrimination of forged water samples, an electronic tongue with orifice electrodes (Fig. 3.6 but with aligned electrodes) and another with tip electrodes constructed as shown on Fig. 3.9.

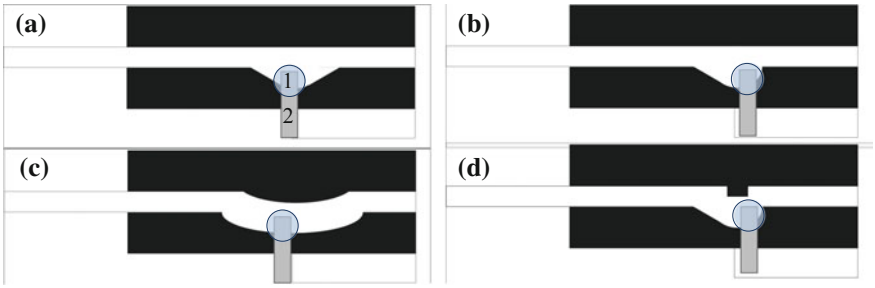

Fig. 3.8 Flow-through devices with integrated working electrode. **a** Channel with triangular electrode niche, **b** Channel with a teardrop shaped electrode niche, **c** oval channel, **d** Architecture B with an inset. *1* ISE membrane, *2* electrical contact

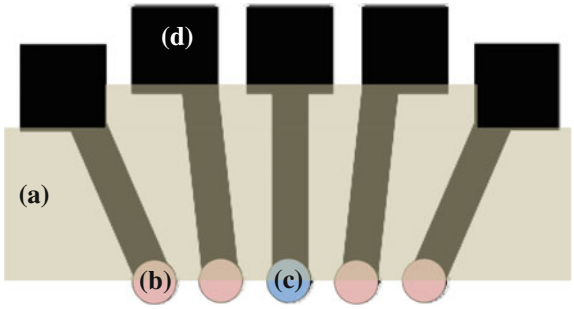

Fig. 3.9 Electronic tongue system for the analysis of wine samples. **a** Lamination sheet, **b** working electrode, **c** Ag/AgCl reference, **d** Silver electrical contact

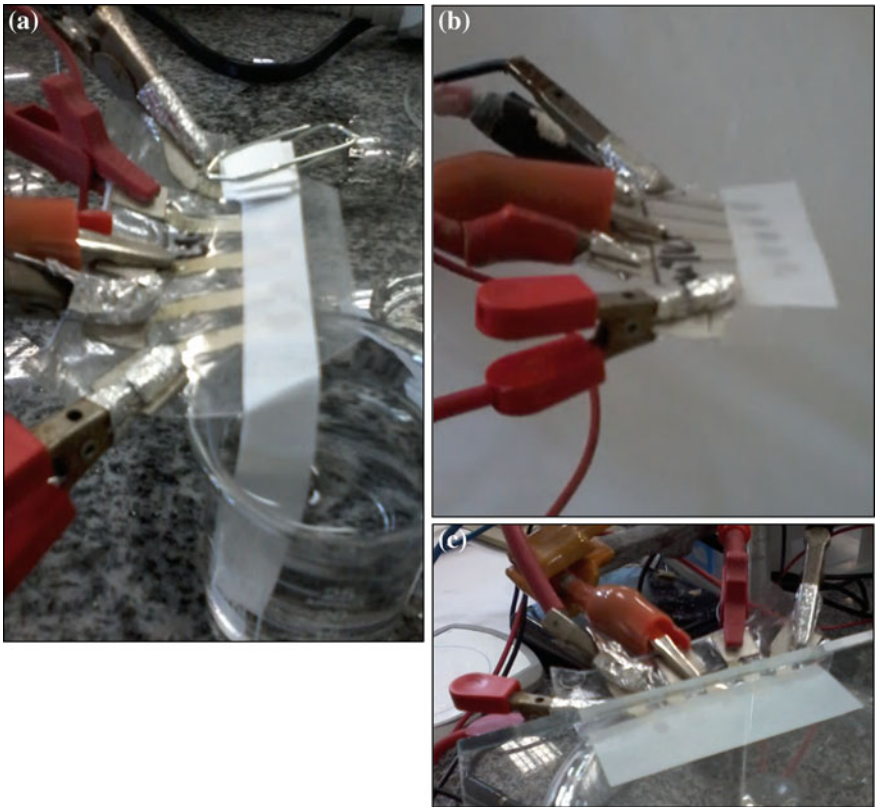

Fig. 3.10 Types of measurement tested to minimize the sample volume necessary for analysis. **a** Measurement in flux, **b** stationary measurement with a paper sample pad, **c** stationary measurement device stacked against glass plaques

To minimize volume of the sample three types of measurement were proposed:

- measurements in flux, accomplished by placing a paper slip with wicking pad attached on top of the electrodes (Fig. 3.10a);
- stationary measurements, accomplished by placing a slip of paper impregnated with the sample solution on top of the electrodes (Fig. 3.10b);
- as above but with a glass plaque stacked against the paper and electronic tongue to assure good contact between electrodes and the paper slip (Fig. 3.10c);

Three devices of each type (tip, orifice) with cation-sensitive electrodes were prepared for each type of measurement (flow, paper sample pad, stacked) and signal repeatability study was carried out as described before. Solution used in repeatability study consisted of $NaNO_3$, KNO_3 $CaCl_2$, $MgCl_2$, NaCl in concentrations equal 0.005 or 0.01 mmol/L.

In the next step three types of paper: Whatman no 1, no 20 and no 3 were tested as sample carriers.

3.2.8 Discrimination of Wines

3.2.8.1 Electrode Matrix for the Discrimination of Wine Samples

Ion-selective electrodes were chosen based on chemical composition of wines and on response of sensing matrixes described in the literature (Table 3.5). To obtain better discrimination capability all four sensors composing the matrix were cross-sensitive (anion-selective (AS), cation-selective (CS), Ca^{2+}/Mg^{2+}, K^{+}/Na^{+}). Final matrix was therefore composed of four sensors, which composition is resumed in Tables 3.6, 3.10 and 3.13.

Mixed conditioning solution used for electronic tongue conditioning: $NaNO_3$ 0.01 mmol/L, KNO_3 0.01 mmol/L, $CaCl_2$ 0.01 mmol/L, $MgCl_2$ 0.01 mmol/L, NaCl 0.01 mmol/L.

3.2.8.2 Electrode Characterization

Calibration curve and sensitivity—four sensors of each type (integrated in one device) were prepared and a calibration curves separate for each electrode type (Tables 3.7 and 3.11), were constructed. Calibration curve for cation-selective electrode was constructed in the same manner as for sodium ISE (Table 3.11).

Table 3.13 Composition of cation-selective electrode. Adapted with permission from [84]

Electrode type	Plasticizer (mg)	Lipophilic salt (mg)	Polymer (mg)	Ionophore (mg)	Conditioning solution (mmol/L)	References
CS	DOS 66.0	KTFPB 1.0	PVC 33.0	–	0.01 NaCl	[64]

Selectivity—was measured as described before, during studies four sensors of each type integrated in one device were used.

Signal repeatability-solution used in repeatability study consisted of $NaNO_3$, KNO_3, $CaCl_2$, $MgCl_2$, NaCl in concentrations equal 0.005 or 0.01 mmol/L. Three electronic tongues were used for this study each consisting of one electrode of each type.

3.2.8.3 Electronic Tongue

Electronic tongue was composed of four working electrodes (AS, CS, Ca^{2+}/Mg^{2+}, K^+/Na^+) and an integrated Ag/AgCl reference electrode. During measurement a paper slip impregnated in sample solution was placed on top of the sensing system covering all 4 sensors and the reference electrode (Fig. 3.11), signal was measured

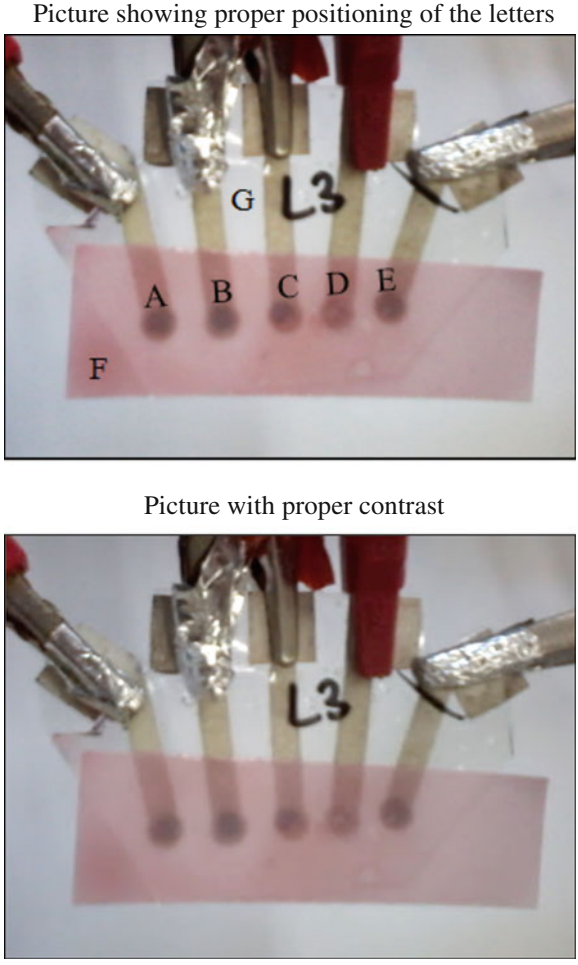

Fig. 3.11 Electronic tongue for measurement of wine samples. **a** Ca^{2+}/Mg^{2+} ISE, **b** AS-ISE, **c** Ag/AgCl reference electrode, **d** CS-ISE, **e** K^+/Na^+ ISE, **f** wine impregnated paper slip, **g** paper-based electronic tongue

Table 3.14 List of wine samples. Adapted with permission from [84]

	Brand	Grape variety	Style	Aged (Y/N)	Type	Alc. vol. %	Year	Vinery	Region	Country of origin	Preservatives	Serial number
1	Chalise	Americanas	White	N	Dry	11	2013	Vinicola Salton	Serra Gaucha, Bento Goncalves RS	Brazil	INS 220	1506313
2	Santa Florentina	Malbec	Red	N	Dry	12,5	2012	La Riojana Coop Vitivinifruticola de la Rioja LTDA	La Rioja Chilecito LR	Argentina	INS 220	L12201 a 06:54
3	Casillero del Diablo	Malbec	Red	Y	Dry	13,5	2013	Vina Concha y Toro	Valle central	Chile	INS 220	L2133714 09:11
4	Santa Helena	Chardonnay	White	Y	Dry	13	2014	Vina San Pedro Tarapaca SA	Valle central	Chile	INS 220	VSPT2014 4287
5	Novecento	Chardonnay	White	N	Dry	14	2013	Bodega Dante Robino	Mendoza	Argentina	INS 220	L9713
6	Santa Carolina	Merlot	Red	Y	Semi-dry	12,5	2013	Vina Santa Carolina SA	Valle central	Chile	INS 220	l4260246802
7	Fincas Privadas	Malbec	Red	N	Dry	13,8	2013	Bodega Luis V Chirino SA	San Juan	Argentina	INS 220	FPMC1314
8	Marcus James	Chardonnay	White	N	Semi-dry	11,5	2014	Cooperativa vinicola aurora LTDA	Serra Gaucha, Bento goncalves RS	Brazil	INS 220, INS 202	51030805115
9	Chalise	Americanas	Red	N	Dry	11	2008	Vinicola Salton	Serra Gaucha, Bento goncalves RS	Brazil	INS 220	152008
10	Saint Germain	Merlot	Red	N	Semi-dry	11	2015	Cooperativa vinicola aurora LTDA	Serra Gaucha, Castas Nobrs	Brazil	INS 220, INS 202	L51035306815
11	Marcus James	Merlot	Red	N	Semi-dry	11,5	2014	Cooperativa vinicola aurora LTDA	Serra Gaucha, Bento goncalves RS	Brazil	INS 220, INS 202	L51020633714

INS 202 -Potassium sorbate, INS 220 -SO_2

for several minutes and subsequent analysis was based on data obtained after signal stabilization but before effects such as drying of the paper slip could influence the result. Three samples were obtained from each wine bottle, next samples were encoded and measured in random order.

3.2.8.4 Wine Samples

Eleven different wines (4 types of grapes, red/white, 3 countries) were tested during this study (Table 3.14).

3.2.8.5 Chemometric Analysis

PCA–discrimination of grape variety–different pretreatment techniques were tested to enhance separation of brands, including: mean-centering, auto-scaling, range scaling, variance scaling and no pretreatment. All data was subjected to analysis (11 samples, 3 replicates).

PLS–prediction of grape variety–data was auto-scaled before analysis. 2/3 of data was used to construct a PLS model. In the next step this model was used to classify the remaining 11 samples.

KNN–Wine style (dry, semi-dry), stabilizer type–data was auto-scaled or variance-scaled before analysis. 2/3 of data was used to construct a KNN model, which was later used to classify remaining samples.

3.2.9 Detection with a Multimeter

As it was already described by Sevilla et al. [27] it is possible to carry out potentiometric measurements using a standard electrician's multimeter. As a proof of concept repeatability studies were carried out using this method. During measurement red tip was connected to working electrode, and black to reference. Signal was written down after stabilization.

Storage stability studies of proposed sensor matrix for beer and wine analysis were performed with a multimeter. Storage stability was analyzed by signal repeatability studies carried out during consecutive weeks. Solution used in this study consisted of $NaNO_3$, KNO_3, $CaCl_2$, $MgCl_2$, NaCl in concentrations equal 0.005, 0.01 and 0.05 mmol/L.

Electronic tongue systems were stored in room temperature in mixed conditioning solution. Measurement for both electronic tongue systems with working electrodes placed around Ag/AgCl reference and aligned were tested with a paper sample pad placed on top of the electrodes.

3.3 Results and Discussion

3.3.1 Development of Potentiometric Sensors

3.3.1.1 Choice of Electrode Material

Silver ink used to paint conductive paths was of poor quality and had to be applied several times to obtain satisfactory resistance. High discrepancies between resistances of individual electrodes were observed. Silver trail was also prone to break on flexible paper surface, especially in preliminary tests (longer 10 cm paths). From all pencil types tested to draw the conductive paths, the softest 6B pencil gave the best results. To obtain steady resistance (50–100 kΩ) the paths had to be drawn for several minutes.

As it can be seen on Fig. 3.12 paper modified with wax still presents porous structure. Each fiber is tightly covered with wax. After drawing with pencil, structure becomes continuous, without any pores or fibers visible.

3.3.1.2 Choice of Insulation

Melted candle wax provided good insulation, but it would break easily upon handling of paper electrodes. When wax was spotted directly on top of paper, the layer resulting was thick and extremely brittle. Because of this, wax was first heated and spread evenly with a spatula. This method could provide low cost, easily available insulation for optimized systems made from thicker paper.

As it comes to glues, cyanoacrylate would break the electrical contact of the both silver and graphite paths. Other types of glue tested did not provide satisfactory insulation. Liquid insulator provided good results, before and after submersion. The layer resulting was rather thick but product could be diluted in tetrahydrofuran.

Covers tested included adhesive tape and lamination. Adhesive tape detached upon submersion in water but laminated layer did not, providing good insulation

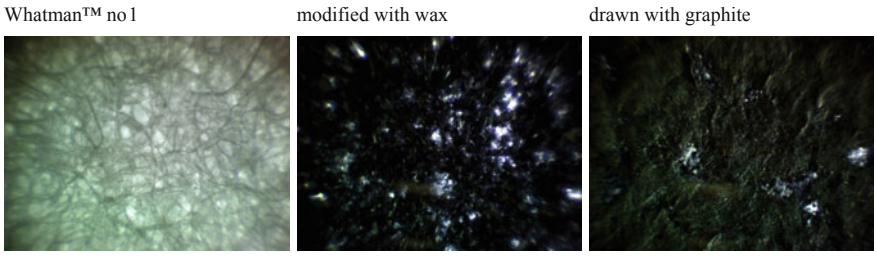

Fig. 3.12 Surface of paper electrode during subsequent steps of preparation seen through an optical microscope (magnification ×10)

and stiffening the construction of electrodes. Lamination became method of choice, as it is more easily available than liquid insulator, and easier to apply.

It was noted that electrodes prepared with the use of carbon paste were harder to insulate, due to uneven and protruding structure.

3.3.1.3 Type of Paper

From different types of paper used (copy paper, Whatman™ Grade 1 and 3, tracing paper) best results were obtained for Whatman™ Grade 1. Thicker Whatman™ Grade 3 was prone to absorb water even when treated with several layers of wax, but electrodes produced from this paper were more rigid. Tracing paper even after impregnation with wax would become corrugated during electrode conditioning, this result may be related to problems with adherence of insulation. It was possible to construct calibration curves for potassium with electrodes prepared on both office and Whatman™ Grade 1 papers. The latter presented better sensitivity probably due to higher volume of graphite deposited on more fibrous Whatman™ Grade 1 paper.

3.3.1.4 Electrode Architecture

Too long electrodes resulted in higher resistance and were more susceptible to insulation failures thus 20 mm was chosen as the path length. Tip electrodes presented slightly better sensitivity (23.1 mV/dec) as compared with orifice electrodes (18.8 mV/dec). Tip electrodes had proven difficult to insulate at the junction of membrane and the electrode, and measurements with not isolated electrodes were laborious (rising level of liquid with each addition during calibration). Therefore orifice electrode was chosen for further tests.

3.3.2 Discrimination of Forged Water Samples

3.3.2.1 Electrode Characterization

Calibration curve and sensitivity—are presentative dynamic response for each electrode type is presented in Fig. 3.13, with respective sensitivities and standard deviation resumed in Table 3.15.

Sensitivity of developed sensors is rather low as compared with theoretical (59.16 [mV/$\log_{(ax)}$]), and with other paper-based potentiometric sensors, for example presented by Novell et al. [23, 24] and by Whitesides group [25]. This fact can be attributed to rather high resistance of pencil graphite as compared with carbon nanotubes and silver used by other research groups. Sensors present good linearity in the range 10^{-5}–10^{-2} (higher range than sensors presented in [25]).

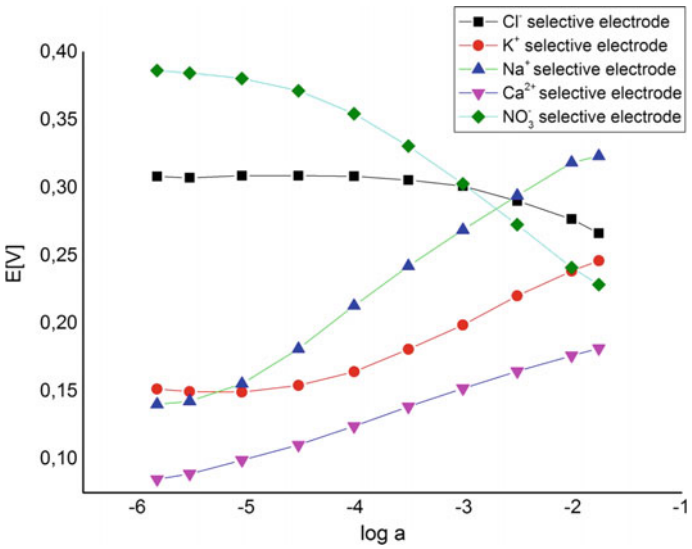

Fig. 3.13 Dynamic response of paper-based ion selective electrodes (electronic tongue for discrimination of forged water samples) (adapted with permission from [77])

Table 3.15 Sensitivity of studied sensors (electronic tongue for discrimination of forged water samples) (adapted with permission from [77])

Ion	Range (mol/L)	Sensitivity (mV/dec)	St. dev. (N = 4)	R^2	Literature data [25]
Na^+	1.2×10^{-5}–1.3×10^{-2}	27.6	2.3	0.998	54.8
K^+	4.0×10^{-5}–2.3×10^{-2}	18.8	0.9	0.998	54.9
Ca^{2+}	4.0×10^{-6}–1.3×10^{-2}	12.6	1.2	0.998	22.9
NO_3^-	4.0×10^{-5}–2.3×10^{-2}	−25.5	2.1	0.991	–
Cl^-	4.0×10^{-4}–2.3×10^{-2}	−18.8	4.9	0.997	−61.8

Selectivity–Tables 3.16 and 3.17 present selectivity coefficients of studied electrodes together with examples from the literature. As it can be seen, the results are with good accordance with data obtained from other systems. It is also noteworthy that all sensors present cross-sensitivity, desired when working with electronic tongue systems.

Signal repeatability–Table 3.18 presents the medium of standard deviations obtained for each electrode type (standard deviation of signal from 3 measurements of the same solution, next taken an average from 3 sensors). The

Table 3.16 Selectivity coefficients of anion-selective paper electrodes (adapted with permission from [77])

Selectivity coefficient towards	Electrode type		Literature data [39]	
	Cl^-	NO_3^-	Cl^-	NO_3^-
Cl^-	0.00	−2.76	0.20	−2.07
Br^-	0.14	−0.30	0.49	−1.18
NO_3^-	0.72	0.00	0.00	0.00
F^-	−1.57	−1.50	−0.80	−2.58
ClO_4^-	1.49	3.28	1.72	2.34
SO_4^-	−1.53	−4.46	−1.85	−3.00

Table 3.17 Selectivity coefficients of cation-selective paper electrodes (adapted with permission from [77])

Selectivity coefficient towards	Electrode type		Literature data	
	K^+/Na^+	Ca^{2+}/Mg^{2+}	K^+/Na^+ [83]	Ca^{2+} [39]
Na^+	−0.17	−6.24	0.00	−3.79
K^+	0.00	−3.77	−1.20	−3.81
NH_4^+	−0.96	−5.42	−1.05	−3.66
Li^+	−0.68	−1.74	−1.55	−1.56
Mg^{2+}	−2.01	0.39	−2.05	−3.38
Ca^{2+}	−1.67	0.00	−1.85	0.00

calcium-magnesium selective electrode optimized during this work shows the lowest variations (∼1 mV).

3.3.2.2 Chemometric Analysis

Principal Component Analysis–PCA 1, 2 and 3 presented 86.7, 9.5 and 2.3 % of total information respectively. As it can be clearly seen on Fig. 3.14 tap, and lake water samples present a separate cluster from mineral waters (more negative Factor 1). Samples similar in chemical composition are grouped close as in the case of Mayrink I and III shown in the lower part of the graph. As it can be seen bottled mineral water and the one obtained directly from the spring do not form separate clusters.

Modeling power of all electrodes was almost equal (K^+/Na^+ ∼ 0.5, other ∼ 0.6). In scaled sensor response (graph not shown) NO_3^- sensor presented lowest standard deviation between the samples. PCA1 versus PCA2 loadings plot (graph not shown) showed that NO_3^- electrode directs samples similarly to Cl^-, thus by removing this sensor more impact would be given to the other two.

Therefore data was analyzed without the NO_3^- sensor. With only 3 sensors left there is no need for dimensionality reduction and 3D graph can be constructed

Table 3.18 Signal repeatability for each sensor type. Adapted with permission from [77]

Electrode type	Cl^-	Na^+/K^+	Ca^{2+}/Mg^{2+}	NO_3^-
St. dev. (N = 3) log a = −3.25	6.8 mV	10.8 mV	1.5 mV	4.2 mV
St. dev. (N = 3) log a = −2.25	4.6 mV	3.5 mV	0.6 mV	4.1 mV

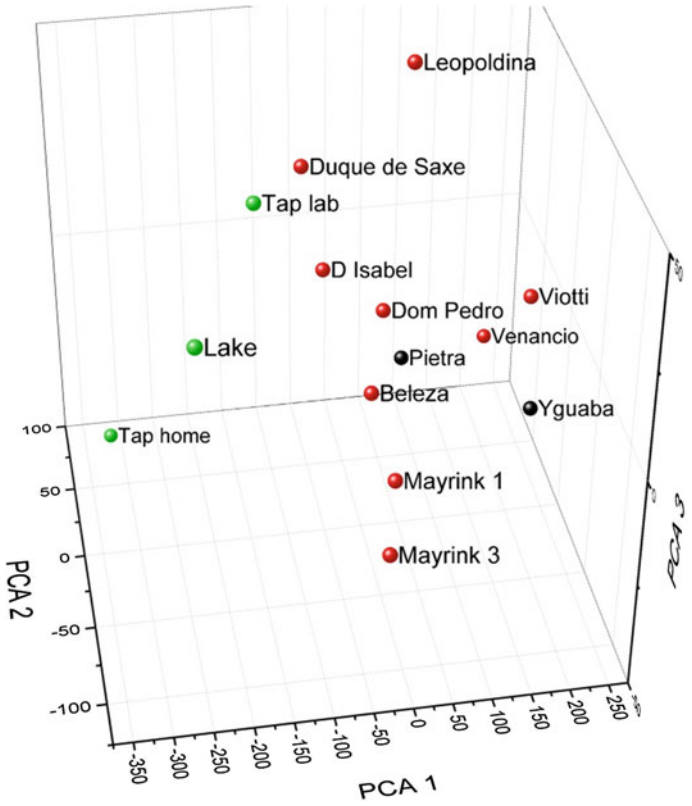

Fig. 3.14 PCA scores plot for all water samples, and all electrodes (*green*–tap and lake water, *black*–commercial, bottled mineral water, *red*–mineral water directly from spring) (adapted with permission from [77])

directly. As it can be seen in Fig. 3.15 separation was not only still possible, but clusters became more pronounced without NO_3^- selective electrode.

K-Nearest Neighbor–2/3 of the data was used to construct a KNN model, and the remaining 1/3 to validate it. As it can be seen in Fig. 3.16 all samples were classified correctly as adulterated or not adulterated.

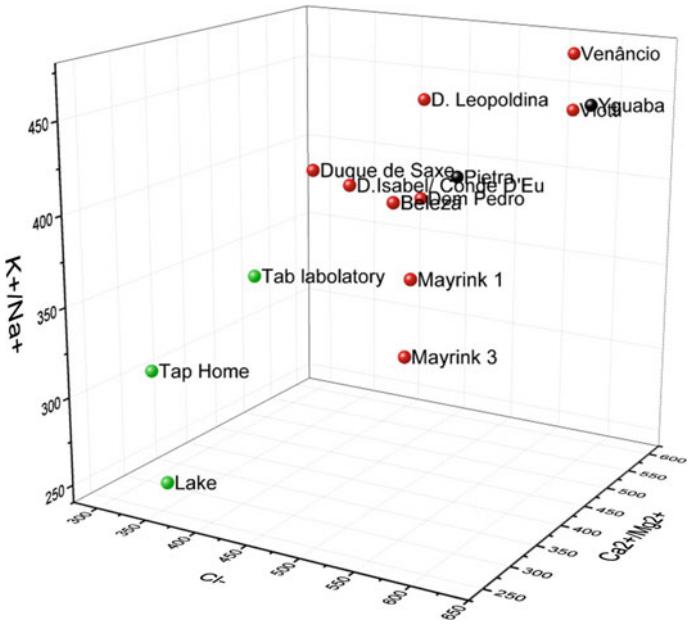

Fig. 3.15 3D plot for all water samples, data without NO_3- sensor (*green*–tap and lake water, *black*–commercial, bottled mineral water, *red*–mineral water directly from spring) (adapted with permission from [77])

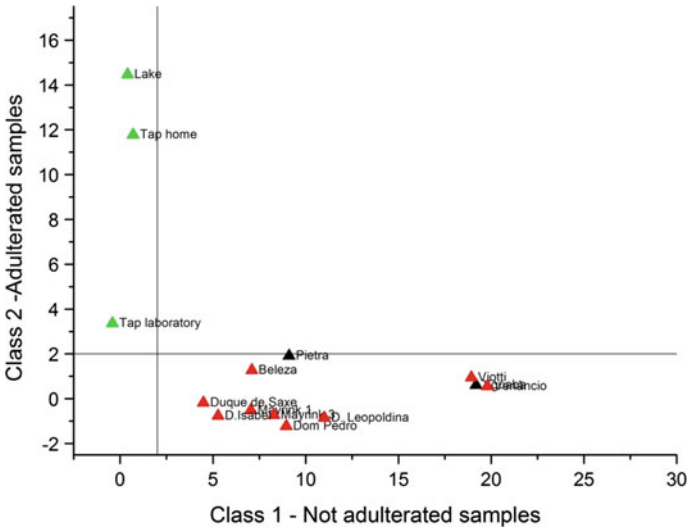

Fig. 3.16 KNN Class fit plot, data without NO_3- sensor (*green*–tap and lake water, *black*–commercial, bottled mineral water, *red*–mineral water directly from spring) (adapted with permission from [77])

3.3.3 Integration of Reference Electrode

3.3.3.1 Preparation of Silver Electrodes

Nanoparticles

Electrodes prepared with two component epoxy resin "Araldite" mixed with nanoparticles showed smooth, even surface, without paper pores visible underneath (Fig. 3.17). When mixed with graphite powder, the same formulation resulted in rugged, continuous structure with clearly visible paper fibers. Silver nanoparticles mixed with mineral oil resulted in uneven surface with patches of silver deposit. The same formulation mixed with graphite generated continuous structure characteristic for graphite without visible silver. Electrodes with graphite powder in formulation presented good conductivity, whereas remaining samples did not. Results are clearly related to preparation procedure of the nanoparticles, which should be repeated and optimized. As this was not focus of this work, use of nanoparticles was discarded from subsequent tests.

Tollens reaction

When silver was deposited on paper by means of Tollens reaction, fibrous structure paper structure was clearly visible. Fibers were tightly covered and appeared stiffened after reaction (Fig. 3.17). Unfortunately, despite the visible deposit, neither of the sides became conductive. After pretreatment with tin chloride (II) paper not treated with wax seemed almost unmodified, and samples with wax presented partial, uneven change of color. During plating silver solution seemed to run off from the surface of electrodes and after drying paper did not present any conductivity when measured with multimeter.

Paper first painted with Electrolube silver paint resulted in even, continuous structure, smoother in the case of wax pretreatment. Side of paper not covered with silver paint became yellow after Tollens reaction and did not conduct electricity. Other side was conductive with resistivity lower for paper without wax (160–300 Ω, with wax $\sim$ 500 Ω).

Silver paint

Independently of wax pretreatment, surface of electrodes covered with SPI Conductive Silver pain was smooth and continuous without visible fibers. Surface became even smoother and more brilliant after sintering. Resistivity after deposition of one layer was much higher for wax treated paper ($\sim$6000 Ω) as compared with untreated ($\sim$1400 Ω). After deposition of second layer and sintering resistivity dropped to 350 Ω for wax treated paper and 200 Ω for untreated.

Electrodes covered with Electrolube silver paint presented resistivity around 1600 Ω independently if covered or not with wax. After sintering resistivity dropped to 200–300 Ω for electrodes without wax, and 300–350 Ω for wax treated paper.

Electrodes prepared by performing Tollens reaction on Electrolube silver paint and produced with SPI Conductive Silver paint, with and without wax were used to prepare Na^+ selective electrodes. Conditioning of electrodes without wax painted

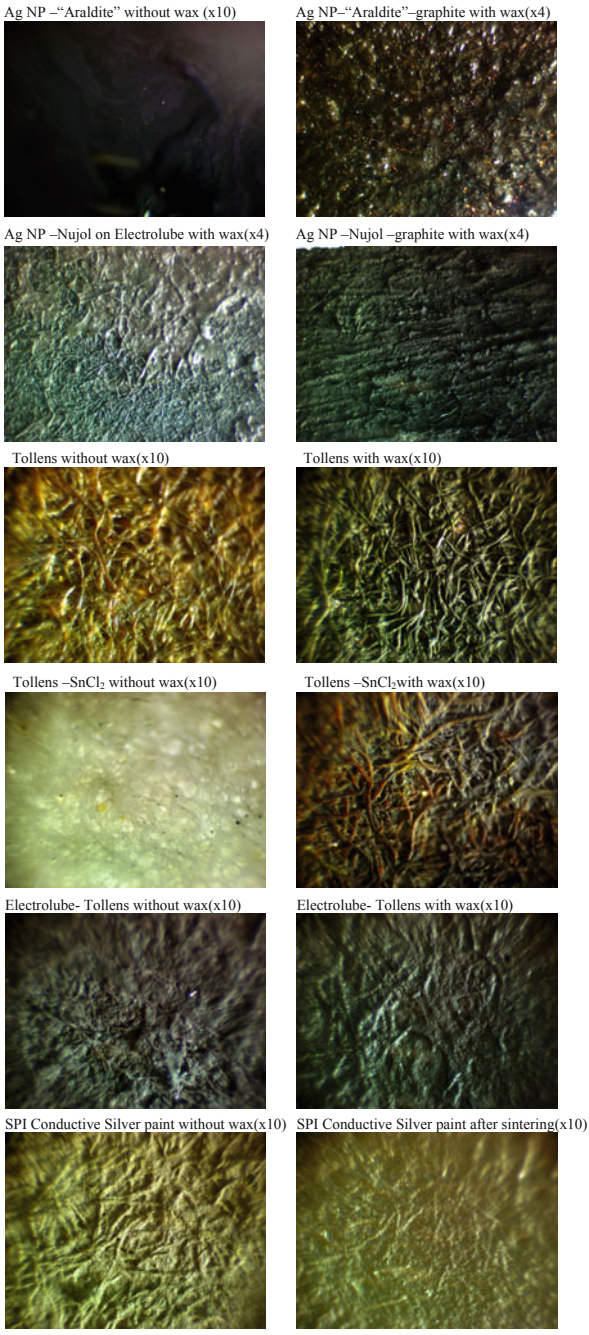

Fig. 3.17 Microscopic images of silver electrodes

with SPI Conductive Silver paint resulted in complete soaking of two of the three electrodes prepared for this study. Other electrodes did not suffer any apparent damage during conditioning.

Electrodes prepared with Electrolube silver paint with silver deposited by Tollens reaction showed lesser repeatability. Highest sensitivity and wider working range was observed for electrodes not treated with wax, probably due to larger surface area of the electrode.

In the case of sensors prepared with SPI Conductive Silver paint higher working range was also observed for electrode without wax. Sensitivity of all electrodes prepared with this paint ranged between 52 and 62 mV/dec.

Signal stabilized quicker in the case of all electrodes treated with wax, probably due to lack of interference caused by residual soaking of paper through the silver paint.

3.3.3.2 Fabrication of Ag/AgCl Reference Electrode

Electrodes prepared with Ag/AgCl nanoparticles did not conduct electricity. Signal stabilized fastest in the case of electrodes modified with wax and painted with SPI Conductive Silver paint (10–45 s), they also presented lowest drift after stabilization ($\sim$0.004 V during 20 min). The same material deposited on untreated paper resulted in longer signal stabilization (150–300 s) and much higher drift ($\sim$0.015 V). Both wax treated and wax free electrodes prepared with Electrolube and Tollens reaction performed less well (without wax 150 s stabilization, drift 0.1 V; with wax 450 s stabilization, drift 0.02 V). Higher drift observed for electrodes without wax layer is probably related with infiltration of liquid inside the electrode.

3.3.4 Discrimination of Beers

3.3.4.1 Electrode Characterization

Calibration curve and sensitivity—a representative dynamic response for each electrode type is presented in Fig. 3.18, with respective sensitivities and standard deviation resumed in Table 3.19.

Sensors based on silver paint presented much higher sensitivity as compared with pencil drawn sensors, which proves that previous results were related to high resistance of the conductive path (100 times higher resistance observed for pencil graphite). Super-Nernstian behavior was observed for NH_4^+ISE for concentrations

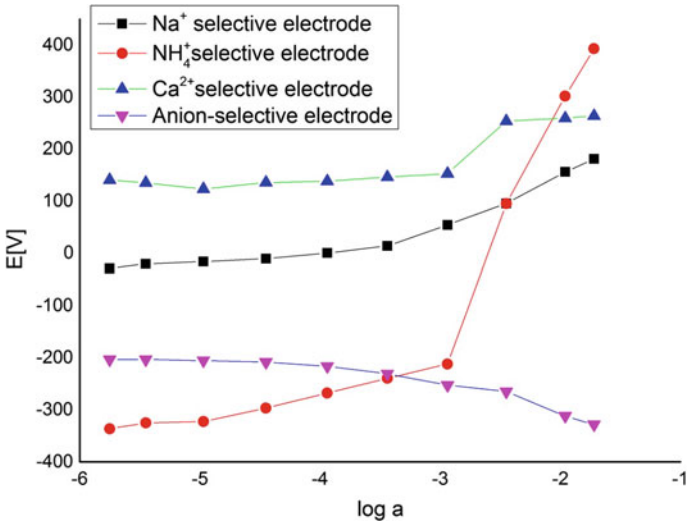

Fig. 3.18 Dynamic response of paper-based ion selective electrodes (electronic tongue for discrimination of beer samples)

Table 3.19 Sensitivity of studied sensors (electronic tongue for discrimination of beer samples). Adapted with permission from [84]

Ion	Range (mol/L)	Sensitivity (mV/dec)	St.dev. (N = 4)
Na^+	4.0×10^{-5}–2.3×10^{-2}	57.7	2.1
Ca^{2+}	2.0×10^{-6}–4.0×10^{-3}	23.8	2.7
NH_4^+	1.2×10^{-5}–1.3×10^{-3}	54.9	1.99
AS	4.0×10^{-5}–2.3×10^{-2}	−50.2	2.1

above 10^{-3}, which can be associated with the solid contact construction of the sensor, and possible diffusion of ammonia through the membrane.

Selectivity–Table 3.20 presents selectivity coefficients of studied electrodes together with examples from the literature. As it can be seen results are with good accordance with data obtained from other systems. Ammonium and calcium selective electrodes are rather selective whereas other sensors present cross-sensitivity, desired when working with electronic tongue systems.

Signal repeatability—Table 3.21 presents the medium of standard deviations obtained for each electrode type (standard deviation of signal from 3 measurements of the same solution, next taken an average from 3 sensors). All electrodes presented satisfactory repeatability, with more uniform results than in the case of pencil drawn electrodes.

Table 3.20 Selectivity coefficients of paper electrodes used for analysis of beer samples. Adapted with permission from [84]

	Electrode type							
	AS	AS [16]		NH_4^+	Na^+	Ca^{2+}	NH_4^+ [83]	Ca^{2+} [83]
Cl^-	−1.67	−1.87	Na^+	−2.56	0.00	−3.02	−2.80	−4.40
Br^-	−0.18	−0.61	K^+	−2.00	−0.54	−2.45	−1.05	−3.10
NO_3^-	0.00	0	NH_4^+	0.00	−0.35	−1.19	0.00	−2.70
F^-	−2.01	−3.13	Li^+	−5.49	−0.74	−1.63	−4.40	−2.15
ClO_4^-	1.15	3.26	Mg^{2+}	−7.03	−1.21	−1.57	−4.85	−2.55
SO_4^-	−1.04	−2.86	Ca^{2+}	−4.54	−0.50	0.00	−4.10	0.00

Table 3.21 Signal repeatability for each sensor type. Adapted with permission from [84]

Electrode type	AS	Na^+	Ca^{2+}	NH_4^+
St. dev. (N = 3)	1.7 mV	1.2 mV	1.9 mV	2.3 mV
0.005 mmol/L				
St. dev. (N = 3)	4.0 mV	1.4 mV	1.7 mV	2.5 mV
0.01 mmol/L				

3.3.4.2 Chemometric Analysis

Analysis of All Beer Samples (34 Samples)

PCR–discrimination of different beer types–first three factors represented 85, 12 and 1.7 % of total variance. As it can be seen in Table 3.22 all electrodes contribute almost equally to the factor with highest variance. With proposed data treatment it was not possible to separate different types of beers, like pilsner, stout, malzbier etc. Nevertheless as it can be seen in Figs. 3.20 and 3.21 data was separated into well-defined clusters.

Replicate measurements were in good accordance with each other, because of this only one data point is shown for each beer sample measured. Both ale beers tested appear in close proximity (green circle in Fig. 3.19), the same can be said for all three Weiss beers (yellow oval in Fig. 3.20).

It is also interesting that both beers produced at the same microbrewery (Zehn Bier) appear together in both planes (black oval in Fig. 3.19 and 3.20). Both beers

Table 3.22 PCR loadings

	Factor 1	Factor 2	Factor 3
Na^+	−0.52	0.3	−0.7
AS	−0.50	0.4	0.1
NH_4^+	−0.56	−0.8	0.04
Ca^{2+}	−0.40	0.3	0.7

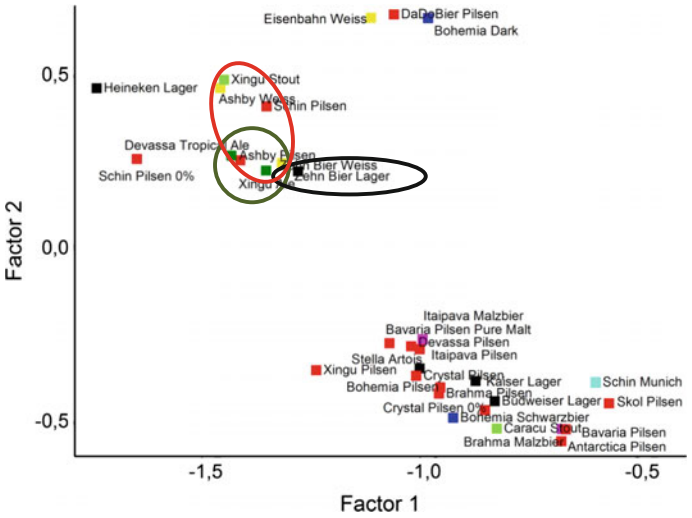

Fig. 3.19 PCR Scores Factor 1 versus Factor 2. Legend: *red*–Pilsner, *black*–Lager, *light green*–Stout, *pink*–Malzbier, *light blue*–Munich, *green*–Ale, *blue*–Schwarzbier and *Dark*, *yellow*–Weiss. Adapted with permission from [84]

from Ashby microbrewery were also grouped in close proximity (red oval in Fig. 3.19). Munich sample also forms a separate cluster, but as there was only one beer of this type in the sample set it is difficult to acclaim correct separation. More data is necessary to explain other clusters, which can be related to i.e. extract or bitterness (both not stated on Brazilian labels).

KNN–presence of antioxidants and stabilizers–KNN analysis (2 neighbors) resulted in only three misclassifications (34 samples, 2 replicates). Beers analyzed during this study contained different antioxidants, such as INS 316, INS 221, INS 224, INS 223. If antioxidant was present, stabilizer INS 405 was also included in the formulation. Three misclassifications obtained for this analysis included one replicate Crystal Pilsen 0 % and both replicates of Eisenbahn Weiss (Fig. 3.21).

PLS–prediction of pH–apart from beers set of samples included also a radler (pilsen mixed with lemon juice) and a distilled lemon alcoholic drink. Error of pH prediction for those two types of drinks was too high but pH of other samples was predicted with good precision (mean of standard deviations between predicted and measured value equal 0.065 pH). pH of 24 types of beer from 34 tested could be predicted with error smaller than 3 %. Results are resumed in Fig. 3.22. Variance of the first three factors was equal: 66.8, 19.7 and 5.36 %.

PLS–alcohol content–it was possible to predict alcohol content of 18 from 34 types of beers tested with error smaller than 5 %. Variance of the first three factors was equal: 14.7, 66.4 and 14.15 %.

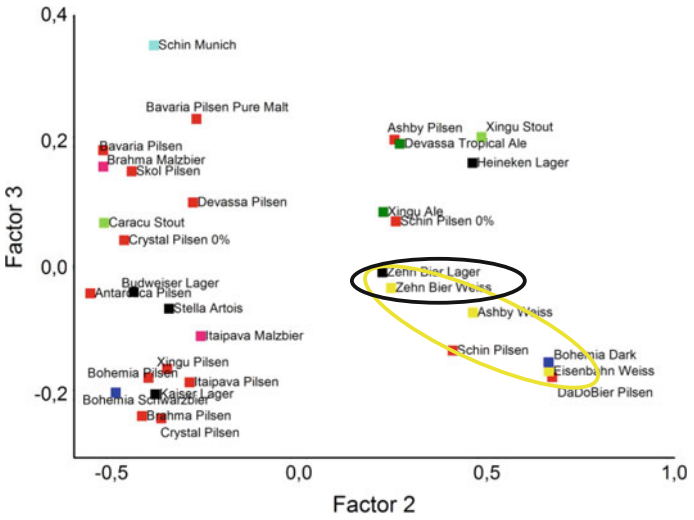

Fig. 3.20 PCR Scores Factor 2 versus Factor 3. Legend: *red*–Pilsner, *black*–Lager, *light green*–Stout, *pink*–Malzbier, *light blue*–Munich, *green*–Ale, *blue*–Schwarzbier and *Dark*, *yellow*–Weiss. Adapted with permission from [84]

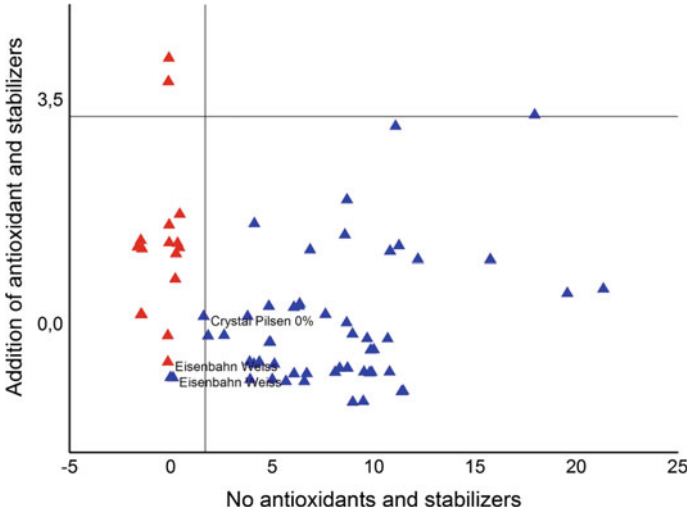

Fig. 3.21 KNN class fit graph for beers with antioxidants and stabilizers. *Blue*-beers without additives, *red* with stabilizers and antioxidants

Analysis of Pilsner Beers (13 Samples)

PCA–discrimination of Pilsner beers–different preprocessing methods were applied, with best separation of samples obtained for range scaled data. First three PC's described 81, 14 and 3 % of total information. Modeling Power was highest

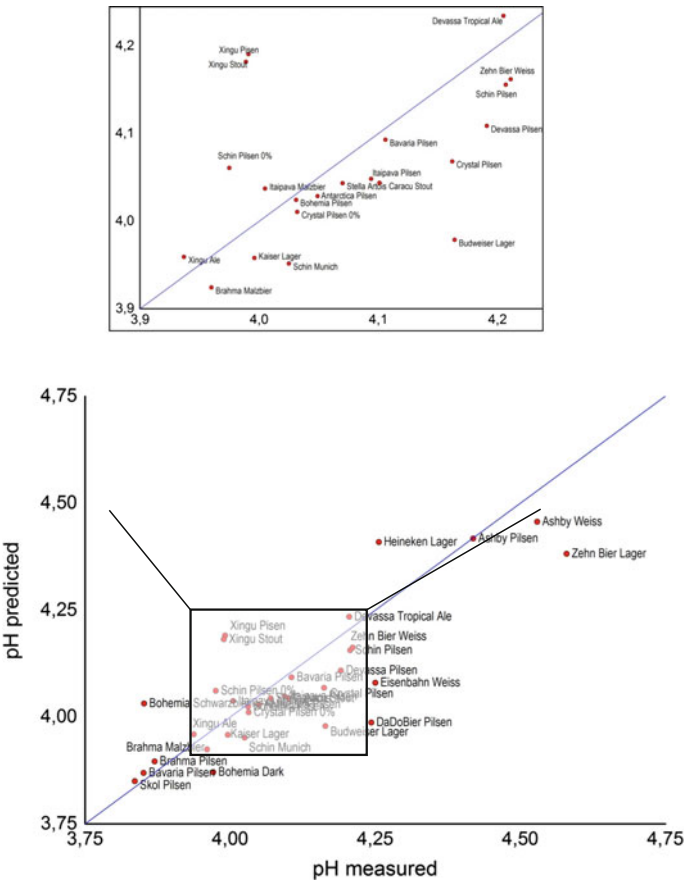

Fig. 3.22 PLS pH prediction for beer samples, Radler and Distilled lemon drink not shown

for NH_4^+ sensor and, equal: Na^+= 0.46, AS = 0.65, NH_4^+ = 0.87, Ca^{2+} = 0.33. As it can be seen in Fig. 3.23 13 samples form 9 separate clusters, 7 of them formed by individual beers. Brahma, Itaipava, Crystal and Bohemia (red oval in Fig. 3.23) as well as Bavaria, Skol (black oval in Fig. 3.23) and Antarctica (blue dots in Fig. 3.24) are all popular Brazilian pilsner beers. This fact can explain their close proximity in the graph and incapability of separation of individual brands (green oval in Fig. 3.23).

Analysis of Other (Non-Pilsner) Beer Types

KNN–type of fermentation–with 1 and 2 neighbors it was possible to assess type of fermentation (low, high, not applicable) with only 2 misclassifications (one replicate for both Crystal Pilsen 0 % and Zehn Bier Weiss).

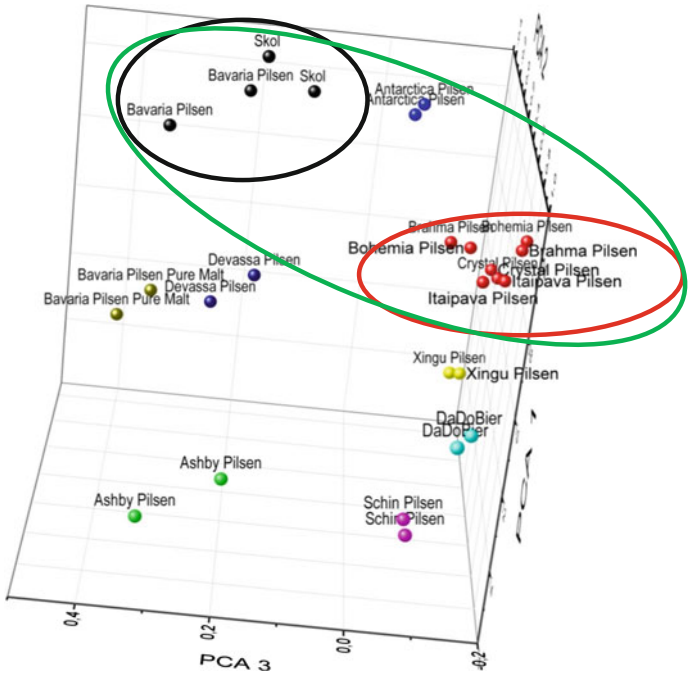

Fig. 3.23 PCA scores plot for Pilsner beer samples. *Colors* indicate separate clusters. Adapted with permission from [84]

KNN–presence of unmalted cereals, carbohydrates and caramel dye–it was also possible to distinguish beers with unmalted cereals added to the wort, with one misclassification for one replicate of Xingu Ale (Fig. 3.24). In the case of beers with carbohydrates added to the wort also only misclassification was obtained for the same replicate of Xingu Ale (Fig. 3.25). It is worth noting that addition of carbohydrates, mainly fermentable sugars to the wort reduces the amount of malt necessary for fermentation. Addition of unmalted cereals can serve the same purpose but in many cases is also associated with obtaining distinct gustatory characteristics.

It was also possible to correctly group beers with and without addition of caramel used as a dye (Fig. 3.26).

3.3.4.3 Stability of Sensor Matrix

Each beer sample was divided in three parts, next samples were coded and measured in random order. After data analysis it was noted that Ca^{2+} selective electrode responded differently for the last 9 samples. 102 samples were tested during this

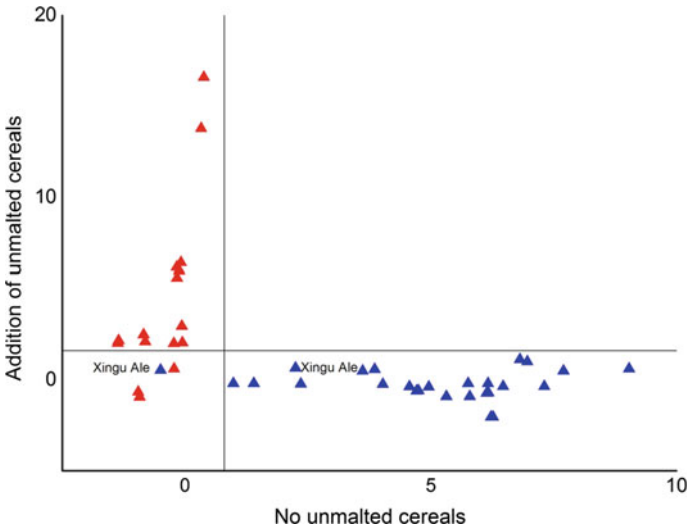

Fig. 3.24 KNN class fit graph for beers with unmalted cereals added to wort. *Blue*-beers without unmalted cereals, *red* with unmalted cereals

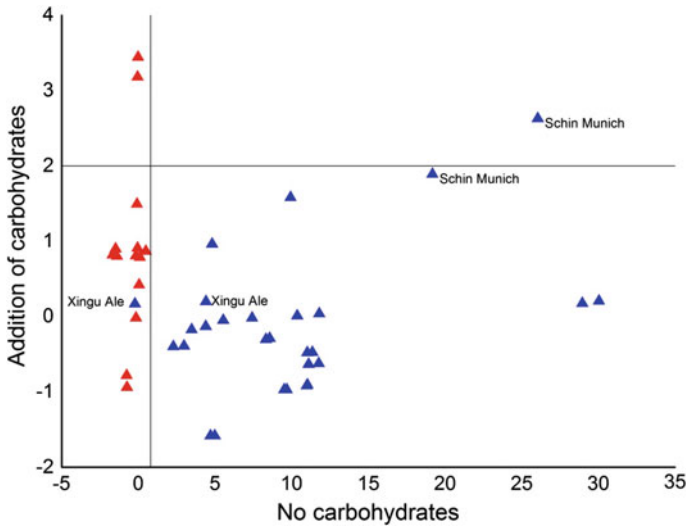

Fig. 3.25 KNN class fit graph for beers with carbohydrates added to wort. *Blue*-beers without carbohydrates, *red* with carbohydrates

study without recalibration or conditioning in between the samples. Therefore electronic tongue presented in this study is stable during analysis of around 90 samples. After analysis signal repeatability study was carried out confirming malfunctioning of the Ca^{2+} selective electrode.

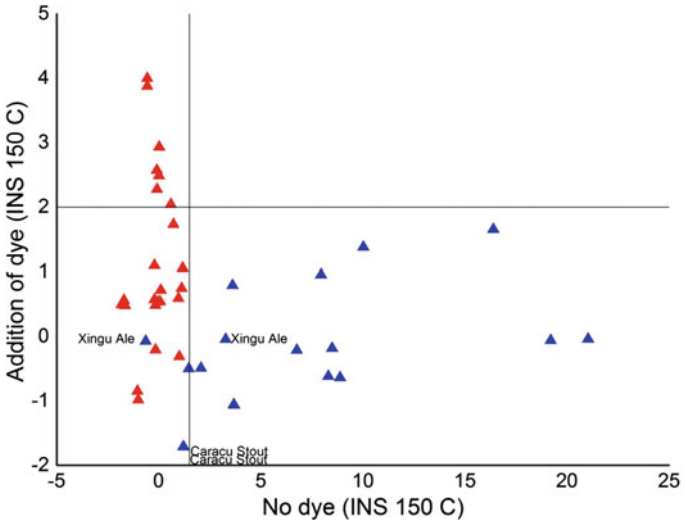

Fig. 3.26 KNN class fit graph for beers with caramel dye. *Blue*-beers without dye, *red* with dye

3.3.5 Minimization of Sample Volume

During first tests with flow-through devices where working electrode was integrated in the channel (Fig. 3.8), several problems were noted. First the deposition of membrane formulation from both sides of the paper was not reproducible. Membrane would in some cases completely block the channel, therefore wider channels had to be applied. During experiments with colored solution passing through a wetted channel it was noted that architectures presented on Fig. 3.8a, b did not allow for full wetting of the electrode. Solution would pass freely on top of the channel almost not entering the triangular or teardrop niche where electrode was placed. In the case of an oval channel presented in Fig. 3.8c electrode would be washed with solution only from the front and upper part. The back part after first wet-out process would not exchange solution, which would result in interference. Architecture proposed in Fig. 3.8d allowed full wetting of the electrode, unfortunately contact of the solution only with the sides of the membrane was too modest to successfully carry out the measurement. This kind of architecture would become too complicated when several electrodes would be introduced in the channel, therefore was discarded from subsequent tests.

In the case of experiments with a laminated, electronic tongue system with aligned electrodes results obtained for measurements in solution and with paper sample pad were in good accordance with each other (Single Factor Anova $F < F_{crit}$). When device was stacked against glass plaques liquid present in the paper sample pad spread over the surface of the glass, therefore amount of sample available around the membrane was lower. It was not possible to obtain results for

Table 3.23 Signal repeatability for three types of measurements destined to minimalize sample volume, cation-selective electrodes

Electrode type	In solution	Paper sample pad	Stacked
St. dev. (N = 3)	2.1 mV	2.9 mV	3.1 mV
0.005 mmol/L			
St. dev. (N = 3)	1.5 mV	2.88 mV	3.5 mV
0.01 mmol/L			

all electrodes during studies in flux due to high noise. Noise increased together with position of the electrode along the flow line (highest for the last electrode). This fact can be associated with the amount of liquid present in different parts of the channel (higher at the inlet) and resulting higher adherence of the paper channel to the electrodes at the beginning of the channel.

Results of the signal repeatability study are resumed in Table 3.23. For further tests measurement with paper sample pad placed on top of the electrode area was chosen. Minimum paper size was equal 3.5 × 0.5 cm and minimum sample volume necessary for analysis 40 μL.

During this study two electrode architectures were tested, namely tip and orifice electrodes. Again, the tip electrode was unreliable due to faults in insulation between the membrane and the lamination sheet. Therefore orifice electrodes were used.

Sample pad was cut from papers of different thickness, namely Whatman no 1, no 20 and no 3. No difference was noted between measurements with Whatman no 1 and no 20, which have similar thickness. Much thicker Whatman no 3 needed larger sample volume and the contact between more rigid and thicker paper and the electrodes was not as good as in the case of thinner sheets. Further tests were carried out with sample pads cut out from Whatman no 1 paper.

3.3.6 Discrimination of Wines

3.3.6.1 Electrode Characterization

Calibration curve and sensitivity–a representative dynamic response for each electrode type is presented in Fig. 3.27, with respective sensitivities and standard deviation resumed in Table 3.24. Measurement with a sample pad (Table 3.24) resulted in lower sensitivity as compared with measurement in solution (Table 3.19). Sensors present good linearity in the range 10^{5}–10^{-2}.

Selectivity–Table 3.25 present selectivity coefficients of studied electrodes together with examples from the literature. As it can be seen results are with good accordance with data obtained from other systems. Ca^{2+}/Mg^{2+} selective electrode is

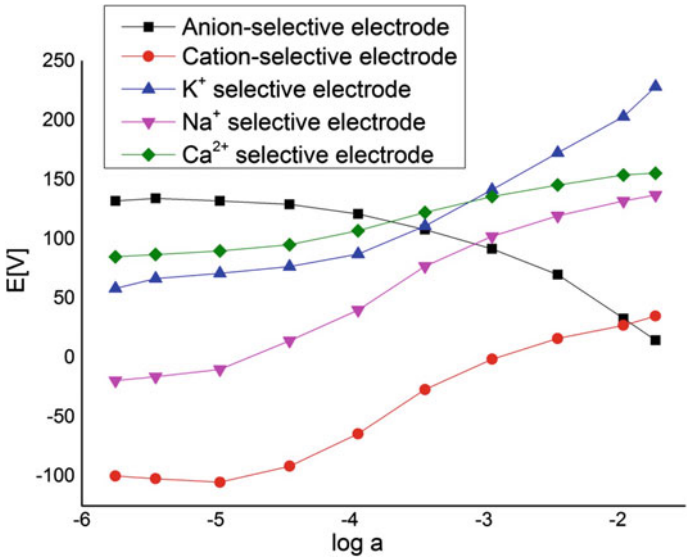

Fig. 3.27 Dynamic response of paper-based ion selective electrodes (electronic tongue for discrimination of wine samples)

Table 3.24 Sensitivity of studied sensors (electronic tongue for discrimination of wine samples). Adapted with permission from [84]

Ion	Range [mol/L]	Sensitivity (mV/dec)	St.dev. (N = 4)
AS	1.3×10^{-4}–2.3×10^{-2}	−47.9	2.1
CS	1.2×10^{-5}–2.3×10^{-2}	46.1	2.6
Na^+	4.0×10^{-5}–2.3×10^{-2}	56.5	2.8
K^+	1.2×10^{-5}–1.3×10^{-2}	49.9	4.0
Ca^{2+}	1.2×10^{-5}–1.3×10^{-2}	22.9	1.7

rather selective whereas other sensors present cross-sensitivity, desired when working with electronic tongue systems.

Signal repeatability–Table 3.26 presents the medium of standard deviations obtained for each electrode type (standard deviation of signal from 3 measurements of the same solution, next taken an average from 3 sensors). All electrodes presented satisfactory repeatability, similar to results obtained from measurements in solution (beer discrimination study) (Table 3.26).

Table 3.25 Selectivity coefficients of paper electrodes used for analysis of wine samples. Adapted with permission from [84]

	Electrode type								
	Cation-selective		Ca^{2+}/Mg^{2+}	Ca^{2+}	K^{+}/Na^{+}			Anion-selective	
	Measured	[64]	Measured	[39]	Measured	[83]		Measured	[16]
Na^{+}	0	0.82	−3.15	–3.79	−0.46	0.00	Cl^{-}	−1.79	−1.87
K^{+}	0.06	0	−3.26	–3.81	0	−1.20	Br^{-}	−0.12	−0.61
NH_4^{+}	0.15	0.62	−3.45	–3.66	−1.19	−1.05	NO_3^{-}	0	0
Li^{+}	0.1	−0.03	−1.79	–1.56	−0.76	−1.55	F^{-}	−3.4	−3.13
Mg^{2+}	−1.45	−1.8	0.43	–3.38	−2.12	−2.05	ClO_4^{-}	1.39	3.26
Ca^{2+}	−1.58	−1.79	0	0.00	2.17	−1.85	SO_4^{-}	−1.52	−2.86

Table 3.26 Signal repeatability for each sensor type. Adapted with permission from [84]

Electrode type	Ca^{2+}/Mg^{2+}	AS	CS	K^{+}/Na^{+}
St. dev. (N = 3)	1.0 mV	1.7 mV	1.1 mV	5.4 mV
0.005 mmol/L				
St. dev. (N = 3)	1.8 mV	0.7 mV	1.4 mV	3.9 mV
0.01 mmol/L				

3.3.6.2 Chemometric Analysis

PCA–discrimination of grape variety—different pretreatment methods were tested, with worst discrimination obtained for data without pretreatment. Other pretreatments provided similar results. For the final analysis data was autoscaled. PC 1, 2 and 3 described 41, 36 and 14 % of total information respectively. Modeling power of the electrodes was comparable: Ca^{2+}/Mg^{2+}:0.45, AS:0.59, CS:0.58, Na^{+}/K^{+}:0.45. Wines produced from different varieties of grapes (Chardonnay, Americanas, Malbec, Merlot) formed separate clusters (Fig. 3.28).

PLS–prediction of grape variety—number of Latent Variables was chosen to minimize standard error of prediction (SEP). Linear fit was performed for the PLS

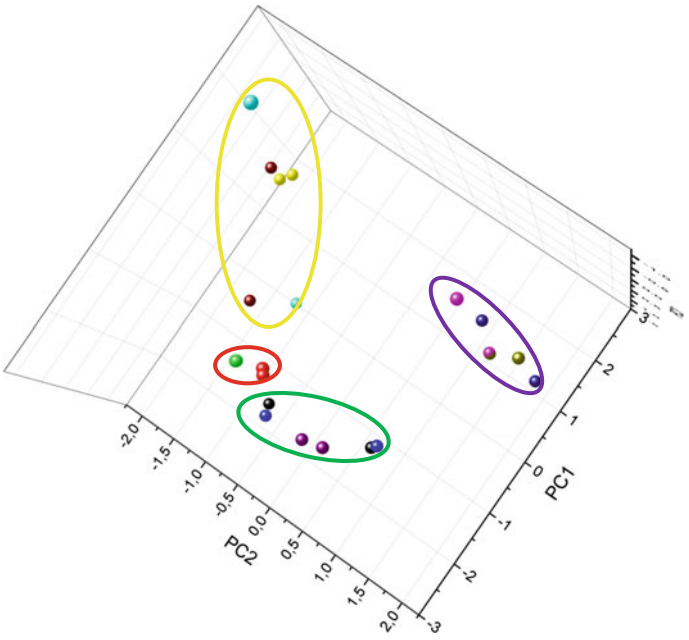

Fig. 3.28 PCA Scores plot for wine samples. *Yellow oval*–Chardonnay (*blue*-Marcus James, *yellow*–Novecento, *brown*–Santa Helena), *Red oval*–Americanas (*green*–*white*, *red*–*red*), *Green oval*–Malbec (*blue*-Fincas Privadas, *black*-, *violet*-Santa Florentina-Casillero del Diablo) *Violet oval*–Merlot (*pink*-Marcus James, *dark blue*–Santa Carolina, *gold*–Saint Germain). Adapted with permission from [84]

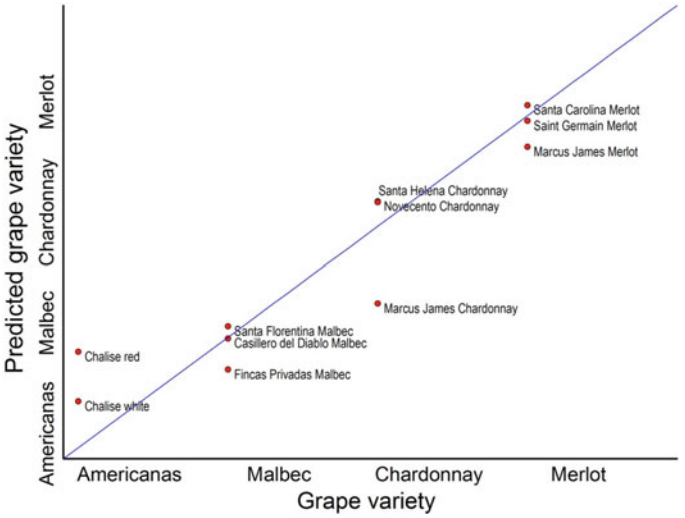

Fig. 3.29 PLS Y-fit plot for different grape varieties

predicted grape varieties versus the one stated on the label. Values of the slope, intercept and determination coefficient R^2, were equal 0.8, 0.3 and 0.93 respectively (in perfect case they should be equal 1.0 and 1). As it can be seen on Fig. 3.29 apart from Chalise red and Marcus James Chardonnay model was able to predict grape variety of tested wines.

KNN–Wine style (dry, semi-dry), type of stabilizer used—it was not possible to predict type of stabilizer used (potassium sorbate, SO_2) regardless the pretreatment method used. In the case of wine style (dry, semi-dry) 1 misclassification for Marcus James Chardonnay sample was obtained. It was noted that wine style is not independent from grape variety in the set of samples tested, therefore obtained result was related to previously presented discrimination.

It was not possible to predict alcohol content, year of production, or origin (including country, region and vinery) of the tested samples with any of the models used (PLS, KNN). Other electrodes should be included in the matrix to enable more robust discrimination.

3.3.7 Detection with Multimeter

Storage stability of proposed electronic tongue systems was evaluated by means of a multimeter (Fig. 3.30). Standard deviations (N = 3) obtained during four consecutive weeks (three test solutions measured alternately), for each electrode were compared by means of Single Factor Anova. No significant difference was found

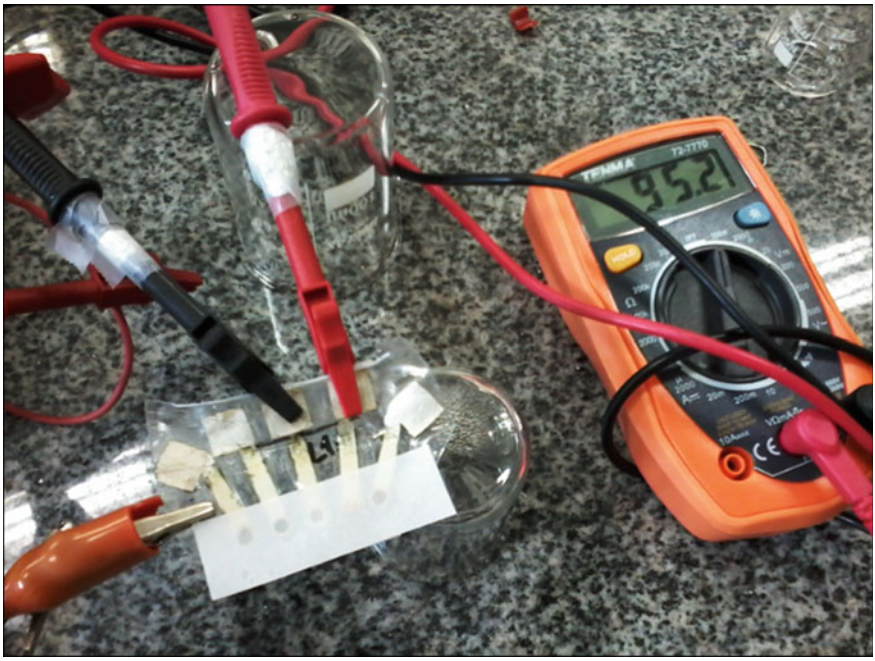

Fig. 3.30 Evaluation of storage stability by means of a multimeter

for both electronic tongue systems with working electrodes placed around Ag/AgCl reference and aligned during 4 weeks of measurements.

More detailed study, including assessment of sensitivity during storage should have to be carried out, but those results obtained for systems stored in room temperature already give some indication of the stability of the proposed system.

3.4 Partial Conclusions

During this part of work two electrode architectures were proposed (tip and orifice electrodes), different insulators were tested, including: wax, different types of glue, commercial liquid insulator, adhesive tape and lamination. Optimization process referred also to the electrode material (pencil graphite, silver ink, silver nanoparticles), length of the electrode and type of paper. It was possible to construct low-cost, paper-based working and reference electrodes integrated in one device, presenting performance close to theoretical and using a minimum amount of sample.

First system destined to indicate adulteration of water samples was able to classify with 100 % accuracy contaminated and original mineral water samples.

System was not influenced by source of mineral water (spring or commercialized product), its carbonation, or the type of adulteration (tap or lake water).

Second electronic tongue was designed for the analysis of beer samples, with 34 different beers tested during study. System was able to indicate presence of stabilizers and antioxidants, as well as dyes or even unmalted cereals and carbohydrates added to the fermentation wort. It was also possible to classify samples by type of fermentation (low, high) and predict pH and alcohol content of tested samples. When analyzed separately it was possible to discriminate 7 out of 13 Pilsner beers. If all samples were subjected to chemometric analysis separate clusters were observed for such beer types as Ale and Weiss, as well as beers fabricated in two micro-breweries.

Last system, devoted to discrimination of wines combined all advances of previous two devices, integrating working and reference electrodes. Apart from that it also introduced a sample pad, which minimized the sample volume. It was not possible to predict alcohol content, year of production, or origin (including country, region and vinery) of the tested samples with any of the models used (PLS, KNN). Other electrodes should be included in the matrix to enable more robust discrimination. Still, proposed matrix was able to group wines produced from different varieties of grapes (Chardonnay, Americanas, Malbec, Merlot), as well as successfully predict grape variety.

References

1. Vlasov Y, Legin A, Rudnitskaya A et al (2005) Nonspecific sensor arrays ("electronic tongue") for chemical analysis of liquids (IUPAC Technical Report). Pure Appl Chem 77:1965–1983. doi:10.1351/pac200577111965
2. Persaud K, Dodd G (1982) Analysis of discrimination mechanisms in the mammalian olfactory system using a model nose. Nature 299:352–355. doi:10.1038/299352a0
3. Otto M, Thomas JDR (1985) Model studies on multiple channel analysis of free magnesium, calcium, sodium, and potassium at physiological concentration levels with ion-selective electrodes. Anal Chem 57:2647–2651. doi:10.1021/ac00290a049
4. Vlasov Y, Legin A (1998) Non-selective chemical sensors in analytical chemistry: from "electronic nose" to "electronic tongue". Fresenius J Anal Chem 361:255–260. doi:10.1007/s002160050875
5. Ciosek P, Wróblewski W (2007) Sensor arrays for liquid sensing–electronic tongue systems. Analyst 132:963–978. doi:10.1039/b705107g
6. del Valle M (2010) Electronic tongues employing electrochemical sensors. Electroanalysis 22:1539–1555. doi:10.1002/elan.201000013
7. Riul A, Dos Santos DS, Wohnrath K et al (2002) Artificial taste sensor: Efficient combination of sensors made from Langmuir-Blodgett films of conducting polymers and a ruthenium complex and self-assembled films of an azobenzene-containing polymer. Langmuir 18:239–245. doi:10.1021/la011017d
8. Rodríguez-Méndez ML, Arrieta A, Parra V et al (2004) Fusion of three sensory modalities for the multimodal characterization of red wines. IEEE Sens J 4:348–354. doi:10.1109/JSEN.2004.824236
9. Rodionova OY, Pomerantsev L (2007) Chemometrics: achievements and prospects. Russ Chem Rev 75:271–287. doi:10.1070/RC2006v075n04ABEH003599

10. Richards E, Bessant C, Saini S (2002) Multivariate data analysis in electroanalytical chemistry. Electroanalysis 14:1533–1542
11. Túlio H, Oliveira AM De (2012) Chemometrics : theory and application. In: Multivar. Anal. Manag. Eng. Sci. pp 121–132
12. Ciosek P, Wróblewski W (2006) The analysis of sensor array data with various pattern recognition techniques. Sensors Actuators, B Chem 114:85–93. doi:10.1016/j.snb.2005.04.008
13. Bratov A, Abramova N, Ipatov A (2010) Recent trends in potentiometric sensor arrays-A review. Anal Chim Acta 678:149–159. doi:10.1016/j.aca.2010.08.035
14. Bobacka J, Ivaska A, Lewenstam A (2008) Potentiometric ion sensors. Chem Rev 108:329–351. doi:10.1021/cr068100w
15. Brzózka Z, Wróblewski W (1999) Sensory chemiczne, 1st edn. Oficyna Wydawnicza Politechniki Warszawskiej, Warsaw
16. Ciosek P, Augustyniak E, Wroblewski W (2004) Polymeric membrane ion-selective and cross-sensitive electrode-based electronic tongue for qualitative analysis of beverages. Analyst 129:639–644. doi:10.1039/b401390e
17. Umezawa Y, Bühlmann P, Umezawa K et al (2000) Potentiometric selectivity coefficients of ion-selective electrodes. part i. inorganic cations (technical report). Pure Appl Chem 72:1851–2082. doi:10.1351/pac200072101851
18. Ivanova NM, Levin MB, Mikhelson KN (2012) Problems and prospects of solid contact ion selective electrodes with ionophore based membranes. Russ Chem Bull 61:926–936
19. Faridbod F, Ganjali MR, Dinarvand R, Norouzi P (2008) Developments in the field of conducting and non-conducting polymer based potentiometric membrane sensors for ions over the past decade. Sensors 8:2331–2412. doi:10.3390/s8042331
20. Ilcheva L, Cammann K (1985) Flow injection analysis of chloride in tap and sewage water using ion-selective electrode detection. Fresenius' Zeitschrift für Anal Chemie 322:323–326
21. Frenzel W, Brätter P (1986) The fluoride ion-selective electrode in flow injection analysis. Anal Chim Acta 188:151–164. doi:10.1016/S0003-2670(00)86039-0
22. Szucs J, Gyurcsányi RE, Gyurcsµnyi E et al (2012) Towards protein assays on paper platforms with potentiometric detection. Electroanalysis 24:146–152. doi:10.1002/elan.201100522
23. Novell M, Parrilla M, Crespo G a et al (2012) Paper-based ion-selective potentiometric sensors. Anal Chem 84:4695–4702. doi:10.1021/ac202979j
24. Novell M, Guinovart T, Blondeau P et al (2014) A paper-based potentiometric cell for decentralized monitoring of Li levels in whole blood. Lab Chip 14:1308–1314. doi:10.1039/c3lc51098k
25. Lan W, Zou XU, Hamedi MM et al (2014) Paper-based potentiometric ion sensing. Anal Chem 86:9548–9553
26. Marple RL, Lacourse WR (2004) Analytical Instrumentation Handbook, 3rd edn. CRC Press
27. Sevilla F, Alfonso RL, Andres RT (1993) The electrician's multimeter in the chemistry teaching laboratory: Part 2: Potentiometry and conductimetry. J Chem Educ 70:580. doi:10.1021/ed070p580
28. Tang D, Zhang B, Liu B et al (2014) Digital multimeter-based immunosensing strategy for sensitive monitoring of biomarker by coupling an external capacitor with an enzymatic catalysis. Biosens Bioelectron 55:255–258. doi:10.1016/j.bios.2013.12.022
29. Liu H, Xiang Y, Lu Y, Crooks RM (2012) Aptamer-based origami paper analytical device for electrochemical detection of adenosine. Angew Chem Int Ed Engl 51:6925–6928. doi:10.1002/anie.201202929
30. Dege N (2011) Technology of bottled water, 3rd edn. Wiley-Blackwell
31. Ahmed W, Yusuf R, Hasan I et al (2013) Fecal indicators and bacterial pathogens in bottled water from Dhaka, Bangladesh. Brazilian J Microbiol 44:97–103. doi:10.1590/S1517-83822013005000026
32. Xing XR, Cao Q, Liu J et al (2008) Water quality of public drinking water sources in some key cities of main environmental protection in China. China Environ Sci 28:961–967

33. Momtaz H, Dehkordi FS, Rahimi E, Asgarifar A (2013) Detection of Escherichia coli, Salmonella species, and Vibrio cholerae in tap water and bottled drinking water in Isfahan, Iran. BMC Public Health 13:556. doi:10.1186/1471-2458-13-556
34. Ajayi A, Sridhar MKC, Adekunle Lola V, Oluwande P (2008) Quality of packaged waters sold in Ibadan, Nigeria. African J Biomed Res 11:251–258. doi:10.4314/ajbr.v11i3.50721
35. Kassinga G, Mbuligwe S (2009) Comparative assessment of physico-chemical quality of bottled and tap water in Dar es Salaam, Tanzania. Int J Biol Chem Sci 3:209–217. doi:10.4314/ijbcs.v3i2.44508
36. Addo K, Mensah G, Donkor B et al (2009) Bacteriological quality of bottled water sold on the Ghanaian market. African J Food, Agric Nutr Dev 9:7–9. doi:10.4314/ajfand.v9i6.46259
37. Gomes FCO, Silveira DMS, Silva LD et al. (2014) Monitoring microbiological and physicochemical quality of bottled mineral water sold in Minas Gerais, Brazil. J Water, Sanit Hyg Dev 4:538. doi:10.2166/washdev.2014.159
38. Scozzari A, Acito N, Corsini G (2007) A novel method based on voltammetry for the qualitative analysis of water. IEEE Trans Instrum Meas 56:2688–2697. doi:10.1109/TIM.2007.903600
39. Ciosek P, Brzózka Z, Wróblewski W (2004) Classification of beverages using a reduced sensor array.pdf. Sensors Actuators B Chem 103:76–83
40. Martínez-Máñez R, Soto J, Garcia-Breijo E et al (2005) An "electronic tongue" design for the qualitative analysis of natural waters. Sensors Actuators, B Chem 104:302–307. doi:10.1016/j.snb.2004.05.022
41. Garcia-Breijo E, Atkinson J, Gil-Sanchez L et al (2011) A comparison study of pattern recognition algorithms implemented on a microcontroller for use in an electronic tongue for monitoring drinking waters. Sensors Actuators, A Phys 172:570–582. doi:10.1016/j.sna.2011.09.039
42. Moreno L, Merlos A, Abramova N et al (2006) Multi-sensor array used as an "electronic tongue" for mineral water analysis. Sensors Actuators, B Chem 116:130–134. doi:10.1016/j.snb.2005.12.063
43. Kundu PK, Kundu M (2011) E-tongue based classification and authentication of mineral water samples following principal component analysis and Sammon's nonlinear mapping. In: Proc 2011 Int Conf Commun Ind Appl ICCIA 2011. doi:10.1109/ICCIndA.2011.6146649
44. Xiao H, Wang J (2012) Electronic tongue technique potential in monitoring quality of bottled water. J Food Agric Environ 10:227–230
45. Sipos L, Kovács Z, Sági-Kiss V et al (2012) Discrimination of mineral waters by electronic tongue, sensory evaluation and chemical analysis. Food Chem 135:2947–2953. doi:10.1016/j.foodchem.2012.06.021
46. Men H, Ge Z, Guo Y et al (2009) Biomimetic electronic tongue for classification of mineral water. IN: 2009 Int Conf Meas Technol Mechatronics Autom ICMTMA 2009 2:621–624. doi:10.1109/ICMTMA.2009.634
47. Hopfer H, Nelson J, Collins TS et al (2015) The combined impact of vineyard origin and processing winery on the elemental profile of red wines. Food Chem 172:486–496. doi:10.1016/j.foodchem.2014.09.113
48. Simoes Costa AM, Costa Sobral MM, Delgadillo I et al (2015) Astringency quantification in wine: comparison of the electronic tongue and FT-MIR spectroscopy. Sensors Actuators B Chem 207:1095–1103. doi:10.1016/j.snb.2014.10.052
49. Nelson M (2005) The Barbarian's beverage - a history of beer in ancient Europe. Taylor & Francis e-Library
50. Hornsey IS (2003) A history of beer and brewing. The Royal Society of Chemistry
51. Blanco CA, de la Fuente R, Caballero I, Rodríguez-Méndez ML (2015) Beer discrimination using a portable electronic tongue based on screen-printed electrodes. J Food Eng 157:57–62. doi:10.1016/j.jfoodeng.2015.02.018
52. Ceto X, Gutierrez-Capitan M, Calvo D, Del Valle M (2013) Beer classification by means of a potentiometric electronic tongue. Food Chem 141:2533–2540. doi:10.1016/j.foodchem.2013.05.091

53. Andrés-Iglesias C, Montero O, Sancho D, Blanco C (2015) New trends in beer flavour compound analysis. J Sci Food Agric 95:1571–1576. doi:10.1002/jsfa.6905
54. Gutiérrez JM, Haddi Z, Amari A et al (2013) Hybrid electronic tongue based on multisensor data fusion for discrimination of beers. Sensors Actuators, B Chem 177:989–996. doi:10.1016/j.snb.2012.11.110
55. Ciosek P, Brzózka Z, Wróblewski W (2006) Electronic tongue for flow-through analysis of beverages. Sensors Actuators, B Chem 118:454–460. doi:10.1016/j.snb.2006.04.051
56. Ghasemi-Varnamkhasti M, Rodríguez-Méndez ML, Mohtasebi SS et al (2012) Monitoring the aging of beers using a bioelectronic tongue. Food Control 25:216–224. doi:10.1016/j.foodcont.2011.10.020
57. Legin A, Rudnitskaya A, Lvova L et al (2003) Evaluation of Italian wine by the electronic tongue: recognition, quantitative analysis and correlation with human sensory perception. Anal Chim Acta 484:33–44. doi:10.1016/S0003-2670(03)00301-5
58. Ouyang Q, Zhao J, Chen Q (2013) Classification of rice wine according to different marked ages using a portable multi-electrode electronic tongue coupled with multivariate analysis. Food Res Int 51:633–640. doi:10.1016/j.foodres.2012.12.032
59. Moreno I, Codinachs L, Kloock JP, Schöning MJ et al (2008) Electronic integrated multisensor tongue applied to grape juice and wine analysis. Analyst 133:1440–1448. doi:10.1039/b801228h
60. Parra V, Arrieta Á, Fernández-Escudero J et al (2006) Electronic tongue based on chemically modified electrodes and voltammetry for the detection of adulterations in wines. Sensors Actuators, B Chem 118:448–453. doi:10.1016/j.snb.2006.04.043
61. Gil M, Cabellos JM, Arroyo T, Prodanov M (2006) Characterization of the volatile fraction of young wines from the Denomination of Origin "Vinos de Madrid" (Spain). Anal Chim Acta 563:145–153. doi:10.1016/j.aca.2005.11.060
62. Kang BS, Lee JE, Park HJ (2014) Electronic tongue-based discrimination of Korean rice wines (makgeolli) including prediction of sensory evaluation and instrumental measurements. Food Chem 151:317–323. doi:10.1016/j.foodchem.2013.11.084
63. Verrelli G, Lvova L, Paolesse R et al (2007) Metalloporphyrin—based electronic tongue: an application for the analysis of Italian white wines. Sensors 7:2750–2762. doi:10.3390/s7112750
64. Ciosek P, Wróblewski W (2006) The recognition of beer with flow-through sensor array based on miniaturized solid-state electrodes. Talanta 69:1156–1161. doi:10.1016/j.talanta.2005.12.029
65. Lvova L, Kim SS, Legin A et al (2002) All-solid-state electronic tongue and its application for beverage analysis. Anal Chim Acta 468:303–314. doi:10.1016/S0003-2670(02)00690-6
66. Cetó X, Céspedes F, delValle M (2013) Assessment of individual polyphenol content in beer by means of a voltammetric bioelectronic tongue. Electroanalysis 25:68–76. doi:10.1002/elan.201200299
67. Arrieta Á, Rodríguez-Méndez ML, de Saja J et al (2010) Prediction of bitterness and alcoholic strength in beer using an electronic tongue. Food Chem 123:642–646. doi:10.1016/j.foodchem.2010.05.006
68. Rudnitskaya A, Polshin E, Kirsanov D et al (2008) Instrumental measurement of beer taste attributes using an electronic tongue. Anal Chim Acta 646:5–6. doi:10.1063/1.3156520
69. Polshin E, Rudnitskaya A, Kirsanov D et al (2010) Electronic tongue as a screening tool for rapid analysis of beer. Talanta 81:88–94. doi:10.1016/j.talanta.2009.11.041
70. Pumtang S, Siripornnoppakhun W, Sukwattanasinitt M, Ajavakom A (2011) Solvent colorimetric paper-based polydiacetylene sensors from diacetylene lipids. J Colloid Interface Sci 364:366–372. doi:10.1016/j.jcis.2011.08.074
71. Links DA, Eaidkong T, Mungkarndee R et al (2012) Polydiacetylene paper-based colorimetric sensor array for vapor phase detection and identification of volatile organic compounds. J Mater Chem 22:5970. doi:10.1039/c2jm16273c
72. Feng L, Li H, Niu LY et al (2013) A fluorometric paper-based sensor array for the discrimination of heavy-metal ions. Talanta 108:103–108. doi:10.1016/j.talanta.2013.02.073

73. Zhang Y, Li X, Li H et al (2014) Postage stamp-sized array sensor for the sensitive screening test of heavy-metal ions. Analyst 00:1–7. doi:10.1039/c4an01022a
74. Lanter F, Erne D, Ammann D, Simon W (1980) Neutral carrier based ion-selective electrode for intracellular magnesium activity studies. Anal Chem 52:2400–2402
75. Sohail M, De Marco R, Lamb K, Bakker E (2012) Thin layer coulometric determination of nitrate in fresh waters. Anal Chim Acta 744:39–44. doi:10.1016/j.aca.2012.07.026
76. Fernandes JCB, De Oliveira Neto G, Rohwedder JJR, Kubota LT (2000) Simultaneous determination of chloride and potassium in carbohydrate electrolyte beverages using an array of ion-selective electrodes controlled by a microcomputer. J Braz Chem Soc 11:349–354. doi:10.1590/S0103-50532000000400004
77. Witkowska Nery E, Guimarães JA, Kubota LT (2015) Paper-based electronic tongue. Electroanalysis. doi:10.1002/elan.201500054
78. Bi Y, Ye J (2009) In situ oxidation synthesis of Ag/AgCl core-shell nanowires and their photocatalytic properties. Chem Commun (Camb) 3:6551–6553. doi:10.1039/b913725d
79. Polk BJ, Stelzenmuller A, Mijares G et al (2006) Ag/AgCl microelectrodes with improved stability for microfluidics. Sensors Actuators, B Chem 114:239–247. doi:10.1016/j.snb.2005.03.121
80. Beer JZ (1961) Quantitative paper radiochromatography using Tollens reagent. Talanta 8:809–816
81. Koura N, Kubota A (1985) Electroless plating of silver. J Met Finish Soc Japan 36:182–190. doi:10.4139/sfj1950.36.182
82. Barlag R, Nyasulu F, Starr R (2014) A student-made silver-silver chloride reference electrode for the general chemistry laboratory: $\sim$10 min preparation. J Chem Educ 91:766–768. doi:10.1021/ed400722e
83. Ciosek P, Mamińska R, Dybko A, Wróblewski W (2007) Potentiometric electronic tongue based on integrated array of microelectrodes. Sensors Actuators, B Chem 127:8–14. doi:10.1016/j.snb.2007.07.015
84. Witkowska Nery E, Kubota LT (2016) Integrated, paper-based potentiometric electronic tongue for the analysis of beer and wine. Anal Chim Acta. 28(918):60–68

Conclusions

In the course of this work two distinct systems were proposed: a paper-based platform for analysis of glucose, cholesterol and uric acid in biological samples (colorimetric and electrochemical detection) and electronic tongue systems for the analysis of beverages. In both cases paper served as the primary substrate for construction of proposed systems. This simple substrate proved to be versatile and practical, however presenting certain problems related to its homogeneity.

Devices destined to quantify glucose, uric acid and cholesterol in biological samples with both colorimetric and electrochemical detection were proposed. Numerous problems were solved during this study, as for example construction method that would enable analysis of compounds such as cholesterol, uniformity of color development in the case of colorimetric detection or electrode positioning in the fibrous structure of paper in the case of electrochemical measurement. Various architectures including spot-test, lateral and tangential flow devices were analyzed. Finally it was possible to construct calibration curves in the range of interest for all three compounds. Glucose and uric acid could be quantified through electrochemical and colorimetric methods and cholesterol only calorimetrically. Glucose and uric acid could be quantified simultaneously in the same device, with both colorimetric (tangential flow device) and electrochemical detection, but efforts to integrate all three assays in one device were unfortunately unsuccessful.

In order to be applicable in real-life situations in resource limited settings, where devices can be exposed to higher temperatures during storage and transport (due to i.e. power outages), proposed devices should be designed for enhanced storage stability. It is widely known that adequate immobilization method can significantly prolong shelf-life of sensors based on enzymatic reactions. One universal immobilization method optimum for all applications does not exist, therefore based on performed study, depending on application indicated methods are:

- short term stationary applications—simple adsorption;
- long term stationary applications—BSA blocking;
- long term flow application—chitosan, starch entrapment or LbL Sodium alginate-PEI (dextran for storage in lower temperatures);
- if covalent linkage is necessary—EDC/NHS;

E. Witkowska Nery, *Analysis of Samples of Clinical and Alimentary Interest with Paper-based Devices*, Springer Theses, DOI 10.1007/978-3-319-28672-3

During the experiments methods for quantification of proteins on paper were proposed, with best results obtained for direct quantification, which could be applied for enzyme and albumin samples, and bromophenol blue only applicable to albumin samples.

Second part of this work was devoted to development of electronic tongue systems. Different electrode materials, insulation methods, architectures were tested leading to an integrated device with four working electrodes and a paper-based Ag/AgCl reference. Performance of the system was close to theoretical and final device that could carry out measurements with sample volume as low as 40 μL. Readily available components such as wax, lamination sheets, bleach were used to assemble the final device. Storage stability was successfully evaluated by means of a multimeter thus, not only fabrication but also detection can be accomplished by means of off-the-shelf components. Each stage of development i.e. construction of working electrodes, integration of paper-based reference, minimization of sample volume, was summarized with a real-life application.

In conclusion, comparing with devices presented in the literature proposed systems for the analysis of glucose, cholesterol and uric acid employ non-toxic, easily available compounds, and do not necessitate the use of auxiliary enzyme such as peroxidase or its substitute (nanoparticles, graphene oxide etc.). Used fabrication methods are also compatible with all analytes including cholesterol. Proposed devices present good repeatability of measurement in the concentration range in question and could be stored for periods up to 20 weeks in 4 °C or 14 weeks in room temperature. In the case of electronic tongue system, two groups already described potentiometric paper-based sensors. Electrodes developed during this work, use more readily available components (as compared with carbon nanotubes), different architecture, and were successfully integrated into multi-electrode system. Up to this date no paper-based electronic tongue with potentiometric detection was described in the literature. Proposed systems were successfully applied for the discrimination of three distinct types of samples.